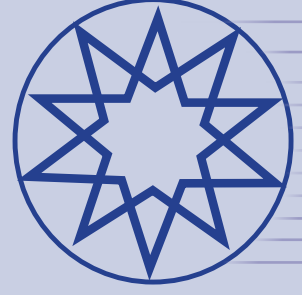


ISSN 2636-8498

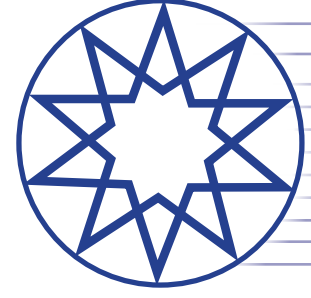


Environmental Research & Technology

Year 2024
Volume 7
Number 2

**YTÜ
PRESS**

www.ert.yildiz.edu.tr



Environmental Research & Technology

Volume 7 Number 2 Year 2024

EDITOR-IN-CHIEF

Prof. Dr. Ahmet Demir, *Yıldız Technical University, İstanbul, Türkiye*

Prof. Dr. Mehmet Sinan Bilgili, *Yıldız Technical University, İstanbul, Türkiye*

ACADEMIC ADVISORY BOARD

Prof. Dr. Adem Baştürk, *Yıldız Technical University, İstanbul, Türkiye*

Prof. Dr. Mustafa Öztürk, *Yıldız Technical University, İstanbul, Türkiye*

Prof. Dr. Lütfi Akça, *İstanbul Technical University, İstanbul, Türkiye*

Prof. Dr. Oktay Tabasaran, *University of Stuttgart, Germany*

SCIENTIFIC DIRECTOR

Prof. Dr. Ahmet Demir, *Yıldız Technical University, İstanbul, Türkiye*

ASSISTANT EDITOR

Dr. Hanife Sarı Erkan, *Yıldız Technical University, İstanbul, Türkiye*

LANGUAGE EDITOR

Prof. Dr. Güleda Engin, *Yıldız Technical University, İstanbul, Türkiye*

Abstracting and Indexing

The following is a list of the Abstracting and Indexing databases that cover

Environmental Research and Technology published by Yıldız Technical University.

TR-DİZİN, Scopus, EBSCO, ROAD, SJIFactor, EurAsianScientific Journal Index (ESJI), Research Bib(Academic Resource Index), ScientificIndexing Services, ASOSIndex, MIAR, IndexCopernicus, Open Ukrainian Citation Index (OUCI), Scilit, Ideal Online, Google Scholar, Directory of Research Journals Indexing

Publisher (Owner)

Yıldız Technical University

Address: Yıldız Technical University, Davutpaşa Kampusu, 34210 Esenler, İstanbul, Türkiye.

Phone: +90 212 383 20 18; **E-mail:** mbilgili@yildiz.edu.tr, ahmetd@yildiz.edu.tr

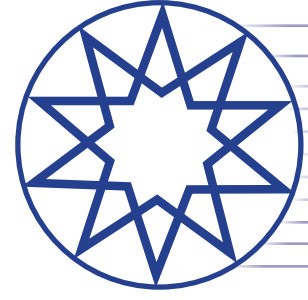
Corporate Contributor (Publishing House)

Kare Publishing - Kare Yayıncılık

Address: Göztepe Mah., Fahrettin Kerim Gökay Cad., No: 200, Da: 2, Göztepe, Kadıköy, İstanbul, Türkiye

Phone: +90 216 550 61 11; **Fax:** +90 216 550 61 12; **Web:** www.karepb.com; **E-mail:** kare@karepb.com

Environmental Research & Technology



Volume 7 Number 2 Year 2024

CO-EDITORS (AIR POLLUTION)

Prof. Dr. Mohd Talib Latif, *Department of National University of Malaysia/Universiti Kebangsaan Malaysia, Malaysia*

Prof. Dr. Nedim Vardar, *Inter American University, Puerto Rico*

Prof. Dr. Sait Cemil Sofuođlu, *İzmir Institute of Technology, İzmir, Türkiye*

Prof. Dr. Wina Graus, *Copernicus Institute of Sustainable Development, Utrecht University, Netherlands*

CO-EDITORS (ENVIRONMENTAL ENGINEERING AND SUSTAINABLE SOLUTIONS)

Prof. Dr. Bülent İnanç, *İstanbul Technical University, İstanbul, Türkiye*

Prof. Dr. Güleda Engin, *Yıldız Technical University, İstanbul, Türkiye*

Prof. Dr. Hossein Kazemian, *University of Northern British Columbia, Canada*

Prof. Dr. Raffaella Pomi, *La Sapienza, Italy*

Prof. Dr. Yılmaz Yıldırım, *Zonguldak Bülent Ecevit University, Zonguldak, Türkiye*

CO-EDITORS (WASTE MANAGEMENT)

Prof. Dr. Bestami Özkaya, *Yıldız Technical University, İstanbul, Türkiye*

Prof. Dr. Bülent Topkaya, *Akdeniz University Faculty of Engineering, Antalya, Türkiye*

Prof. Dr. Kahraman Unlu, *Department of Environmental Engineering, Middle East Technical University, Ankara, Türkiye*

Prof. Dr. Mohamed Osmani, *Loughborough University, School of Architecture, Building and Civil Engineering, United Kingdom*

Prof. Dr. Pin Jing He, *Tongji University, China*

CO-EDITORS (WATER AND WASTEWATER MANAGEMENT)

Prof. Dr. Ayşe Filibeli, *Dokuz Eylül University, İzmir, Türkiye*

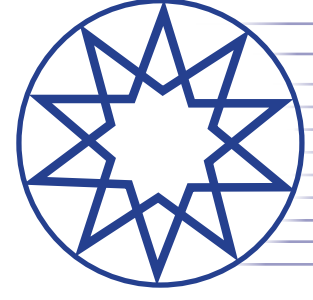
Prof. Dr. Barış Çallı, *Marmara University, İstanbul, Türkiye*

Prof. Dr. Marina Prisciandaro, *University Of L'aquila, Italy*

Prof. Dr. Md. Ahmaruzzaman, *National Institute of Technology Silchar, India*

Prof. Dr. Selvam Kaliyamoorthy, *Mie University, Japan*

Prof. Dr. Subramanyan Vasudevan, *Academy For Scientific and Innovative Research, New Delhi, India*



Environmental Research & Technology

Volume 7 Number 2 Year 2024

EDITORIAL BOARD

Prof. Dr. Andjelka Mihajlo, *Department of Environmental Engineering and Occupational Safety and Health, Faculty of Technical Sciences, University of Novi Sad, Serbia*

Prof. Dr. Artur J. Badyda, *Warsaw University of Technology, Poland*

Prof. Dr. Azize Ayol, *Dokuz Eylül University, İzmir, Türkiye*

Prof. Dr. Didem Balkanlı, *Yıldız Technical University, İstanbul, Türkiye*

Prof. Dr. Erwin Binner, *University of Natural Resources and Life Science Vienna, Austria*

Prof. Dr. Eyüp Debik, *Yıldız Technical University, İstanbul, Türkiye*

Prof. Dr. Dilek Sanin, *Middle East Technical University, Ankara, Türkiye*

Prof. Dr. Gülsüm Yılmaz, *İstanbul University-Cerrahpaşa, İstanbul, Türkiye*

Prof. Dr. Hamdy Seif, *Beirut Arab University, Beirut, Lebanon*

Prof. Dr. Hanife Büyükgüngör, *Ondokuz Mayıs University, Samsun, Türkiye*

Prof. Dr. Ilirjan Malollari, *University of Tirana, Albania, Albanian Academy of Sciences, Albania*

Prof. Dr. İsmail Koyuncu, *İstanbul Technical University, İstanbul, Türkiye*

Prof. Dr. Jaakko Puhakka, *Tampere University of Applied Sciences, Tampere, Finland*

Prof. Dr. Lucas Alados Arboledas, *University of Granada, Granada, Spain*

Prof. Dr. Mahmoud A. Alawi, *University of Jordan, Amman, Jordan*

Prof. Dr. Marcelo Antunes Nolasco, *University of São Paulo, São Paulo, Brasil*

Prof. Dr. Martin Kranert, *University of Stuttgart, Stuttgart, German*

Prof. Dr. Mesut Akgün, *Yıldız Technical University, İstanbul, Türkiye*

Prof. Dr. Mukand S. Babel, *Asian Institute of Technology, Pathum Thani, Thailand*

Prof. Dr. Mustafa Odabaşı, *Dokuz Eylül University, İzmir, Türkiye*

Prof. Dr. Müfide Banar, *Eskişehir Technical University, Eskişehir, Türkiye*

Prof. Dr. Mufit Bahadır, *Technische Universität Braunschweig, German*

Prof. Dr. Neslihan Doğan Sağlamtimur, *Niğde Ömer Halisdemir University, Niğde, Türkiye*

Prof. Dr. Nihal Bektaş, *Gebze Technical University, Gebze, Türkiye*

Prof. Dr. Osman Arıkan, *İstanbul Technical University, İstanbul, Türkiye*

Prof. Dr. Osman Nuri Ağdağ, *Pamukkale University, Denizli, Türkiye*

Prof. Dr. Pier Paolo Manca, *University of Cagliari, Italy*

Prof. Dr. Saim Özdemir, *Sakarya University, Sakarya, Türkiye*

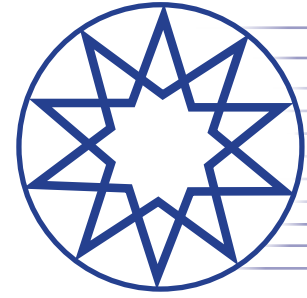
Prof. Dr. Serdar Aydın, *İstanbul University-Cerrahpaşa, İstanbul, Türkiye*

Prof. Dr. Timothy O. Randhir, *University of Massachusetts Amherst, USA*

Prof. Dr. Ülkü Yetis, *Middle East Technical University, Ankara, Türkiye*

Prof. Dr. Victor Alcaraz Gonzalez, *University of Guadalajara, Mexico*

Prof. Dr. Ejaz Khan, *Health Services Academy, Pakistan*



Environmental Research & Technology

Volume 7 Number 2 Year 2024

CONTENTS

- Preface**
148 Güleda ENGİN, Azize AYOL, Tasnim ALMOULKI
- Research Articles**
- 149 **Energy sources as a function of electric vehicle emission: The case of Bosnia and Herzegovina**
Jasmin ŠEHOVIĆ, Dževad BIBIĆ
- 160 **Performance evaluation of a simple electrochemical treatment model for saline wastewaters: Part B**
Ezekiel Oluwaseun FEHINTOLA, Enoch Adedayo ADEKUNBI, Babatunde Moses OJO, John Olugbemiga AWOTUNDE, Isaiah Adesola OKE
- 175 **PbO₂/graphite and graphene/carbon fiber as an electrochemical cell for oxidation of organic contaminants in refinery wastewater by electro-fenton process; electrodes preparation, characterization and performance**
Rowaida N. ABBAS, Ammar S. ABBAS
- 186 **Text mining on sustainability reports of top 40 airlines and bibliometric analysis of airline's sustainability**
İbrahim ŞAPALOĞLU
- 194 **Smart environmental drone utilization for monitoring urban air quality**
Yeliz DURGUN, Mahmut DURGUN
- 201 **Evaluation of characterization and adsorption kinetics of natural organic matter onto nitric acid modified activated carbon**
Betül AYKUT ŞENEL, Nuray ATEŞ, Şehnaz Şule Kaplan BEKAROĞLU
- 212 **Dispersion model of NOx emissions from a liquefied natural gas facility**
İlker TÜRKYILMAZ, S. Levent KUZU
- 223 **Factorial experimental design for removal of Indigo Carmine and Brilliant Yellow dyes from solutions by coagulation**
Mustafa KORKMAZ
- Reviews Articles**
- 233 **Impact of dissolved organic nitrogen (DON) to the formation of disinfection byproducts (DBP) during water/wastewater treatment: A review**
Ashik AHMED, Sumaya TABASSUM, Debo Brata PAUL ARGHA, Pranta ROY
- 256 **Fostering sustainability: The environmental advantages of natural fiber composite materials – a mini review**
Sivasubramanian PALANISAMY, Thulasi Mani MURUGESAN, Murugesan PALANIAPPAN, Carlo SANTULLI, Nadir AYRILMIŞ
- 270 **Application of Scheffe's Simplex Lattice Model in concrete mixture design and performance enhancement**
Jonah AGUNWAMBA, Fidelis OKAFOR, Michael Toryila TÍZA
- Case Report**
- 280 **Potential recycling of mine tailings for PMC's Padcal Mine, Philippines**
Idongesit Ime IKOPBO, Melissa May BOADO



Environmental Research and Technology

<https://ert.yildiz.edu.tr> - <https://dergipark.org.tr/tr/pub/ert>

Environmental
Research & Technology

Preface

Güleda ENGİN¹, Azize AYOL², Tasnim ALMOULKI¹

¹Department of Environmental Engineering, Yıldız Technical University, Faculty of Civil Engineering, İstanbul, Türkiye

²Department of Environmental Engineering, Dokuz Eylül University, Faculty of Engineering, İzmir, Türkiye

In this special edition of Environmental Research and Technology, we are pleased to introduce the ECO-SPHERE postdoctoral fellowship programme, an interdisciplinary research initiative dedicated to promoting sustainability and circular economies. Funded by the European Union under the renowned Marie Skłodowska-Curie Actions (MSCA) COFUND program agreement No. 101126655, and The Scientific and Technological Research Institution of Turkey (TÜBİTAK), ECO-SPHERE was designed to foster cutting edge research and work collaboratively to address global environmental challenges.

The program is coordinated by Yıldız Technical University, with Dokuz Eylül University, as the implementing partner. As two of Türkiye's most prestigious educational institutions, they offer dynamic environments that permit comprehensive training and mentorship opportunities, in addition to their rich educational and industrial partnerships.

ECO-SPHERE stands for "Circular Economy for the Sustainable Earth Spheres - Geosphere, Biosphere, Hydro-

sphere & Atmosphere". This five-year framework, under two separate calls, will bring together 12 leading researchers each, in which they will conduct research over the course of 24 months.

Our wide range of domains include but are not limited to: Energy, Water and/or Wastewater Management, Material Recovery, Waste Management, Economic and Environmental Policy, Policy Instruments for Circular Economy, Structural Health Monitoring of Structures, Business Models, Bioeconomy, Digitalisation, Decision Making, Eco-Design, Technological Change, and Climate Change.

As you engage in the findings and research presented in this special edition, we invite you to apply and join our team and mission in Researching for a Sustainable Future.

Thank you for your interest in ECO-SPHERE. You can find detailed information at <https://ecosphere-msca.org.tr>.

Sincerely,

*Corresponding author.

*E-mail address: gengin@yildiz.edu.tr





Research Article

Energy sources as a function of electric vehicle emission: The case of Bosnia and Herzegovina

Jasmin ŠEHOVIĆ^{*} , Dževad BIBIĆ

Department for IC Engines and Vehicles, Faculty of Mechanical Engineering, University of Sarajevo, Sarajevo, Bosnia and Herzegovina

ARTICLE INFO

Article history

Received: 08 December 2023

Revised: 05 February 2024

Accepted: 08 February 2024

Key words:

Copert; CO₂ pollution; Electric vehicles; Renewable energy sources

ABSTRACT

This paper deals with the analysis of challenges and perspectives of the transition to electric vehicles as a sustainable solution for the transport sector in the context of global energy challenges and the need to reduce negative environmental impacts. With an emphasis on the energy situation in Bosnia and Herzegovina, the paper explores the possibilities of switching to electric vehicles (EVs) and analyses the effects of energy sources on CO₂ emissions. The paper highlights the motivation to switch to EVs, driven by the need to reduce greenhouse gas emissions and rely on renewable energy sources. After analysing relevant studies, it is concluded that smaller and lighter electric vehicles have lower CO₂ emissions and that the participation of renewable sources in electricity production reduces these emissions. The conducted analysis of the vehicle fleet specifies that the CO₂ emissions of electric vehicles are not zero and that they depend on the source of electricity. Furthermore, other factors, such as the production of batteries, also play an important role in the overall environmental impact. Although the motivation to switch to electric vehicles is emphasized to reduce greenhouse gas emissions and use renewable energy sources, it has been shown that the CO₂ emissions of electric vehicles (EVs) are not zero and significantly depend on the energy sources. Calculations performed on the vehicle fleet of the Federation of Bosnia and Herzegovina for the year 2021, using Copert as the tool, showed that vehicles driven by fossil fuels emit about 1.6 million tonnes of CO₂. In comparison, if all vehicles were replaced with electrical ones, the CO₂ emissions would be about 1.15 million tonnes. As for the required electricity to power EVs, it is calculated that the required amount would be about 1,539 GWh per year. This paper acknowledges the presence of emissions associated with battery production, storage, and disposal, as well as vehicles themselves. However, it does not delve into this issue in detail. Future research will aim to address this matter more thoroughly.

Cite this article as: Šehovic J, Bibic D. Energy sources as a function of electric vehicle emission: The case of Bosnia and Herzegovina. Environ Res Tec 2024;7(2)149–159.

INTRODUCTION

In today's world, we are encountering significant energy challenges that require sustainable solutions to minimize the adverse impact on the environment. The transition in the transport sector is one of the primary concerns, as it contributes to harmful gas emissions and air pollution. Therefore,

shifting to electric vehicles (EVs) is crucial in achieving sustainable mobility and reducing environmental impact. This paper will discuss the energy challenges of transitioning to electric vehicles. We will focus on the global situation, specifically in the European Union and Bosnia and Herzegovina. We aim to explore this transition's advantages, challenges, and possibilities towards a more sustainable future. We

***Corresponding author.**

*E-mail address: sehovic@mef.unsa.ba



hope to provide insight into this crucial step's current state and perspectives. The motivation to transition to electric vehicles stems from the growing awareness of climate change and the need to reduce emissions. Vehicles with engines that use fossil fuels by the nature of their operation emit exhaust gases that have a harmful effect on air quality and human health. The transition to EVs should make it possible to reduce dependence on fossil fuels, which would achieve a reduction in the emissions of CO₂ and other harmful substances from exhaust gases. However, the transition to EVs faces challenges. Adequate charging infrastructure is essential to ensure electric vehicles' practicality and reliability. Issues related to vehicle range and battery charging time and questions about the sustainability of battery production and waste management need to be addressed.

Research carried out in China [1] considered the influence of the vehicle category, the origin of the source of electricity used to charge electric vehicle batteries, and the technology used to produce batteries for electric vehicles on Carbon emissions. The results indicate that smaller and lighter vehicles have lower CO₂ emissions than larger and heavier ones. Also, the CO₂ emissions of electric vehicles depend on the share of energy sources in electricity production. These findings highlight the importance of optimising battery technology, battery manufacturing materials and vehicle energy efficiency to reduce CO₂ emissions in electric mobility. A similar study was conducted in Poland [2], where CO₂ emissions were also analysed from vehicles using fossil fuels and EVs. It has been concluded that introducing EVs in regions that rely on non-renewable sources of electricity, like coal, leads to higher CO₂ emissions than in regions that use renewable energy sources for electricity production. The usage of renewable energy sources does not contribute to additional CO₂ emissions. The use of batteries for EVs and their impact on the environment is shown in the example given in the research [3], where it is stated that the production and application of batteries also significantly impact the environment. In particular, the materials used in batteries are harmful to human health and the environment. The research focused on two types of batteries: LiFePO₄ batteries and Li(NiCoMn)O₂. The results show that LiFePO₄ batteries are more environmentally friendly in the production phase, while Li(NiCoMn)O₂ batteries are more environmentally friendly in the exploitation phase. Despite this, from a life cycle perspective, LiFePO₄ batteries are generally more environmentally friendly than Li(NiCoMn)O₂ batteries. Another research assesses various methods of recycling waste lithium-ion batteries, employing a multi-criteria decision-making approach. The study concludes that direct recycling exhibits advantages, particularly in environmental impact and technical, economic, and social aspects, despite its reliance on specific cathode materials [4]. Direct recycling aims to recover the cathode material without any chemical change in the structure of the recovered material and to produce new batteries by renewing them. The study [5] delves into diverse battery technologies for electric vehicles (EVs) and hybrid electric vehicles (HEVs). It highlights their benefits and drawbacks,

focusing on aspects like energy density, costs, efficiency, and temperature range. The conclusion underscores the significance of EVs and HEVs in reducing noise, fossil fuel consumption, and environmental pollution in transport. However, it emphasizes the importance of advancing battery technology, which is crucial in determining vehicle range and performance, and acknowledges the high cost of batteries as a key challenge. The studies mentioned above [1–5] agree that EVs can have a lower pollution level than the vehicles using fossil fuels but that the source of electricity largely influences this. According to these studies, pollution reduction is achieved only when the sources of electricity are decarbonised. In the study given in [6], the authors consider that recent studies that have questioned whether driving EVs emit less greenhouse gases or whether we should wait for further decarbonization of electricity have several shortcomings. According to them, proper calculations show that EVs already emit less than half of the greenhouse gases than those using fossil fuels. Speculating on a future where production and driving are done using renewable energy results in at least ten times fewer emissions than vehicles using fossil fuels. This study lists six biggest mistakes in studies that claim EVs have greenhouse gas emissions similar to vehicles using fossil fuels. However, one gets the impression that the researchers in the study mentioned above [6] focused on geographical areas where significant progress has already been made in the decarbonization of electricity, which means that they relied on electrical grids with a high share of renewable energy sources. It is important to note that it cannot be concluded that this study considered areas where coal is still the dominant source of electricity. For this reason, the results of this study should be taken with a certain amount of caution. It is important to note that findings cannot be applied to regions or countries where coal is still intensively used to generate electricity. More research and analysis are necessary for a complete understanding of the impact of EVs on greenhouse gas emissions in all contexts. Research in the study [7] examined EV emissions across leading G20 countries, focusing on their electricity generation sources. France and Canada are highlighted as environmentally friendly due to their reliance on low-emission energy sources like nuclear and hydropower. In contrast, nations like Saudi Arabia and South Africa exhibited higher emissions owing to their reliance on oil and coal. The research emphasized the significance of cleaner energy sources to curb vehicle emissions without delving into specific pollutants. Research [8] focuses on analysing the economic aspects of electric roads compared to battery-powered EVs, particularly investigating their ability to reduce costs and CO₂ emissions. By exploring various scenarios involving electric roads and vehicles, the study confirms that implementing electric roads can significantly decrease costs, lower CO₂ emissions, and reduce the reliance on large batteries in EVs. The conclusions emphasize the potential of electric roads to create an unlimited range for EVs, contributing to reducing emissions and costs in road transport and positioning them as a pivotal element for sustainable transportation electrification. Similar

research conducted in Türkiye [9] focused on analysing the daily electricity demand in transportation by implementing electric roads. The aim was to explore the variation in daily electricity demand in transportation on eight busiest roads connecting seven major cities in Türkiye and to estimate the impact of electric roads on CO₂ emissions in the road transport sector. The study's results highlight a significant increase of 3.7% in the daily electricity demand on the observed roads with complete electrification of existing traffic. However, if all roads in the country were converted into electric roads with full vehicle conversion, that increase would rise by as much as 100%. Furthermore, applying electric roads on high-traffic routes could reduce CO₂ emissions from the road transport sector by an impressive 18.8 million tons. This research lays the groundwork for further assessments of the sustainability and practicality of developing electric roads in Türkiye. It emphasizes the potential of electric roads to reduce CO₂ emissions but also underscores the complexity of challenges associated with developing electromobility on highways. It sets guidelines for future research and evaluations of the justification for implementing this technology in Türkiye transportation. Similar research to ones in [8, 9] can be found in [10].

The increase in the number of EVs will affect the emissions and the load on the power grid. The research [11] focused on the impact of EVs on the power grid and the required infrastructure for charging stations. Analyses revealed significant loads on transformers and lines during vehicle charging, emphasizing the need for long-term solutions due to the expected increase in EVs. Similar research was conducted in [12], concluding that EVs are a significant addition to the power grid, necessitating comprehensive research into their impact. By modelling EV charging behaviour and validating it with real data, the study establishes a foundation for analysing grid sufficiency, network quality, and how EVs as a new load will affect them. Research in [13] investigates the adverse effects of electric vehicle charging stations on the power grid. It proposes integrating solar power plants to mitigate these impacts, enhancing grid efficiency and quality. Careful planning of this integration is crucial in supporting sustainable energy practices.

Taking into consideration the existing literature review, this paper contributes to the field in the following areas: (I) Analysis of the impact of different energy sources in Bosnia and Herzegovina on CO₂ emissions from EVs, providing localized insights into the influence of energy sources on CO₂ emissions from EVs. (II) Identifying factors influencing CO₂ emissions from EVs, specifically highlighting the significance of energy sources in reducing CO₂ emissions in electromobility. (III) Analysis of energy consumption and CO₂ emissions from EVs in the Federation of Bosnia and Herzegovina and Sarajevo, ensuring a localized understanding of the impact of EVs on energy and CO₂ emissions in the domestic context. Additionally, the contributions made in this paper can be extended to other regions with diverse energy sources, offering a framework for evaluating the influence of varied energy mix on CO₂ emissions from EVs.

The paper is structured as follows: in Chapter 1, an introduction to the motivation of the research, an overview of current research, and the contribution of this paper to the existing literature are given. Chapter 2 analyses the state of energy sources in 2021. For electricity production in the world, the EU and Bosnia and Herzegovina. The share of different energy sources in electricity production is analysed, and trends and plans for the future are presented. Also, the difference in the use of renewable energy sources between the EU, where significant progress is being made, and Bosnia and Herzegovina, where a dominant share of non-renewable sources is still present, is highlighted. In Chapter 3, an analysis of passenger vehicles in the Federation of BiH and taxi vehicles in Sarajevo for the year 2021 was conducted. Based on these data, the emissions of passenger and taxi vehicles were calculated with special emphasis on CO₂. After that, a hypothetical replacement of the aforementioned vehicles with electric ones was carried out. Finally, the required amount of electricity was calculated and the CO₂ emission analysis of EVs was performed, considering Bosnia and Herzegovina's energy mix. Finally, in Chapter 4, concluding considerations are presented, limitations of this research are highlighted, and recommendations for future research are given. It is important to note that the analysis of energy sources and the calculation of emissions were carried out based on data from 2021 because we had a database of vehicles from the Federation of Bosnia and Herzegovina for 2021 at our disposal.

The Current State and Perspectives of Energy Sources in the World, the European Union and Bosnia and Herzegovina

This chapter will analyse the current state and perspectives of energy sources worldwide in the European Union and Bosnia and Herzegovina. The goal is to provide more specific information about the share of different sources of electricity, trends, and plans for the future.

Current State of Energy Sources

According to available data for 2021 [14], fossil fuels have the largest share of global electricity production, accounting for about 61.4% of total production. Coal is still a dominant source in many parts of the world, although its share is gradually decreasing due to the faster growth of renewable energy sources.

Renewable energy sources, such as solar, wind, and hydropower, have significantly increased their share and currently account for around 25.1% of the total electricity production in the world. Solar energy has greatly increased in the last decade, with the continuous decline in solar panel prices and incentive policies. Nuclear power is also seeing strong growth, especially in Europe and China. Nuclear energy accounts for about 9.8% of the global electricity production. Nuclear power plants are a significant energy source in some countries, such as France and Japan, but they face challenges and issues of safety and nuclear waste management. Figure 1 shows the share of individual sources of electricity in the total world production for the year 2021 [14].

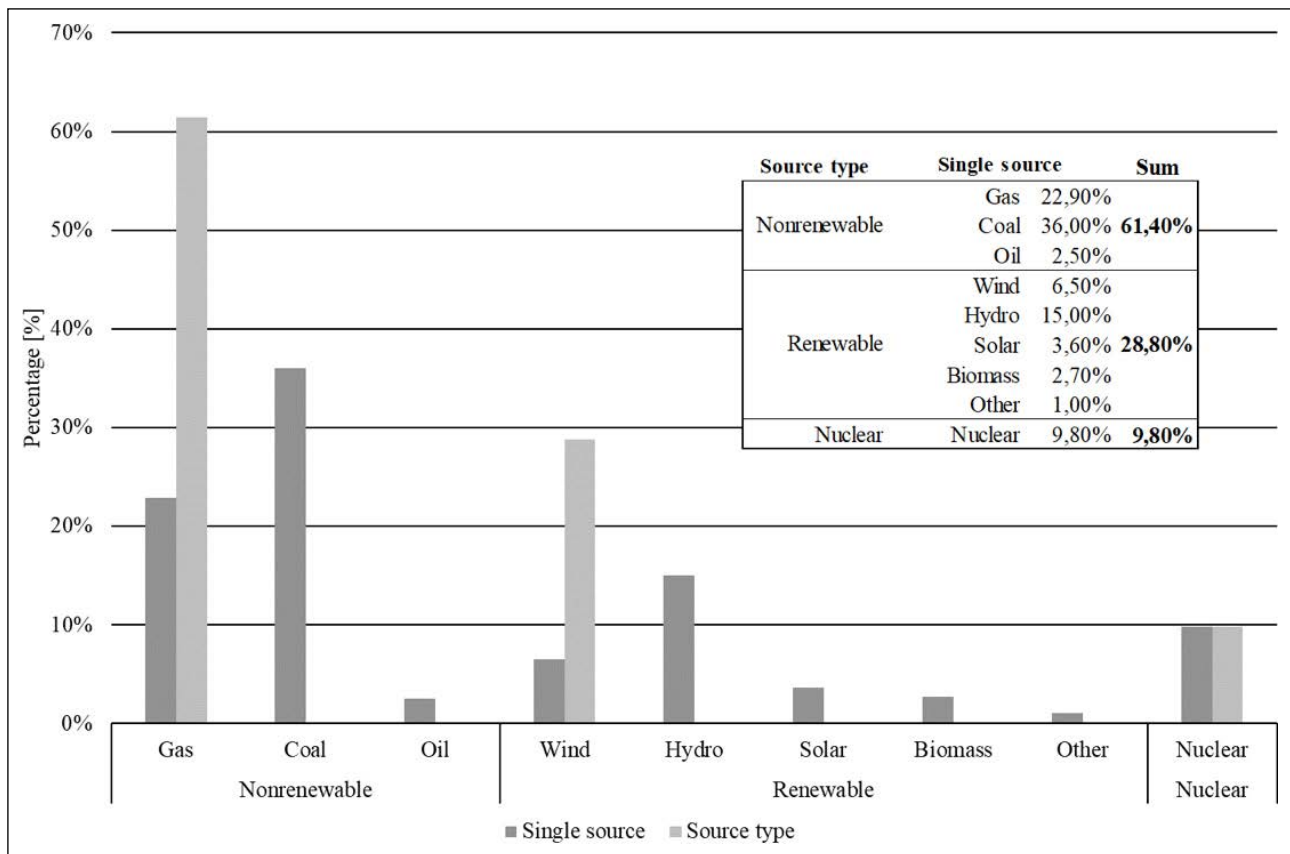


Figure 1. The share of individual sources of electricity in the total production in the world for the year 2021 [14].

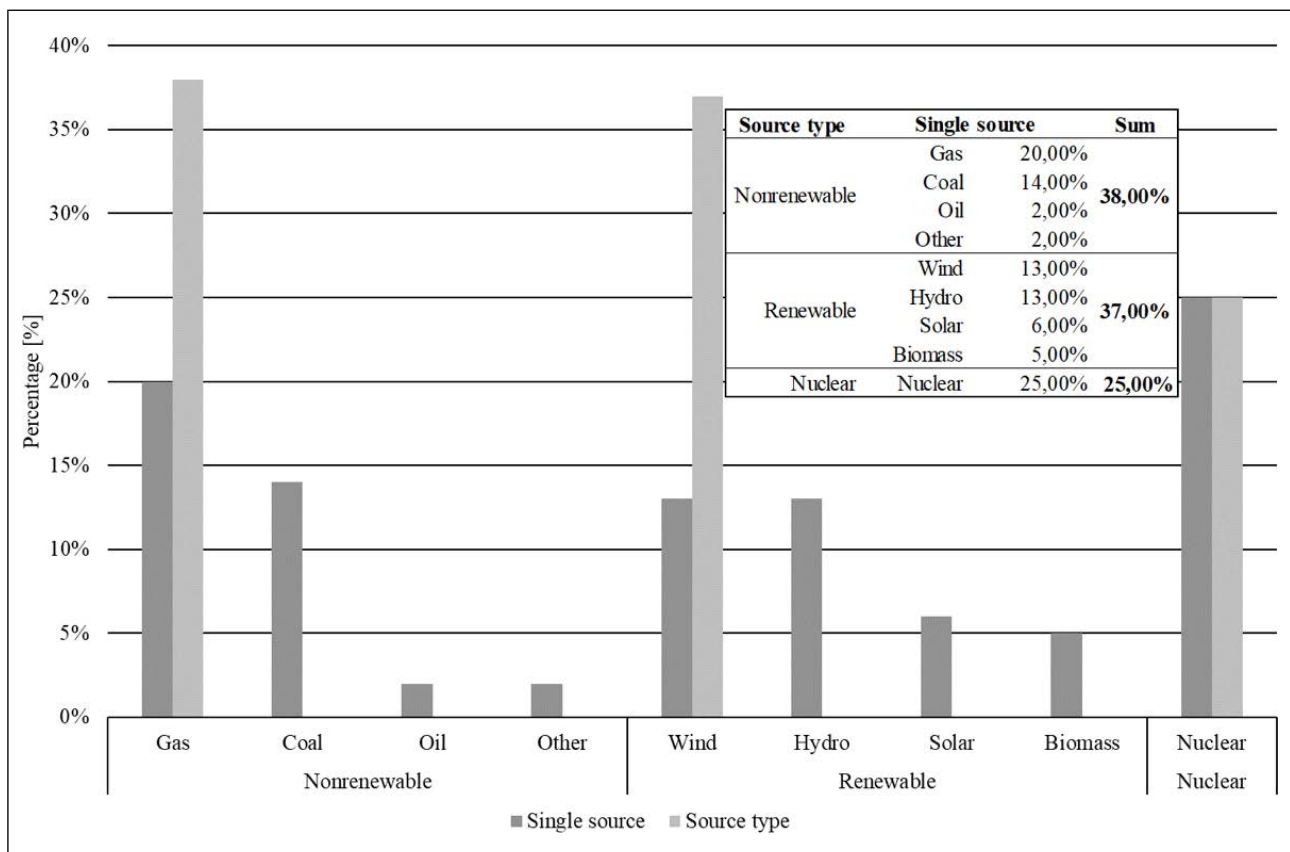


Figure 2. The participation of individual sources of electricity in the total production in the European Union for the year 2021 [15].

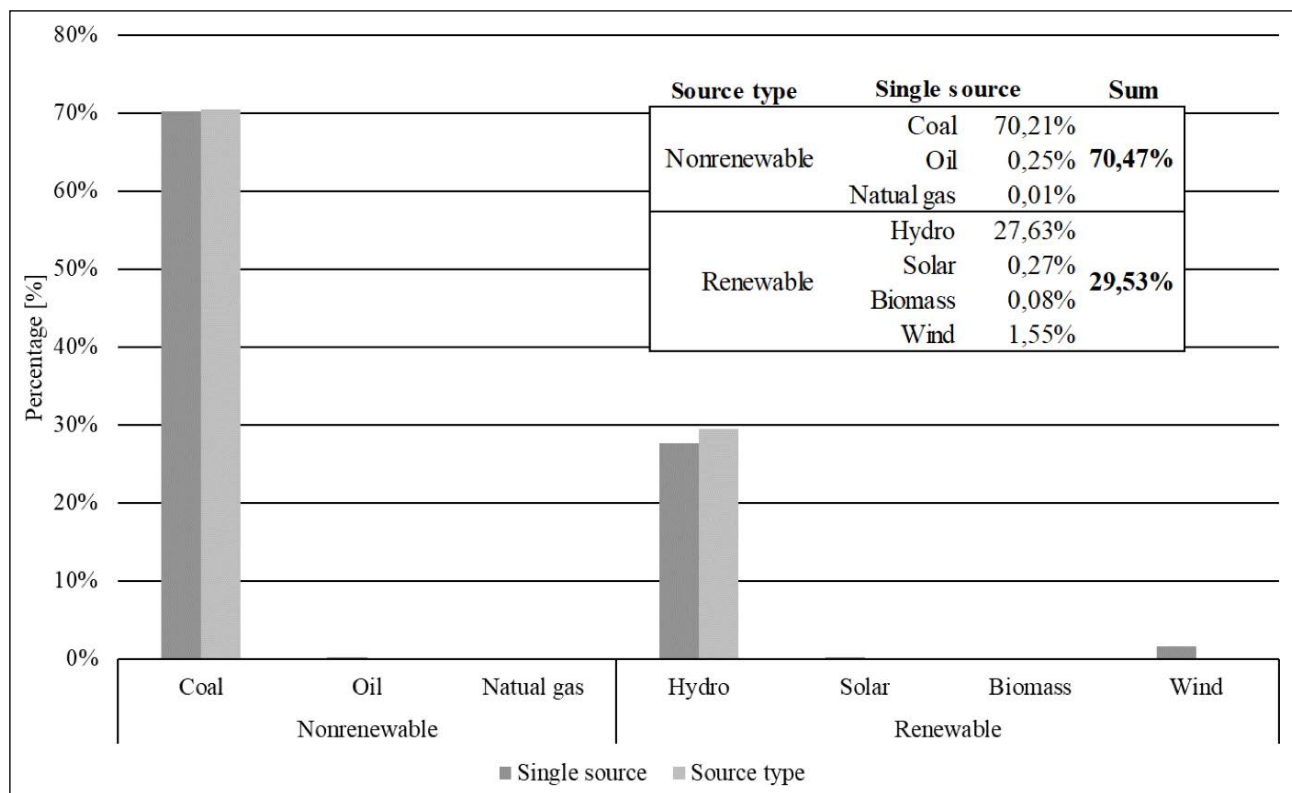


Figure 3. The participation of individual sources of electricity in the total production in Bosnia and Herzegovina for the year 2021 [16].

The European Union is one of the leading regions in the global transition towards sustainable electricity production. According to available data for 2021, the share of renewable energy sources in the total electricity production in the European Union was 38%, non-renewable 37% and nuclear 25% [6]. Countries such as Germany, Sweden, Denmark and Portugal are leading the way in using renewable energy sources, especially wind and solar. Germany is one of the world’s leading producers of solar panels, while Denmark and Sweden have a significant share in electricity production with wind power. In the European Union, there is also a trend of gradual abandonment of nuclear energy in some countries, such as Germany.

Figure 2 shows the participation of individual sources of electricity in the total production in the European Union for the year 2021 [15].

According to data from the International Energy Agency for the year 2021, the energy sector in Bosnia and Herzegovina is characterised by a diversity of energy sources. Coal takes the largest share in electricity production and accounts for about 70% of the total production. Bosnia and Herzegovina has a significant potential for the development of hydro-power, whose participation in the production of electricity amounts to about 27%. However, other renewable energy sources, such as solar and wind, are still limited. Solar energy accounts for only 0.27% of total production, while biomass and wind account for 1.63%. Figure 3 shows the participation of individual sources in the production of electricity in Bosnia and Herzegovina for the year 2021 [16].

Based on the data presented, it can be concluded that in the European Union in 2021, significant participation of renewable energy sources in electricity production is noticeable, while in Bosnia and Herzegovina, non-renewable sources still prevail. These data indicate a global transition towards sustainable electricity production, especially in the European Union, where significant progress is made in using renewable energy sources. However, in Bosnia and Herzegovina, there is a need for further development of renewable energy sources to reduce the share of non-renewable sources and greenhouse gas emissions. In the future, further plans and initiatives are expected to improve the energy sector in the world, Europe and Bosnia and Herzegovina to increase the share of renewable energy sources and reduce greenhouse gas pollution.

Plans for Electricity Decarbonisation

Plans and goals in the world and Europe aim to reduce greenhouse gas emissions by transitioning to renewable energy sources for electricity production. This transition aims to combat climate change and create a sustainable energy sector.

There is a growing awareness of the importance of transitioning to renewable energy sources to reduce dependence on fossil fuels and greenhouse gas emissions. Many countries have adopted ambitious plans and targets for electricity decarbonisation. These plans include increasing the share of renewable energy sources, such as solar, wind, hydro, geothermal, and tidal energy.

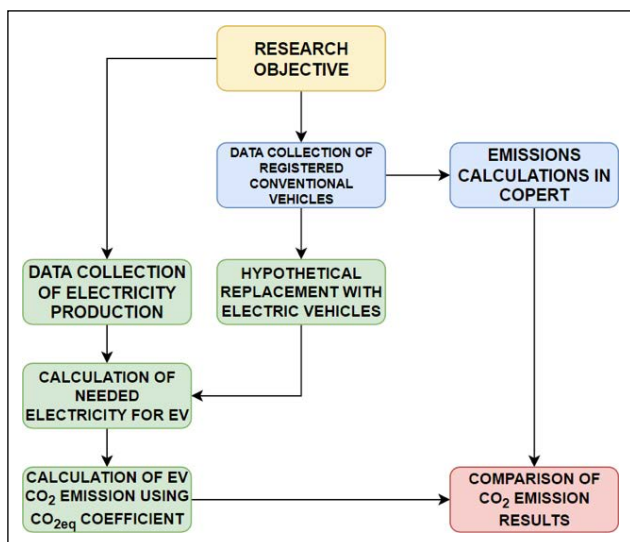


Figure 4. Methodology flowchart.

In Europe, the European Union is a leader in this area. One of the critical plans is the European Green Deal, which aims to achieve climate neutrality by 2050 [17]. As part of that plan, the European Union has set targets to reduce greenhouse gas emissions by at least 55% by 2030. This includes the goal for renewable energy sources to make up at least 32% of energy consumption in Europe by 2030.

Bosnia and Herzegovina also has the potential to develop renewable energy sources and reduce greenhouse gas emissions in the electricity sector. Plans for decarbonisation in Bosnia and Herzegovina include increasing the share of renewable energy sources, mainly hydropower, solar, and wind power plants. These plans aim to reduce dependence on fossil fuels, such as coal, and create a sustainable and clean energy sector.

To achieve these plans, it is crucial to invest in the infrastructure for renewable energy sources, encourage research and development of new technologies, and adopt incentive policies and measures to support the transition to renewable energy sources.

It is important to point out that Bosnia and Herzegovina has adopted the Framework Energy Strategy of Bosnia and Herzegovina until 2035 [18], which aims to increase the share of renewable energy sources and improve energy efficiency. To achieve these goals, further development of renewable energy sources in the country is expected.

All these measures aim to create a sustainable energy sector that will contribute to reducing greenhouse gas emissions, promoting environmental protection, and fighting against climate change.

To show the impact of the current situation in Bosnia and Herzegovina from the point of view of the source of electricity, modelling and comparison of the emissions of vehicles using fossil fuels and EVs will be carried out below.

Table 1. Vehicle fleet in the Federation of Bosnia and Herzegovina for 2021 [20]

Vehicle category	Quantity	Share
Motorcycles	9,669	1.45%
Passenger vehicles	576,450	86.65%
Busses	2,645	0.40%
Trucks, vans and lorries	54,694	8.22%
Trailers	17,793	2.67%
Tractors	2,854	0.43%
Others	1,120	0.17%
Total	665,225	100%

Electric Vehicles’ Impact on Energy and CO₂ in Bosnia and Herzegovina

To analyse the impact of the introduction of electric vehicles on energy consumption and CO₂ emissions in the current conditions of electricity production in Bosnia and Herzegovina, an analysis of vehicles registered in the Federation of Bosnia and Herzegovina (FBiH) and Sarajevo will be conducted, with a particular emphasis on passenger vehicles. Also, the vehicle fleet in Sarajevo will be analysed. Still, only taxi vehicles will be singled out for the calculation to gain insight into their impact on electricity consumption and CO₂ emissions.

To model the emission of polluting substances, the Copert program was used, which enables a detailed analysis of vehicle emissions based on vehicle characteristics and driving conditions. The methodology of emission calculations using the Copert program is given in the EMEP/EEA air pollutant emission inventory guidebook 2023 [19].

Given that the goal is to explore the impact of the transition to EVs, in further calculation, all vehicles in FBiH will be hypothetically replaced with EVs of appropriate characteristics and battery capacity. Then, using the data on electricity production in the FBiH, the CO₂ emissions resulting from that transition will be calculated. A similar calculation will be performed on the example of taxi vehicles in Sarajevo.

After that, the results obtained from the CO₂ emission analysis for conventional and electric vehicles will be compared. The flowchart of the research methodology is shown in Figure 4.

It is essential to note that although vehicles using fossil fuels also emit components such as CO, NO_x, HC, and soot particles in their exhaust gases, these components are not included in this analysis. This is due to their small presence in exhaust gases, which makes them local rather than global parameters. As technology advances, these components are increasingly removed from exhaust gases, highlighting CO₂ as a major global challenge and still the most critical factor. Even vehicle manufacturers, when describing the technical characteristics of their vehicles, emphasise only CO₂ as a crucial parameter.

Table 2. Emission standards by fuel type [20]

Fuel	Emission standard (ES)							NO ES
	Conventional	Euro 1	Euro 2	Euro 3	Euro 4	Euro 5	Euro 6	
Gasoline	9,309	2,708	13,394	41,146	18,406	14,765	13,082	
Gasoline/LPG	741	399	1,285	5,497	2,938	1,610	631	
Diesel	31,608	9,475	20,983	151,778	109,344	83,025	44,264	
Diesel/CNG	0	0	0	3	3	3	0	
Electro								53
Total	41,658	12,582	35,662	198,424	130,691	99,403	57,977	53
Total M1 category	576,450							

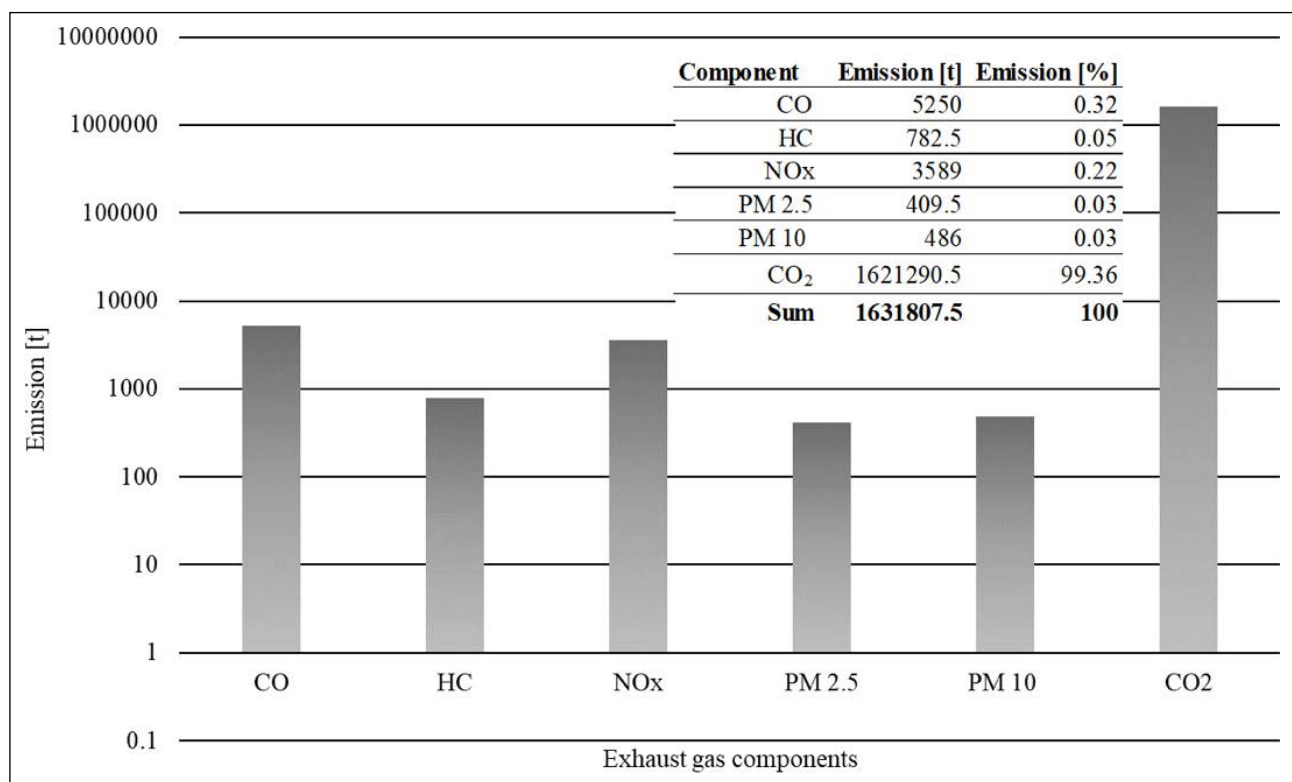


Figure 5. The results of exhaust gas emissions modelling of passenger vehicles in FBiH.

Modelling of Passenger Vehicle Emissions in the Federation of Bosnia and Herzegovina

To provide an insight into the state of the vehicle fleet in the Federation of Bosnia and Herzegovina, the database [20] of technical inspections of vehicles for the year 2021 was used. The Federal Ministry of Transport and Communications obtained the database officially, and the data set did not use any personal data of vehicle owners, only the technical characteristics of the vehicles. Table 1 shows the condition of the vehicle fleet in the Federation of Bosnia and Herzegovina for 2021 [20].

Table 2 provides an overview of the passenger vehicles' emission standards according to the type of fuel [20].

The Copert program was used to calculate the emissions of passenger motor vehicles from Table 1. Detailed data on the number of vehicles according to eco characteristics, type,

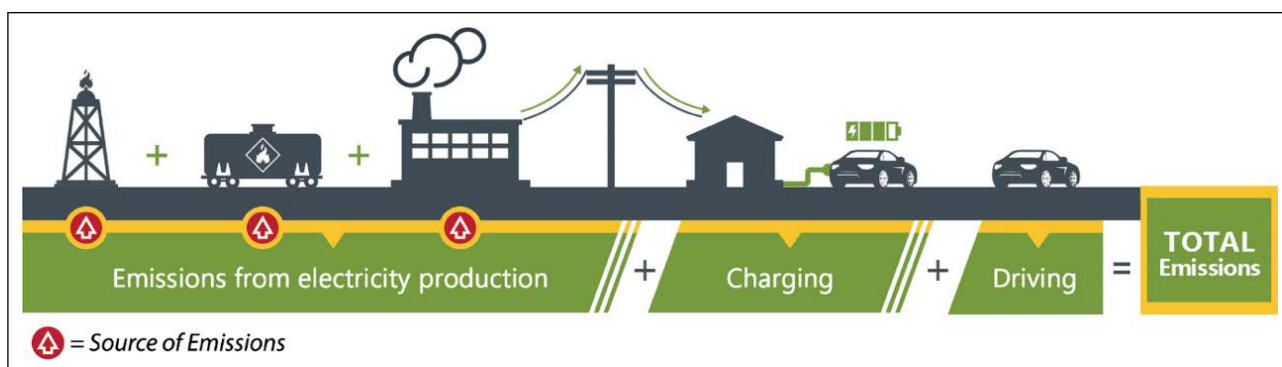
and engine volume was determined from the database of vehicle technical inspections for 2021 [20]. Data for the fuel consumed in 2021 were obtained based on data from the Federal Ministry of Trade for 2021 [21], while climatological data were taken from the Meteorological Yearbook for 2021 published by the Federal Hydrometeorological Institute [22].

Figure 5 shows the results of the modelling of exhaust gas emissions of passenger vehicles using fossil fuels.

The components of exhaust gases from Figure 5 are given in tons and displayed on a logarithmic scale. The reason for this is the largest CO₂ emission, which is significantly higher than other components of exhaust gases, typically considered polluting. The ratio of polluting components (CO, HC, NO_x, PM) to the amount of CO₂ is expected because these components occupy a very small percentage of exhaust gases in modern vehicles using fossil fuels.

Table 3. Electric vehicles that would replace the fleet in the Federation of Bosnia and Herzegovina

Vehicle class	Curb mass [kg]	Battery capacity [kWh]	Range [km]	Consumption of the el. energy [kWh/100 km]	Number of vehicles	Average annual mileage [km/yr]	El. energy consumption [kWh]	CO ₂ eq emission [t]
A	<1,100	17.7	151	11.67	202,347	20,000	472,277,898	354,208
B	1,101–1,500	24.4	177	13.71	256,063	20,000	702,124,746	526,594
C	1,501–1,750	42.1	281	14.98	86,234	20,000	258,357,064	193,768
D	≥1,751	59.9	357	16.77	31,753	20,000	106,499,562	79,875
				Total	576,397		1,539,259,270	1,154,444

**Figure 6.** The emission mechanism of EVs due to the source of electricity [24].

To compare the exhaust gas emissions of conventional passenger vehicles given in Table 1 with EVs, a hypothetical assumption is made that the complete fleet of passenger vehicles from Table 1 is replaced with EVs of similar characteristics. Table 3 shows the proposal to replace the fleet with EVs. EVs are divided into four groups based on the weight of the empty vehicle, according to recommendations from [1].

Table 3 also shows the calculation of the required electricity based on data on the number of vehicles and characteristics of electricity consumption. By multiplying the number of vehicles by the electricity consumption per vehicle and the average annual mileage, the total electricity consumption for certain categories of vehicles is obtained.

Also shown is the calculation of CO₂ emissions of EVs due to the type of energy source used to power those vehicles. The analysis was made so that the electric energy consumption of the vehicle given in Table 3 is multiplied by the CO₂eq given by the electricity producer in Bosnia and Herzegovina, which is 0.75 kg/kWh [23]. This equivalent contains all the pollutants that are formed during the production of electricity. The calculation shows that, in such a case, the annual CO₂ emission due to the power supply of EVs would amount to an additional 1,154,444 tons of CO₂. Although EVs locally do not directly impact the environment because they do not emit exhaust gases like vehicles using fossil fuels due to the type of source for producing electricity, EVs can also significantly contribute to CO₂ emissions. The emission mechanism of EVs due to the source of electricity is shown in Figure 6.

According to the calculation from Table 3, the required amount of electricity to power these vehicles annually is slightly more than 1,539 GWh (Gigawatt hour) of electricity. The current electricity production in Bosnia and Herzegovina is about 17,000 GWh, and consumption, according to official data in Bosnia and Herzegovina [25], is about 12,000 GWh of electricity. To conclude, the required electricity to power EVs would have to be provided from the difference sold to third parties or produced additionally, which would increase the amount of CO₂ shown in the calculation in Table 3.

In the following, the modelling of taxi vehicle emissions in Sarajevo will be analysed to gain better insight and more realistic possibilities of replacing them with EVs in the future.

Modelling Taxi Vehicle Emissions in the City of Sarajevo

Using the methodology from the previous chapter, an analysis of the fleet of taxi vehicles in the city of Sarajevo for the year 2021 was performed. Based on that data, these vehicles' exhaust gas emissions were analysed using the Copert program. Data on Sarajevo's fuel consumption and climatological conditions were taken from [21] and [22]. Table 4 shows the analysis of the taxi fleet in Sarajevo.

Using the data from Table 4 [20] and other input data in the Copert program, an analysis of the vehicle's exhaust gas emissions from Table 4 was performed. Figure 7 shows the result of the calculation. As in the previous example, the base ten logarithmic scale distribution was used here to display the results.

Table 4. Emission standards by fuel type for the taxi vehicles in Sarajevo [20]

Fuel	Emission standard (ES)							
	Conventional	Euro 1	Euro 2	Euro 3	Euro 4	Euro 5	Euro 6	NO ES
Gasoline	0	0	0	0	2	7	4	0
Gasoline/LPG	0	0	1	6	29	42	23	0
Diesel	0	0	4	87	230	324	194	0
Diesel/CNG	0	0	0	0	0	0	0	0
Electro	0	0	0	0	0	0	0	0
Total	0	0	5	93	261	373	221	0
Total taxi vehicles	953							

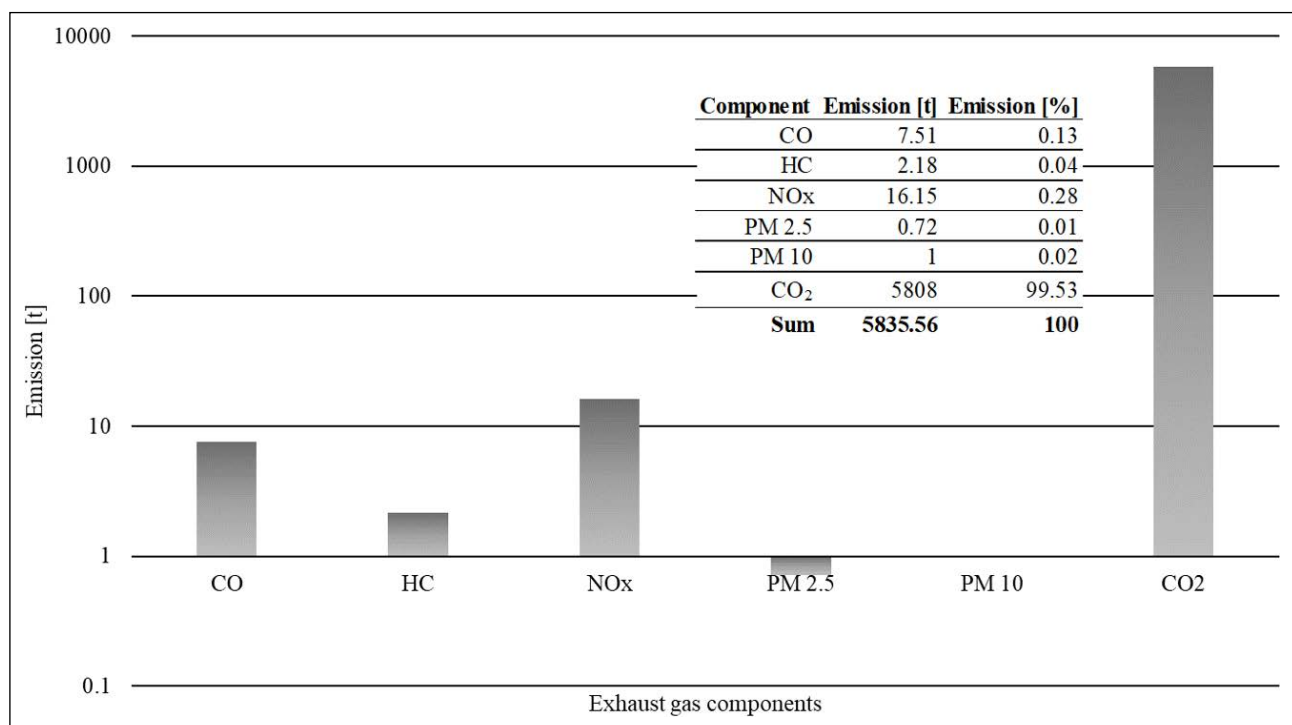


Figure 7. The results of modelling of exhaust gas emissions of taxi vehicles in Sarajevo.

Table 5. EVs that would replace the taxi fleet in Sarajevo

Vehicle class	Curb mass [kg]	Battery capacity [kWh]	Range [km]	Consumption of the el. energy [kWh/100 km]	Number of vehicles	Average annual mileage [km/yr]	El. energy consumption [kWh]	CO ₂ eq emission [t]
A	< 1,100	17.7	151	11.67	5	30,000	17,505	13
B	1,101-1,500	24.4	177	13.71	412	30,000	1,694,556	1,271
C	1,501-1,750	42.1	281	14.98	525	30,000	2,359,350	1,770
D	≥1,751	59.9	357	16.77	11	30,000	55,341	42
Total					953		4,126,752	3,095

The next step is, as in the previous section, the analysis of emissions when all engine-powered vehicles are replaced with equivalent EVs. For this purpose, the criterion is again used according to the recommendations from the literature [1], that vehicles using fossil fuels are assumed to be replaced with EVs. Table 5 shows a suggested pro-

posal to replace the taxi fleet in Sarajevo with EVs, according to the established criteria.

Table 5 also shows the results of the calculation of the required electrical energy and the CO₂ emissions that would be achieved by consuming that amount of electricity. Accord-

ing to the data of Public Enterprise Electric Utility of Bosnia and Herzegovina for Sarajevo, the total amount of electricity consumed in 2021 was 1,309 GWh [26]. The required electrical energy to power EV taxi fleet of Sarajevo would be 4.12 GWh, which is negligible compared to the actual consumption and distribution to current consumers in Sarajevo.

When looking at the CO₂ emissions given in Table 5 due to electricity consumption to power EV taxi fleet, a 47% reduction is noticeable compared to the CO₂ emissions emitted by taxis with vehicles using fossil fuels. It is also important to note that in the calculation of taxi vehicles example in Sarajevo, vehicles were assumed to travel an average of 30,000 km per year, but when modelling the emissions of the vehicle fleet in the Federation of Bosnia and Herzegovina, an annual average of 20,000 km was taken.

CONCLUSIONS

This paper aimed to analyse the influence of energy sources on the emission of EVs in Bosnia and Herzegovina. Based on the available data, it has been shown that in Bosnia and Herzegovina, non-renewable sources are still used in a higher percentage to produce electricity, which results in a high coefficient of CO₂ emissions during electricity production.

To model the emission of vehicles using fossil fuels an analysis of the fleet of passenger vehicles in the Federation of Bosnia and Herzegovina was carried out. The study was performed using the Copert program. After that, the existing vehicle fleet was hypothetically replaced with EVs according to criteria from the literature. The CO₂ emission of EVs, which results from the electricity production that would power these vehicles, was calculated next. The adopted parameter used to compare emissions was CO₂, as the component that is most prevalent in the exhaust gases of vehicles using fossil fuels and globally has the most significant impact on the environment and climate. The results of vehicle CO₂ emissions for the year 2021 showed that vehicles using fossil fuels have an emission of 1.6 million tons of CO₂. In comparison, CO₂ emissions from electric vehicles would amount to 1.15 million tons. From this result, it can be concluded that the source from which the electrical energy is obtained is essential and that the emissions of EVs cannot be taken as zero. Although it is an indirect emission, it is still present and poses a significant global environmental problem. As for the required electricity to power EVs, it is calculated that the required amount would be 1,539 GWh per year. This means that the current resources from which the electricity is produced would have to be increased, or part of the electricity sold to third parties would have to be taken.

A similar analysis was carried out on the example of Sarajevo, where the fleet of taxi vehicles transporting passengers was analysed. As for the CO₂ emission, a very similar ratio was calculated as in the previous example, while the required electrical energy is significantly below the actual consumption that Sarajevo consumes annually.

It should be noted here that although in vehicles using fossil fuels, there are components in the exhaust gases such as

CO, NO_x, HC, soot particles, etc. they were not considered here because these components are minimally represented in exhaust gases. Also, they are a local and not a global parameter. Furthermore, with the advancement of technology, these components are more and more efficiently removed from exhaust gases every day, so the CO₂ parameter is still the most significant global problem.

It is essential to point out that the emissions and pollution from EVs, in addition to the source of energy that powers them, are also affected by the production process of EVs and their components, primarily batteries, as well as their subsequent disposal after use. This parameter was not considered here, which leads to the conclusion that EV emissions and pollution are even higher than calculated. This is certainly a motivation for further research and deepening of this topic.

Based on the shown examples of fleet analysis, realistically, the example of taxi vehicles could take place, with the added fact that a grid of charging stations for these vehicles would have to be developed, which was not considered here.

In the end, it can be concluded, based on the conducted analysis, that in the conditions of the current energy situation in Bosnia and Herzegovina, where about 70% of electricity is produced from non-renewable sources and where there is a minimal representation of solar and wind power plants, it is still not possible to consider EVs as vehicles with zero emissions. In the future, if energy strategies are adopted and the transition to clean sources for electricity production is made, we should expect a lower CO₂ coefficient due to the production of electricity from clean sources and, thus, a reduction in indirect pollution by EVs.

DATA AVAILABILITY STATEMENT

The authors confirm that the data that supports the findings of this study are available within the article. Raw data that support the finding of this study are available from the corresponding author, upon reasonable request.

CONFLICT OF INTEREST

The authors declared no potential conflicts of interest with respect to the research, authorship, and/or publication of this article.

USE OF AI FOR WRITING ASSISTANCE

Authors declare no use of AI for writing assistance.

ETHICS

There are no ethical issues with the publication of this manuscript.

REFERENCES

- [1] Y. Li, N. Ha, and T. Li, "Research on carbon emissions of electric vehicles throughout the life cycle assessment taking into vehicle weight and grid mix composition," *Energies*, Vol. 12(19), Article 3612, 2019. [CrossRef]
- [2] P. Albrechtowicz, "Electric vehicle impact on the en-

- vironment in terms of the electric energy source — Case study,” *Energy Reports*, Vol. 9, pp. 3813–3821, 2023. [CrossRef]
- [3] X. Shu, Y. Guo, W. Yang, K. Wei, and G. Zhu, “Life-cycle assessment of the environmental impact of the batteries used in pure electric passenger cars,” *Energy Reports*, Vol. 7, pp. 2302–2315, 2021. [CrossRef]
- [4] M. Öztürk, E. Evin, A. Özkan, and M. Banar, “Comparison of waste lithium-ion batteries recycling methods by different decision making techniques,” *Environmental Research and Technology*, Vol. 6(3), pp. 226–241, 2023. [CrossRef]
- [5] Z. N. Kurtulmuş, and A. Karakaya, “Review of lithium-ion, fuel cell, sodium-beta, nickel-based and metal-air battery technologies used in electric vehicles,” *International Journal of Energy Applications and Technologies*, Vol. 10(2), pp. 103–113, 2023. [CrossRef]
- [6] A. Hoekstra, and M. Steinbuch, “Comparing the lifetime greenhouse gas emissions of electric cars with the emissions of cars using gasoline or diesel,” TU/e Eindhoven University of Technology, 2020.
- [7] A. Uğurlu, “A Benchmarking analysis on electric vehicle emissions of leading countries in electricity generation by energy sources,” *International Journal of Automotive Engineering and Technologies*, Vol. 12(4), pp. 165–171, 2023. [CrossRef]
- [8] H. H. Coban, A. Rehman, and A. Mohamed, “Analyzing the societal cost of electric roads compared to batteries and oil for all forms of road transport,” *Energies*, Vol. 15(5), Article 1925, 2022. [CrossRef]
- [9] H. H. Coban, and W. Lewicki, “Daily electricity demand assessment on the example of the Turkish road transport system – a case study of the development of electromobility on highways,” *Prace Komisji Geografii Komunikacji PTG*, Vol. 25(2), pp. 52–63, 2022. [CrossRef]
- [10] H. H. Coban, “Smart steps towards sustainable transportation: Profitability of electric road system,” *Balkan J Electric Comput Eng* Vol. 11(1), pp. 88–99, 2023. [CrossRef]
- [11] D. Yıldızhan, A. K. Erenoğlu, and O. Erdiñç, “Elektrikli araç entegrasyonunun dağıtım sistemine etkilerinin incelenmesi ve şarj istasyonu altyapısının tayin edilmesi,” *Mühendislik Bilimleri ve Tasarım Dergisi*, Vol. 10(4), pp. 1232–1242, 2022. [CrossRef]
- [12] N. Aslan, E. Kilic, and M. Şekkelı, “Modeling of electric vehicles as a load of the distribution grid,” *International Journal of Automotive Science and Technology*, Vol. 7(1), pp. 54–62, 2023. [CrossRef]
- [13] K. Olcay, and N. Çetinkaya, “Investigation of the effects of electric vehicle charging stations and solar energy integration on grid performance,” *Journal of Scientific Reports-A*, Vol. 055, pp. 206–219, 2023. [CrossRef]
- [14] World Energy Data, “World Electricity Generation,” Available at: <https://www.worldenergydata.org/world-electricity-generation/> Accessed on Dec 12, 2023.
- [15] Statista Inc., “Distribution of electricity production in the European Union in 2011 and 2021, by source,” Available at: <https://www.statista.com/statistics/620693/sources-of-power-generation-european-union/> Accessed on Dec 12, 2023.
- [16] International Energy Agency, “Electricity Information,” Available at: <https://www.iea.org/data-and-statistics/data-product/electricity-information> Accessed on Dec 12, 2023.
- [17] European Commission, “Delivering the European green deal,” Available at: https://commission.europa.eu/strategy-and-policy/priorities-2019-2024/european-green-deal/delivering-european-green-deal_en Accessed on Dec 12, 2023.
- [18] Ministry of Foreign Trade and Economic Relations of Bosnia and Herzegovina, “Framework Energy Strategy of Bosnia and Herzegovina by 2035,” Available at: http://www.mvteo.gov.ba/data/Home/Dokumenti/Energetika/Okvirna_energetska_strategija_Bosne_i_Hercegovine_do_2035_BIH_FINALNA.PDF Accessed on Dec 12, 2023.
- [19] European Environment Agency, “EMEP/EEA air pollutant emission inventory guidebook 2023,” Available at: https://www.emisia.com/wp-content/uploads/2023/09/1.A.3.b.i-iv-Road-transport-2023_Sep.pdf Accessed on Dec 12, 2023.
- [20] Database of registered vehicles in Federation of Bosnia and Herzegovina for 2021, Federal Ministry of Transport and Communications.
- [21] Federal Ministry of Trade, “Overview of Imports of Oil Derivatives in The Federation of BiH for The 2021,” Available at: <https://www.fmt.gov.ba/novosti/pregled-uvoza-n-d-u-federaciji-bih-za-period-i-%E2%80%93xii-mjeseca-2021-god.html> Accessed on Dec 12, 2023.
- [22] Federal Hydrometeorological Institute, “Meteorological Yearbook for 2021,” Available at: <https://www.fhmzbih.gov.ba/podaci/klima/godisnjak/G2021.pdf> Accessed on Dec 12, 2023.
- [23] Public Enterprise Electric Utility of Bosnia and Herzegovina, “Energy Efficiency,” Available at: <https://www.epbih.ba/stranica/energetska-efikasnost> Accessed on Dec 12, 2023.
- [24] U.S. Department of Energy, “Greenhouse Gas Emissions from Electric and Plug-In Hybrid Vehicles – Results,” Available at: <https://www.fueleconomy.gov/feg/Find.do?zipCode=94102&year=2016&vehicleId=37066&action=bt3> Accessed on Dec 12, 2023.
- [25] State Regulatory Commission for Electric Energy, “Report of The State Regulatory Commission for Electricity Work in 2021,” Available at: <https://www.derk.ba/DocumentsPDFs/DERK-Izvjestaj-o-radu-2021-b.pdf> Accessed on Dec 12, 2023.
- [26] Data was obtained through e-mail communication with the Public Enterprise Electric Utility of Bosnia and Herzegovina on 25.08.2023.



Research Article

Performance evaluation of a simple electrochemical treatment model for saline wastewaters: Part B

Ezekiel Oluwaseun FEHINTOLA¹, Enoch Adedayo ADEKUNBI¹, Babatunde Moses OJO¹,
John Olugbemiga AWOTUNDE¹, Isaiah Adesola OKE^{*2}

¹Department of Chemistry, Adeyemi Federal University of Education, Ondo, Nigeria

²Department of Civil Engineering, Obafemi Awolowo University, Osun, Nigeria

ARTICLE INFO

Article history

Received: 19 August 2023

Revised: 13 October 2023

Accepted: 14 February 2024

Key words:

Brine; Efficiency; Factors;
Factorial experiments;
Interactions electrochemical
treatment process

ABSTRACT

This paper investigated the performance of the electrochemical treatment technique in removing chloride from saline wastewater (brine) with the critical objective of purifying the wastewater, evaluated the efficacies of selected mathematical models and particular attention to selected polynomial regression models as a follow-up to previous studies. The saline wastewaters were prepared and subjected to electrochemical treatment using developed carbon–resin (anode) and aluminium (cathode) electrodes. Electrochemical treatment of the synthesised saline wastewaters (between 10×10^3 mg/l and 40×10^3 mg/l of chloride) was conducted on a laboratory scale. The influences of selected or picked-out operational factors on the functioning or efficacy of the electrochemical purification process of the wastewater were monitored using fractional factorial experiments. Three mathematical models were formulated using Microsoft Excel Solver and evaluated statistically. The study revealed that the current, the time and the interval distance between the electrodes were significant and vital factors that impacted on the performance of the electrochemical purification treatment of brine. The factors with negative special effects on the performance of the treatment process of brine were separation distance between the electrodes, pH, the depth of the electrode, the initial and primary concentration of the chloride and the flow and discharge rate of the wastewater. The performances or efficacy of the polynomial regression models in predicting the performance of the treatment technique were with average errors of 2.99%, 2.97% and 2.94% and accuracy of 97.01%, 97.03% and 97.06% for Models A, B and C, respectively. It was concluded that the electrochemical treatment of brine with carbon-resin electrodes is efficient in removing chloride from brine and the selected models predicted the performance of the treatment technique well.

Cite this article as: Fehintola EO, Adekunbi EA, Ojo BM, Awotunde JO, Oke IA. Performance evaluation of a simple electrochemical treatment model for saline wastewaters: Part B. Environ Res Tec 2024;7(2)160–174.

INTRODUCTION

The world is facing problems with different solutions in relation to the provision of potable water through water treatment techniques, which are meant at producing safe

water and protecting the environment [1]. Presently, a vital research focus is on the next-generation wastewater and water treatment techniques to solve global potable water shortage and pollution issues [2]. In the case of conventional water treatment techniques, their performances in

*Corresponding author.

*E-mail address: okeia@hotmail.com



removing emerging pollutants from aqueous are not dependable. These conventional water and wastewater treatment techniques are categorised as physical (screening, filtration, sedimentation, floatation, evaporation, distillation and aeration), chemical (coagulation, flocculation, precipitation, adsorption, chlorination), biological and advanced. In the present-day water treatment techniques for saline water and wastewater are membrane-based techniques, irradiation, electric-current-based techniques and a combination of two or more of these conventional techniques. Among these present-day water and wastewater treatment techniques, membrane and electric-current-based (electrochemical) techniques play a prevailing role in the worldwide market and engineering applications. In line with the comparative advantages of electric-current-based and membrane-based techniques of higher and dependable efficiency, higher energy utilization efficiency and lower footprint [2]. Among these two techniques (electric-current-based techniques and electric-current-based techniques), electric-current-based techniques have attracted wider attention [1] than membrane-based techniques, based on some limitations and disadvantages of membrane techniques [3]. In the last three decades, the electrochemical technique of treating water and wastewater has been suggested as a substitute process for the removal of contaminants in wastewater or effluents discharge into the environment. These electrochemical treatment techniques have shown reliable performance results in several matrices of polluted and contaminated wastewater such as herbicides and pesticides, textile dyes, dairy, pulp and paper, heavy metals, landfill leachate, aquaculture, pharmaceutical residues, and other industrial effluents or wastewaters [1]. In addition, a wide range and varieties of electrode substances and materials have been utilised and suggested in electrochemical treatment techniques. Some of the utilised and suggested electrodes (active, non-active or passive) are noble metals (silver, platinum, gold and graphite), dimensionally stable anodes, PbO₂ based, carbon or graphite-based anodes, and Boron Doped Diamond (BDD). These utilised and suggested electrodes have attained different removal and reduction efficacies of organic matter [1]. These non-active anodes, which include BDD, are beneficial for direct electrooxidation of organic material through hydroxyl radicals. The Dimensionally Stable Anode (DSA) another non-active electrode, which includes Ti and IrO₂ with Ta₂O₅, are active in enhancing hypochlorite-mediated chemistry in the presence of chloride ions. The anodic electrooxidation of brine created by petroleum exploration of the Petrobras plant in Brazil utilises an electrochemical reactor with electrode made of a Ti and RuO₂ with TiO₂ and SnO₂ was recently evaluated [1]. The evaluation was under the current density of 89 mA cm⁻² (galvanostatic conditions and situations). The study confirmed that the degradation of the organic pollutants at different discharge and flow rates (1.3, 0.8, 0.5 and 0.25 dm⁻³ h) attained the removal efficacies of 84%, 95%, 97% and 98%, respectively. Da Silva et al. [1] reported that the electrooxidation (electrochemical oxidation) of brine in galvanostatic situations and conditions utilising

platinum supported on titanium (Ti and Pt) and BDD anodes, in a batch reactor. The results showed that complete Chemical Oxygen Demand (COD) removal was achieved using BDD electrode. The study stated that the production of high amounts of hydroxyl radicals (OH⁻) and oxidizing species (Cl₂, HClO, ClO⁻) aided the performances. Utilization of these electrooxidation techniques and materials to create very strong oxidant materials and species (such as chlorine) has been anticipated due to the electrocatalytic characteristics of these treatment techniques and materials. Several studies have reported the treatment and remediation of petrochemicals and brine effluents in the literature. The other treatment techniques for the treatment of brine can be summarized as follows:

- a) Biological treatment techniques as indicated in Akyon et al. [4]; Baptista et al. [5]; Beneduce et al. [6]; Kargi and Dincer [7]; Zhang et al. [8] and Ziemkiewicz et al. [9],
- b) Electrochemical, electrocoagulation and other electric current techniques as documented in Soni et al. [10]; Madrona et al. [11]; Al-Raad et al. [12]; Al-Raad et al. [13] and Ayadi et al. [14]
- c) Photocatalysis as highlighted by Andreozzi et al. [15]; Feroz [16] and Ye [17];
- d) Soil remediation as indicated in Ekama et al. [18]; Estabragh et al. [19]; and Jiang et al. [20];
- e) Electromagnetization techniques as documented in Hachicha et al. [21];
- f) Chemical as highlighted by Jin et al. [22]; Kaith et al. [23]; Pfennig et al. [24]; and Shrivastava [25]; and
- g) The membrane as indicated in Zhang et al. [26]; Xu et al. [27] and Yue et al. [28].

More information and data on the treatment of brine wastewater and water are established in the literature and can be summarized as follows:

- a) Treatment using osmotic agent in water flux enhancement during osmotic membrane distillation (OMD) for treatment of highly saline brines osmotic agent in water flux enhancement during osmotic membrane distillation (OMD) for treatment of highly saline brines and a microbial desalination cell for sustainable wastewater treatment and saline water desalination, in Zhang et al. [8], and Zhang et al. [26];
- b) Treatment using Carbide coated tools in Yusof et al. [29]; Adsorption techniques in Aber and Sheydari [30];
- c) Treatment of the Brine Generated from Reverse Osmosis Advanced Membrane Wastewater Treatment Plant Using Epuvalisation System. Qurie et al. [31];
- d) Electrochemical Catalytic Oxidation Treatment of Coking Wastewater RO Brine in Wang et al. [32];
- e) Innovative Application of Water Quality and Flow Modeling to Design a Softening, UF/RO and Brine Handling System for Copper and Gold Mining Wastewater Treatment in the Peruvian Andes in Burbano et al. [33];

treatment of meat industry wastewater using electrochemical treatment method in Thirugnansanhanghan et al. [34];

- f) Bioelectrochemical treatment of table olive brine processing wastewater for biogas production and phenolic compounds removal in Marone et al. [35];
- g) Treatment of a hypersaline brine, extracted from a potential CO₂ sequestration site, and an industrial wastewater by membrane distillation and forward osmosis in Salih et al. [36];
- h) Treatment of brine wastewater through a flow-through technology integrating desalination and photocatalysis in Ye et al. [37];
- i) Assessment of three brine recycle humidification-dehumidification desalination systems applicable for industrial wastewater treatment in Ghofrani and Moosavi [38];
- j) Membrane distillation treatment of municipal wastewater desalination brine and its mitigation by foam fractionation in Rajwade et al. [39];
- k) Sonophotocatalytic treatment of AB113 dye and real textile wastewater using ZnO/persulfate: Modeling by response surface methodology and artificial neural network in Asgari et al. [40];
- l) Removal from aqueous solutions using ionic liquid-modified magnetic activated carbon in Bazrafshan et al. [41]; and
- m) Techno-economic assessment of minimal liquid discharge (MLD) treatment systems for saline wastewater (brine) management and treatment in Panagopoulos [42].

With reference to the importance of these electrochemical treatment techniques in removing both conventional and emerging pollutants from aqueous solutions the performance of the techniques in removing chloride from brine wastewater and polynomial models that relate and simulate operational factors to their removal efficacies are limited in the literature. The main objectives of the current study are to evaluate the performance electrochemical process (using carbon-resin and aluminium electrodes) in removing chloride from saline water, to establish mathematical (polynomial regression form) models that relate the performance of the system to selected operational factors and to evaluate accuracy of these models statistically.

MATERIALS AND METHODS

Carbon-resin or graphite-resin electrodes (CRE) were produced from wasted dry cells. The discarded and spent dry cells were collected and picked from several dumpsites located in Nigeria. These collected dry cells were segmented and carbon (graphites) were separated from these cells and crushed. Powdered carbon was separated into different British standard particle sizes. A fixed mass of the powdered carbon was mixed with resin (organic binder), and moulded into 25- a millimetre diameter, 100-millime-

tre-long electrode utilising a plunger and extruder, with a compaction or compressive device. Details of the development and characteristics of the electrodes were presented in previous and other studies as follows:

- a) Development, stability and properties of carbon-resin electrode Oke et al. [43];
- b) Orthogonal experiment in the development of carbon-resin electrode Oke [44];
- c) Establishment of factors that influence stability and properties of carbon-resin electrode Oke et al. [45];
- d) Properties of doped carbon-resin electrode in Oke et al. [46]; aluminium and Calcium oxide doped Oke et al. [47];
- e) Utilization of Weibull distribution in the development of carbon-resin electrode in Oke et al [48];
- f) Effects of carbonization on stability and electrical conductivity of carbon-resin electrode in Oke [49];
- g) Development and optimization of carbon-resin electrode Oke et al. [50] and
- h) Thermal properties of carbon-resin electrode in Oke et al. [51]

Microstructures of the electrode were monitored to ascertain the composition of the electrode utilising a scanning electron microscope (of model Carl Zeiss Smart Evo 10 available at the Department of Materials Science and Engineering, Obafemi Awolowo University, Ile-Ife, Nigeria). Electrolysing equipment was developed from local materials. The development and performance of the device are as presented in previous publications such as Oke and Ogedengbe [52]; and Fehintola et al. [53]. The synthesised chloride wastewaters (salty water, brine) were prepared and calibrated by utilising procedures, techniques and methods stated and specified in the Standard Methods for Water and Wastewater Examination such as APHA [54], and van Loosdrecht et al. [55]. The analytical Sodium Chloride (60.0 grams) salt was dissolved in 1000 ml of distilled water as a stock solution, and secondary solutions for calibration and working salty wastewater were prepared from the stock. Selected calibration solutions of 0.0 mg/l, 250 mg/l, 500 mg/l, 1000 mg/l; 5000 mg/l; 10000 m/l and 15000 mg/l of chloride were used to calibrate the equipment used in the determination of chloride concentrations. Salty wastewaters were subjected to electrochemical treatment utilising developed carbon-resin or graphite-resin (anode) and aluminium (cathode) electrodes. Figure 1a, b present the laboratory setup of the electrochemical treatment of the simulated wastewater.

The impacts of selected operational factors (volume of the wastewater used, separation distance between the electrodes, flow and discharge rate, pH, applied current, initial concentration of the chloride, contact surface area of the electrode used and depth of the electrode) on the performance of electrochemical purification process were monitored using fractional factorial experiment and optimised using Microsoft Excel Solver. Table 1 presents the standard fractional factorial experiments and the factors. Sta-

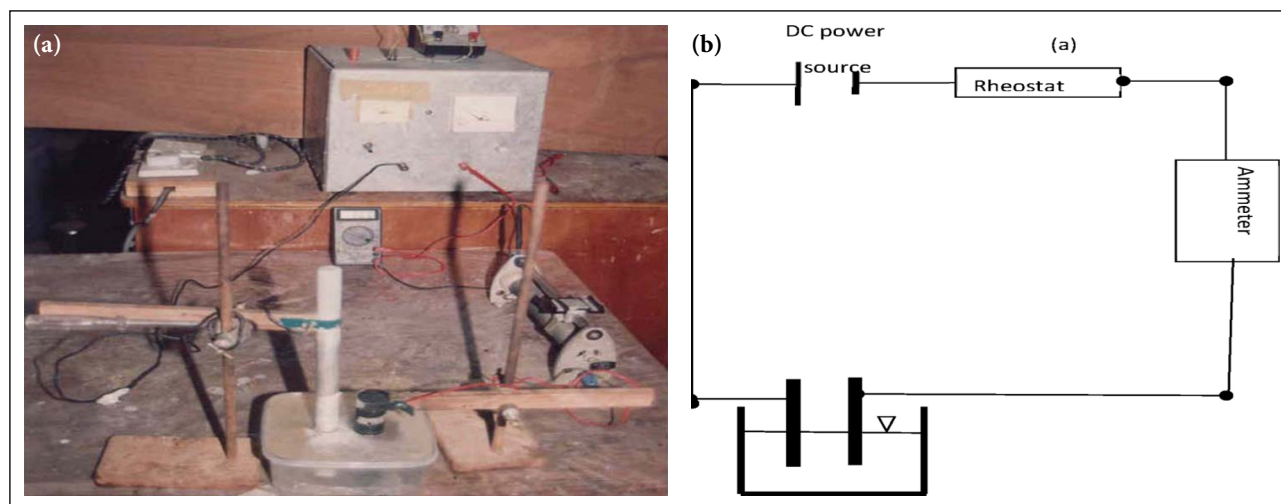


Figure 1. (a) Laboratory setup of the electrochemical treatment process. (b) Schematic diagram laboratory setup of the electrochemical treatment process.

Table 1. Standard fractional experiment (2^{k-P}) and factors used

Experiment	Initial concentration of chloride (g/l)	Current (A)	Separation distance (cm)	Time (hr)	Flow (l/hr)	Depth (cm)	Area (cm ²)	pH
1	10.0	1.0	2.0	1.0	1.0	0.4	4.91	3.0
2	40.0	1.0	2.0	1.0	2.5	0.4	19.64	10.0
3	10.0	10.0	2.0	1.0	2.5	1.0	4.91	10.0
4	40.0	10.0	2.0	1.0	1.0	1.0	19.64	3.0
5	10.0	1.0	10.0	1.0	2.5	1.0	19.64	3.0
6	40.0	1.0	10.0	1.0	1.0	1.0	4.91	10.0
7	10.0	10.0	10.0	1.0	1.0	0.4	19.64	10.0
8	40.0	10.0	10.0	1.0	2.5	0.4	4.91	3.0
9	10.0	1.0	2.0	4.0	1.0	1.0	19.64	10.0
10	40.0	1.0	2.0	4.0	2.5	1.0	4.91	3.0
11	10.0	10.0	2.0	4.0	2.5	0.4	19.64	3.0
12	40.0	10.0	2.0	4.0	1.0	0.4	4.91	10.0
13	10.0	1.0	10.0	4.0	2.5	0.4	4.91	10.0
14	40.0	1.0	10.0	4.0	1.0	0.4	19.64	3.0
15	10.0	10.0	10.0	4.0	1.0	1.0	4.91	3.0
16	40.0	10.0	10.0	4.0	2.5	1.0	19.64	10.0

tistical parameters (average, median, standard deviation, Skewness, coefficient of variation) of the performances of the treatment technique were determined using standard techniques. The choice of the Microsoft Excel Solver for the computation was grounded on the accessibility of the software at no extra cost (established in all Microsoft Excel packages). The models were modified to accommodate interactions between the selected factors (in this case the interactions were considered to be significant factors). The modified and qualified model equations were solved Microsoft Excel Solver (MiES) technique. These results from modified models were evaluated using statistical methods. The modified and qualified model equations are expressed as follows Asgari et al. [40], and Bazrafshan et al. [41]:

$$\text{Model A: } Y = \beta_0 + \beta_i \sum_{i=1}^k X_i + \xi \tag{1}$$

$$\text{Model B: } Y = \beta_0 + \beta_i \sum_{i=1}^k X_i + \beta_{ii} \sum_{ii=1}^k X_{ii}^2 + \xi \tag{2}$$

$$\text{Model C: } Y = \beta_0 + \beta_i \sum_{i=1}^k X_i + \beta_{ij} \sum_{i=1}^k \sum_{j=1}^k X_i X_j + \xi \tag{3}$$

The experimental data was fitted to polynomial models. The coefficients of polynomial models were determined using Microsoft Excel Solver. The Solver is an Add-in software for the Microsoft Excel packages which is typically or originally not enabled during the initial or primary installation of Microsoft Office (which includes Excel). The procedures

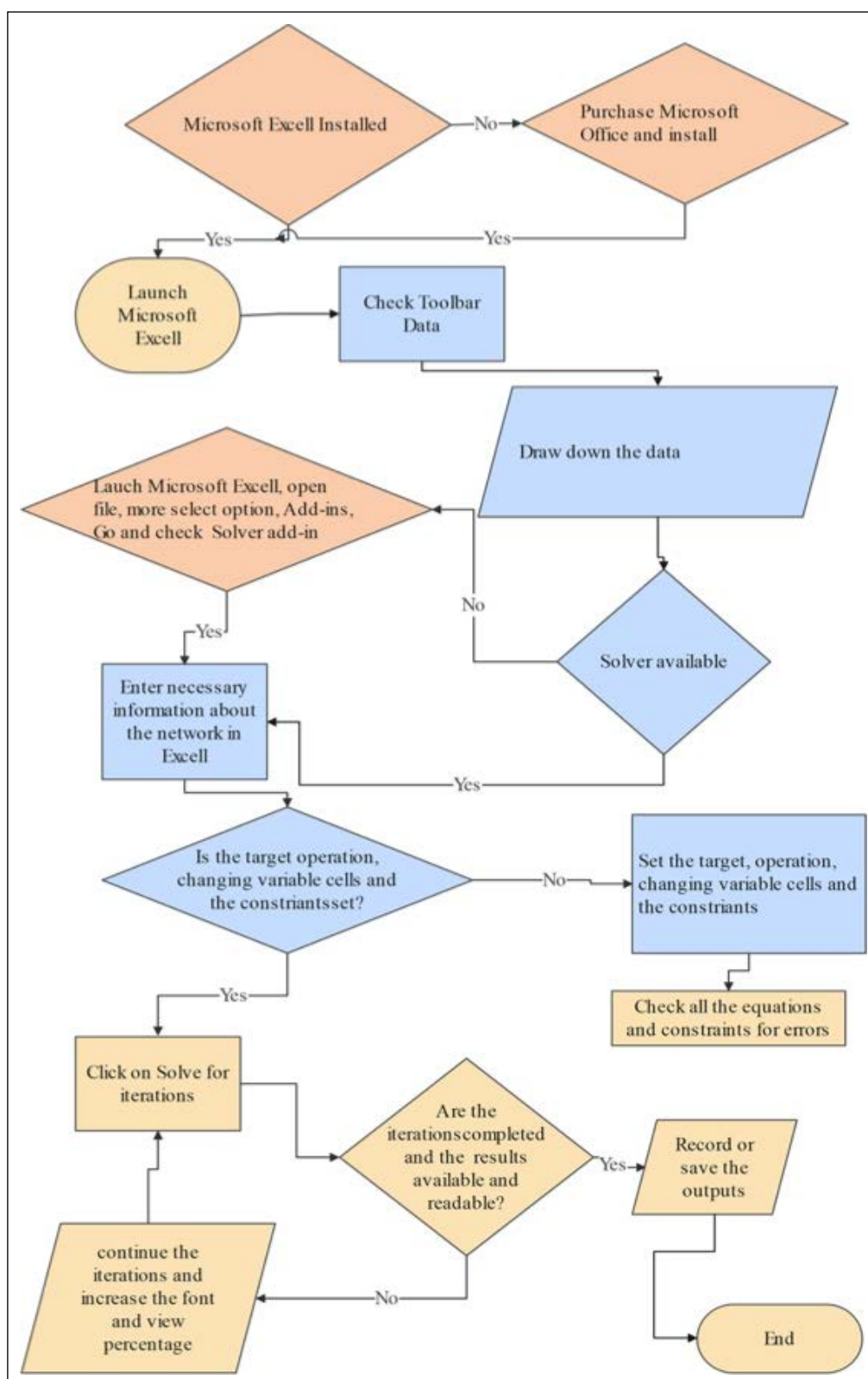


Figure 2. Procedure and flow chart for utilising Microsoft Excel Solver in the calculation of the unknown coefficients.

required in using Microsoft Excel Solver can be summarized as indicated in Figure 2. Figure 2 presents the flow chart of the procedures. The selection of these factors to be researched or studied was based on the theoretical information and data about numerous factors that establish the performance of the electrochemical treatment process

and the knowledge regarding graphite-resin or carbon-resin and aluminium electrodes. Chloride determinations in both raw and treated salty wastewater were carried out using the argenotometric technique or method specified in APHA [54]. Chloride concentration was calculated using equation (5) as follows:

$$Cl^{-} (mg/l) = 35450 \times C_f \left(\frac{(A-B) \times N_0 \times P_1}{V_s} \right) \quad (4)$$

Where; N_0 is the normality of Silver Nitrate used, P_1 is the dilution factor; V_s is the volume of effluent or sample used (ml), A is the volume of the titrate used for the sample (ml), C_f is the calibration factor and B is the volume of the titrate used for the blank (ml).

Efficiencies of the process were based mainly on pollutant (chloride) removal ($Y, \%$), which was computed using equation (5). The choices of the argenotometric and instrumentation methods [54] were based on accuracy, type of wastewater (clear aqueous solution) and availability of required reagents.

$$Y = 100 \times \left(\frac{(Z_0 - Z_t)}{Z_0} \right) \quad (5)$$

Where: Z_0 is the initial concentration of the chloride in the synthetic wastewater (mg/l). Z_t is the final concentration of chloride in the synthetic wastewater (mg/l) and Y is the chloride ions removed (%).

Statistical evaluations were conducted utilising Analysis of Variance (ANOVA), Coefficient of Determination (CD), Model of Selection Criterion (MSC), average relative error (A_{re}), accuracy (E_r) and total error. Average Relative Error (A_{re}), Accuracy (E_r) and Total error (Err^2) were computed as follows:

$$A_{re} = \frac{1}{N} \sum_{i=1}^N \left(\frac{(X_i - X_{ci})}{X_i} \right) \quad (6)$$

Where; X_i is the observed concentration and X_{ci} is the calculated concentration.

$$E_r = 100 \times \left(1 - \frac{(X_i - X_{ci})}{X_i} \right) \quad (7)$$

$$Err^2 = \sum_{i=1}^N (X_i - X_{ci})^2 \quad (8)$$

The coefficient of Determination can be shown and computed as follows:

$$CD = \frac{\sum_{i=1}^N (X_i - \bar{X}_{ci})^2 - \sum_{i=1}^N (X_i - X_{ci})^2}{\sum_{i=1}^N (X_i - \bar{X}_{ci})^2} \quad (9)$$

Where; \bar{X}_i is the average or statistical means of experimental concentration and \bar{X}_{ci} is the average or statistical means of calculated concentration. The model of Selection Criterion can be calculated utilizing equation (9) indicated as:

$$MSC = \ln \left(\frac{\sum_{i=1}^N (X_i - \bar{X}_i)^2}{\sum_{i=1}^N (X_i - X_{ci})^2} \right) - \frac{2p}{N} \quad (10)$$

Where; p is the number of variables or parameters and N is the number of experimental and data points

Skewness is a quantity of symmetry, proportion or exact of the data. The data set or information is symmetric when it

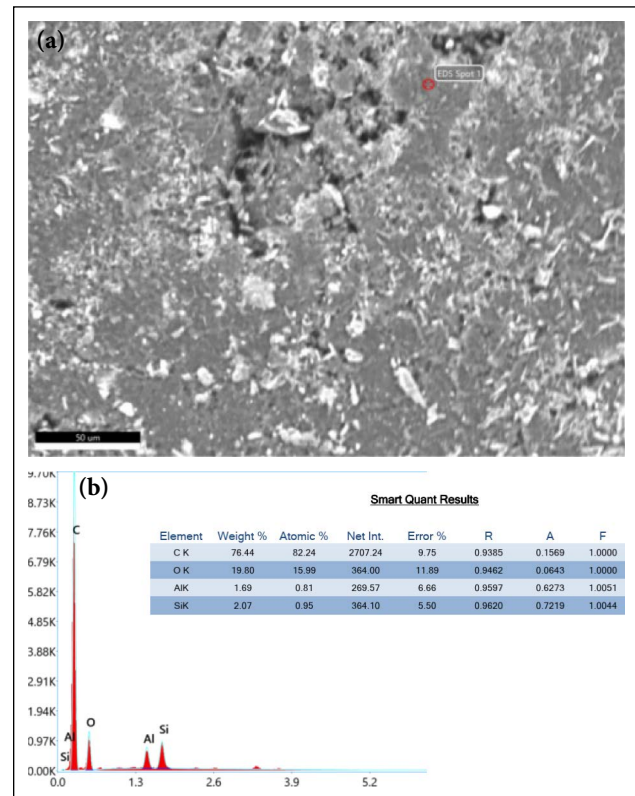


Figure 3. (a) The Spot for major composition of the carbon resin electrode. (b) The major composition of the Carbon resin electrode.

looks the same or similar to the left and right from the centre point. Skewness was computed as follows (Equation 11):

$$\gamma = \frac{\sum_{i=1}^N (Y - \bar{Y})^3}{N\delta^3} \quad (11)$$

Where; γ is the skewness, δ is the standard deviation, Y is the performance of the treatment process in removing chloride; \bar{Y} is the mean of of the performance of the treatment process in removing chloride and N is the number of samples.

Kurtosis is an important ingredient in statistical measurement and engineering design of treatment facility was computed as follows (equation 12):

$$\beta = \frac{\sum_{i=1}^N (Y - \bar{Y})^4}{N\delta^4} \quad (12)$$

RESULTS AND DISCUSSION

Figure 3a, b shows the major compositions of the Carbon resin electrode. The figure revealed that the major components of the electrode are Carbon (76.44%) Oxygen (19.80%), Si (2.07%) and Al (1.69%). The result indicated the presence of Carbon and Oxygen at the spot, which had the highest portion of the electrode, which can be attributed to the binder used and the size of the powdered graphite [3]. This result of the composition established and discovered that the removal and reduction of chloride may

be attributed to adsorption by the pores and conversion of some of the components to silicon, aluminium, chloride and oxygen products such as $Al(OCl)_3$, $SiCl_4$ and $AlCl_3$. The $SiCl_4$ reacts with water to give silicon dioxide and acidic end products (equation 13).



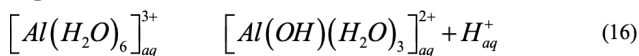
This reaction of $SiCl_4$ can be attributed to the bigger size of the Silicon atom, which provides more room and space around the atom to enable the water molecule to attach. In addition, the silicon atom has empty 3d orbitals available to accept a lone pair from the water molecule. This reaction indicated that the oxygen atom can bond to the silicon atom before the need to break the silicon-chlorine bond and support the whole process energetically. Aluminium chloride ($AlCl_3$) is an influential Lewis acid, industrial catalyst, non-explosive, non-flammable but corrosive solid and reacts violently with water or bases. $AlCl_3$ is believed to be a hygroscopic salt. Usually, this salt fumes in the moist - air. The reaction creates a heckling sound as it comes in connection with water. As these reactions take place or occur the Cl^- ions are displaced and replaced with water molecules and form hexahydrate $(Al(H_2O)_6)Cl_3$. At an anhydrous state, $AlCl_3$ is lost and as the heat is utilised HCl is dissipated and aluminium hydroxide is the final product that is attained.



As the temperature is increased further to a level of 400 °C, aluminium oxide is transformed from the hydroxide.



One distinct characteristic of $AlCl_3$ in aqueous solutions is that the solutions are ionic in character. With reference to this reason, these solutions are good conductors of electricity. The solutions are also acidic, which can result in the partial hydrolysis in Al^{3+} ion. The overall reaction can be expressed as follows:



Aluminium compounds and salts that is made up of hydrated Al^{3+} ions are similar in reaction to the behaviour of aqueous solutions of aluminium chloride. These solutions behave in the same way or similar by giving a profuse precipitate of $Al(OH)_3$ in reaction with a dilute basic oxide such as sodium hydroxide.

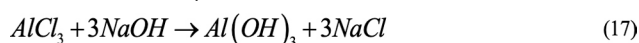


Figure 4a–c shows the Scanned electromagnetic (SEM) structures of the electrode. From the figure, it is clearly revealed that the powdered particles of carbon electrode were closely parked and the porosity is very low. This lower porosity can be attributed to a lower concentration of binder, higher compressive pressure and nano-particle sizes used in the development of the electrode [53]. Table 2 presents the arrangement of the fractional factorial experiment, the performance of electrochemical treatment in removing chloride from aqueous solutions and the statistical summary of the performance of electrochemical treatment.

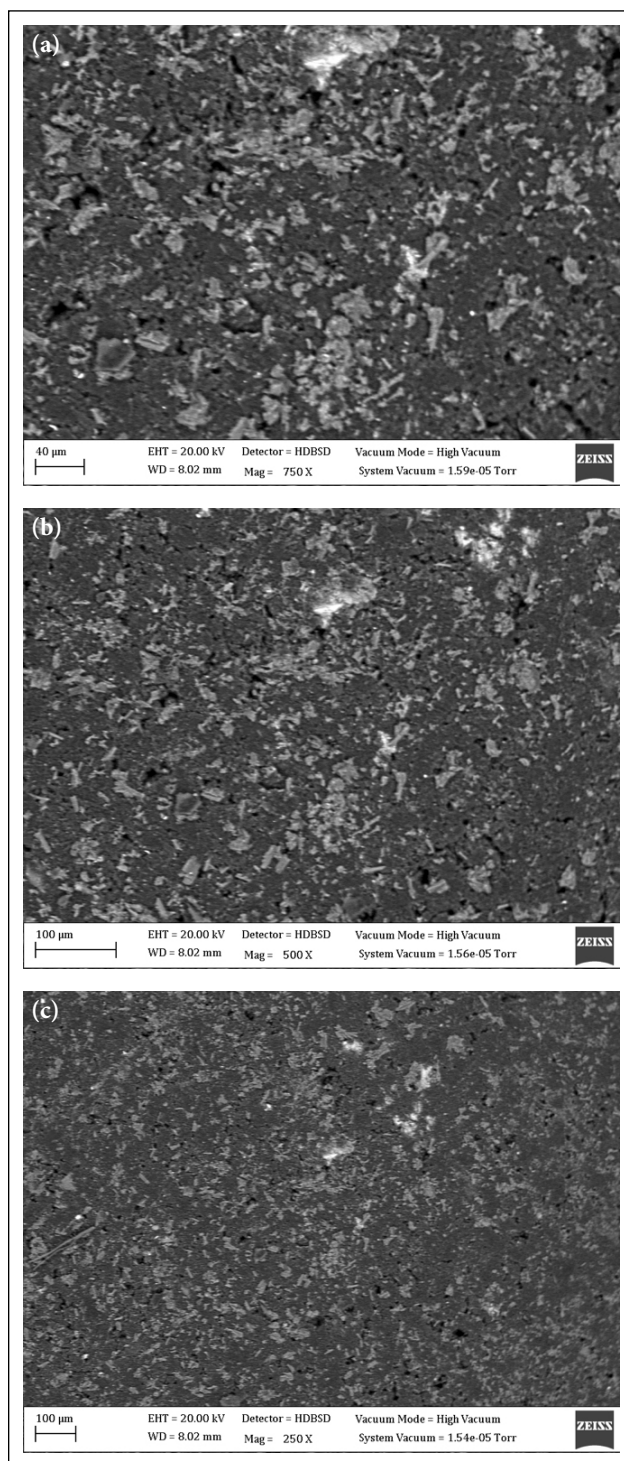


Figure 4. (a) Scanned Electro Magnetic (SEM) structures of the electrode at 40 µm. (b) Scanned Electro Magnetic (SEM) structures of the electrode at 100 µm. (c) Another Scanned Electro Magnetic (SEM) structures of the electrode at 100 µm.

The Table revealed that the maximum values the performance occurred at experiment number 11 with 94.82% removal of chloride concentration when the surface area (19.64 cm²), the flow (2.0l/hr), the treatment time (4.0 hr) and the current (10.0 A) were at their higher levels, which indicated that these selected and mentioned factors had positive influences on the performance of electrochemical

Table 2. Fractional factorial experiment, and the statistical summary of the performance of electrochemical treatment in removing chloride from aqueous solution

Exp.	Response				Total	Ave.	Ske.	Max.	Min.	SD	Med.	CV	Kur.
1	89.55	89.25	87.06	83.79	349.65	87.41	-1.12	89.55	83.79	2.66	88.16	3.04	0.160
2	85.77	85.67	83.78	80.5	335.72	83.93	-1.29	85.77	80.50	2.46	84.73	2.93	0.903
3	91.94	91.74	89.85	86.17	359.7	89.93	-1.35	91.94	86.17	2.67	90.80	2.97	1.232
4	88.46	88.46	86.47	82.98	346.37	86.59	-1.32	88.46	82.98	2.58	87.47	2.98	1.039
5	71.54	71.64	69.85	67.06	280.09	70.02	-1.25	71.64	67.06	2.14	70.70	3.05	0.701
6	70.5	69.95	68.36	65.27	274.08	68.52	-1.22	70.50	65.27	2.35	69.16	3.43	0.855
7	85.5	85.37	83.48	80.2	334.55	83.64	-1.28	85.50	80.20	2.47	84.43	2.95	0.875
8	83.5	83.38	81.59	78.31	326.78	81.70	-1.32	83.50	78.31	2.42	82.49	2.96	1.080
9	96.1	96.52	94.23	90.45	377.3	94.33	-1.32	96.52	90.45	2.77	95.17	2.94	1.174
10	88.9	87.66	86.76	83.28	346.6	86.65	-1.23	88.90	83.28	2.41	87.21	2.78	1.832
11	96.9	96.81	94.62	90.94	379.27	94.82	-1.27	96.90	90.94	2.79	95.72	2.94	0.802
12	87.9	87.76	85.87	82.49	344.02	86.01	-1.30	87.90	82.49	2.52	86.82	2.93	0.978
13	83.3	83.56	81.29	78.11	326.26	81.57	-1.18	83.56	78.11	2.52	82.30	3.09	0.407
14	81.09	81.09	79.2	90.94	332.32	83.08	1.83	90.94	79.20	5.32	81.09	6.40	3.518
15	91.14	90.84	89.05	85.47	356.5	89.13	-1.34	91.14	85.47	2.61	89.95	2.92	1.226
16	87.04	86.96	85.07	81.59	340.66	85.17	-1.34	87.04	81.59	2.55	86.02	3.00	1.140

Exp: Experiment; Ave: Average; Ske: Skewness; Max: Maximum; Min: Minimum; SD: Standard deviation; Med: Median; Kur: Kurtosis.

Table 3. ANOVA of the performance

Source of variation	Sum of squares	Degree of freedom	Mean Sum of square	F-value	P-value
Within experiment	3034.023	15	202.2682	55.41323	6.19x10 ⁻²⁴
Between runs	209.3126	3	69.77087	19.11437	3.87x10 ⁻⁰⁸
Error	164.2581	45	3.650179		
Total	3407.594	63			

during the treatment process. The lowest value of the performance of the process occurred in experiment numbered 6 with 68.52% removal of the chloride by the treatment process [27, 28, 32, 45]. This level of performance occurred when the initial concentrations of chloride (40 x 10³ mg/l), the separation distances between electrodes (10.0 cm), the depth of the electrode (1.0 cm) and pH (10.0) were at higher factorial factor levels, which meant that these latter mentioned selected factors contributed negatively to the performance of the treatment process. From Table 2, the Skewness of the performance of electrochemical treatment in removing chloride from an aqueous solution was between -1.12 and 1.83. With the exception of experiment number 14, which has positive Skewness, all the other experiments were of negative Skewness, which indicated that most values are concentrated on the right of the mean, with extreme values to the left. Kurtosis (β) is a degree of data peakedness or horizontalness relative to a normal distribution pattern. The data sets or information with higher values of kurtosis tend to have a distinct peak near the mean, either decline and reduce rapidly or have heavier tails than necessary. From Table 2, the Kurtosis of the performance of electrochemical treatment in removing chloride from

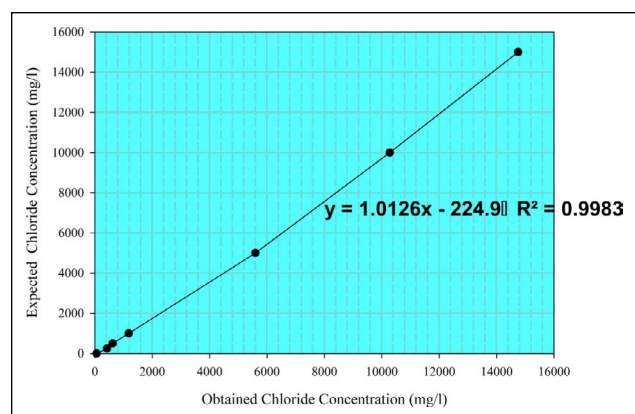


Figure 5. Calibration curve (relationship between obtained and expected chloride concentrations).

aqueous solution was between 0.160 and 3.518. The Kurtosis values of the performance of electrochemical treatment in removing chloride from an aqueous solution were positive, which indicated the data sets have a distinct peak near the mean, decline rather rapidly, and have heavy tails. With the exception of experiment number 14, which has Kurtosis greater than 3, all the other experiments had Kurtosis less

Table 4. Result of ANOVA for the calibration

Source of variation	Sum of squares	Degree of freedom	Mean Sum of square	F-value	P-value
Between groups	96114.29	1	96114.28571	0.002819033	0.95853
Within groups	4.09E+08	12	34094771.43		
Total	4.09E+08	13			

Table 5. The coefficient for the mathematical polynomial regression models

Experiment	Average	Model A's coefficients		Model B's coefficients		Model C's coefficients			
1	87.41	Constant	87.629	Constant	86.671	Constant	86.930	Cubic Initial Con	-6.5E-07
2	83.93	Initial Con	-0.122	Initial Con	-0.110	Initial Con	-0.108	Cubic Current	0.002882
3	89.93	Current	0.576	Current	0.675	Current	0.362	Cubic Sep D	-0.00377
4	86.59	Sep D	-1.044	Sep D	-0.980	Sep D	-0.515	Cubic Time	0.051667
5	70.02	Time	2.042	Time	2.193	Time	1.113	Cubic Flow (l/hr)	-0.01613
6	68.52	Flow (l/hr)	-0.411	Flow (l/hr)	-0.292	Flow (l/hr)	-0.157	Cubic Depth(cm)	-0.00316
7	83.64	Depth(cm)	-2.462	Depth(cm)	-1.440	Depth(cm)	-1.432	Cubic Area	-7E-06
8	81.70	Area	0.091	Area	0.113	Area	0.116	Cubic pH	-6.2E-05
9	94.33	pH	-0.113	pH	-0.078	pH	-0.070	Cubic Initial Con	-6.5E-07
10	86.65			Sq. Initial Con	-0.00024	Sq. Initial Con	-0.00024		
11	94.82			Sq. Current	-0.00902	Sq. Current	-0.00964		
12	86.01			Sq. Sep D	-0.0054	Sq. Sep D	-0.00523		
13	81.57			Sq. Time	-0.03026	Sq. Time	-0.03129		
14	83.08			Sq. Flow (l/hr)	-0.03373	Sq. Flow (l/hr)	-0.02743		
15	89.13			Sq. Depth(cm)	-0.72951	Sq. Depth(cm)	-0.72654		
16	85.17			Sq. Area	-0.00089	Sq. Area	-0.00089		
				Sq. pH	-0.00272	Sq. pH	-0.0026		

Table 6. The statistical evaluation of the mathematical model equation

	Average	Accuracy	MSC	CD	R	AIC	SC
Model A	2.99	97.01	0.630	0.804	0.897	96.023	96.658
Model B	2.97	97.03	0.690	0.874	0.935	95.945	96.602
Model C	2.94	97.06	0.705	0.893	0.945	95.945	96.602

than 3, which indicated that experiment 14 is a leptokurtic distribution, sharper than a normal distribution, with values concentrated around the mean and thicker tails.

Table 3 presents the ANOVA of the performance of the treatment process. The table revealed that there were significant differences between the performances and the runs (experiments) at a 95% confidence level. Table 4 presents the results of ANOVA for the calibration conducted on the equipment used in the determination of the chloride concentrations. The table revealed that there was no significant difference between obtained and expected chloride concentrations at a 95% confidence level ($F_{1,12}=0.0028$; $p=0.95853$). Figure 5 presents the relationship between obtained and expected chloride concentrations. The Figure established that there is a good relationship between the obtained and expected chloride concentrations ($R^2=0.9983$). Table 5

shows the analysis of the fractional factorial experiment, the effects and the coefficient of each of the selected factors for model A. The table revealed that these selected factors can be classified into two groups as positive and negative factors. The current through the wastewater, the treatment time and the surface area of the electrodes were the positive factors. The above-mentioned factors are the factors with increment in magnitude that improved the performance of the treatment process. The initial concentration of the salt, the distance between the electrodes, the flow rate of the wastewater, the depth of the electrodes and the pH value of the wastewater were the negative factors, that reduced the performance of the treatment process. These negative factors were the factors with a decrement in the magnitude of the performance of the treatment process. From the table, the significant factors (at a 90% confidence level) on

Table 7. Effects of selected factors on performance of electrochemical treatment in removing chloride from aqueous solution, optimum and statistical evaluation (Model A)

	Initial concentration of chloride	Current	Separation distance between electrodes	Treatment time	Flow rate	Depth of electrode	Surface area of electrodes	pH	Error	Total
Sum of squares	0.06	1.33	4.36	16.67	0.67	24.24	0.03	0.05	3.15	758.51
Degree of freedom	1	1	1	1	1	1	1	1	7.00	15.00
Means Sum of squares	0.06	1.33	4.36	16.67	0.67	24.24	0.03	0.05	0.45	50.57
F-value	0.13	2.95	9.70	37.05	1.50	53.86	0.07	0.11		

F-critical values at 90 %, 95 %, 97.5 %, 99 % and 99.5 % are 3.59, 5.59, 8.07, 12.25 and 16.24, respectively.

Table 8. Effects of selected factors on the performance of electrochemical treatment in removing chloride from aqueous solution, optimum and statistical evaluation (Model B)

	Initial concentration of chloride	Current	Separation distance between electrodes	Treatment time	Flow rate	Depth of electrode	Surface area of electrodes	pH	Error	Total
Sum of Squares	0.05	1.82	3.84	19.24	0.34	8.30	0.05	0.02	16.91	758.51
Degree of Freedom	1	1	1	1	1	1	1	1	7.00	15.00
Means Sum of Squares	0.05	1.82	3.84	19.24	0.34	8.30	0.05	0.02	2.42	50.57
F-value	0.11	4.05	8.53	42.74	0.76	18.44	0.11	0.05		

Table 9. Effects of Selected Factors on the performance of electrochemical treatment in removing chloride from an aqueous solution, optimum and statistical evaluation (Model C)

	Initial concentration of chloride	Current	Separation distance between electrodes	Treatment time	Flow rate	Depth of electrode	Surface area of electrodes	pH	Error	Total
Sum of Squares	0.05	0.52	1.06	4.96	0.10	8.20	0.05	0.02	35.61	758.51
Degree of Freedom	1	1	1	1	1	1	1	1	7.00	15.00
Means Sum of Squares	0.05	0.52	1.06	4.96	0.10	8.20	0.05	0.02	5.09	50.57
F-value	0.10	1.16	2.35	11.01	0.22	18.21	0.12	0.04		

electrochemical performance toward chloride removal are current, separation distance between electrodes and time. Table 5 revealed the coefficient for the mathematical polynomial regression models as follows (equations [18–20]):

a) For Model A.

$$Y(\%) = 87.629 - 0.122I_c + 0.576C_u - 1.0424D_s + 2.042T_t - 0.411Q_f - 0.2.462D_p + 0.091A_s - 0.113pH \quad (18)$$

b) For Model B.

$$Y(\%) = 87.629 - 0.122I_c + 0.576C_u - 1.0424D_s + 2.042T_t - 0.411Q_f - 0.2.462D_p + 0.091A_s - 0.113pH \quad (19)$$

For Model C.

$$Y(\%) = 87.629 - 0.122I_c + 0.576C_u - 1.0424D_s + 2.042T_t - 0.411Q_f - 0.2.462D_p + 0.091A_s - 0.113pH \quad (20)$$

Table 6 shows the statistical evaluation of the mathematical model equations. The table revealed that average error, accuracy, MSC, CD, and R of these model equations

(Models A, B and C) were 2.99%, 97.01, 0.41183, 0.804, and 0.897; 2.97%, 97.03%, 0.690, 0.874, 0.935; 2.94%, 97.06%, 0.705, 0.893 and 0.945, respectively. This result indicated that these mathematical models are reliable with 97.01%, 97.03% and 97.06% accurate, which indicates that Model A can predict 97.01% of the experimental data, Model B predicts 97.03% and Model C provide information on 97.06% of the experimental data. Tables 7 to 9 present the results of ANOVA on the effects of the selected factors in each of the model equations. Table 7 presents the effects of selected factors on the performance of electrochemical treatment in removing chloride from aqueous solution, optimum and statistical evaluation (Model A). Table 8 shows the effects of Selected Factors on the performance of electrochemical treatment in removing chloride from aqueous solution, optimum and statistical evaluation (Model B) and Table 9 is for the effects of selected factors on the performance of electrochemical treatment in removing chloride from an aqueous solution, optimum and

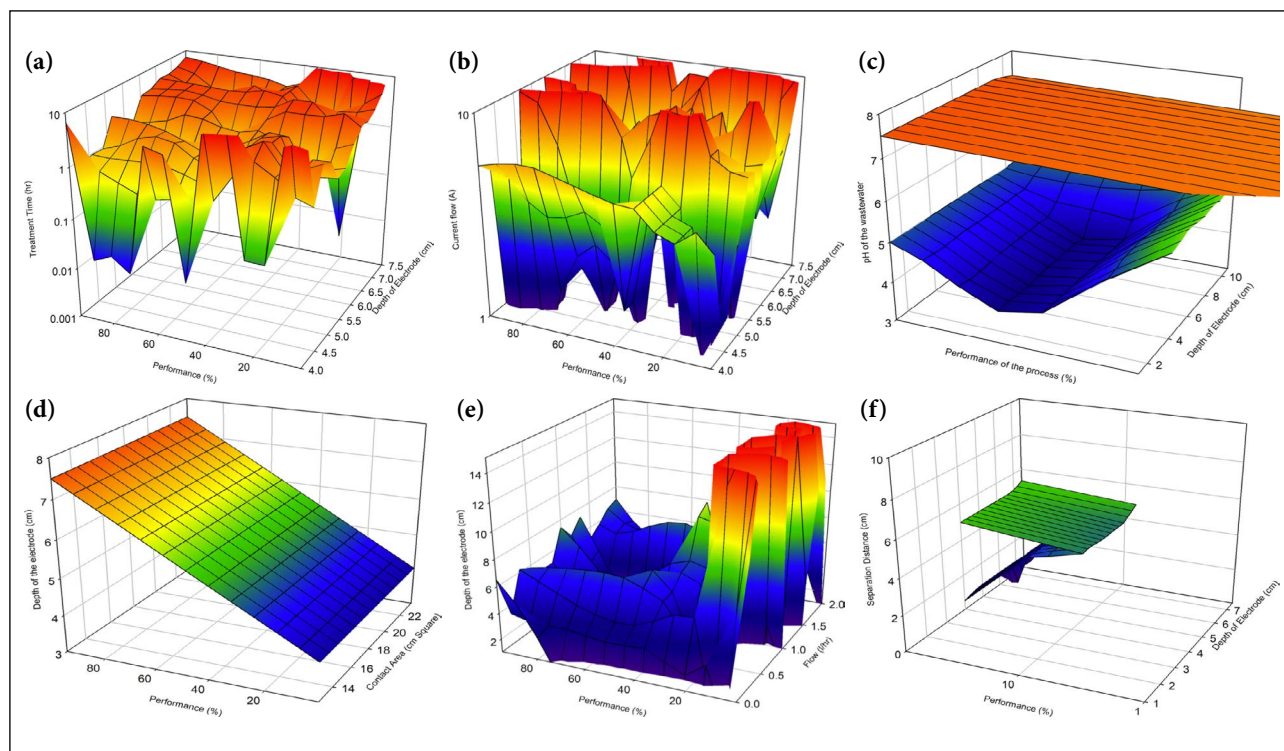


Figure 6. (a) Relationship between treatment time, depth of electrodes and performance of electrochemical treatment in removing chloride from an aqueous solution. (b) Relationship between the current, depth of electrodes and performance of electrochemical treatment in removing chloride from an aqueous solution. (c) Relationship between the pH, depth of electrodes and performance of electrochemical treatment in removing chloride from an aqueous solution. (d) Relationship between Contact Area, depth of electrodes and performance of electrochemical treatment in removing chloride from an aqueous solution. (e) Relationship between the flow rate, depth of electrodes and performance of electrochemical treatment in removing chloride from an aqueous solution. (f) Relationship between the separation distance between the electrodes, depth of electrodes and performance of electrochemical treatment in removing chloride from an aqueous solution.

statistical evaluation (Model C). From these Tables (Table 7–9) the factors can be grouped into two factors with effects but not significant and factors with effects and factors are significant. The factors with effects and significance are separation distance between electrodes, treatment time, current and depth of electrodes. Figure 6 presents the relationship between the performance of the treatment process and selected operational factors. Figure 6a shows the relationship between treatment time, depth of electrodes and performance of electrochemical treatment in removing chloride from an aqueous solution.

Figure 6b presents the relationship between the current, depth of electrodes and performance of electrochemical treatment in removing chloride from an aqueous solution. Figure 6c shows the relationship between the pH, depth of electrodes and performance of electrochemical treatment in removing chloride from an aqueous solution. Figure 6d is for the relationship between Contact Area, depth of electrodes and performance of electrochemical treatment in removing chloride from an aqueous solution. Figure 6e is for the relationship between the flow rate, depth of electrodes and performance of electrochemical treatment in removing chloride from an aqueous solution. Finally, Figure 6f presents the relationship between the flow rate, depth of electrodes and

performance of electrochemical treatment in removing chloride from an aqueous solution. All these figures revealed that there were polynomial relationships between the selected operational factors and the performance of the treatment process. These revelations indicated that optimizations of these factors are necessary and will be helpful in operational techniques.

It was observed that these relationships were similar to the surface response of the influence of some the operational variables and parameters on the arsenic reduction and removal by electrocoagulation utilising iron electrodes and other techniques in Oke et al. [56], Vijaya Bhaskar et al [57], Can et al. [58], Darvishi et al. [59], and Majumder and Gupta [60], the response surface technique and methodological examination or evaluation of the adsorption of textile dye onto biosilica or alginate nano-biocomposite: kinetic, and isotherm studies and thermodynamic behaviour in Darvishi et al. [59], the removal and elimination of methylene blue dye from aqueous solutions by zeolite composite from shrimp waste and new chitosan in Gilhotra et al. [61], Yao et al. [62], Gadkari et al [63], and Elimelech and Phillip [64], and electrocoagulation technology for high strength arsenic wastewater: process optimization and mechanistic study in Can et al. [58].

CONCLUSIONS

It can be concluded based on the study that:

- a. Electrochemical treatment with carbon electrodes is efficient in removing chloride from salty wastewater. The system was able to reduce chloride concentration from 15000 mg/l to 5% of the initial concentration at a current flow of 9.68 A and retention time of 5 hours.
- b. The operational factors with negative effects (increasing these operational factors decreases the removal performance) on the performance of the treatment process were separation distance between the electrodes, pH, depth of the electrode, initial concentration of the chloride and flow rate.
- c. These operational factors applied current, treatment time and contact surface area of the electrode used are positive factors (increasing these operational factors increases the removal performance) that influence the electrochemical treatment of salty wastewaters.
- d. The operational factors that had significant effects on the performance of the treatment process are current, time and separation distance between the electrodes.
- e. In the case of models and their evaluations Model C performed better than Model B and Model A based on average errors of 2.99%, 2.97% and 2.94%, respectively and R values of 0.945, 0.935 and 0.897 for Models C, B and A, respectively, which supported conclusions on nonlinear models in Mahmoud [65] and Amin et al. [66].

DATA AVAILABILITY STATEMENT

The authors confirm that the data that supports the findings of this study are available within the article. Raw data that support the finding of this study are available from the corresponding author, upon reasonable request.

CONFLICT OF INTEREST

The authors declared no potential conflicts of interest with respect to the research, authorship, and/or publication of this article.

USE OF AI FOR WRITING ASSISTANCE

The authors confirmed that AI was not use in the writing or as a writing assistant in the manuscript.

ETHICS

There are no ethical issues with the publication of this manuscript.

REFERENCES

- [1] A. J. C. Da Silva, E. V. dos Santos, C. C. de Oliveira Morais, C. A. Martínez-Huitle, and S. S. L. Castro, "Electrochemical treatment of fresh, brine and saline produced water generated by petrochemical industry using Ti/IrO₂-Ta₂O₅ and BDD in flow reactor," *Chemical Engineering Journal*, Vol. 233, pp. 47–55, 2013. [\[CrossRef\]](#)
- [2] S. Kaith, and R. Shabnam, "Synthesis of pH — Thermosensitive gum arabic based hydrogel and study of its salt-resistant swelling behavior for saline water treatment," *Desalination and Water Treatment*, Vol. 24(1-3), pp. 28–37, 2010. [\[CrossRef\]](#)
- [3] N. A. Ahmad, P. S. Goh, A. K. Zulhairun, and A. F. Ismail, "Antifouling property of oppositely charged titania nanosheet assembled on thin film composite reverse osmosis membrane for highly concentrated oily saline water treatment," *Membranes*, Vol. 10(9), pp. 237–243, 2020. [\[CrossRef\]](#)
- [4] B. Akyon, E. Stachler, N. Wei, and K. Bibby, "Microbial Mats as a Biological Treatment Approach for Saline Wastewaters: The Case of Produced Water from Hydraulic Fracturing," *Environmental Science and Technology*, Vol. 49(10), pp. 6172–6180, 2015. [\[CrossRef\]](#)
- [5] A. T. A. Baptista, P. F. Coldebella, P. H. F. Cardines, R. G. Gomes, M. F. Vieira, R. Bergamasco, and A. M. S. Vieira, "Coagulation–flocculation process with ultrafiltered saline extract of *Moringa oleifera* for the treatment of surface water," *Chemical Engineering Journal*, Vol. 276, pp. 166–173, 2015. [\[CrossRef\]](#)
- [6] L. Beneduce, G. Spano, F. Lamacchia, M. Bellucci, F. Consiglio, and I. M. Head, "Correlation of seasonal nitrification failure and ammonia-oxidizing community dynamics in a wastewater treatment plant treating water from a saline thermal spa," *Annals of Microbiology*, Vol. 64(4), pp. 1671–1682, 2014. [\[CrossRef\]](#)
- [7] F. Kargi, and A. R. Dincer, "Biological treatment of saline wastewater by fed-batch 545 operation," *Journal of Chemical Technology and Biotechnology*, Vol. 69(2), pp. 167–172, 1999. [\[CrossRef\]](#)
- [8] J. Zhang, H. Yuan, Y. Deng, Y. Zha, I. M. Abu-Reesh, Z. He, and C. Yuan, "Life cycle assessment of a microbial desalination cell for sustainable wastewater treatment and saline water desalination," *Journal of Cleaner Production*, Vol. 200, pp. 900–910, 2015. [\[CrossRef\]](#)
- [9] P. Ziemkiewicz, P. H. Stauffer, J. Sullivan-Graham, S. P. Chu, W. L. Bourcier, T. A. Buscheck, and J. L. Wagoner, "Opportunities for increasing CO₂ storage in deep, saline formations by active reservoir management and treatment of extracted formation water: Case study at the GreenGen IGCC facility, Tianjin, PR China," *International Journal of Greenhouse Gas Control*, Vol. 54, pp. 538–556, 2016. [\[CrossRef\]](#)
- [10] B. D. Soni, U. D. Patel, A. Agrawal, and J. P. Ruparelia, "Application of BDD and DSA electrodes for the removal of RB 5 in batch and continuous operation," *Journal of Water Process Engineering*, Vol. 17, pp. 11–21, 2017. [\[CrossRef\]](#)
- [11] G. S. Madrona, R. Bergamasco, V. J. Seolin, and M. R. Fagundes Klen, "The potential of different saline solution on the extraction of the moringa oleifera Seed's active component for water treatment," *International Journal of Chemical Reactor Engineering*, Vol. 9(1), 2011. [\[CrossRef\]](#)

- [12] A. A. Al-Raad, M. M. Hanafiah, A. S. Naje, and M. A. Ajeel, "Optimized parameters of the electrocoagulation process using a novel reactor with rotating anode for saline water treatment," *Environmental Pollution*, Vol. 265, Article 115049, 2020. [CrossRef]
- [13] A. Al-Raad, M. M. Hanafiah, A. S. Naje, M. A. O. Ajeel, A. Basheer, T. Ali Aljayashi, and T. M. Ekhwan, "Treatment of saline water using electrocoagulation with combined electrical connection of electrodes," *Processes*, Vol. 7(5), Article 242, 2019. [CrossRef]
- [14] A. Ayadi, D. J. Ennigrou, F. Proietto, A. H. Hamzaoui, and M. Jaouadi, "electrochemical degradation of phenol in aqueous solutions using activated Carbon-ZnO composite," *Environmental Engineering Science*, pp. 349–361, 2023. [CrossRef]
- [15] M. Andreozzi, M. G. Álvarez, S. Contreras, F. Medina, L. Clarizia, G. Vitiello, and R. Marotta, "Treatment of saline produced water through photocatalysis using rGO-TiO₂ nanocomposites," *Catalysis Today*, Vol. 315, pp. 194–204, 2018. [CrossRef]
- [16] S. Feroz, "Treatment of saline water by solar nano photocatalysis. *Synthesis and Catalysis: Open Access*, Vol. 02(01), 2017. [CrossRef]
- [17] Z. Ye, S. Wang, W. Gao, H. Li, L. Pei, M. Shen, and S. Zhu, "Synergistic effects of micro-electrolysis-photocatalysis on water treatment and fish performance in saline recirculating aquaculture system," *Scientific Reports*, Vol. 7(1), 2017. [CrossRef]
- [18] G. A. Ekama, J. A. Wilsenach, and G. H. Chen, "Saline sewage treatment and source separation of urine for more sustainable urban water management," *Water Science and Technology*, Vol. 64(6), pp. 1307–1316, 2011. [CrossRef]
- [19] A. R. Estabragh, M. Kouchakzadeh, and A. A. Javaidi, "Treatment of a clay soil deposited in saline water by cement," *European Journal of Environmental and Civil Engineering*, Vol. 25(8), pp. 1521–1537, 2019. [CrossRef]
- [20] B. Jiang, S. Jiang, A. L. Ma, and Y. G. Zheng, "Effect of heat treatment on erosion-corrosion behavior of electroless Ni-P coatings in saline water," *Materials and Manufacturing Processes*, Vol. 29(1), pp 74–82, 2014. [CrossRef]
- [21] M. Hachicha, B. Kahlaoui, N. Khamassi, E Misle, and O. Jouzdan, "Effect of electromagnetic treatment of saline water on soil and crops," *Journal of the Saudi Society of Agricultural Sciences*, Vol. 17(2), pp. 154–162, 2018. [CrossRef]
- [22] P. Jin, X. Jin, L. Zhou, and X. Wang, "A study on the removal of highly concentrated organic matters in saline lake water and the mechanism of magnesium ion loss in water treatment," *Desalination and Water Treatment*, Vol. 42(1-3), pp. 241–247, 2012. [CrossRef]
- [23] B. S. Kaith, and S. Ranjta, "Synthesis of pH — Thermosensitive gum Arabic based hydrogel and study of its salt-resistant swelling behavior for saline water treatment," *Desalination and Water Treatment*, Vol. 24(1-3), pp. 28–37, 2010. [CrossRef]
- [24] A. Pfennig, H. Wolthusen, M. Wolf, and A. Kranzmann, "Effect of heat treatment of injection pipe steels on the reliability of a saline aquifer water CCS-site in the Northern German Basin," *Energy Procedia*, Vol. 63, pp. 5762–5772, 2014. [CrossRef]
- [25] B. K. Shrivastava, "Technological innovation in the area of drinking water for treatment of saline water," *Asian Journal of Water, Environment and Pollution*, Vol. 13(3), pp. 37–44, 2016. [CrossRef]
- [26] Z. Zhang, G. Q. Chen, B. Hu, H. Deng, L. Feng, and S. Zhang, "The role of osmotic agent in water flux enhancement during osmotic membrane distillation (OMD) for treatment of highly saline brines," *Desalination*, Vol. 481, Article 114353, 2020.
- [27] J. Xu, Y. B. Singh, G. L. Amy, and N. Ghaffour, "Effect of operating parameters and membrane characteristics on air gap membrane distillation performance for the treatment of highly saline water," *Journal of Membrane Science*, Vol. 512, pp. 73–82, 2016. [CrossRef]
- [28] Y. Yue, S. Liu, and F. Han. "Desalination advancement by membrane water heating in vacuum membrane distillation," *Environmental Engineering Science*, pp. 394–401, 2023. [CrossRef]
- [29] N. M. Yusof, V. C. Venkatesh, S. Sharif, S. Elting and A. Abu, "Application of response surface methodology in describing the performance of coated carbide tools when turning AISI 104 steel," *Journal of Materials Processing Technology*, Vol. 145, pp. 46–58, 2004. [CrossRef]
- [30] S. Aber, and M. Sheydaei, "Removal of COD from industrial effluent containing indigo dye using adsorption method by activated carbon cloth: Optimization, kinetic, and isotherm studies," *Clean – Soil, Air, Water*, Vol. 40(1), pp. 87–94, 2012. [CrossRef]
- [31] M. Qurie, J. Abbad, L. Scranò, G. Mecca, S. Bufo, M. Khamis, and R. Karaman, "Inland treatment of the brine generated from reverse osmosis advanced membrane wastewater treatment plant using epuvalisation system," *International Journal of Molecular Sciences*, Vol. 14(7), pp. 13808–13825, 2013. [CrossRef]
- [32] H. D. Wang, K. L. Gao, and B. T. Lu, "Electrochemical Catalytic Oxidation Treatment of Coking Wastewater RO Brine," *Advanced Materials Research*, Vol. 838–841, pp. 2751–2758, 2013. [CrossRef]
- [33] A. Burbano, S. Sansom, K. Kinser, J. Rozas, and P. Corser, innovative application of water quality and flow modeling to design a softening, UF/RO and brine handling system for copper and gold mining wastewater treatment in the peruvian andes. *Proceedings of the Water Environment Federation*, Vol. 13, pp. 4124–4131, 2014. [CrossRef]
- [34] K. Thirugnanasambandham, V. Sivakumar, and J. M. Prakash, "Response surface modelling and optimization of treatment of meat industry wastewater using electrochemical treatment method," *Journal of the Taiwan Institute of Chemical Engineers*, Vol. 39, pp. 432–456, 2014.

- [35] A. Marone, A. A. Carmona-Martínez, Y. Sire, E. Meudec, J. P. Steyer, N. Bernet, and E. Trably, “Bio-electrochemical treatment of table olive brine processing wastewater for biogas production and phenolic compounds removal,” *Water Research*, Vol. 100, pp 316–325, 2016. [\[CrossRef\]](#)
- [36] H. H. Salih, and S. A. Dastgheib, “Treatment of a hypersaline brine, extracted from a potential CO₂ sequestration site, and an industrial wastewater by membrane distillation and forward osmosis,” *Chemical Engineering Journal*, Vol. 325, pp. 415–423, 2017. [\[CrossRef\]](#)
- [37] G. Ye, Z. Yu, Y. Li, L. Li, L. Song, L. Gu, and X. Cao, “Efficient treatment of brine wastewater through a flow-through technology integrating desalination and photocatalysis,” *Water Research*, Vol. 157, pp 134–144, 2019. [\[CrossRef\]](#)
- [38] I. Ghofrani, and A. Moosavi, “Energy, exergy, exergoeconomics, and exergoenvironmental assessment of three brine recycle humidification-dehumidification desalination systems applicable for industrial wastewater treatment” *Energy Conversion and Management*, Vol. 205, Article 112349, 2020. [\[CrossRef\]](#)
- [39] K. Rajwade, A. C. Barrios, S. Garcia-Segura, and F. Perreault, “Pore wetting in membrane distillation treatment of municipal wastewater desalination brine and its mitigation by foam fractionation,” *Chemosphere*, Vol. 257, Article 127214, 2020. [\[CrossRef\]](#)
- [40] G. Asgari, A. Shabanloo, M. Salari, and F. Eslami, “Sonophotocatalytic treatment of AB113 dye and real textile wastewater using ZnO/persulfate: Modeling by response surface methodology and artificial neural network,” *Environmental Research* Vol. 184, Article 109367, 2020. [\[CrossRef\]](#)
- [41] E. Bazrafshan, A. A. Zarei, I. Mohammadi, M. N. Zafar, M. Foroughi, S. Aman, F. Sabri, A. Mahvi, F. Barahuie, and M. Zafar, “Efficient tetracycline removal from aqueous solutions using ionic liquid modified magnetic activated carbon (IL@mAC),” *Journal of Environmental Chemical Engineering*, Vol. 9, Article 106570, 2021. [\[CrossRef\]](#)
- [42] A. Panagopoulos, “Techno-economic assessment of minimal liquid discharge (MLD) treatment systems for saline wastewater (brine) management and treatment,” *Process Safety and Environmental Protection*, Vol. 146, pp 656–669, 2021. [\[CrossRef\]](#)
- [43] I. A. Oke, L. E. Umoru, and M. O. Ogedengbe, “Properties and stability of a carbon-resin electrode,” *Journal of Materials and Design*, Vol. 28(7), pp. 2251–2254, 2007. [\[CrossRef\]](#)
- [44] I. A. Oke, “Orthogonal experiments in the development of carbon –resin for chloride ions removal,” *Statistical Methodology*, Vol. 6, pp. 109–119, 2009. [\[CrossRef\]](#)
- [45] I. A. Oke, L. E. Umoru, and M. O. Ogedengbe, “2k factorial experiments on factors that influence stability of carbon resin electrodes,” *FUTAJEET*, Vol. 5(2), pp. 135–141, 2007.
- [46] I. A. Oke, L. E. Umoru, O. E. Olorunniwo, F. I. Alo, and M. A. Asani, “Chapter 16: Properties and Structures of Iron Doped Carbon Resin Electrodes for Wastewaters Treatment,” *Solid Waste Management and Environmental Remediation*. Edited by Faerber, T and Herzog, J. Nova Science Publisher Inc New York. pp. 467–484, 2010.
- [47] I. A. Oke, M. A. Asani, J. A. Otun, N. O. Olarinoye, and S. Lukman, “Chapter 10: Effects of Aluminium and Calcium Oxide on Carbon Resin Electrodes Developed for Use in Electrochemical Treatment of Wastewaters. Edited by Adeyemo, R. Cuviller Verlag Gottingen, Internationaler Wissenschaftlicher Fachverlag. pp. 67–74, 2010.
- [48] I. A. Oke, L. E. Umoru, K. T. Oladepo, and M. O. Ogedengbe, “Utilization of weibull techniques to describe stability distribution of carbon resin electrodes,” *Ife Journal of Technology*, Vol. 17(1), pp. 35–46, 2008.
- [49] I. A. Oke, “Influence of carbonization on selected engineering properties of carbon resin electrodes for electrochemical treatment of wastewater,” *Canadian Journal of Chemical Engineering*, Vol. 87(10), pp. 801–811, 2009. [\[CrossRef\]](#)
- [50] I. A. Oke, D. B. Adie, A. Ismail, S. Lukman, S. B. Igboro, and M. I. Sanni, “Computer Simulation In The Development And Optimization Of Carbon Resin Electrodes For Water And Wastewater Treatment Electrochemically,” *Ife Journal of Science*, Vol. 16(2), pp 227– 239, 2014.
- [51] I. A. Oke, S. Lukman, T. A. Aladesanmi, E. O. Fehintola, S. J. Amoko, and O. O. Hammed, “Chapter 8 Electrochemical Treatment of Wastewater: An Emerging Technology for Emerging Pollutants,” in *Effects of Emerging Chemical Contaminants on Water Resources and Environmental Health*. Edited by Victor Shikuku. Published in the United States of America by IGI Global. pp. 133–157, 2020. [\[CrossRef\]](#)
- [52] I. A. Oke, and M. O. Ogedengbe, “The performance of a locally developed electrolysing equipment,” *FUTAJEET*, Vol. 5(2), pp 142–146, 2007.
- [53] E. O. Fehintola, E. A. Adekunbi, B. M. Ojo, L. Gbadamosi, O. K. Olayanju, and I. A. Oke, “Performance evaluation of a simple electrochemical treatment model for saline wastewaters: Part A,” *Egyptian Journal of Chemistry*, 2022.
- [54] APHA, “Standard Method for the Examination of Water and Wastewater”, 22nd edn, America Water Works Association and Water Pollution Control Federation, Washington DC. 2012.
- [55] M. C. M. van Loosdrecht, P. H. Nielsen, C. M. Lopez-Vazquez, and D. Brdjanovic, “Experimental Methods in Wastewater Treatment,” 1st ed, International Water Publishing Alliance House, 2016. [\[CrossRef\]](#)
- [56] I. A. Oke, O. A. Obijole, E. A. Adekunbi, J. O. Babajide, M. D. Iidi, and O. T. Aladesanmi, “Thermal property of carbon resin electrodes developed for electrochemical treatment of water and wastewaters,” *FUTAJEET*, Vol. 15(1), pp. 84–91, 2021. [\[CrossRef\]](#)

- [57] A. Vijaya Bhaskar, R. Zulkifii, Y. J. Jaafar, A. B. Aris, and A. M. Zaiton, "Simulation of a conventional water treatment plant for the minimization of new emerging pollutants in drinking water sources: process optimization using response surface methodology," *RSC Advances*, Vol. 7, Article 11550, 2017. [\[CrossRef\]](#)
- [58] B. Z. Can, R. Boncukcuoglu, A. E. Yilmaz, and B. A. Fil, "Effect of some operational parameters on the arsenic removal by electrocoagulation using iron electrodes," *Journal of Environmental Health Science & Engineering*, Vol. 12, pp. 95–98, 2014. [\[CrossRef\]](#)
- [59] C. Darvishi R. Soltani, A. Khataee, H. Godini, M. Safari, M. Ghanadzadeh, and M. Rajaei, "Response surface methodological evaluation of the adsorption of textile dye onto biosilica/alginate nanobio-composite: thermodynamic, kinetic, and isotherm studies," *Desalination and Water Treatment*, Vol. 56, pp.1389–1402, 2015. [\[CrossRef\]](#)
- [60] C. Majumder, and A. Gupta, "Prediction of arsenic removal by electrocoagulation: Model development by factorial design," *The Journal of Hazardous, Toxic, and Radioactive Waste*, Vol. 15, pp. 48–54, 2010. [\[CrossRef\]](#)
- [61] V. Gilhotra, L. Das, A. Sharma, T. S. Kang, P. Singh, R. S. Dhuria, and M. S. Bhatti, "Electrocoagulation technology for high strength arsenic wastewater: process optimization and mechanistic study," *Journal of Cleaner Production*, Vol. 198, pp. 693–703, 2018. [\[CrossRef\]](#)
- [62] M. Yao, L. D. Tijing, G. Naidu, S. H. Kim, H. Matsuyama, A. G. Fane, and H. K. Shon, "A review of membrane wettability for the treatment of saline water deploying membrane distillation," *Desalination*, Vol. 479, Article 114312, 2020. [\[CrossRef\]](#)
- [63] S. Gadkari, S. Gu, and J. Sadhukhan, "Towards automated design of bioelectrochemical systems: A comprehensive review of mathematical models," *Chemical Engineering Journal*, Vol. 343, pp. 303–316, 2018. [\[CrossRef\]](#)
- [64] M. Elimelech, and W. A. Phillip, "The future of seawater desalination: Energy, technology, and the environment. *Science*, Vol. 333, pp. 712–717, 2011. [\[CrossRef\]](#)
- [65] A. E. D. Mahmoud, "Graphene-based nanomaterials for the removal of organic pollutants: Insights into linear versus nonlinear mathematical models," *Journal of Environmental Management*, Vol. 270, Article 110911, 2020. [\[CrossRef\]](#)
- [66] I. S. Amin, A. N. Neysari, R. H. Althomali, E. A. Musad Saleh, S. Baymakov, A. H. Radie Alawady, A. Hashiem Alsaalamy, M. F. Ramadan, and A. Juyal, "Development of microextraction methods for the determination of sulfamethoxazole in water and biological samples: modelling, optimization and verification by central composite design," *Frontiers in Environmental Science*, Vol. 11, Article 1242730, 2023. [\[CrossRef\]](#)



Research Article

PbO₂/graphite and graphene/carbon fiber as an electrochemical cell for oxidation of organic contaminants in refinery wastewater by electro-fenton process; electrodes preparation, characterization and performance

Rowaida N. ABBAS¹, Ammar S. ABBAS²

¹Department of Refining, Baghdad Oil Training Institute, Ministry of Oil, Baghdad, Iraq

²Department of Chemical Engineering, College of Engineering, University of Baghdad, Baghdad, Iraq

ARTICLE INFO

Article history

Received: 19 October 2023

Revised: 26 February 2024

Accepted: 27 February 2024

Key words:

Carbon fiber; Electro-fenton;
Graphene; Graphite; Oxidation;
Phenol removal

ABSTRACT

The electro-Fenton oxidation process was used to treat organic pollutants in industrial wastewater as it is one of the most efficient advanced oxidation processes. The novel cell in this process consists of a prepared PbO₂ electrode by electrodeposition on graphite substrate and carbon fiber modified with graphene as a cathode. X-ray diffraction, fluorescence, analysis system, atomic force microscopy, and scan electron microscopy were used to characterize the prepared anode and cathode. XRD patterns clearly show the characteristic reflection of the mixture of α - and β phases of PbO₂ on graphite and carbon fiber, and AFM results for cathode and anode present that PbO₂ on graphite substrate and graphene on carbon fiber surface are on a nanoscale. Contact angle measurement was determined for the carbon fiber cathode before and after modification. The anodic polarization curve showed a higher anodic current when utilizing the PbO₂ anode than the graphite anode. Phenol in simulated wastewater was removed by electro-Fenton oxidation at 8 mA/cm² current density, 0.4 mM of ferrous ion concentration at 35 °C up to 6 h of electrolysis. Chemical oxygen demand for the treated solution was removed by 94.02% using the cell consisting of modified anode and cathode compared with 81.23% using modified anode and unmodified cathode and 79.87% when using unmodified anode and modified cathode.

Cite this article as: Abbas RN, Abbas AS. PbO₂/graphite and graphene/carbon fiber as an electrochemical cell for oxidation of organic contaminants in refinery wastewater by electro-fenton process; electrodes preparation, characterization and performance. Environ Res Tec 2024;7(2)175–185.

INTRODUCTION

Organic pollutants such as benzoic acid, oxalic acid, phenols, and phenolic derivatives have been used in a variety of industries, such as formaldehyde resins, pharmaceuticals, pesticides, textiles, dyes, petroleum refineries, paint removal, varnish printing, and dyeing fabrics [1, 2]. After these industrial processes, this compound is discharged into the water effluents. The extensive pollution of these compounds

in aqueous streams has been considered the most harmful and persistent organic contaminants in wastewater produced by various industries [3, 4]. Degradation of aqueous effluent containing phenol and phenolic derivatives is of primary concern due to its toxicity to human and aquatic life, even at low concentrations. Phenolic wastewater is listed among the most severe environmental pollutants [5–7]. Complete oxidation of these organic pollutants is significant at the end of wastewater treatment [8].

*Corresponding author.

*E-mail address: ammarabbas@coeng.uobaghdad.edu.iq



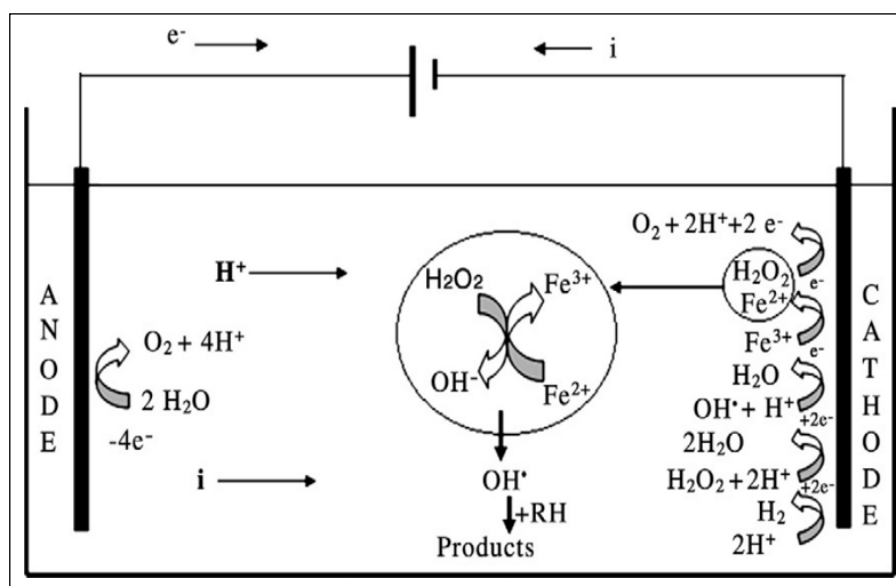


Figure 1. Electro-Fenton process.

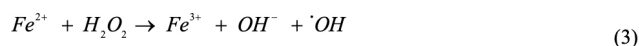
The traditional treatment technique, such as biological and chemical oxidation, no longer satisfies modern industry requirements for processes, so they need alternative methods [6]. Biodegradation is a very economical method for wastewater treatment for organic compounds, but this technique cannot treat phenolic wastes because of their resistance to microorganisms [9]. Phenol adsorption by some adsorbents like activated carbon adsorbs phenolic and phenolic compounds by firm contact between phenols and the positive charge of activated carbon. Adsorption is considered an economical and efficient method to remove pollutants, but the adsorption capacity of the adsorbent limits it and cannot be renewable easily [10]. Phenol removed by activated carbon is not degraded but removed from the aqueous stream and passed into another phase. Adsorption of a phenolic compound may cause the formation of hazardous by-products (secondary pollution) [11].

The chemical oxidation process utilizes strong oxidants that degrade phenolic pollutants with a fast oxidation rate and do not produce secondary pollutants. However, this process is costly and has some operational problems [12, 13]. Other treatment methods include Fenton oxidation, photocatalytic degradation, ozone treatment, and electrochemical [14].

Recently, a more efficient and non-selective process, advanced oxidation processes (AOPs), offer an effective and rapid alternative treatment for various pollutants. In AOPs, a strong oxidant, hydroxyl radical ($\cdot\text{OH}$), generated in situ, destroyed more organic pollutants until their complete mineralization into CO_2 , water, and inorganic ions [15–17]. One of these AOPs is Fenton oxidation. The Fenton process is an essential treatment method as it is simple, does not need special equipment, and gives high efficiency in removing organic pollutants [18].

The Fenton oxidation process has some disadvantages, such as the storage and transportation of hydrogen peroxide (H_2O_2); its activity is less than the modified one called the

electro-Fenton oxidation process. In the electro-Fenton oxidation process, ferrous ion (Fe^{2+}) is added, and H_2O_2 is generated electrochemically in situ at the cathode by two-electron oxygen reduction as shown in Figure 1 (RH represents an organic molecule) [15]. The cathode must have an appropriate potential to form H_2O_2 from the two-electron reduction of O_2 (Eq. 1), and the famous electrodes used for his purpose are the carbonous electrodes such as reticulated vitreous carbon, carbon felt, carbon sponge, and graphite [15, 19, 20]. Electro-decomposition of H_2O_2 produced ($\cdot\text{OH}$) also at the cathode (Eqs. 2 and 3) [21, 22].



Through (Eq. 3), Fe^{3+} is formed continuously, and through (Eq. 4), continuous regeneration of Fe^{2+} at the cathode, thus avoiding Fe^{3+} accumulation in the reaction medium and accordingly eliminating the production of iron sludge [23].



The anode material is one of the leading parameters in the electrochemical reaction processes because it intensely influences the mechanism of the decomposition reaction and, accordingly, the products of the anodic reaction [24]. The generally used anode materials for decomposing organic contaminants in wastewater are graphite, lead dioxide, nickel, and platinum. Some electrodes lose their activity rapidly or have high cost and mechanical resistance problems; also, it is difficult to find a suitable material that deposits on it [25]. Other electrodes have a short lifetime, and they have partially oxidized the organic pollutants in wastewater [26]. Active anodes, such as platinum (Pt), ruthenium oxide (RuO_2), and iridium oxide (IrO_2), have been used a lot recently because they have high electrocatalytic activity and high chemical stability [27, 28]. Active anodes partially

oxidize organic pollutants because of their low oxygen evolution potential, which reduces their current efficiency for degradation reactions [29]. On the other hand, the PbO₂ electrode has high electrochemical stability [30], good electrical conductivity, high chemical inertness, and high stability in corrosive solutions [31, 32], and oxidized organic compounds such as phenol effectively [33]. PbO₂ electrodes can be efficiently and economically prepared [30].

The cathode anode material is also crucial in electrochemical oxidation, especially in electro-Fenton oxidation. Carbonous material is used extensively as cathodes in electro-Fenton oxidation due to its surface area, porosity, chemical inertness, etc. In order to increase the efficiency of the electro-Fenton process, effective H₂O₂ must be produced. The cathode is the working electrode in the electro-Fenton process, and its modification can be achieved by different methods to improve H₂O₂ production. The H₂O₂ rate produced in situ through the reaction and the hydroxyl radical rate depends mainly on the cathode material's nature and properties. Some modification methods aim to increase the cathode's specific surface area and hydrophilicity. Others raise catalytic activity by increasing the active site on its surface and electrode conductivity. This modification will increase the production rate of H₂O₂ and thereby increase the degradation rate of organic pollutants [34, 35].

This work deals with preparing PbO₂ electrodeposited on graphite substrate as an anode and carbon fiber modified by graphene as a cathode. PbO₂ was used to promote the electrochemical activity of graphite electrodes, and graphene was utilized to improve the H₂O₂ production on the cathode electrode. The prepared anode electrode was characterized by X-ray diffraction (XRD), X-ray fluorescence (XRF), scan electron microscopy (SEM), energy dispersive X-ray analysis system (EDX), and atomic force microscopy (AFM.) The modified cathode was characterized by XRD, XRF, SEM, EDX, AFM, and contact angle measurement. The novel cell consists of modified electrodes used in the electro-Fenton oxidation process of phenolic derivatives in simulated wastewater.

MATERIALS AND METHODS

All chemicals used in the experiments were of reagent grade, and there was no need for further purification. Lead Nitrate Pb(NO₃)₂, Sodium Laureth Sulfate (SLS surfactant), Nitric Acid (HNO₃), phenol, sulfuric acid (H₂SO₄), and distilled water were used in the preparation of all aqueous solutions.

The electrochemical cell had a 400 mL capacity. A hot plate magnetic stirrer reserved the cell heat (LABINCO, model L-81) supplied by power by DC power supply (KA3005D Digital Control DC Power Supply 30V 5A) with outlet voltage (0–30V) and output current (0–5 A).

PbO₂ Electrode Preparation (Anode Modification)

Before the deposition process, the graphite plate with dimensions of (3*10 cm²) was well cleaned and boiled in dis-

tilled water for 30 min. The graphite plate was then activated electrochemically in an open, undivided cell in a 1.44 M (H₂SO₄) solution, and a 14 mA/cm² current density was applied at 90 °C for 30 min. Electrode modification occurs by depositing a film of PbO₂ on electrode surfaces. The cell consists of two graphite plates as anode and a cathode used to prepare the anode electrode. The distance between the anode and the cathode in the electrodeposition cell was 3 cm. The PbO₂ film on the graphite plate was produced using an electrolyte (pH 1.6) containing 0.2 M of lead nitrate (Pb(NO₃)₂), 0.1 M of HNO₃, and 0.4 ml of SLS surfactant. The electrolytic solution was heated to 65 °C, and the current density applied was 1.1 mA/cm². After 3 h of electrodeposition, the electroplated electrode was washed with distilled water and kept dry for electrochemical oxidation of simulated wastewater [30].

Graphene Electrode Preparation (Cathode Modification)

Carbon fiber with a dimension of (3*10 cm²) was used as the base cathode, and 0.5 g of graphene was used to modify it. Mixing 0.14 mL of Polytetrafluoroethylene (PTFE), 3 mL of ethanol, and 2 mL of deionized water, a kind of slurry was formed, coated on the carbon fiber's two sides. Then, it dried at room temperature and was calcinated for 30 min at 360 °C [36].

Electro-Fenton Oxidation Process

The electro-Fenton oxidation process degraded phenolic pollutants in simulated wastewater. The simulated wastewater was prepared with 150 ppm of phenol by adding 150 mg to 1 L of distilled water. Sodium sulfate (Na₂SO₄) with a concentration of 0.05M was used as a supporting electrolyte, and the pH of the solution was justified to 2–3 by 0.1M of H₂SO₄. The two electrodes (anode and cathodes) were dipped into the electrolytic solution and connected to the DC power supply that applied a constant current density at 8 mA/cm² up to 6 h at 35 °C and 200 rpm rotation speed. Compressed air was bubbled into the solution at a flow rate of 1 liter per minute using an electromagnetic air pump (ACO-001), externally added FeSO₄·7H₂O with a concentration of (0.4 mM). Finally, the samples were collected during the electrolysis process, and the concentration of phenol was determined by measuring the chemical oxygen demand (COD) using a COD reactor (Lovibond® Water Testing, MD 200 COD, tube tests, Germany) (Eq. 5).

$$\text{COD removal, \%} = \frac{\text{COD}_0 - \text{COD}_t}{\text{COD}_0} \times 100 \quad (5)$$

RESULTS AND DISCUSSION

Characterization of the Electrodes

XRD

XRD technique was used to find out the phase and structure of the prepared anode electrode in the range between 0 and 80° of 2θ for electrodeposition of PbO₂ on graphite at 65 °C, and the current density applied was 1.1 mA/cm².

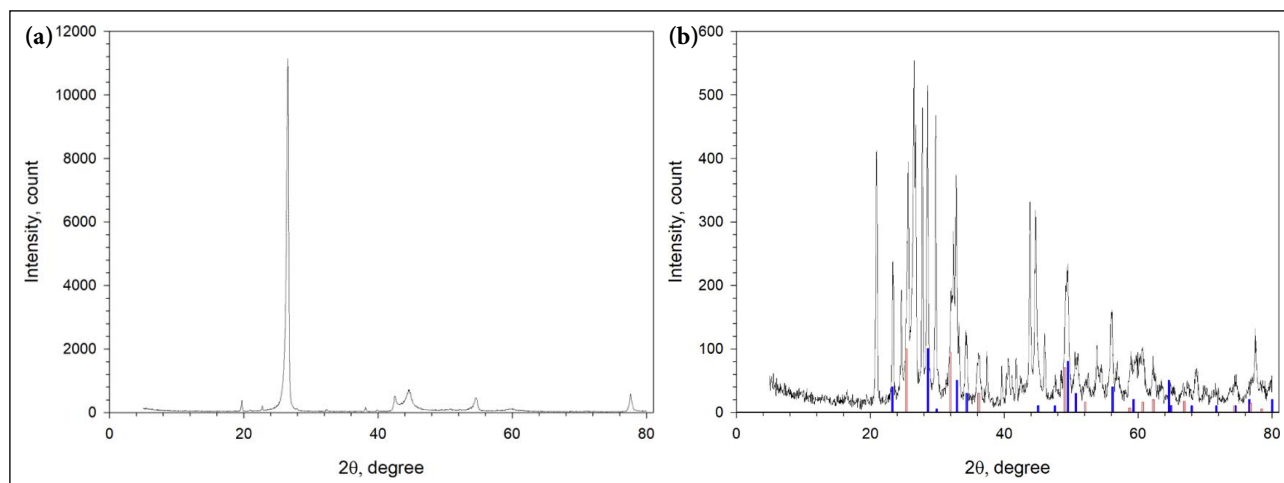


Figure 2. XRD pattern of graphite anode (a) original (b) modified by PbO_2 .

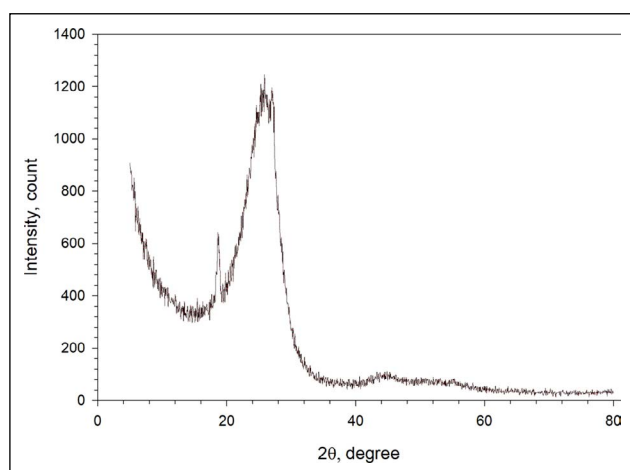


Figure 3. XRD pattern for carbon fiber cathode after modification with graphene.

Figure 2a shows the XRD patterns of the original graphite anode electrode before the electrodeposition process, and Figure 2b shows the XRD patterns of PbO_2 on the graphite anode electrode.

XRD pattern for graphite before the electrodeposition process (Fig. 2a) showed that it is identical to the standard card and has a distinctive peak at 26° of 2θ . After the deposition process, (Fig. 2b), the XRD peaks of orthorhombic PbO_2 were assigned at 2θ values of 23.402° (1 1 0), 28.549° (1 1 1), 32.611° (0 0 2), 34.3193° (0 2 1), 36.1743° (2 0 0), 40.5751° (1 1 2), 45.3306° (0 2 2), 47.6418° (2 2 0), 49.3314° (1 3 0), 50.7798° (2 2 1), 55.9957° (1 1 3) and 58.9747° (2 2 2) and these angles refer to the existence of the phase α - PbO_2 as compared with the standard card JCPDS:75-2414 and literature [37].

Furthermore, there are peaks presented in XRD patterns for the prepared electrode indicated to the presence of β phases of PbO_2 at 2θ values of 25.6413° (1 1 0), 32.0908° (0 1 1), 52.0773° (2 2 0), 54.4201° (0 0 2), 60.6214° (1 1 2), and 62.2500° (0 3 1), 66.6972° (0 2 2). XRD patterns clearly show the characteristic reflection of a mixture of α - and β phases of PbO_2 compared with the standard card JCPDS:75-2414

Table 1. XRF elemental composition report of PbO_2 deposit on graphite (normalized)

Symbol	Element	Conc., %
K_2O	Potassium	0.16
CaO	Calcium	3.26
PbO	Lead	95.97
ZrO_2	Zirconium	0.22
Ta_2O_5	Tantalum	0.39
Sum of concentration		100

for α - PbO_2 and JCPDS:75-2420 for β - PbO_2 (standard cards of α - PbO_2 and β - PbO_2 shown in Figure 2b the red and blue line, respectively) [37, 38]. The average crystallite size of electrodepositing PbO_2 on graphite was 27.05 nm, and the crystallinity was 80.02%.

The XRD pattern of the modified carbon fiber cathode electrode with graphene on its surface is shown in Figure 3. The pattern showed a sharp diffraction peak at 2θ values of 26.99° (0 0 2), which was attributed to the crystalline graphitic structure. There is a weaker sharp peak at 2θ values of 18.81° , which refers to PTFE as it is used in the modification process.

XRF

The quantitative chemical composition of the electrodeposit PbO_2 on the anode electrode surface was investigated by the XRF analytical technique, and the results were listed in Table 1 as the weight percent of each component. Clearly, lead (Pb) (as oxide) had the highest weight percentage of 95.97%.

SEM

SEM images of the graphite plate coated with a layer of PbO_2 can be detected at two different magnifications (with different scales) in Figure 4. PbO_2 is coated on the graphite plate substrate uniformly and without cracking, mostly in clusters and highly compressed structures that firmly adhere to the graphite electrode surface. The layer-coated graphite

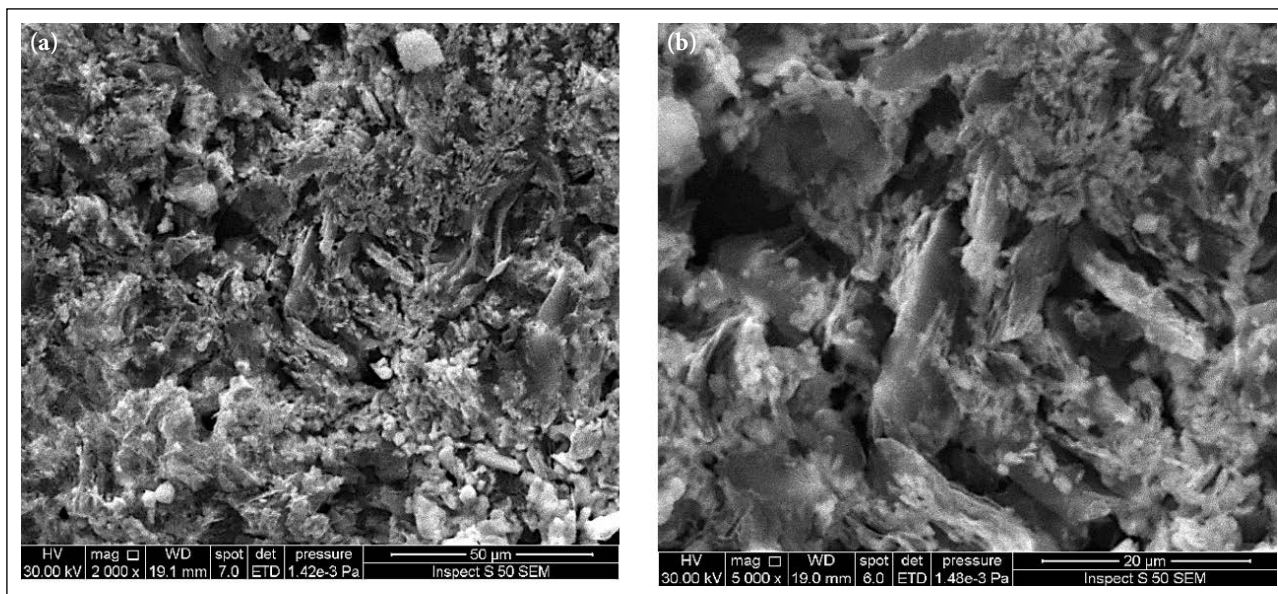


Figure 4. SEM images of PbO₂ deposit on graphite plate from an acidic electrolyte at 65 °C, 1.1 mA/cm², and 200 rpm for 3 hours (a) 50 μm and (b) 20 μm.

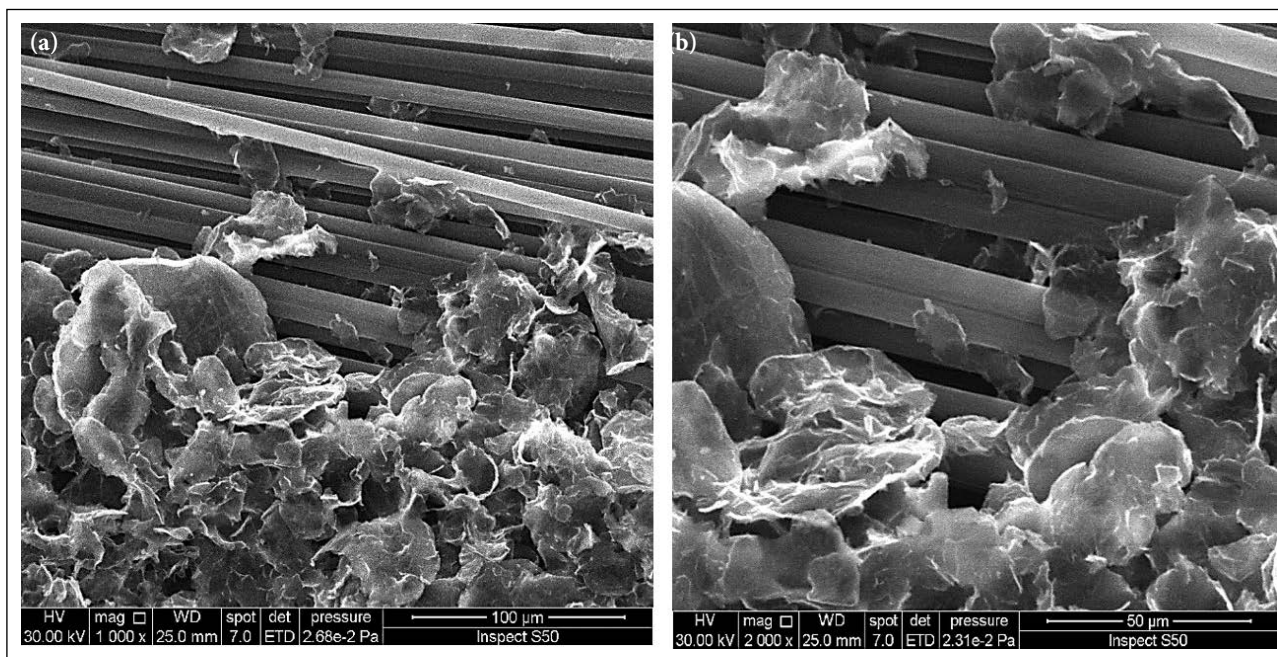


Figure 5. SEM image of graphene on carbon fiber (a) 100 μm, and (b) 50 μm.

showed tiny rough crystals of PbO₂ over the graphite plate. The crystals may have different growth rates. A more specific surface area can be obtained with the rough surface, leading to better interaction during the degradation of phenol and phenolic derivatives through the electrochemical reaction. The even surface obtained after deposition supported the adherence between the electrodeposited layer and the graphite substrate. This results in agreement with previous researchers [2, 4, 39].

The morphology of graphene on carbon fiber cathode electrode was also detected by using SEM. The SEM micrographs of the prepared cathode are shown in Figure 5.

The graphene flakes were thin sheets, and all of them were arranged on the surface of carbon fiber.

Figure 6a, b presented the original and modified carbon fiber, and the thickness of each felt in carbon fiber increases with modification. Carbon fiber has a smooth surface, and improvement with graphene made its surface rough, increasing its surface and active sites. The graphene has formed a clear layer on the carbon fiber, and penetration of graphene between the carbon fiber threads can be noticed, which increases the surface area, improves electrode performance, H₂O₂ production, and the chance of entering the reaction solution mixture between the carbon fiber threads [34].

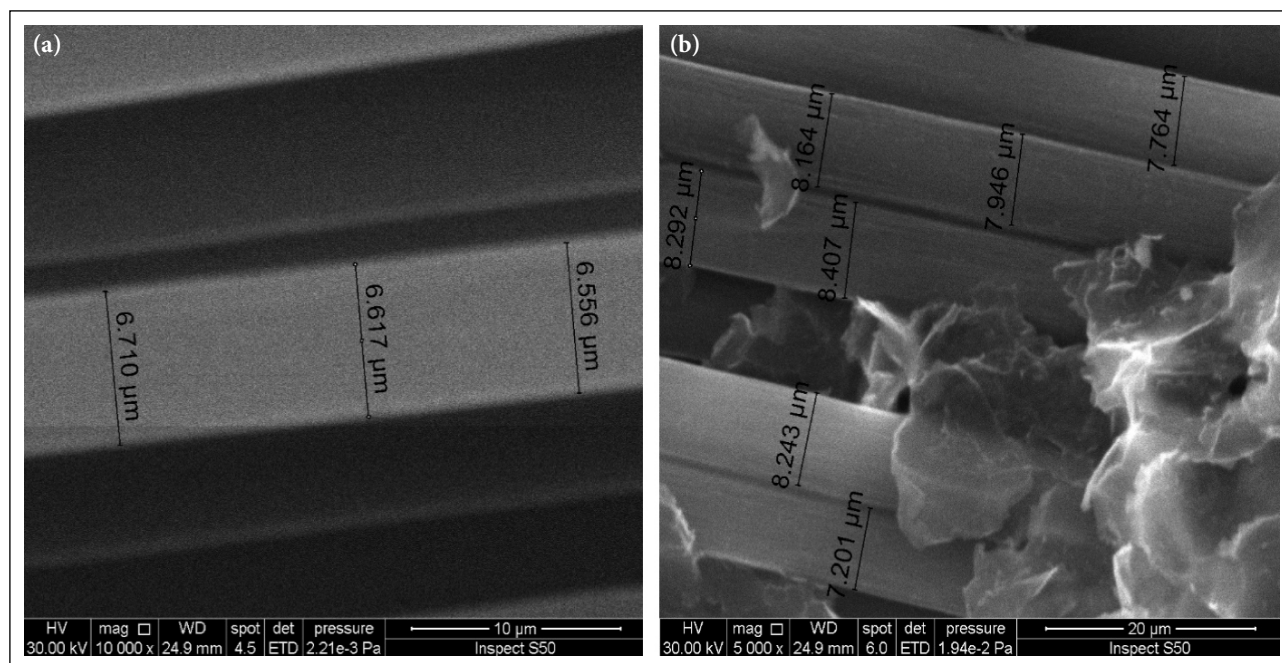


Figure 6. SEM image of carbon fiber (a) before modification with graphene and (b) after modification with graphene.

Table 2. Amplitude parameters for PbO_2 on graphite and graphene on carbon fiber

Amplitude parameters	PbO_2 on graphite	Graphene on carbon fiber
Roughness average (S_a), nm	100.3	32.86
Root mean square (S_q), nm	123.40	48.15
Surface skewness (S_{sk})	-0.097	2.219
Surface kurtosis (S_{ku})	2.558	10.901
Maximum peak height (s_p), nm	377.8	401.6
Maximum pit height (s_v), nm	379.6	97.86
Ten-point height (S_z), nm	757.4	499.5

AFM

The surface topography was evaluated quantitatively to understand the surface texture and morphology. One of the techniques used to characterize nanoscale surface topography is the AFM technique. This technique is better than other microscopic techniques because of its flexibility and facilities. AFM test made for PbO_2 on graphite anode electrode and graphene on carbon fiber cathode electrode and amplitude parameters of the obtained graphite and carbon fiber after modification on their surfaces presented in (Table 2).

The graphite statistical summary for the electrodeposit PbO_2 shows that the mean diameter was 449 nm, the minimum diameter was 242 nm, and the maximum was 772 nm.

Contact Angel Measurement

The contact angles were utilized regularly to measure the hydrophilicity of carbon materials. The contact angle of carbon fiber before modification was 90.67° and became 81.32° after modification with graphene, as shown in Figure

7. These contact angle values evidenced that the hydrophobic property of carbon fiber decayed noticeably by modification with the graphene. A Droplet of water dispersed when it contacted the modified carbon fiber surface. One of the essential features that affect the electro-Fenton oxidation process is the hydrophilicity of the cathode material. The cathode with the highest hydrophilicity provides helpfulness to O_2 diffusion and, accordingly, the highest H_2O_2 production [40, 41].

Raman Spectrometer

Raman test is considered the most active, fast, and non-destructive technique used to describe the structure and quality of carbon material and identify defects and irregular structures [42, 43]. In the Raman technique, G-band and D-bands are characteristics of ordered and disordered materials, respectively [44]. The ratio of the intensity of the D-line and G-line was used to indicate the defects in the material [43, 45, 46].

A typical Raman spectrum for the origin carbon fiber is shown in Figure 8a, and for modified carbon fiber, it is shown in Figure 8b. D-band peak at about 1350 cm^{-1} indicates the presence of significant defects. The D band was usually correlated to a series of defects, including bonding disorders and vacancies in graphene lattice [47]. G-band at about 1600 cm^{-1} peak corresponds to the graphitic carbon [48, 49].

The modified carbon fiber exhibited a clear D-band (as shown in Figure 8b, whereas the original carbon fiber did not have the D-band (there is a valley at about 1350 cm^{-1} , not a peak), as shown in Figure 8a. The valley in this region indicates the absence of significant defects. D-band was related to the disorder and defect in the structure because of the disorderliness in the graphene sheets [49].

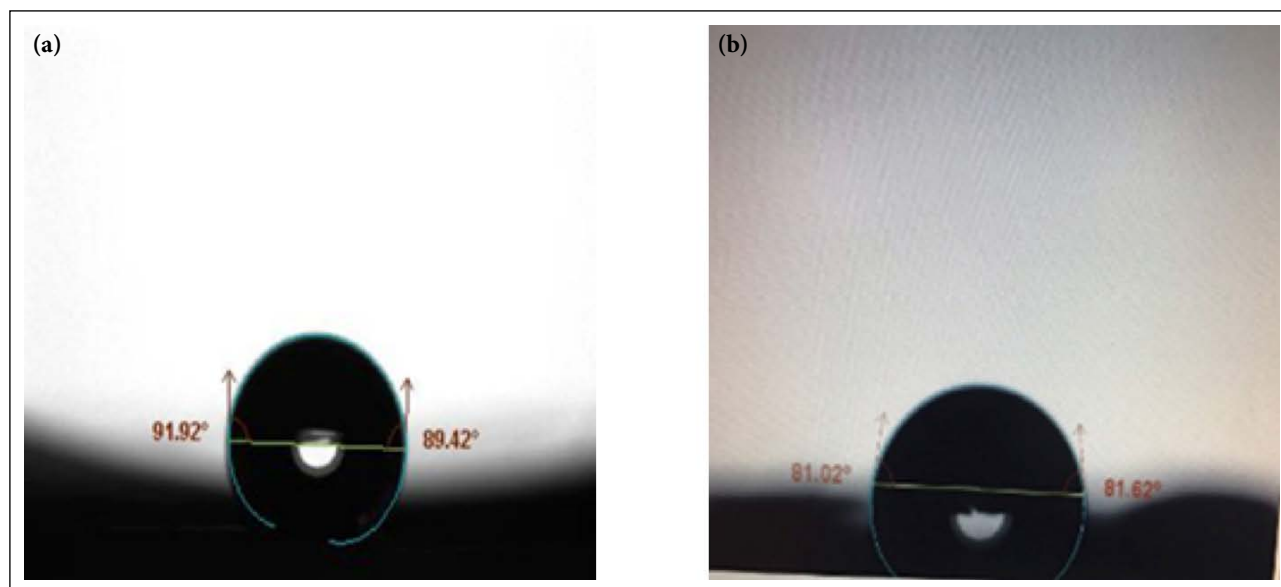


Figure 7. Contact angle for carbon fiber cathode (a) before modification (b) after modification with graphene.

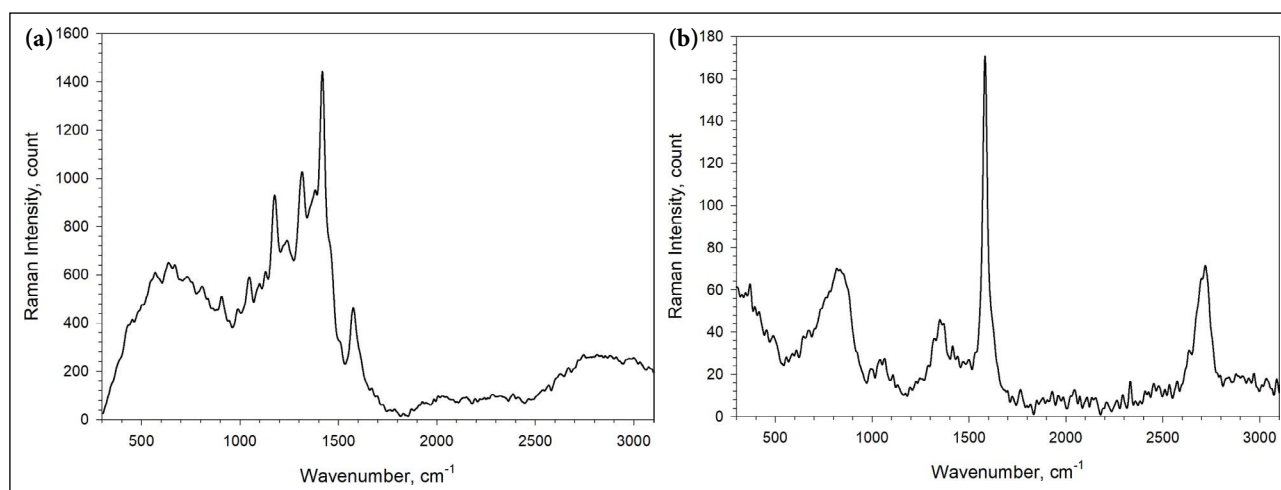


Figure 8. A typical Raman spectrum of carbon fiber (a) before modification (b) after modification with graphene.

Defects and distortion were efficiently enhanced by modification of carbon fiber with graphene, which will improve the activity of oxidation-reduction reaction and provide more active sites and, thereby, H_2O_2 generation [50–54].

The intensity ratio of the D-band to G-band (ID/IG) obtained from Raman spectra results after modification with graphene was about 0.314.

Anodic Polarization

The electrochemical performance of the PbO_2 electrode was studied by linear sweep voltammetry in an acidic solution of 0.1 M H_2SO_4 in the potential window of 0–3V versus SCE at a scan rate of 50 mV/s. The anodic linear sweep voltammograms for phenol oxidation on graphite and PbO_2 on graphite anodes were shown in Figure 9. A higher anodic current was detected when utilizing the PbO_2 anode electrode than the graphite anode electrode in the oxidation of phenol and its derivatives in simulated wastewater. A higher current of the PbO_2 electrode, perhaps because of the electrodeposited

layer of PbO_2 , improves the anode electrode's performance in the electro-Fenton oxidation technique. Consequently, PbO_2 anode denotes a capable anode electrode material for wastewater treatment comprising phenolic compounds compared to graphite or carbon-based materials.

Cod Removal

Figure 10 shows the effect of using modified electrodes (anode and cathodes) on the COD removal efficiency by the electro-Fenton oxidation process. Figure 10 shows that the COD removal after 6 h was 62.33% using unmodified electrodes (anode and cathode). COD removal was 81.23% using a modified anode (PbO_2 on graphite) and unmodified cathode (carbon fiber) and 79.87% by using an unmodified anode (graphite) and modified cathode (Graphene on carbon fiber). Using the two modified electrodes, the COD removal reached 94.02%. Oxidation efficiency using an unmodified anode electrode increased slightly after four hours of electrolysis. Modified anode by deposition layer of PbO_2 on it led to increase oxidation efficiency of organic pollutants.

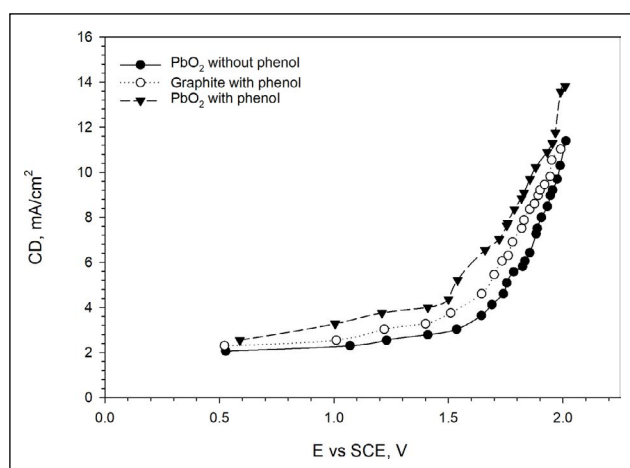


Figure 9. Anodic polarization curves (a) H_2SO_4 (0.1M)- PbO_2 anode (b) phenol (150 ppm) - H_2SO_4 (0.1M) - graphite anode (c) phenol (150 ppm) - H_2SO_4 (0.1M)- PbO_2 anode.

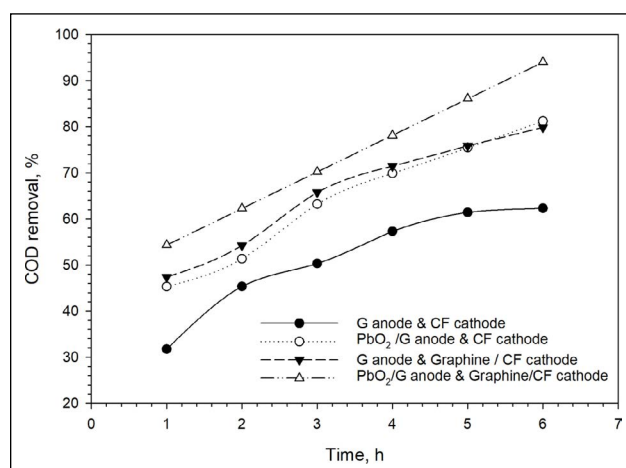


Figure 10. Comparison of COD removal between modified and unmodified electrodes by the electro-Fenton oxidation process.

Oxidation efficiency was still increasing noticeably after four hours because the modified anode has high stability and resistance to corrosion. Also, the deposition of PbO_2 on graphite gives an anode electrode with good electrochemical oxidation of COD removal because it has high electrical conductivity and increases the overpotential for oxygen evolution. PbO_2 layer deposit increases the hydroxyl radical yield, decreases the energy consumption, and increases the current efficiency [30, 32, 55]. Modified cathode using graphene increases the COD removal efficiency because graphene has a high surface area and excellent conductivity. It leads to an increase in the electron transfer rate and thereby improves the production of (H_2O_2) from the reaction of oxygen reduction that occurs on the cathode electrode [34, 36, 47]. The generation of H_2O_2 controls the rate of Fenton reaction and the formation rate of homogeneous $\cdot\text{OH}$ in the medium [36, 56, 57].

Organic pollutants in real wastewater from one of the Iraqi refineries were also treated by using this cell sand electro-Fenton oxidation process at 8 mA/cm^2 CD, 35°C operating temperature, 0.4 mM of Fe^{2+} up to 6h. Figure 11 compares the COD removal results for simulated and real wastewater. It was evident from Figure 11 that the removal efficiency for simulated wastewater is higher than that of real wastewater and that, perhaps because of the formation of intermediate, many side reactions occur when treating real refinery wastewater. Real wastewater contains different contaminants that might participate in unknown reactions or act as a catalyst to improve the unwanted reactions or increase the indirect electrochemical oxidation process because of existing highly dissolved salts that need higher current applied.

Using PbO_2 /Graphite and Graphene/Carbon Fiber as the anode and cathode, respectively, the electro-Fenton process was applicable for treating simulated wastewater at the best conditions. After 6 hours of electrolysis, a 94.02% COD removal efficiency was possible by starting with an initial COD concentration of about 320 ppm. The current research results were encouraging and were in the same

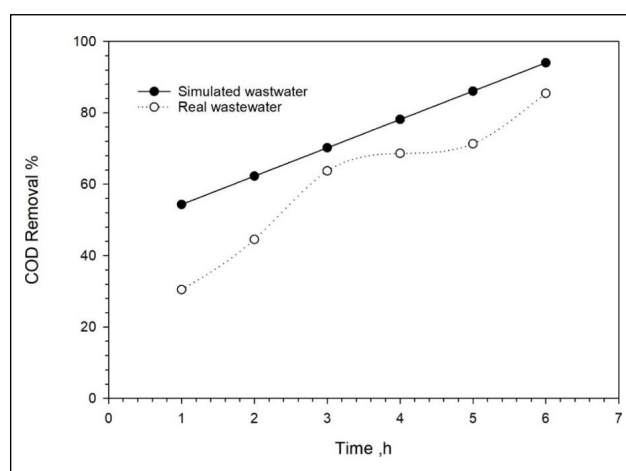


Figure 11. Comparison of COD removal between simulated and real wastewater by the electro-Fenton oxidation process.

magnitude for removing organics pollutants and COD from wastewater of petroleum refineries compared to the results of removal using electro-Fenton [36, 40, 58] or Fenton using heterogeneous catalysts [59–61].

CONCLUSION

A PbO_2 on graphite anode electrode was prepared for COD removal from phenolic wastewater. Characterization of the prepared anode electrode showed a mixture of α and β phases of PbO_2 with an average crystal size of 27.05 nm and an average particle size of 449 nm. Pb was the primary element in the electrodeposited material, with 95.97 weight %. (As oxide). Analysis of the morphology of the PbO_2 film deposit on graphite showed that the particles were well crystallized to form a uniform surface. Carbon fiber was modified using graphene, and morphology analysis showed that the graphene flakes were thin sheets. All of them were arranged on the surface of carbon fiber with an average particle size of 322 nm. Contact angle measurement presents that it increases with modification from 81.32° to 90.67° ,

and that improves the oxidation-reduction reaction. Raman test showed that the (ID/IG) for the modified carbon fiber cathode was about 0.314, which enhanced the oxidation-reduction reaction. The mechanism of the electro-Fenton oxidation process depends on $\cdot\text{OH}$ generated from H_2O_2 decomposition in the presence of Fe^{2+} . COD removal reached 94.02% using a modified anode and cathode at 8 mA/cm^2 and 0.4 mM of Fe^{2+} after 6 h of electrolysis at $35 \text{ }^\circ\text{C}$.

DATA AVAILABILITY STATEMENT

The author confirm that the data that supports the findings of this study are available within the article. Raw data that support the finding of this study are available from the corresponding author, upon reasonable request.

CONFLICT OF INTEREST

The author declared no potential conflicts of interest with respect to the research, authorship, and/or publication of this article.

USE OF AI FOR WRITING ASSISTANCE

Not declared.

ETHICS

There are no ethical issues with the publication of this manuscript.

REFERENCES

- [1] H. Abbar, and A. S. Abbas, "A kinetic study of oxalic acid electrochemical oxidation on a manganese dioxide rotating cylinder anode," *Portugaliae Electrochimica Acta*, Vol. 36(5), pp. 325–337, 2018. [\[CrossRef\]](#)
- [2] X. Duan, F. Ma, Z. Yuan, L. Chang, and X. Jin, "Electrochemical degradation of phenol in aqueous solution using PbO_2 anode," *Journal of the Taiwan Institute of Chemical Engineers*, Vol. 44(1), pp. 95–102, 2013. [\[CrossRef\]](#)
- [3] R. G. Saratale, K.-J. Hwang, J.-Y. Song, G. Dattatray Saratale, and D.-S. Kim, "Electrochemical oxidation of phenol for wastewater treatment using Ti/PbO_2 electrode," *Journal of Environmental Engineering(United States)*, Vol. 142(2), pp. 1–9, 2016. [\[CrossRef\]](#)
- [4] R. N. Abbas, and A. S. Abbas, "Feasibility of using carbon fiber, graphite, and their modified versions by PbO_2 as electrodes in electrochemical oxidation of phenolic wastewater," *AIP Conference Proceedings*, Vol. 2660, 2022. [\[CrossRef\]](#)
- [5] I. Polaert, A. M. Wilhelm, and H. Delmas, "Phenol wastewater treatment by a two-step adsorption-oxidation process on activated carbon," *Chimie-Ingenieur-Technik*, Vol. 73(6), pp. 1585–1590, 2001. [\[CrossRef\]](#)
- [6] F. Zhang, M. Li, W. Li, C. Feng, Y. Jin, X. Guo, and J. Cui, "Degradation of phenol by a combined independent photocatalytic and electrochemical process," in *Chemical Engineering Journal*, Vol. 175(1), pp. 349–355, 2011. [\[CrossRef\]](#)
- [7] R. N. Abbas, and A. S. Abbas, "The Taguchi approach in studying and optimizing the electro-fenton oxidation to reduce organic contaminants in refinery wastewater using novel electrodes," *Engineering, Technology & Applied Science Research*, Vol. 12(4), pp. 8928–8935, 2022. [\[CrossRef\]](#)
- [8] N. Bensalah, and A. Bedoui, "Enhancing the performance of electro-peroxone by incorporation of UV irradiation and BDD anodes," *Environmental Technology*, Vol. 38(23), pp. 1–28, 2017. [\[CrossRef\]](#)
- [9] P. H. Britto-Costa and L. A. M. M. Ruotolo, "Phenol removal from wastewaters by electrochemical oxidation using boron doped diamond (BDD) and $\text{Ti/TiO}_2/\text{RuO}_4$ electrodes," *Brazilian Journal of Chemical Engineering*, Vol. 29(4), pp. 763–773, 2012. [\[CrossRef\]](#)
- [10] P. Jin, R. Chang, D. Liu, K. Zhao, L. Zhang, and Y. Ouyang, "Phenol degradation in an electrochemical system with TiO_2 /activated carbon fiber as electrode," *The Journal of Environmental Chemical Engineering*, Vol. 2(2), pp. 1040–1047, 2014. [\[CrossRef\]](#)
- [11] M. H. El-Naas, S. Al-Zuhair, and M. A. Alhajja, "Removal of phenol from petroleum refinery wastewater through adsorption on date-pit activated carbon," in *Chemical Engineering Journal*, Vol. 162(3), pp. 997–1005, 2010. [\[CrossRef\]](#)
- [12] Y. X. Liu, Z. Y. Liao, X. Y. Wu, C. J. Zhao, Y. Xin Lei, and D. B. Ji "Electrochemical degradation of methylene blue using electrodes of stainless steel net coated with single-walled carbon nanotubes," *Desalination and Water Treatment*, Vol. 54(10), pp. 2757–2764, 2015. [\[CrossRef\]](#)
- [13] N. Jarrah, and N. D. Mu'azu, "Simultaneous electro-oxidation of phenol, CN^- , S^{2-} and NH_4^+ in synthetic wastewater using boron doped diamond anode," *Journal of Environmental Chemical Engineering*, Vol. 4(3), pp. 2656–2664, 2016. [\[CrossRef\]](#)
- [14] Q. J. Rasheed, K. Pandian, and K. Muthukumar, "Treatment of petroleum refinery wastewater by ultrasound-dispersed nanoscale zero-valent iron particles," *Ultrasonics Sonochemistry*, Vol. 18(5), pp. 1138–1142, 2011. [\[CrossRef\]](#)
- [15] M. Zhou, Q. Yu, L. Lei, and G. Barton, and "Electro-Fenton method for the removal of methyl red in an efficient electrochemical system," *Separation and Purification Technology*, Vol. 57, pp. 380–387, 2007. [\[CrossRef\]](#)
- [16] E. Rosales, M. Pazos, M. A. Longo, and M. A. Sanromán, "Electro-Fenton decoloration of dyes in a continuous reactor : A promising technology in colored wastewater treatment," *Chemical Engineering Journal*, Vol. 155, pp. 62–67, 2009. [\[CrossRef\]](#)
- [17] I. Sirés, E. Brillas, M. A. Oturan, M. A. Rodrigo, and M. Panizza, "Electrochemical advanced oxidation processes: Today and tomorrow. A review," *Environmental Science and Pollution Research*, Vol. 21(14),

- pp. 8336–8367, 2014. [CrossRef]
- [18] M. S. Lucas, and J. A. Peres, “Decolorization of the azo dye Reactive Black 5 by Fenton and photo-Fenton oxidation,” *Dyes and Pigments*, Vol. 71(3), pp. 236–244, 2006. [CrossRef]
- [19] A. Alvarez-Gallegos, and D. Pletcher, “The removal of low level organics via hydrogen peroxide formed in a reticulated vitreous carbon cathode cell, Part 1. The electrosynthesis of hydrogen peroxide in aqueous acidic solutions,” *Electrochimica Acta*, Vol. 44(5), pp. 853–861, 1998. [CrossRef]
- [20] M. Panizza, and G. Cerisola, “Electrochemical generation of H₂O₂ in low ionic strength media on gas diffusion cathode fed with air,” *Electrochimica Acta*, Vol. 54(2), pp. 876–878, 2008. [CrossRef]
- [21] Z. I. Abbas, and A. S. Abbas, “Oxidative degradation of phenolic wastewater by electro-fenton process using MnO₂-graphite electrode,” *The Journal of Environmental Chemical Engineering*, Vol. 7(3), Article 103108, 2019. [CrossRef]
- [22] R. N. Abbas, and A. S. Abbas, “Kinetics and energetic parameters study of phenol removal from aqueous solution by electro-fenton advanced oxidation using modified electrodes with PbO₂ and graphene,” *Iraqi Journal of Chemical and Petroleum Engineering*, Vol. 23(2), pp. 1–8, 2022. [CrossRef]
- [23] M. Panizza, and M. A. Oturan, “Degradation of Alizarin Red by electro-Fenton process using a graphite-felt cathode,” *Electrochimica Acta*, Vol. 56(20), pp. 7084–7087, 2011. [CrossRef]
- [24] Y. Yavuz, A. S. Kopalal, and Ü. B. Ögütveren, “Treatment of petroleum refinery wastewater by electrochemical methods,” *Desalination*, Vol. 258(1–3), pp. 201–205, 2010. [CrossRef]
- [25] A. S. Abbas, M. H. Hafiz, and R. H. Salman, “Indirect electrochemical oxidation of phenol using rotating cylinder reactor,” *Iraqi Journal of Chemical and Petroleum Engineering*, Vol. 17(4), pp. 43–55, 2016. [CrossRef]
- [26] A. H. Abbar, R. H. Salman, and A. S. Abbas, “Electrochemical incineration of oxalic acid at manganese dioxide rotating cylinder anode: Role of operative parameters in the presence of NaCl,” *Journal of the Electrochemical Society*, Vol. 163(13), pp. E333–E340, 2016. [CrossRef]
- [27] D. Rajkumar, J. G. Kim, and K. Palanivelu, “Indirect electrochemical oxidation of phenol in the presence of chloride for wastewater treatment,” *Chemical Engineering & Technology*, Vol. 28(1), pp. 98–105, 2005. [CrossRef]
- [28] Y. Jiang, H. Zhao, J. Liang, L. Yue, T. Li, Y. Luo, Q. Liu, S. Lu, A. M. Asiri, Z. Gong, and X. Sun, “Anodic oxidation for the degradation of organic pollutants: Anode materials, operating conditions, and mechanisms. A mini review,” *Electrochemistry Communications*, Vol. 123, Article 106912, 2021. [CrossRef]
- [29] C. Shao, F. Zhang, X. Li, J. Zhang, Y. Jiang, H. Cheng, and K. Zhu, “Influence of Cr doping on the oxygen evolution potential of SnO₂/Ti and Sb-SnO₂/Ti electrodes,” *Journal of Electroanalytical Chemistry*, Vol. 832, pp. 436–443, 2019. [CrossRef]
- [30] R. M. Farinos, R. L. Zornitta, and L. A. M. M. Ruoto-lo, “Development of three-dimensional electrodes of PbO₂ electrodeposited on reticulated vitreous carbon for organic electrooxidation,” *Journal of the Brazilian Chemical Society*, Vol. 28(1), pp. 187–196, 2017. [CrossRef]
- [31] X. Wu, H. Xu, L. Lu, H. Zhao, J. Fu, Y. Shen, P. Xu, and Y. Dong, “PbO₂-modified graphite felt as the positive electrode for an all-vanadium redox flow battery,” *Journal of Power Sources*, Vol. 250, pp. 274–278, 2014. [CrossRef]
- [32] V. Suryanarayanan, I. Nakazawa, S. Yoshihara, and T. Shirakashi, “The influence of electrolyte media on the deposition/dissolution of lead dioxide on boron-doped diamond electrode - A surface morphologic study,” *Journal of Electroanalytical Chemistry*, Vol. 592(2), pp. 175–182, 2006. [CrossRef]
- [33] C. Borrás, P. Rodríguez, T. Laredo, J. Mostany, and B. R. Scharifker, “Electrooxidation of aqueous p-methoxyphenol on lead oxide electrodes,” *Journal of Applied Electrochemistry*, Vol. 34(6), pp. 583–589, 2004. [CrossRef]
- [34] Y. Wang, Y. Liu, K. Wang, S. Song, P. Tsiakaras, and H. Liu, “Preparation and characterization of a novel KOH activated graphite felt cathode for the electro-Fenton process,” *Applied Catalysis B: Environmental*, Vol. 165, pp. 360–368, 2015. [CrossRef]
- [35] Z. Pan, K. Wang, Y. Wang, P. Tsiakaras, and S. Song, “In-situ electrosynthesis of hydrogen peroxide and wastewater treatment application: A novel strategy for graphite felt activation,” *Applied Catalysis B: Environmental*, Vol. 237, pp. 392–400, 2018. [CrossRef]
- [36] W. Yang, M. Zhou, N. Oturan, Y. Li, and M. A. Oturan, “Electrocatalytic destruction of pharmaceutical imatinib by electro-Fenton process with graphene-based cathode,” *Electrochimica Acta*, Vol. 305, pp. 285–294, 2019. [CrossRef]
- [37] H. Mo, Y. Tang, X. Wang, J. Liu, D. Kong, Y. Chen, P. Wan, H. Cheng, T. Sun, L. Zhang, M. Zhang, S. Liu, Y. Sun, N. Wang, L. Xing, L. Wang, Y. Jiang, X. Xu, Y. Zhang, and X. Meng, “Development of a three-dimensional structured carbon fiber Felt/ β -PbO₂ electrode and its application in chemical oxygen demand determination,” *Electrochimica Acta*, Vol. 176, pp. 1100–1107, 2015. [CrossRef]
- [38] N. Yu, L. Gao, S. Zhao, and Z. Wang, “Electrodeposited PbO₂ thin film as positive electrode in PbO₂/AC hybrid capacitor,” *Electrochimica Acta*, Vol. 54(14), pp. 3835–3841, 2009. [CrossRef]
- [39] T. M. Garakani, P. Norouzi, M. Hamzehloo, and M. R. Ganjali, “Electrodeposition of nano-structured PbO₂ on glassy carbon electrodes by FFT continuous cyclic voltammetry,” *International Journal of Electrochemical Science*, Vol. 7(1), pp. 857–874, 2012. [CrossRef]

- [40] W. Yang, M. Zhou, J. Cai, L. Liang, G. Ren, and L. Jiang, "Ultra-high yield of hydrogen peroxide on graphite felt cathode modified with electrochemically exfoliated graphene," *Journal of Materials Chemistry A*, Vol. 5(17), pp. 8070–8080, 2017. [CrossRef]
- [41] T. X. Houng Le, M. Bechelany, S. Lacour, N. Oturan, M. A. Oturan, and M. Cretin, "High removal efficiency of dye pollutants by electron-Fenton process using a graphene-based cathode," *Carbon NY*, Vol. 94, pp. 1003–1011, 2015. [CrossRef]
- [42] L. P. Bicelli, B. Bozzini, C. Mele, and L. D. Urzo, "A review of nanostructural aspects of metal electrodeposition," *International Journal of Electrochemical Science*, Vol. 3, pp. 356–408, 2008. [CrossRef]
- [43] J. Liu, X. Sun, P. Song, Y. Zhang, W. Xing, and W. Xu, "High-performance oxygen reduction electrocatalysts based on cheap carbon black, nitrogen, and trace Iron," *Advanced Materials*, Vol. 25(47), pp. 6879–6883, 2013. [CrossRef]
- [44] C. Trelu, N. Oturan, F. K. Keita, C. Fourdrin, Y. Pechaud, and M. A. Oturan, "Regeneration of activated carbon fiber by the electro-fenton process," *Environmental Science & Technology*, Vol. 52(13), pp. 7450–7457, 2018. [CrossRef]
- [45] J. Guo, T. Zhang, C. Hu, and L. Fu, "A three-dimensional nitrogen-doped graphene structure: A highly efficient carrier of enzymes for biosensors," *Nanoscale*, Vol. 7(4), pp. 1290–1295, 2015. [CrossRef]
- [46] S. D. Sklari, K. V. Plakas, P. N. Petsi, V. T. Zaspalis, and A. J. Karabelas, "Toward the development of a novel electro-fenton system for eliminating toxic organic substances from water. Part 2. Preparation, characterization, and evaluation of iron-impregnated carbon felts as cathodic electrodes," *Industrial & Engineering Chemistry Research*, Vol. 54(7), pp. 2059–2073, 2015. [CrossRef]
- [47] W. Yang, M. Zhou, and L. Liang, "Highly efficient in-situ metal-free electrochemical advanced oxidation process using graphite felt modified with N-doped graphene," *Chemical Engineering Journal*, Vol. 338, pp. 700–708, 2018. [CrossRef]
- [48] G. Divyapriya, I. M. Nambi, and J. Senthilnathan, "An innate quinone functionalized electrochemically exfoliated graphene/Fe₃O₄ composite electrode for the continuous generation of reactive oxygen species," *Chemical Engineering Journal*, Vol. 316, pp. 964–977, 2017. [CrossRef]
- [49] Y. Zhou, Q. Bao, L. A. L. Tang, Y. Zhong, and K. P. Loh, "Hydrothermal dehydration for the 'green' reduction of exfoliated graphene oxide to graphene and demonstration of tunable optical limiting properties," *Chemistry of Materials*, Vol. 21(13), pp. 2950–2956, 2009. [CrossRef]
- [50] T. H. Magn, A. Ping, G. Jingyang, S. Caroline, M. Christos, and C. G. Chen, "Highly-Ordered Magnéli Ti₄O₇ Nanotube Arrays as Effective Anodic Material for Electro-oxidation," Elsevier Ltd, 2014.
- [51] G. Li, and Y. Zhang, "Highly selective two-electron oxygen reduction to generate hydrogen peroxide using graphite felt modified with N-doped graphene in an electro-Fenton system," *New Journal of Chemistry*, Vol. 43, pp. 12657–12667, 2019. [CrossRef]
- [52] A. Mir, D. K. Singh, and A. Shukla, "Size distribution of trilayer graphene flakes obtained by electrochemical exfoliation of graphite: Effect of the synthesis parameters," *Materials Chemistry and Physics*, Vol. 220, pp. 87–97, 2018. [CrossRef]
- [53] T. X. Houng Le, B. Alemán, J. J. Vilatela, M. Bechelany, and M. Cretin, "Enhanced electro-fenton mineralization of acid orange 7 using a carbon nanotube fiber-based cathode," *Frontiers of Materials*, Vol. 5, pp. 5–10, 2018. [CrossRef]
- [54] S. Akcöltekin, M. El Kharrazi, B. Köhler, A. Lorke, and M. Schleberger, "Graphene on insulating crystalline substrates," *Nanotechnology*, Vol. 20(15), 2009. [CrossRef]
- [55] Q. Zhou, X. Zhou, R. Zheng, Z. Liu, and J. Wang, "Application of lead oxide electrodes in wastewater treatment: A review," *Science of Total Environment*, Vol. 806, Article 150088, 2022. [CrossRef]
- [56] Z. Zhang, H. Meng, Y. Wang, L. Shi, X. Wang, and S. Chai, "Fabrication of graphene@graphite-based gas diffusion electrode for improving H₂O₂ generation in Electro-Fenton process," *Electrochimica Acta*, Vol. 260, pp. 112–120, 2018. [CrossRef]
- [57] R. N. Abbas, and A. S. Abbas, "Phenol deterioration in refinery wastewater through advanced electrochemical oxidation reactions using different carbon fiber and graphite electrodes configurations," *Egyptian Journal of Chemistry*, Vol. 65(12), pp. 463–472, 2022.
- [58] A. S. Fahem, and A. H. Abbar, "Treatment of petroleum refinery wastewater by electro-Fenton process using porous graphite electrodes," *Egyptian Journal of Chemistry*, Vol. 63(12), pp. 4805–4819, 2020.
- [59] S. K. Kamal, Z. M. Mustafa, and A. S. Abbas, "Comparative study of organics removal from refinery wastewater by photocatalytic fenton reaction coupled with visible light and ultraviolet irradiation," *Iraqi Journal of Industrial Research*, Vol. 10(3), pp. 22–32, 2023. [CrossRef]
- [60] S. K. Kamal, and A. S. Abbas, "Fenton oxidation reaction for removing organic contaminants in synthetic refinery wastewater using heterogeneous Fe-Zeolite: An experimental study, optimization, and simulation," *Case Studies in Chemical and Environmental Engineering*, Vol. 8, pp. 100458–100458, 2023. [CrossRef]
- [61] S. K. Kamal and A. Abbas, "Decrease in the organic content of refinery wastewater by photocatalytic Fenton oxidation using iron-doped zeolite: Catalyst preparation, characterization, and performance," *Chemical Engineering and Processing - Process Intensification*, Vol. 193, pp. 109549–109549, 2023. [CrossRef]



Research Article

Text mining on sustainability reports of top 40 airlines and bibliometric analysis of airline's sustainability

İbrahim ŞAPALOĞLU*

Department of Management Engineering, İstanbul Technical University, Faculty of Management, İstanbul, Türkiye

ARTICLE INFO

Article history

Received: 26 September 2023

Revised: 06 January 2024

Accepted: 10 February 2024

Key words:

Civil aviation; SDG;

Sustainability; Text mining

ABSTRACT

This study aims to comprehensively explore sustainability practices, guidelines, and emerging trends in the airline industry through an in-depth analysis of their sustainability reviews. A thorough bibliometric analysis of airline sustainability was conducted using the Scopus Database. Additionally, employing text-mining techniques, a meticulous analysis focused on the sustainability reports of the leading 20 airlines compared to the subsequent 20, considered as followers, in the textual examination of sustainability reports. The results revealed thematic disparities between these two cohorts. The top 20 airlines prioritized significant concerns such as safety and other sustainability-related aspects like biodiversity. In contrast, follower companies placed a higher emphasis on financial considerations. This analysis illuminates the primary focuses of airlines and the spectrum of sustainability-related issues. Moreover, offering valuable insights for both researchers and industry practitioners, this study presents a repository of pertinent data related to sustainability practices in the aviation sector. Integrating text mining and bibliometric analysis emphasizes essential facets of airline sustainability, resulting in a comprehensive overview of the research landscape.

Cite this article as: Şapaloğlu İ. Text mining on sustainability reports of top 40 airlines and bibliometric analysis of airline's sustainability. Environ Res Tec 2024;7(2)186–193.

INTRODUCTION

In recent decades, sustainability has emerged as a critical concern for companies worldwide. Organizations now focus on sustainable solutions to utilize resources effectively and contribute to a more habitable world. Solutions prioritizing environmental protection have created new opportunities for gaining a competitive advantage through the efficient use of corporate assets [1].

The aviation industry, in particular, faces significant challenges in balancing operational requirements with environmental stewardship. Airlines have responded to society's increasing demand for environmentally sensitive practices by incorporating sustainability into their operations, regu-

lations, and reporting methods. While the aviation industry offers the opportunity to explore the world, it also places a substantial demand on the world's resources. Passenger traffic, which stood at 34.4 million (domestic and international) in 2003, reached 161 million by November 2022. Over the past decade, the aviation sector has witnessed an energy consumption increase of over 6% [2]. Currently, aviation contributes to more than 2% of the world's greenhouse gas emissions, and in the European Union (EU), this proportion is approximately 3% [3]. Aviation companies have heightened their interest in sustainability to avoid carbon taxes, reduce operational costs, and build a positive reputation. Consequently, they have shifted from merely publishing annual financial reports to including "sustainability re-

*Corresponding author.

*E-mail address: sapaloglu19@itu.edu.tr



ports." Numerous studies in the literature demonstrate the relationship between sustainability reports and corporate reputation [4–8]. Analyzing sustainability reports, a crucial input for corporate reputation is also valuable in examining the current situation and concerns of the aviation industry.

This study comprises two main parts: the first involves researching the subject through both bibliometric analysis and the Scopus database, and the second aims to discuss the findings by applying text mining to the sustainability reports published by the top 40 airline companies. The selection of the top 40 is based on their awareness of the importance of sustainability reporting and their status as flag carrier companies of different countries.

On the regulatory front, governments are pushing companies towards greater environmental friendliness, exemplified by initiatives such as the Emission Trading Scheme (ETS).

This research contributes to the body of knowledge by examining thematic variations between the sustainability reports of the top 20 airlines and those of their competitors. The comparative analysis elucidates the unique priorities of these clusters and underscores thematic patterns in sustainability reporting in the aviation industry. By employing text-mining techniques, the study provides a new perspective, offering a thorough understanding of the linguistic patterns and emphasized topics in sustainability reports. These reports play a crucial role in portraying airline companies as environmentally friendly to their stakeholders. Consequently, this study aims to answer the following research questions:

- RQ1: What are the most emphasized topics in the sustainability reports of airline companies?
- RQ2: Are there thematic differences between the sustainability reports of the top 20 and the followers?
- RQ3: Are there similarities and/or differences in trends between the airline companies' sustainability reports and the literature?

The aviation industry's rapid growth poses challenges in striking a balance between environmental responsibility and operational needs. Grasping the thematic nuances becomes critical as airlines increasingly publish sustainability reports alongside financial reports. The need to understand airline priorities and concerns in the sustainability space is the driving force behind this study. Despite the growing importance of sustainability reporting, there are still few studies systematically comparing the sustainability reports of leading airlines. This research aims to fill this knowledge gap by providing a thorough analysis of thematic differences and commonalities, advancing both academic and practical knowledge in the field.

The study's data comprises information obtained from the Scopus database as well as reports published by various companies. The presentation of the study results will commence alongside the methodology section in the third part.

Literature Review

The civil aviation sector has started to pay attention to its commitment to minimizing and lowering its environmental consequences as one of the major sources of energy use and carbon emissions [9]. Because of this attention, companies, society, governments, and regulators want the aviation industry to be more sustainable. One of the ways aviation companies prove that they are sustainable is through the reports they have published. The practice of non-financial reporting began in the 1970s with social disclosures, then expanded to include broader social and environmental reporting in the 1990s. After the turn of the millennium, these reports increasingly combined and came to be known as sustainability reports [10, 11]. Sustainability reports can be used in impression management to keep the company's credibility high and as a tool for actions being beneficial [12]. One of the methods used in the analysis of sustainability reports is text mining. Text mining is the use of natural language processing and data mining together, it is a way of conducting research with the aim of processing and using all human-specific languages [13].

Seo and Itoh, [14] highlight the potential of text mining in analyzing passenger word-of-mouth to gain insight into the evolution of global airline alliance efforts. Similarly, Tian et al. [15] propose a new methodology that uses text mining and sentiment analysis to evaluate service quality in the airline industry, highlighting the potential to extract valuable insights from social media data. Additionally, Menezes et al. [16] advocate combining quantitative longitudinal data analysis with text mining and qualitative inferences from sustainability reports to improve understanding and decision-making.

In addition to methodological considerations, it is also crucial to understand the specific focus areas in sustainability reports. Moreover, Zhang [17] highlights the importance of comparative studies of sustainability reports in different regions, highlighting the attention paid by European and Asia-Pacific airlines to economic, social, and environmental issues. That study highlights the importance of considering regional differences and specific sustainability issues in the airline industry.

Additionally, the temporal aspect of sustainability reporting is also important. Yang et al. [18] found changing trends in corporate social responsibility reporting among the world's leading airlines, highlighting the dynamic nature of sustainability disclosures over time and across regions. Similarly, Paraschi (2022) [19] discusses the importance of sustainability reporting strategies, especially during crises such as the COVID-19 pandemic, and argues that investments in ESG (Environmental, Social and Governance) and sustainability practices can lead to sustainable profitability and market performance.

In the study of Kim and Kim [20] by analyzing sustainability reports and newspaper articles with text mining, they determined that the concepts of ethical issues, sustainable production, quality, and customer roles are emphasized in the texts analyzed the most. Health and safety, human rights, lowering greenhouse gas emissions, conserving en-

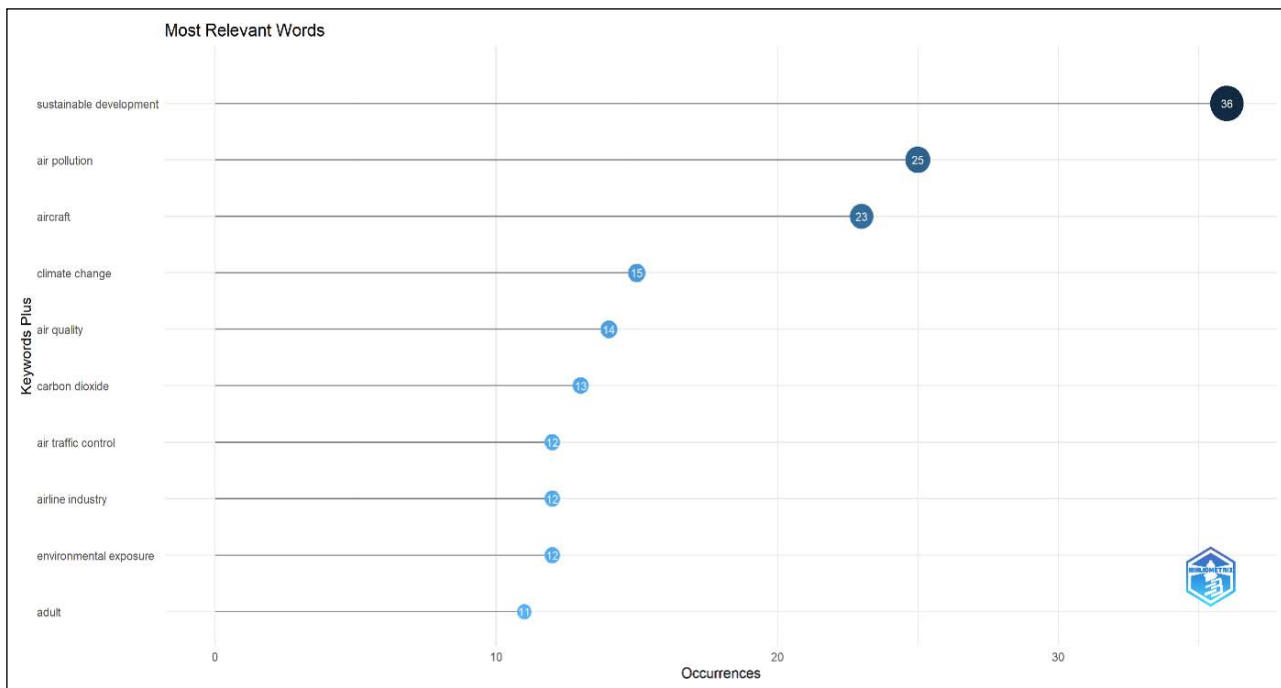


Figure 2. Most relevant words.

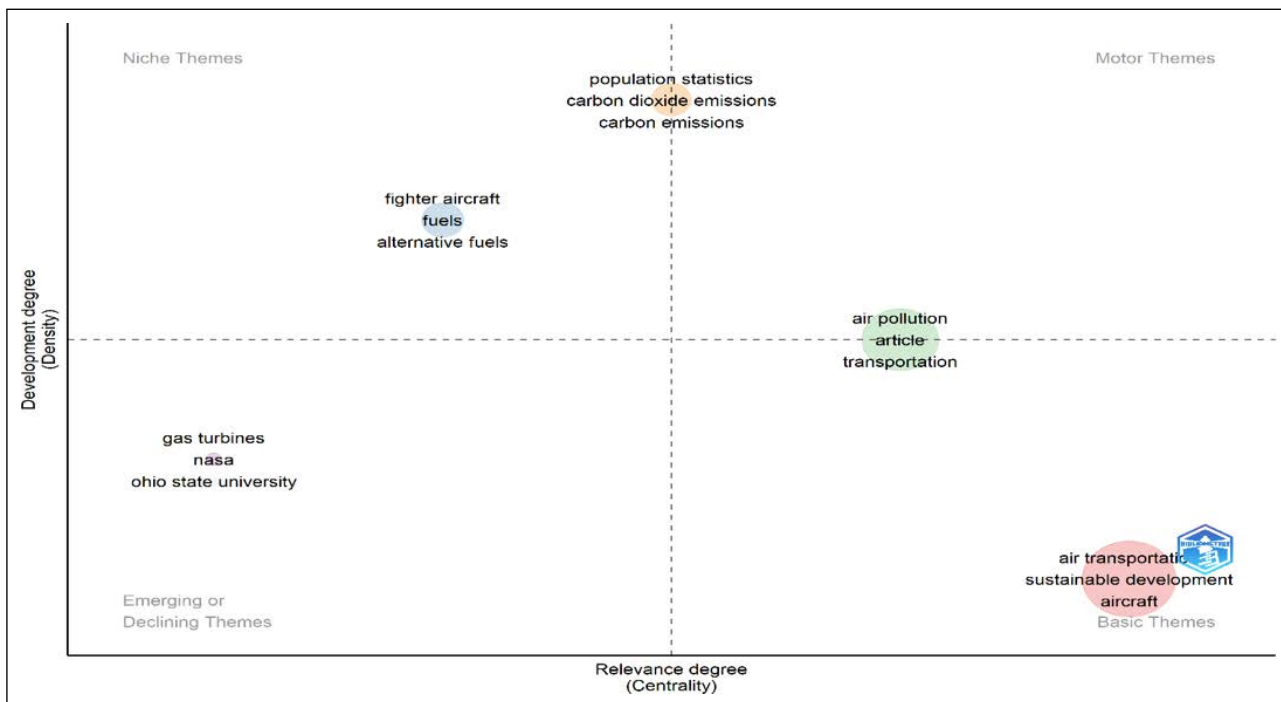


Figure 3. Thematic clustering of documents from the literature.

As seen in Figure 1, "environmental sustainability" seems to be more prominent in the studies in the context of sustainability related to the aviation industry. On the other hand, it is observed that economic sustainability and human health and quality concerns are also emphasized.

According to the most relevant words in Figure 2, the word meaning is sustainable development. This especially shows the importance of SDGs even in terms of airways. There are positive reflections on the performance of the companies that act with the awareness of the SDGs [36, 37].

As has been pointed out in Figure 3 the thematic map had five clusters. When the results were considered, niche themes were fighter aircraft and alternative fuels. Emerging themes were gas turbines and NASA. The Basic (developing) themes were air transportation, sustainable development, and aircraft. Motor (developed) themes although the boundaries are not exactly clear were air pollution, pollution, carbon emission, and carbon dioxide emissions.

As depicted in Table 1, illustrating the frequencies and country-specific distribution of documents within the top

Table 1. The list of the top 40 airways by country

Airways	Country	Airways	Country
Id1	Qatar	Id21	Finland
Id2	Singapore	Id22	Bahrain
Id3	UAE	Id23	Thailand
Id4	Japan	Id24	USA
Id5	Australia	Id25	Spain
Id6	Japan	Id26	Ethiopia
Id7	Türkiye	Id27	Thailand
Id8	France	Id28	Greece
Id9	Korea	Id29	Singapore
Id10	Switzerland	Id30	New Zealand
Id11	Britain	Id31	Indonesia
Id12	UAE	Id32	Australia
Id13	China	Id33	Korea
Id14	China	Id34	Saudi Arabia
Id15	Germany	Id35	USA
Id16	China	Id36	Fiji
Id17	Netherlands/France	Id37	Oman
Id18	Taiwan	Id38	Kazakhstan
Id19	USA	Id39	Canada
Id20	India	Id40	Ireland

Source: [38].

40 airline lists, it is noteworthy that China, the Netherlands, and the USA emerge as prominent contributors, as evident in Table 2, where a substantial number of academic studies have been conducted. Additionally, the airlines from these countries hold positions within the Top 20 airline list. Top 20 airlines list gathered from Skytrax website [38].

The next part of the study aims to answer the research questions by analyzing the companies' sustainability reports.

Text Mining on Sustainability Reports

The analysis at this stage compares the top 20 companies and the other 20 companies that are followers of them. To carry out the analysis in this section, it is necessary to prepare the data first. In this context, the sustainability reports in the dataset, which are pdf, have been converted to text file format. The average word count of the 40 files examined in this section is 7302.154.

Companies in the top 40 in the research were divided into two clusters: top 20 and followers. In this way, it is aimed to reveal the thematic differences behind the success of the top 20. It is aimed to compare these two clusters and to provide the opportunity to see a shortcoming of the following companies. The variables used in the analysis process are shown in Table 3. In the text files, many elements could not be analyzed because these files were company reports. To get rid of all these, the cleaning processes mentioned in the 3rd part were carried out.

Table 2. Academic documents frequency by country

Academic documents on Scopus	
Country	Frequency
Usa	48
China	21
Italy	17
Germany	15
Netherlands	14
Spain	14
Malaysia	10
India	9
UK	9
France	8

Source: Scopus database.

Table 3. Variables of sustainability reports analysis

Variable	Definition
Txt files	An independent document id spanning from 1 to 40
Text	Text of the under-inquiry work
Cluster 1	Data of top 20 companies [1–20]
Cluster 2	Data of followers companies [21–40]

Findings of Analysis of the Sustainability Reports

The analysis findings of the documents listed as 40 separate document IDs and divided into two clusters, the first 20 and the next 20, will be discussed in this section.

When Figure 4 is examined, it is possible to have an idea about the priorities of the top 20 companies. For example, while safety is the most important issue for the top 20 companies, on the other hand, finances have emerged for the followers. It is not surprising that a concept like biodiversity is in the top 20 and not in the followers. This may show that these companies are aware that they cannot be sustainable by using only resources less.

When the bi-gram words in Table 4 are examined, it is seen that there are distinctive differences between the top 20 and the followers in parallel with Figure 4. While the top 20 focus mainly on sustainability, the followers focus more on financial issues.

Drawing insights from the content and frequency of the text data, themes outlined in Table 5 came to the forefront. A few overarching observations emerge from this analysis:

Topic 1 elucidates the intricate interplay among environmental responsibility, ethical conduct, security considerations, and the realm of business operations. The relationship between sustainability and employees, as well as monetary concerns, is highlighted in Topic 2. The significance of data and reporting on air, carbon, and the environment is demonstrated in Topic 3. Topic 4 demonstrates how companies integrate their sustainability objectives with corporate responsibility.

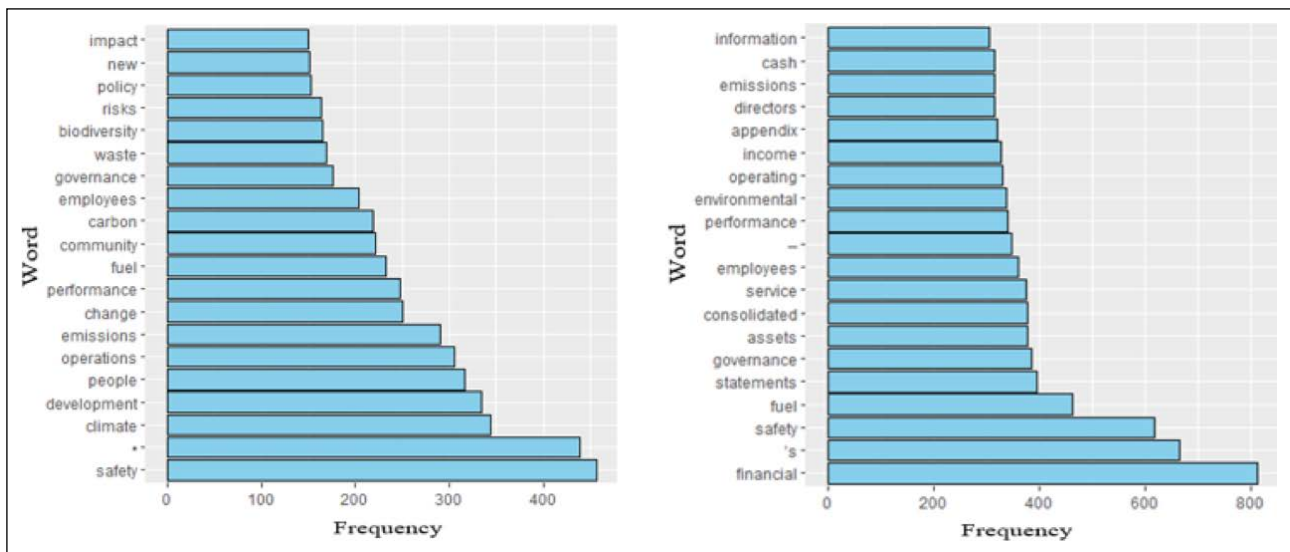


Figure 4. Word/frequency graphs of the top 20 and next 20 companies' reports (left side top 20, right side followers).

Table 4. Bi-gram word frequencies of the top 20 and followers

Top 20	Followers		
Safety standards	455	Financial statement	470
Climate change	349	Financial assets	390
Sustainable development	319	Aviation fuel	349
Carbon emission	312	Jet fuel	346
Fuel efficiency	310	Health safety	346
Waste management	306	Supply chain	341
Corporate governance	279	Fuel efficiency	339
Employee engagement	262	Carbon emission	320
Risk management	237	Cash flow	220
Environmental impact	192	Corporate governance	217

Table 5. Topic modeling analysis on airline sustainability reports (id1-id40)

Topic 1: statement, safety, operation, sustain, green
Topic 2: financial, flight, sustainable, operation, employees
Topic 3: report, air, carbon, green, environment
Topic 4: operation, sustainable, board, social, efficiency
Topic 5: consolidation, operation, governance, safety, sustainable

ty and social responsibility. The effects of consolidation are highlighted in Topic 5, along with the relationship between business performance, security, and sustainability.

When evaluated together with the literature findings that were mentioned in bibliometric analysis, it is seen that companies do not only refer to environmental and economic sustainability but also to social sustainability to emphasize that they are aware of their responsibilities towards society and their stakeholders.

Figure 2, which shows the most relevant words in the literature, is mentioned in the reports, although there is



Figure 5. Word cloud of the sustainability reports [id1-id40].

no term related to the employees or other social environment elements. In this context, in Figure 5, words such as human, community, employee, and training in the word cloud are prominent.

CONCLUSION

This study employs both bibliometric analyses from the literature and text-mining techniques on sustainability reports from the top 40 airlines, providing a comprehensive examination. The robustness of the findings is strengthened by this dual approach, offering a thorough understanding of thematic differences. The integration of quantitative and qualitative methodologies contributes to the expansion and depth of knowledge within the field of airline sustainability.

Results obtained from the bibliometric analysis reveal a pronounced emphasis on environmental aspects in sustainability studies within the aviation industry. Countries such as China, the Netherlands, India, and the USA emerge as key contributors to the academic discourse, featuring a

multitude of scientific inquiries, with their respective airlines prominently represented in the cohort of the top 40 airlines. A meticulous nation-wise assessment of scientific document frequency underscores these trends.

The research findings hold significant implications for practitioners and policymakers in the aviation industry. Airlines can refine their strategies to align with evolving sustainability goals by thoroughly understanding the thematic priorities highlighted in sustainability reports. Using these insights, managers can enhance their reporting procedures and ensure that sustainability projects are communicated to stakeholders more comprehensively and effectively.

Additional insights were derived from text-mining analysis of the sustainability reports of the top 20 airlines and their followers. The analysis reveals distinct themes in the reports of the top 20 airlines and those of the followers. Safety, environmental sustainability, and social responsibility take precedence in the reports of the top 20 airlines, while followers place greater emphasis on financial considerations. The reports of the top 20 airlines also feature terms like biodiversity more frequently, demonstrating their recognition of the importance of considering a broader range of sustainability issues. As discussed by Paraschi (2022) [19], sustainability reporting strategies and investments in ESG and sustainability practices can lead to sustainable profitability and market performance. Conversely, Yang et al. (2020) [18] state in their study that there are changing trends in sustainability reports or corporate social responsibility reports, emphasizing the need for airline companies to adapt to maintain competitiveness. This study did not identify clear distinctions between the top 20 airlines and their followers regarding regional differences, as both clusters include airlines from countries with both Western and Eastern cultures.

While this study provides valuable insights, it is essential to acknowledge its limitations. Firstly, the analysis is based on sustainability reports made available to the public, which may or may not be comprehensive. Additionally, the study's focus on the top 40 airlines might overlook the diversity present in smaller or regional airlines. The quality and format of the reports may impact the efficacy of text-mining techniques, influencing the extent of the analysis. Furthermore, the study does not delve into regional differences in sustainability priorities, a potential avenue for further investigation.

Future studies may explore whether regional differences exist in reports based on the countries or regions where airline companies are located. Additionally, examining whether company structures or management types affect differentiation in reports could be a valuable area for investigation.

DATA AVAILABILITY STATEMENT

The author confirm that the data that supports the findings of this study are available within the article. Raw data that support the finding of this study are available from the corresponding author, upon reasonable request.

CONFLICT OF INTEREST

The author declared no potential conflicts of interest with respect to the research, authorship, and/or publication of this article.

USE OF AI FOR WRITING ASSISTANCE

Not declared.

ETHICS

There are no ethical issues with the publication of this manuscript.

REFERENCES

- [1] R. Wüstenhagen and M. Starik, "Sustainable Innovation and Entrepreneurship Reducing permitting risks of large wind energy projects in Switzerland View project UNISG former research work View project," Edward Elgar Publishing Limited, 2008. [\[CrossRef\]](#)
- [2] A. Hadi-Vencheh, P. Wanke, A. Jamshidi, and Z. Chen, "Sustainability of Chinese airlines: A modified slack-based measure model for CO2 emissions," in *Expert Systems*, Blackwell Publishing Ltd, 2020.
- [3] M. Efthymiou, and A. Papatheodorou, "EU Emissions Trading Scheme in aviation: Policy analysis and suggestions," *Journal of Cleaner Production*, Vol. 237, Article 117734, 2019. [\[CrossRef\]](#)
- [4] D. L. Brown, R. P. Guidry, and D. M. Patten, "Sustainability reporting and perceptions of corporate reputation: An analysis using fortune," in *Sustainability, environmental performance and disclosures*, Emerald Group Publishing Limited, 2009. [\[CrossRef\]](#)
- [5] Zimon, A. Arianpoor, and M. Salehi, "Sustainability reporting and corporate reputation: the moderating effect of CEO opportunistic behavior," *Sustainability*, Vol. 14(3), Article 1257, 2022. [\[CrossRef\]](#)
- [6] Y. A. Abbas, W. Mehmood, Y. Y. Lazim, and A. Aman-Ullah, "Sustainability reporting and corporate reputation of Malaysian IPO companies," *Environmental Science and Pollution Research*, Vol. 29(52), pp. 78726–78738, 2022. [\[CrossRef\]](#)
- [7] M. D. Odriozola, and E. Baraibar-Diez, "Is corporate reputation associated with quality of CSR reporting? Evidence from Spain," *Corporate Social Responsibility and Environmental Management*, Vol. 24(2), pp. 121–132, 2017. [\[CrossRef\]](#)
- [8] D. L. Brown, R. P. Guidry, and D. M. Patten, "Sustainability reporting and perceptions of corporate reputation: An analysis using fortune," in *Sustainability, environmental performance and disclosures*, Emerald Group Publishing Limited, 2009. [\[CrossRef\]](#)
- [9] A. Hadi-Vencheh, P. Wanke, A. Jamshidi, and Z. Chen, "Sustainability of Chinese airlines: A modified slack-based measure model for CO2 emissions," *Expert Systems*, Vol. 37(3), Article e12302, 2020. [\[CrossRef\]](#)
- [10] M. S. Fifka, "Corporate Responsibility Reporting and its Determinants in Comparative Perspective – a Review of the Empirical Literature and a Meta-analysis," *Business Strategy and the Environment*,

- Vol. 22(1), pp. 1–35, 2013. [CrossRef]
- [11] M. Zieba, and E. Johansson, “Sustainability reporting in the airline industry: Current literature and future research avenues,” *Transportation Research Part D: Transport and Environment*, Vol. 102, Article 103133, 2022. [CrossRef]
- [12] P. Bansal, and G. Kistruck, “Seeing is (not) believing: Managing the impressions of the firm’s commitment to the natural environment,” *Journal of Business Ethics*, Vol. 67, pp. 165–180, 2006.
- [13] T. Kaşıkçı, and H. Gökçen, “Metin Madenciliği ile E-Ticaret Sitelerinin Belirlenmesi,” *Bilişim Teknolojileri Dergisi*, Vol. 7(1), pp. 25–32, 2014.
- [14] G.-H. Seo, and M. Itoh, “Perceptions of customers as sustained competitive advantages of global marketing airline alliances: A hybrid text mining approach,” *Sustainability*, Vol. 12(15), Article 6258, 2020.
- [15] X. Tian, W. He, C. Tang, L. Li, H. Xu, and D. Selover, “A new approach of social media analytics to predict service quality: evidence from the airline industry,” *Journal of Enterprise Information Management*, Vol. 33(1), pp. 51–70, 2020. [CrossRef]
- [16] L. M. de Menezes, A. B. Escrig-Tena, and J. C. Bou-Llugar, “Sustainability and Quality Management: has EFQM fostered a Sustainability Orientation that delivers to stakeholders?,” *International Journal of Operations & Production Management*, Vol. 42(13), pp. 155–184, 2022. [CrossRef]
- [17] X. Zhang, “Communicating social responsibilities through CSR reports: Comparative study of top European and Asia-Pacific airlines,” *PLoS One*, Vol. 16(10), Article e0258687, 2021. [CrossRef]
- [18] L. Yang, C. S. B. Ngai, and W. Lu, “Changing trends of corporate social responsibility reporting in the world-leading airlines,” *PLoS One*, Vol. 15(6), pp. e0234258, 2020. [CrossRef]
- [19] E. P. Paraschi, “Why ESG Reporting is Particularly Important for the Airlines during the Covid-19 Pandemic,” *Journal of Business and Management Studies*, Vol. 4(3), pp. 63–67, 2022. [CrossRef]
- [20] D. Kim, and S. Kim, “Sustainable supply chain based on news articles and sustainability reports: Text mining with Leximancer and DICTION,” *Sustainability (Switzerland)*, Vol. 9(6), Article 1008, 2017. [CrossRef]
- [21] W. Te Liew, A. Adhitya, and R. Srinivasan, “Sustainability trends in the process industries: A text mining-based analysis,” *Computers in Industry*, Vol. 65(3), pp. 393–400, 2014. [CrossRef]
- [22] J. R. Modapothala, and B. Issac, “Study of economic, environmental and social factors in sustainability reports using text mining and Bayesian analysis,” in *2009 IEEE Symposium on Industrial Electronics & Applications*, pp. 209–214, 2009. [CrossRef]
- [23] Y. Zhou, X. Wang, and K. F. Yuen, “Sustainability disclosure for container shipping: A text-mining approach,” *Transport Policy (Oxford)*, Vol. 110, pp. 465–477, 2021.
- [24] M. Kılıç, A. Uyar, and A. S. Karaman, “What impacts sustainability reporting in the global aviation industry? An institutional perspective,” *Transport Policy (Oxford)*, Vol. 79, pp. 54–65, 2019. [CrossRef]
- [25] S. Vijayarani, and R. Janani, “Text mining: open source tokenization tools-an analysis,” *Advanced Computational Intelligence: An International Journal*, Vol. 3(1), pp. 37–47, 2016. [CrossRef]
- [26] D. Munková, M. Munk, and M. Vozár, “Data pre-processing evaluation for text mining: transaction/sequence model,” *Procedia Computer Science*, Vol. 18, pp. 1198–1207, 2013. [CrossRef]
- [27] A. Correia, M. F. Teodoro, and V. Lobo, “Statistical methods for word association in text mining,” *Recent Studies on Risk Analysis and Statistical Modeling*, Springer, pp. 375–384, 2018. [CrossRef]
- [28] P. T. Eles, B. Pennell, and M. Richter, “Assessing NATO policy alignment through text analysis: An initial study,” in *2016 International Conference on Military Communications and Information Systems (ICMCIS)*, IEEE, 2016, pp. 1–7. [CrossRef]
- [29] M.-J. Kim, K. Ohk, and C.-S. Moon, “Trend analysis by using text mining of journal articles regarding consumer policy,” *New Physics: Sae Mulli*, Vol. 67(5), pp. 555–561, 2017. [CrossRef]
- [30] V. Lertnattee and T. Theeramunkong, “Effect of term distributions on centroid-based text categorization,” *Information Science (NY)*, Vol. 158, pp. 89–115, 2004. [CrossRef]
- [31] J. Gadge, S. Sane, and H. B. Kekre, “N-layer approach to web information retrieval,” *International Journal of Applied Information Systems*, Vol. 5, pp. 45–49, 2013. [CrossRef]
- [32] W. B. Croft, “Document Retrieval system,” *Information Technology*, Vol. 2, pp. 1–21, 1983.
- [33] E. S. Negara, D. Triadi, and R. Andryani, “Topic modeling twitter data with latent Dirichlet allocation method,” in *2019 International Conference on Electrical Engineering and Computer Science (ICECOS)*, IEEE, 2019, pp. 386–390. [CrossRef]
- [34] Y. Haralambous, “Text mining methods applied to mathematical texts,” 2012. Accessed on Jun 11, 2023. <https://hal.science/hal-01864536>
- [35] I. Feinerer, K. Hornik, and D. Meyer, “Text mining infrastructure in R,” *The Journal of Statistical Software*, Vol. 25(5), pp. 1–54, 2008. [CrossRef]
- [36] P. A. Khan, S. K. Johl, and S. Akhtar, “Firm sustainable development goals and firm financial performance through the lens of green innovation practices and reporting: a proactive approach,” *Journal of Risk and Financial Management*, Vol. 14(12), Article 605, 2021. [CrossRef]
- [37] D. L. Ramos, S. Chen, A. Rabeeu, and A. B. Abdul Rahim, “Does SDG Coverage Influence Firm Performance?,” *Sustainability*, Vol. 14(9), Article 4870, 2022. [CrossRef]
- [38] World Airline Awards, “World’s Top 100 Airlines 2022 | SKYTRAX.” Accessed on Jun 11, 2023. <https://www.worldairlineawards.com/worlds-top-100-airlines-2022/>



Research Article

Smart environmental drone utilization for monitoring urban air quality

Yeliz DURGUN¹, Mahmut DURGUN²

¹Turhal Vocational School, Tokat Gaziosmanpaşa University, Tokat, Türkiye

²Faculty of Turhal Applied Sciences, Tokat Gaziosmanpaşa University, Tokat, Türkiye

ARTICLE INFO

Article history

Received: 01 October 2023

Revised: 24 October 2023

Accepted: 14 February 2024

Key words:

Air pollution measurement;
Environmental drone; Urban air
quality; Real time measurement

ABSTRACT

Urban air quality has significant and far-reaching impacts on both human health and the broader environment. Pollutants like particulate matter (PM2.5 and PM10), for instance, are associated with a range of health issues including respiratory conditions, asthma, heart diseases, and even contribute to low birth weight in newborns. These health implications extend to larger environmental concerns such as air pollution, greenhouse gas emissions, and global climate change. Recognizing the urgent need for effective and dynamic air quality monitoring solutions, this paper explores the use of smart environmental drones as a promising approach. Our drone is equipped with a state-of-the-art, low-cost particulate matter sensor that can accurately measure PM2.5 and PM10 concentrations. Operating at a flight speed of 10 m/s and capable of covering a range of 5 km, the drone executes a pre-programmed flight plan to autonomously map pollution levels across urban areas. With a 95% accuracy rate in sensor readings, our model significantly minimizes potential errors commonly associated with traditional air quality monitoring methods. Furthermore, it simplifies maintenance procedures, reducing both time and financial costs. By employing drone technology in this innovative manner, our model offers a cost-effective, reliable, and dynamic solution for monitoring urban air quality. It provides real-time, actionable pollution indices that can inform public health decisions, regulatory policies, and community awareness, thereby contributing to the broader goal of improving air quality and public health.

Cite this article as: Yeliz Durgun, Mahmut Durgun. Smart environmental drone utilization for monitoring urban air quality. Environ Res Tec 2024;7(2)194–200.

INTRODUCTION

In recent years, the increasing industrial activities in the world and in our country, as well as the rapid population growth in cities, have become the main source of environmental problems [1]. The fact that environmental problems not only affect the areas where they occur, but also the entire world, has become a significant factor in the universalization of environmental awareness and approach [2]. Air pollution refers to the increase of pollutants such as dust, smoke, gas, odor, and non-pure water vapor that can negatively affect human and animal health and cause financial damages [3, 4].

The emissions that cause air pollution are produced as a result of natural events and necessary activities, and when they are released at high levels, they negatively impact the environment and human health [5]. These activities include burning industrial waste, conducting industrial and commercial activities, energy production, transportation, and agriculture [6]. The emissions may contain harmful substances such as carbon dioxide, nitrogen oxides, sulfur dioxide, particulate matter, and sulfur dioxide [7]. Additionally, particulate matter of different sizes (PM10, PM2.5) is released into the atmosphere [8]. When these substances are present in the air at high levels, they negatively impact

*Corresponding author.

*E-mail address: yeliz.durgun@gop.edu.tr



the environment and human health [9–11]. Carbon dioxide can cause consequences such as acceleration of the global climate change process, rising sea levels, changing climate conditions, and increasing natural disasters [12]. Nitrogen oxides and sulfur dioxide are one of the causes of air pollution and can lead to respiratory problems, asthma, heart diseases, and other human health problems [13]. Particulate matter can increase the risk of lung and heart diseases [14–16]. Therefore, monitoring and reducing emissions that cause air pollution is important to protect human health and the environment [17].

World Health Organization (WHO), affiliated with the United Nations, has established air quality standards with the aim of protecting human health and the sustainability of the environment [7]. To this end, certain restrictions have been imposed on the emission of gases and particulate matter. These standards encourage efforts towards a cleaner and healthier air quality by limiting the emission of substances that pose a potential danger to human health and the environment. In Türkiye, the Ministry of Environment and Urbanization (MOEU) continuously monitors air quality at stations established at predetermined points throughout the country, under the control of the Ministry [18]. The purpose of these measurements is three-fold: firstly, to provide information about the general condition and pollution level of the city's air quality in a comprehensible manner; secondly, to increase awareness of health problems caused by increased air pollution levels; and thirdly, to create a dynamic ranking system based on air pollution levels in cities and towns with measuring stations. The air quality is determined by measuring the pollutants present in the environment through the National Air Quality Monitoring Stations (NAQMS) system [19].

According to the Air Quality Assessment and Management Regulation in Türkiye, limit values for certain pollutants have been determined and it is aimed to reach the European Union limit values for decreasing pollutant emissions gradually by the specified dates [20]. To prevent people from being negatively affected by air pollution, it is necessary to measure the pollution level as soon as possible and take action. For this reason, in 2007, the Tokat Central Air Quality Monitoring (AQM) station was established, followed by the Tokat Square, Erbaa, and Turhal Air Quality Monitoring (AQM) stations in 2015.

Recent advancements in technology have opened up innovative avenues for air quality monitoring. For instance, one study employed Smart Drones designed to monitor 9 different pollutants in metropolitan cities, using a deep learning model, the Bi-GRU network, for real-time data analysis, yielding high accuracy rates in various urban settings [21]. Another research integrated microcontrollers like Arduino Nano and ESP32 with various sensors to measure air quality parameters such as CO, NO₂, O₃, and PM, employing both standalone devices and drone technology for real-time monitoring through an application called Blynk App [22].

Similarly, research has been conducted to counter the absence of national regulations and expensive monitoring

networks by developing a smart multi-sensor system using unmanned aerial vehicles and LoRa communication [23]. Another study from Dhaka, Bangladesh, used an unmanned aerial vehicle built on a DJI F450 frame with various sensors to monitor air quality both indoor and outdoor, focusing on areas with more industries and construction sites [24].

There are also systems designed for monitoring hard-to-reach areas using Arduino Uno and NodeMcu microcontrollers, which not only provide real-time monitoring but also allow data logging to a remote server [25]. Furthermore, the growing availability of small drones equipped with advanced sensing technology has expanded the scope for environmental applications, including the mapping of pollutant distributions and monitoring of greenhouse gases [26].

The versatility of drone technology has been further extended through various innovative approaches. One project focused on a combined deployment of ground robots and drones equipped with sharp-branded dust sensors for indoor air quality monitoring, aiming to create a 3D air pollution map of the targeted area [27]. Another study presented an autonomous multi-rotor aerial platform capable of real-time air quality monitoring across large cities, offering high spatial resolution at a relatively low cost [28].

The evolution of drone technology has expanded beyond its original military applications. Now integrated with IoT and machine learning, drones serve diverse functions ranging from traffic management to pollution monitoring. They have become vital tools in the development and sustenance of smart cities, contributing significantly to various stages such as operation, citizen engagement, and data collection [29].

In this study, a low-cost drone system was developed to measure and evaluate the pollution levels in Tokat province, Turhal district by using drones that can measure from different points in the city as an alternative to the Turhal Air Quality Monitoring (AQM) station in the city. In this study, a low-cost drone system was created to monitor and detect environmental air pollution in Turhal district of Tokat province. The drones are designed for environmental data monitoring and long-term analysis in the city, with the aim of obtaining detailed information about the air quality in the area. The data obtained from the drone measurements is compared to the data obtained from the fixed AQM station, and the results show that the drone system is capable of providing accurate and reliable air quality data.

Air Quality Index (AQI) is an index used to report daily air quality. It provides information on how clean or polluted the air in our region is and what type of health effects may result. The AQI also determines the levels of different air quality levels and their general effects on public health, as well as the steps to be taken when levels become unhealthy. The National Air Quality Index is based on the EPA Air Quality Index and adjusted to our national regulations and limit values. The AQI is calculated for 5 main pollutants:

Table 1. Turkish National Air Quality Index

Air Quality Index (AQI)	Health anxiety levels	Colors	Meaning
0–50	Good	Green	Air quality is satisfactory and air pollution poses little or no risk.
51–100	Medium	Yellow	Air quality is favorable but for a very small number of people who are unusually sensitive to air pollution, there may be a moderate health concern for some pollutants.
101–150	Sensitive	Orange	Health effects may occur for vulnerable groups. The general public is unlikely to be affected.
151–200	Unhealthy	Red	Everyone can begin to experience health effects, serious health effects for vulnerable groups.
201–300	Bad	Purple	May create a health emergency. The entire population is likely to be affected.
301–500	Dangerous	Brown	Health alarm:Everyone with more serious health effects may encounter.

particulate matter (PM10), carbon monoxide (CO), sulfur dioxide (SO₂), nitrogen dioxide (NO₂), and ozone (O₃). The AQI consists of 6 categories ranging from 1 (Good) to 6 (Hazardous). There is no mathematical calculation, only classification. The value for the highest pollutant determines the AQI value. Table 1 shows the National Air Quality Index Values determined for Türkiye [30].

MATERIALS AND METHODS

Design of Environmental Drone System

A drone sensor system has been designed to collect air quality information in the city. The system consists of a dust sensor DSM501A and ESP8266 dust measurement module, LTE modem, and drone. The dust sensor and ESP8266 are placed on top of the drone, while the LTE modem is placed beneath the drone.

Dust Measurement Component

The proposed module includes a dust detection sensor and a microcontroller capable of wireless communication. This unit is capable of detecting levels of dust and particulate matter in the air. The particulate matter (PM) level measurement is obtained as the ratio of the Low Pulse Occupancy time (LPO time) to a specific time unit. The LPO time itself is proportional to the detected particulate matter concentration levels (DIY Projects, 2017). A fan mounted on top of the sensor draws air and passes it over the sensor to obtain readings. The DSM501a operates by sending a low pulse for a constant time of 30 seconds, which is what we need to measure. Then, the total of low pulses is divided by a constant time period to calculate the value. The PM1.0 and PM2.5 measurements are carried out through PWM lines on the microcontroller. For the microcontroller, Wi-Fi unit, and IoT connector, we chose NodeMCU, which is an open-source IoT platform equipped with an ESP8266 Wi-Fi SoC produced by Espressif Systems and hardware of the ESP-12 module (Espressif Systems, 2018). The ESP8266 relies on system design on the chip, with a 32-bit microprocessor operating at 80 MHz and equipped with 4 MB flash memory from Tensilica L106. In addition to having many GPIO pins, the ESP8266 has Wi-Fi functions and features that are compatible with the standard IEEE 802.11 b/g/n Wi-Fi protocol and support the TCP/IP stack.

LTE Modem

In this study, the Huawei E5573S LTE modem was used. This modem also operates as a wireless router. It provides NodeMCU Wifi wireless connection through its functioning as a WiFi access point. It has an internal battery. The modem is mounted under the drone.

Drone

In this study, a four-rotor unmanned aerial vehicle (UAV) was selected as the test platform. The main structure is made of high-strength and lightweight carbon fiber with a weight of 108 g and a frame diameter of 235 mm. The UAV is equipped with four 2306 brushless motors, each with three-blade propellers. The speed parameter of the motors is 2750 kV, indicating the increase in speed with each voltage increase. A single motor has a full-load voltage of 977 g and a kinetic energy conversion efficiency of 3.372 g/w. The UAV uses a STM32 microcontroller unit (MCU) as the controller and the main auxiliary sensors include an optical flow sensor, a laser range sensor, a gyroscope (Gyr), and an accelerometer (Acc) sensor.

Communication Protocol

In this work, Message Queuing Telemetry Transfer (MQTT), a lightweight publish/subscribe messaging protocol that is an ISO standard (ISO/IEC PRF 20922) and one of the popular protocols for Internet of Things (IoT) concept, was used for data transfer to the server. MQTT is useful for devices with limited resources, such as NodeMCU. The MQTT protocol is based on the pub/sub principle of message publishing and subscribing. In this work, the sensor operation is ensured by subscribing to a topic to receive messages, and the sensor's readings are sent to a specified topic by publishing.

Cloud Service

In the study, the Ubuntu Server software was installed on a Fujitsu Siemens S7 workstation. Remote access was provided with approximately 100 Mbit network access and a static IP address. Cloud service is provided using Ubuntu Server and Docker. Ubuntu Server is a Linux distribution regularly used as a powerful and flexible operating system. Docker is a platform that allows applications and data to be distributed and managed in a container-based manner. When used

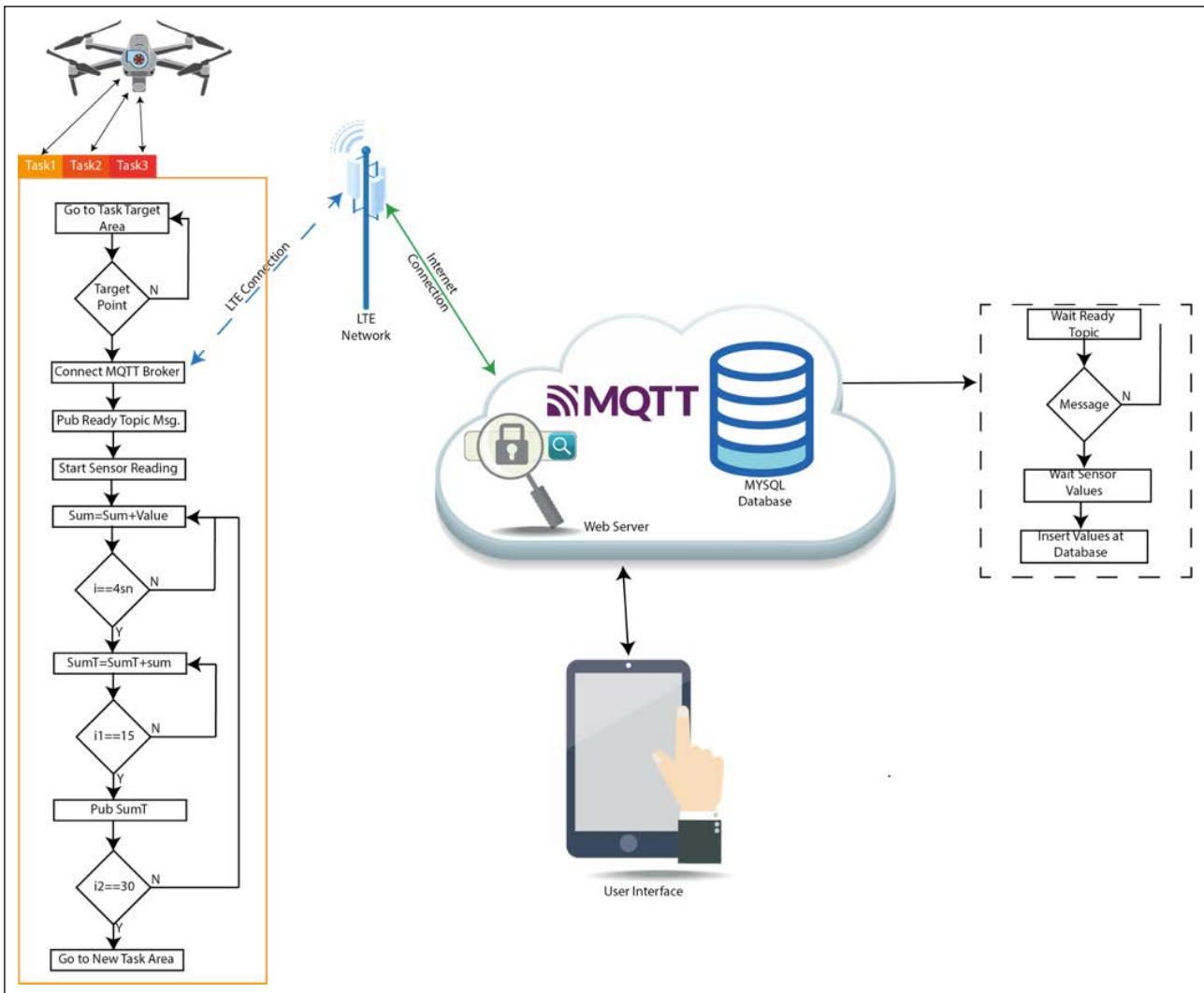


Figure 1. System overview of environmental drone measurement.

together, they can be used to distribute, manage, and scale the resources required for creating a cloud service, such as server and storage space. The MySQL database was installed as a container for data storage, the Apache web server for web interface, and the Eclipse Broker for MQTT messaging.

Cloud-Based Applications

In order to create graphical visualizations on the server, a software based on PHP, HTML and Javascript has been developed. This interface allows the data on the cloud to be displayed through wireless internet connections. This enables all of the data collected by the sensors from the designated points to be reflected in a format that can be easily understood by end-users. It assists in monitoring historical data and mapping it.

RESULTS

In the study, a sequential testing strategy was used to determine the PM1.0 and PM2.5 concentration at different locations. For each minute, fifteen different slices were created, each lasting 4 seconds. A reading is made for each

slice with a 4-second sampling time, and an average is taken after each reading. At the end of the minute, the average of all the values is sent to the cloud database using publish, so that the values are stored in the server database for visualization and analysis purposes. In this way, PM values on the drone are always stored in the cloud server database and can be easily accessible. The database ensures that the PM values are continuously and up-to-date stored and can be accessed whenever needed. This process guarantees a safe and direct data transfer from the PM sensor on the drone to the MySQL database in the cloud server.

An experiment was conducted using drones in three different areas within the Turhal district of Tokat from noon 12:00 to 14:00 on January 12th, 2023. The algorithms using Figure 1 were utilized in the experiment. Task 1 was selected as an agricultural area, Task 2 as an industrial area in the industrial area, and Task 3 as an area within the university campus. The data was collected every minute and mapping was performed based on the measured values.

The line graph showing PM values measured from different locations using drone provides more information and can be interpreted about air quality (Fig. 2). Trend Analysis:

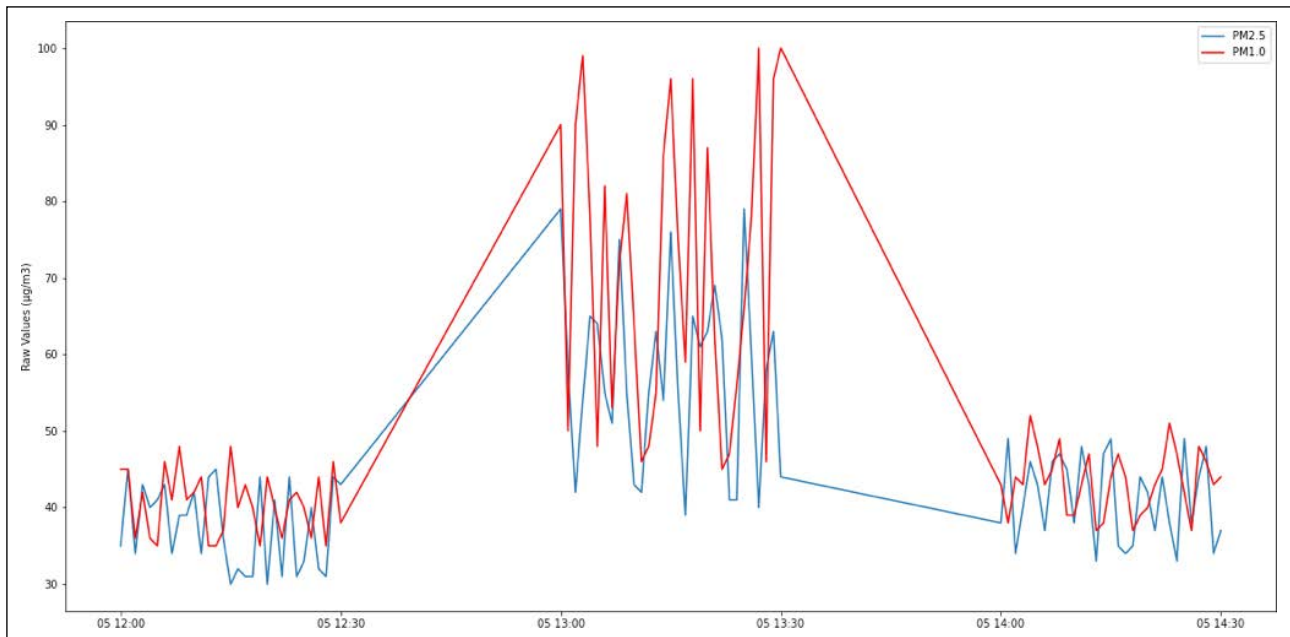


Figure 2. PM_{2.5} and PM_{1.0} as measured by proposed pollution measurement kit in real time.

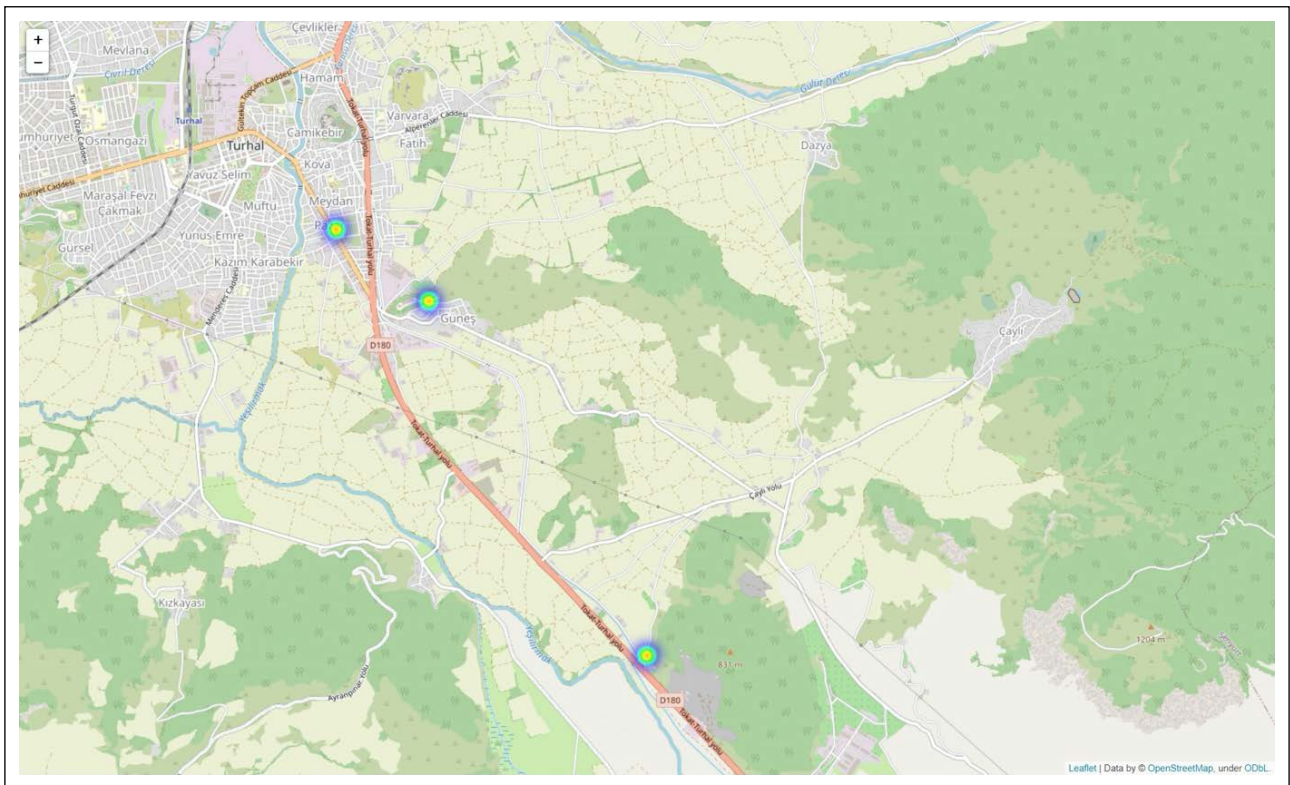


Figure 3. Heat map according to air pollution values.

Using the line graph, it is possible to see the trend of PM values (increase or decrease) within a certain time period. These trends indicate the change in air quality at a certain point. For example, an increase trend of PM values at a certain point shows that the air quality has declined. Comparisons: The line graph allows for comparison of PM values at different locations. This shows how different the air quality is at certain points and gives more ideas about air quality at specific locations. Time-of-Day Analysis: Using the line

graph, it is possible to see the change of PM values within a certain time period with respect to time. This change indicates the daily change in air quality at a certain point. For example, if it is seen that PM values are low at the beginning of the day but show an increase throughout the day at a certain point, it can be understood that the air quality at that point can deteriorate during the day. These features enable the interpretation and gaining of more information about air quality using the line graph of PM values.

The display of Particulate Matter (PM) values on the Figure 3 as a temperature map provides the following advantages:

Visualization: When PM values are presented in a visual form such as a temperature map, it becomes possible to understand and easily evaluate the values. The colors on the temperature map indicate the high or low levels of PM concentration in certain regions. Thus, a more rapid and understandable idea about air quality can be gained. **Geographical Context:** Showing PM concentrations on a map allows you to see how high or low these values are in certain regions. This provides more information about the air quality in certain regions. For example, when high PM concentrations are seen in a certain region, it can be understood that the air quality in that region is poor. **Real-Time Data:** The temperature map displayed on the map is updated continuously with PM values measured by a drone, so it always provides the latest and real-time data. This allows you to gain an idea about air quality more quickly and accurately. **Decision Making:** Obtaining more information about PM concentrations enables you to make more informed decisions about air quality and take the necessary measures to improve it. For example, if high PM concentrations are seen in a certain region, necessary measures can be taken to improve the air quality in that region. These features demonstrate the advantages of displaying PM values as a temperature map on an online map.

In this study, air quality measurements were conducted at predetermined intervals and locations using drones. Upon reaching a designated point for measurement, the drone executed a safe landing to carry out the readings for that specific location. The focus of this approach primarily leverages the advantages of drone technology. Instead of setting up multiple stationary measurement stations, we have utilized a single drone to collect data from different areas. This strategy significantly reduces costs associated with station setup, maintenance, and other logistical concerns. Particularly, the use of drones enables quicker and more efficient local air quality measurements, thus expanding our capability to monitor air quality across a broader geographical area.

CONCLUSIONS AND FUTURE WORK

Our article proposes an open platform architecture consisting of a drone-supported particulate measurement system capable of conducting measurements from various points through an interface. The study particularly leverages the technological advantages of using drones for air quality measurements. Upon reaching a specific measurement point, the drone executes a safe landing to collect readings, thus ensuring accurate and localized data capture. This approach significantly minimizes the logistical and financial burdens typically associated with setting up multiple stationary measurement stations.

The line graph of PM values measured from different points by the drone not only provides a more comprehensive understanding of air quality but also allows for techniques such as trend analysis, comparisons, and time-of-day analysis. These techniques visualize changes in air quality over time and

space, thereby helping us understand the state of air quality at specific locations. Additionally, displaying PM values as a temperature map on an online platform offers another layer of understanding, elucidating the interaction between air quality and temperature and its effects on the former.

For future work, further development of this drone-based technology and the collection of more extensive data will refine our results and deepen our understanding of air quality variables. Moreover, incorporating other environmental factors such as humidity and wind speed into the analysis alongside PM values and temperature maps will enable a more holistic understanding of air quality determinants and facilitate the development of more effective preservation strategies.

DATA AVAILABILITY STATEMENT

The author confirm that the data that supports the findings of this study are available within the article. Raw data that support the finding of this study are available from the corresponding author, upon reasonable request.

CONFLICT OF INTEREST

The author declared no potential conflicts of interest with respect to the research, authorship, and/or publication of this article.

USE OF AI FOR WRITING ASSISTANCE

Not declared.

ETHICS

There are no ethical issues with the publication of this manuscript.

REFERENCES

- [1] H. Angelo and D. Wachsmuth, "Why does everyone think cities can save the planet?," *Urban Studies*, Vol. 57(11), pp. 2201–2221, 2020. [\[CrossRef\]](#)
- [2] H. Baykal, and T. Baykal, "Environmental problems in a globalized World," *Mustafa Kemal Üniversitesi Sosyal Bilimler Enstitüsü Dergisi*, Vol. 5(9), 2008.
- [3] I. Manisalidis, E. Stavropoulou, A. Stavropoulos, and E. Bezirtzoglou, "Environmental and health impacts of air pollution: a review," *Frontiers in Public Health*, Vol. 8, Article 14, 2020. [\[CrossRef\]](#)
- [4] A. L. Melnik, "What Will You Drink?: Quenching Thirst Through the Ages," *Post Hill Press*, 2020.
- [5] H. A. Shahriyari, Y. Nikmanesh, S. Jalali, N. Tahery, A. Zhiani Fard, N. Hatamzadeh, K. Zarea, M. Cheraghi, and M. J. Mohammadi, "Air pollution and human health risks: mechanisms and clinical manifestations of cardiovascular and respiratory diseases," *Toxin Rev*, Vol. 41(2), pp. 606–617, 2022. [\[CrossRef\]](#)
- [6] N. Z. Muller, R. Mendelsohn, and W. Nordhaus, "Environmental accounting for pollution in the United States economy," *Am. Econ. Rev.*, Vol. 101(5), pp. 1649–1675, 2011. [\[CrossRef\]](#)

- [7] World Health Organization, Air quality guidelines: global update 2005: particulate matter, ozone, nitrogen dioxide, and sulfur dioxide. World Health Organization, 2006.
- [8] X. Querol, A. Alastuey, S. Rodriguez, F. Plana, E. Mantilla, and C. R. Ruiz, "Monitoring of PM10 and PM2.5 around primary particulate anthropogenic emission sources," *Atmospheric Environment*, Vol. 35(5), pp. 845–858, 2001. [CrossRef]
- [9] M. A. Zoran, R. S. Savastru, D. M. Savastru, and M. N. Tautan, "Assessing the relationship between surface levels of PM2.5 and PM10 particulate matter impact on COVID-19 in Milan, Italy," *Science of The Total Environment*, Vol. 738, Article 139825, 2020. [CrossRef]
- [10] M. H. Vahidi, F. Fanaei, and M. Kermani, "Long-term health impact assessment of PM2.5 and PM10: Karaj, Iran," *International Journal of Environmental Health Engineering*, Vol. 9, pp. 1–7, 2020.
- [11] L. Luo, X. Bai, S. Liu, B. Wu, W. Liu, Y. Lv, Z. Guo, S. Lin, S. Zhao, Y. Hao, J. Hao, K. Zhang, A. Zheng, and H. Tian, "Fine particulate matter (PM2.5/PM1.0) in Beijing, China: Variations and chemical compositions as well as sources," *Journal of Environmental Sciences*, Vol. 121, pp. 187–198, 2022. [CrossRef]
- [12] H. Buhaug, N. P. Gleditsch, and O. M. Theisen, "Implications of climate change for armed conflict," *World Bank*, Vol. 2, 2008.
- [13] T.-M. Chen, W. G. Kuschner, J. Gokhale, and S. Shofer, "Outdoor air pollution: nitrogen dioxide, sulfur dioxide, and carbon monoxide health effects," *The American Journal of the Medical Sciences*, Vol. 333(4), pp. 249–256, 2007. [CrossRef]
- [14] Y. Du, X. Xu, M. Chu, Y. Guo, and J. Wang, "Air particulate matter and cardiovascular disease: the epidemiological, biomedical and clinical evidence," *Journal of Thoracic Disease*, Vol. 8(1), pp. E8–E19, 2016.
- [15] P. Yin, J. Guo, L. Wang, W. Fan, F. Lu, M. Guo, S. B. R. Moreno, Y. Wang, H. Wang, M. Zhou, and Z. Dong, "Higher risk of cardiovascular disease associated with smaller size-fractioned particulate matter," *Environmental Science & Technology Letters*, Vol. 7(2), pp. 95–101, 2020. [CrossRef]
- [16] Y. A. Alemayehu, S. L. Asfaw, and T. A. Terfie, "Exposure to urban particulate matter and its association with human health risks," *Environmental Science and Pollution Research*, Vol. 27, pp. 27491–27506, 2020. [CrossRef]
- [17] K. Kuklinska, L. Wolska, and J. Namiesnik, "Air quality policy in the US and the EU—a review," *Atmospheric Pollution Research*, Vol. 6(1), pp. 129–137, 2015. [CrossRef]
- [18] H. Erdun, A. Öztürk, Ö. Çapraz, H. Toros, S. Dursun, and A. Deniz, "Spatial variation of PM10 in Turkey," in *7th Atmospheric Sciences Symposium, Istanbul, Turkey*, 2015, pp. 311–323. [CrossRef]
- [19] T. Büke, and A. Ç. Köne, "Assessing air quality in Turkey: A proposed, air quality index," *Sustainability*, Vol. 8(1), Article 73, 2016. [CrossRef]
- [20] E. O. Gaga, T. Döğeroğlu, Ö. Özden, A. Ari, O. D. Yay, H. Altuğ, N. Akyol, S. Örnektekin, and W. Van Doorn, "Evaluation of air quality by passive and active sampling in an urban city in Turkey: current status and spatial analysis of air pollution exposure," *Environmental Science and Pollution Research*, Vol. 19, pp. 3579–3596, 2012. [CrossRef]
- [21] R. R. Hemamalini, R. Vinodhini, B. Shanthini, P. Partheeban, M. Charumathy, and K. Cornelius, "Air quality monitoring and forecasting using smart drones and recurrent neural network for sustainable development in Chennai city," *Sustainable Cities and Society*, Vol. 85, Article 104077, 2022. [CrossRef]
- [22] M. F. T. Babierra, N. N. Carandang, A. Mangubat, C. T. Mercado, A. Santos, and C. Escarez, "AQMoD: An IoT Implementation of Air Quality Monitoring, Mapping, and Warning System Using Drone Technology," in *Tencon 2022-2022 IEEE Region 10 Conference (Tencon)*, 2022, pp. 1–5. [CrossRef]
- [23] R. Camarillo-Escobedo, J. L. Flores, P. M. Montoya, G. García-Torales, and J. M. Camarillo-Escobedo, "Smart multi-sensor system for remote air quality monitoring using unmanned aerial vehicle and LoRaWAN," *Sensors*, Vol. 22(5), Article 1706, 2022. [CrossRef]
- [24] A. Hossain, M. J. Anee, R. Faruqui, S. Bushra, P. Rahman, and R. Khan, "A gps based unmanned drone technology for detecting and analyzing air pollutants," *IEEE Instrumentation & Measurement Magazine*, Vol. 25(9), pp. 53–60, 2022. [CrossRef]
- [25] J. Burgués and S. Marco, "Drone-based monitoring of environmental gases," in *Air Quality Networks: Data Analysis, Calibration & Data Fusion*, Springer, pp. 115–137, 2023. [CrossRef]
- [26] I. A. Limon, A. D. Hossain, K. F. Ibne Faruque, M. R. Uddin, and M. Hasan "Drone-Based Real-Time Air Pollution Monitoring for Low-Access Areas by Developing Mobile-Smart Sensing Technology," in *2023 3rd International Conference on Robotics, Electrical and Signal Processing Techniques (ICREST)*, 2023, pp. 90–94, 2023. [CrossRef]
- [27] A. Cozma, Adrian-Cosmin Firculescu, D. Tudose, and L. Ruse, "Autonomous Multi-Rotor Aerial Platform for Air Pollution Monitoring," *Sensors*, Vol. 22(3), Article 860, 2022. [CrossRef]
- [28] B. Yılmaz, B. Kütük, and İ. Korkamz, "Real Time Air Quality Sensing with Ground Robot and Drone." file:///Users/batti/Downloads/RealTimeAirQualitySensingwithGroundRobot.pdf Accessed on Feb 16, 2024.
- [29] B. Prabu, R. Malathy, M. N. A. Gulshan Taj, and N. Madhan "Drone networks and monitoring systems in smart cities," in *AI-Centric Smart City Ecosystems*, CRC Press, pp. 123–148, 2022. [CrossRef]
- [30] U. Isikdag and K. Sahin, "Web based 3D visualisation of time-varying air quality information," *The International Archives of the Photogrammetry, Remote Sensing and Spatial Information Sciences*, Vol. 42, pp. 267–274, 2018. [CrossRef]



Research Article

Evaluation of characterization and adsorption kinetics of natural organic matter onto nitric acid modified activated carbon

Betül AYKUT ŞENEL¹, Nuray ATEŞ², Şehnaz Şule KAPLAN BEKAROĞLU¹

¹Department of Environmental Engineering, Süleyman Demirel University, Isparta, Türkiye

²Department of Environmental Engineering, Erciyes University, Kayseri, Türkiye

ARTICLE INFO

Article history

Received: 01 November 2023

Revised: 13 February 2024

Accepted: 27 February 2024

Key words:

Activated carbon; Adsorption;

Kinetic model; Modification;

Natural organic matter

ABSTRACT

Natural organic substances (NOM) found in drinking water are a major contributor to disinfection by-product formation and are potentially toxic to humans. Conventional water treatment techniques may not always effectively treat NOMs. Therefore, an advanced treatment method such as adsorption can be inexpensive, simple and efficient. The selected adsorbent's and the NOMs properties both affect the removal effectiveness of the adsorption method. Activated carbon (AC), which is widely used in real-scale water treatment plants, has been modified and used in recent years in order to oxidize the porous carbon surface, raise its acidic qualities, eliminate mineral components, and enhance the surface's hydrophilic qualities. In this research, AC was modified with nitric acid (M-PAC) and NOM removal was investigated. In addition, it is discussed how the modification with nitric acid changes the adsorbent structure and chemistry. A morphology with smooth and irregular voids was observed as a result of nitric acid modification of the original AC by scanning electron microscopy (SEM) analysis. The particle size increased from 387.65 nm to 502.07 nm for the M-PAC adsorbent. The fourier transform infrared spectrophotometer (FTIR) spectrum indicates that structures connected to aromatic rings get formed in the M-PAC adsorbent as a result of the modification. The highest NOM removal for the original powdered activated carbon (PAC), 47%, was observed at 36 hours of contact time. On the other hand, M-PAC adsorbent achieved 40% NOM removal at contact times of 72 hours and above. It was concluded that the pseudo-second order kinetic model better represented NOM adsorption for both adsorbents.

Cite this article as: Aykut Şenel B, Ateş N, Kaplan Bekaroğlu ŞŞ. Evaluation of characterization and adsorption kinetics of natural organic matter onto nitric acid modified activated carbon. Environ Res Tec 2024;7(2)201–211.

INTRODUCTION

Over the last two decades, increased natural organic matter (NOM) concentration because of global warming, soil erosion, heavy rains [1, 2] and water pollution [3], poses challenges for water treatment plants in terms of operational optimization and proper process control [4, 5]. In addition to the increase in the amount of NOM in drinking water, changes in its quality (for example UV, SUVA)

also have a substantial effect on how water treatment systems function [6]. Furthermore, the interaction of NOM with chlorine-based disinfectants leads to the formation of disinfection by-product (DBPs) in drinking water [7]. Chronic exposure to these DBPs for example, trihalo-methanes (THMs) and haloacetic acids (HAAs) in drinking water through eating, inhalation, and skin contact can result in mutagenic and carcinogenic adverse health consequences [5, 8].

*Corresponding author.

*E-mail address: betulaykut32@gmail.com



The most effective method for reducing and controlling DBPs formation is to remove precursors (such as NOM) prior to disinfection. Kristiana et al. [9] study is a good example of this situation. According to the study, adding powdered activated carbon (PAC) to the coagulation process increased NOM removal efficiency by 70% and significantly decreased the generation of DBPs (80–95%). Similarly, Álvarez-Uriarte et al. [10] observed that the addition of 50 mg/L PAC resulted in a reduction in coagulant dose and increased removal of high molecular weight fractions of NOM. This confirmed that the THM formation potential increases the removal tendency. On the other hand, Joseph et al. [11] achieved a similar NOM removal efficiency (71.2%) using only commercially activated carbon.

NOMs are commonly removed from drinking water using a variety of treatment techniques, including adsorption, electrochemical treatment, membrane filtration, oxidation, biochemical treatment, coagulation, and flocculation [12]. Owing to its advantages, including high efficiency, the absence of toxic byproducts, practicability, and affordability, the adsorption method is widely regarded as one of the most effective water treatment technologies for NOM removal [13, 14]. It is used in the appropriate dosages before, during, and after coagulation to remove NOM more effectively, particularly during the adsorption process utilizing PAC. The drawback of PAC is the potential for carbon leakage into treated water [15].

Worldwide, studies has concentrated on many methods of modification to improve the important characteristics of AC, including surface chemistry, surface area, and morphological characteristics. Particularly in modification research, the factors impacting AC's properties and the impact of modifying agents on the morphological/adsorptive properties of the adsorbent are discussed [16]. It consists of three main categories of chemical, physical, and biological AC modification procedures and is further divided into subcategories according on the methods applied to change the surfaces [17, 18]. The porous surface of the AC is modified using an acidic process to boost its acidic properties, remove rid of undesired minerals, and make it more hydrophilic [19]. Nitric and sulfuric acids are the most often employed acids for this modification. There are more acidic functional groups and structures with –N–O– linkages and various oxygen groups formed on the surface of activated carbon due to nitric acid (HNO₃) modification [20].

Modification with nitric acid increases and/or decreases the pore volume and surface area and increases the amount of carbonyl, carboxyl, phenolic and lactone groups that give acid character to the surface. The modification of activated carbon with nitric acid resulted in the occurrence of functional groups with high amounts of accessible oxygen on the adsorbent surface, as observed by Gökçe and Aktaş [21] and Valentin-Reyes et al. [22]. Similar to this, Li et al. [23] observed that following modification, groups like carboxyl and lactone increase the oxygen-containing groups on the AC surface while also increasing the surface's hydrophilicity. Numerous investigations have found that nitric acid

oxidation has a positive effect on the micro and mesopore volume. Nitric acid modification, according to Su et al. [24], increased the maximum surface area by 15%, which had a substantial impact on micropore formation and enhanced the adsorption area for the required pollutant removal. Our previous studies showed that the total pore volume of powdered activated carbon modified with nitric acid increased significantly from 0.22 cm³/g to 0.76 cm³/g [25]. On the other hand, in a different study, nitric acid modification of AC resulted in a major reduction in total surface area (from 13% to 25%), a slight increase in mesopore volume, some expansion of average pore size, and a slight increase in adsorption capacity [26].

The modification method using acids like nitric acid and sulfuric acid had favorable impacts by enhancing the adsorption capacity in the adsorption of organic pollutants like NOM. Yang and Fox [27] as a consequence of modification with nitric acid, isotherm data showed that the adsorption capacity of humic acid increased from 30 mg/g to 45 mg/g compared to unmodified PAC. It was also stated that the acid-modified carbon adsorption fits the pseudo-second-order model. However, only a small number of studies have taken into account the adsorption of organic matter and its compounds using AC modified with nitric acid. The use of nitric acid modified AC is frequently encountered in metal adsorption research [20, 24, 28–31].

The performance of powdered activated carbon treated with nitric acid during the removal of NOMs from water has been the subject of numerous investigations [5, 27, 32], but the information is still insufficient. There are no investigations in the literature on the modification and characterization of the Purolite AC20 powder activated carbon chosen for this investigation using nitric acid. On the other hand, the research differs from other studies in that it was carried out using drinking water that actually contained NOM.

The objective of this study i) to investigate the effect of surface modification with nitric acid on the characterization of powder activated carbon, ii) to evaluate the adsorptive removal performance of original and nitric acid-modified PAC, iii) to determine the adsorption kinetic model of original and modified adsorbents. In the scope of the study, Purolite AC20 activated carbon was selected and modified with nitric acid. Additionally, NOM adsorption capacity was estimated using kinetic models (pseudo-first-order and pseudo-second-order) in water samples collected from the coagulation unit inlet for evaluation.

MATERIALS AND METHODS

Purolite AC20 is a commercially activated black spherical bead-like carbon obtained from the bituminous coal mineral. The adsorbent has a size range of 0.4–1.4 mm, a BET surface area of 900–1000 m²/g, and a maximum moisture content of 2%. Purolite AC20 activated carbon was supplied in granular form and was used in experimental studies after grinding and sieving under laboratory con-

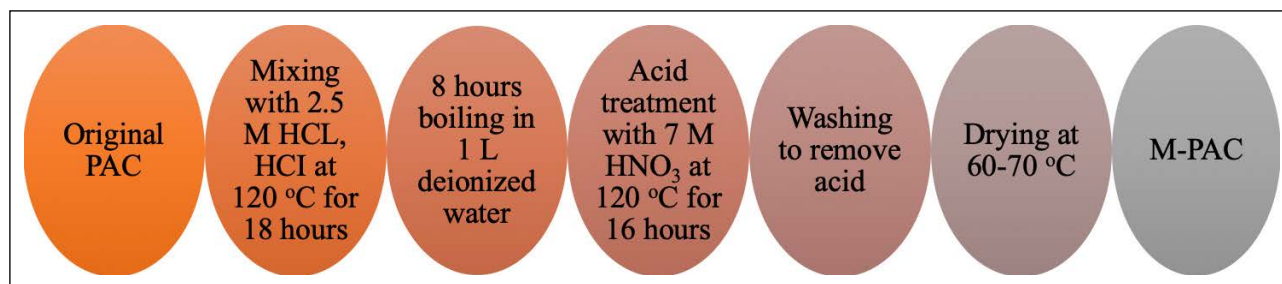


Figure 1. Nitric acid modification steps of original PAC.

ditions. High purity concentrated nitric acid from Merck (specific gravity 1.43 g/m³, 65% purity) was provided for modification. On the other hand, hydrochloric acid with a specific gravity of 1.19 g/m³ and 37% purity was bought from Sigma Aldrich.

Preparation of Modified Activated Carbon

Guha et al. [33] method with a few minimal changes was applied for the nitric acid modification procedure of the original PAC. Before AC modification, it was washed with distilled and deionized water and dried in an oven at 105 °C. Modification of AC was carried out in 5 stages as seen in Figure 1. In the initial stage of the modification, a flask containing 15 g of the adsorbent sample was slowly stirred in 500 ml of a 2.5 M HCl solution for 18 hours at 120 °C. After pre-treatment, in the second step, the samples were boiled in 1 L of distilled water at 120 °C for 8 hours. Nitric acid was used for the alteration process after pretreatment. The adsorbents added to 1 L of 7 M HNO₃ were shaken quietly for 16 hours at 120 °C using a magnetic stirrer in a flask. Following acid treatment, the adsorbent and acid phase were separated by precipitation in a flask.

Step 4 involved washing the samples with distilled and deionized water until they acquired a consistent pH of between 5 and 6. Following the washing procedure, the samples were dried in a vacuum oven at 60 °C to 70 °C. The drying process was continued for approximately 48 hours. In order to understand that the activated carbons are dry, weightings were made at certain intervals until they reach the constant weight, and after reaching the constant weight, the dry activated carbons are kept in the desiccator. In the samples weighed after drying, a loss of approximately 40% was observed due to the washing processes compared to the pre-modification. The resulting adsorbent was labeled as M-PAC.

Characterization Methods

Surface characteristics, pore size distributions, and structural characteristics of modified and unmodified activated carbons were determined by characterization analysis using scanning electron microscopy (SEM), Brunauer, Emmet, and Teller (BET) analysis, fourier transform infrared spectrophotometer (FTIR), and dynamic light scattering (DLS). The surface morphology of the adsorbents was determined by Zeiss Evo LS10 scanning electron microscope (SEM) at Erciyes University TAUM center. In the 400–4000 cm⁻¹

Table 1. The characteristics of the water used in adsorption experiments

Parameters	Unit	Value
pH	–	7.84
UV ₂₅₄	(cm ⁻¹)	0.044
TOC	(mg/L)	3.05
SUVA ₂₅₄	(L/(mgTOC.m))	1.73
Alkalinity	(mgCaCO ₃ /L)	210
Total hardness	(mgCaCO ₃ /L)	225
Electrical conductivity	(µS/cm)	400

wavelength range, FTIR analyses were carried out using a Perkin Elmer 400 Ft-IR/FT-FIR spectrometer at Erciyes University Technology Research and Application Center. The surface areas and total pore volumes of the adsorbents were determined with the micromeritics gemini VII surface area and porosity surface analyzer device. The surface area of the adsorbents was determined using N₂ adsorption-desorption isotherms. At the Technology Research and Application Center of Erciyes University, BET analyses were conducted through service procurement. The point of zero charge (pH_{PZC}) and pH equilibrium methods were employed for evaluating the surface chemistry of the adsorbents. Total surface acidic groups (NaOH adsorption) and total surface basic groups (HCl adsorption) were measured using the Boehm method (alkalimetric titration) with minor modifications [34].

Water Characterization

Water samples collected from the coagulation process's input at Konya Drink Water Treatment Plant (KOSKİ) Plant were used in the kinetic testing for the adsorption experiments. The characteristics of the coagulation process inlet water are given in Table 1. The removal efficiencies of UV₂₅₄ and NOM from filtrate were computed as a result of kinetic testing, and models were developed.

Adsorption and Kinetic Analysis

Adsorption kinetic tests were conducted for the original and nitric acid modified activated carbon. In the kinetic tests, the contact time required for the adsorbent to reach equilibrium was determined. The kinetic tests were carried out in 125 ml (solution volume 100 ml) polytetrafluoroethylene (PTFE) capped, dark (amber) glass bottles, on

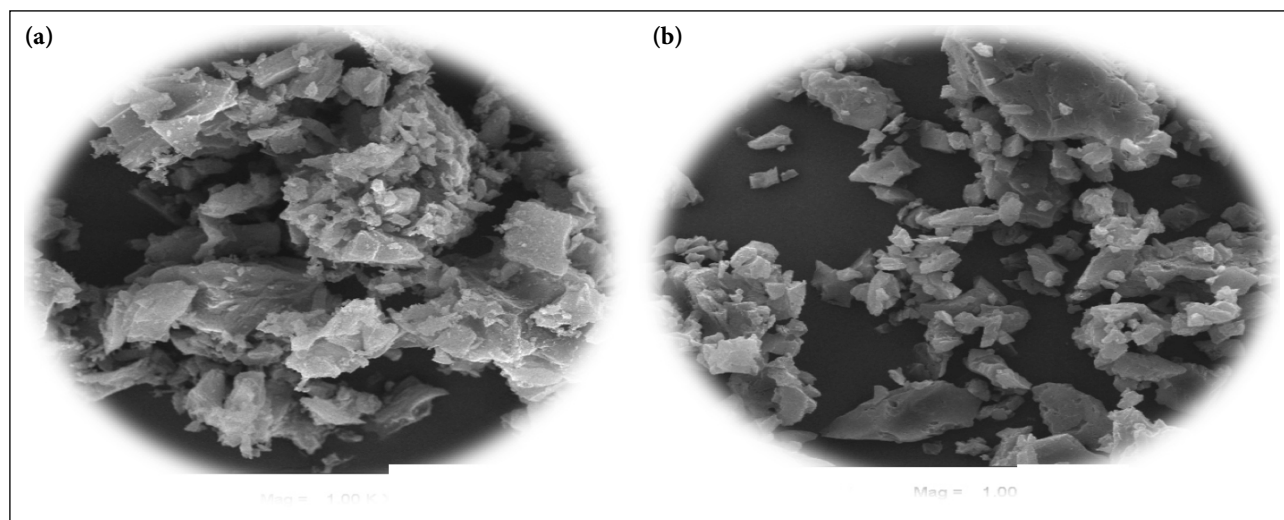


Figure 2. SEM images original PAC (a) and nitric acid modified M-PAC (b) (1 μm mag: 5.00 KX).

the samples taken from the coagulation inlet unit of the KOSKÍ Drinking Water Treatment Plant. The pH value of natural waters is required to be between 6.5 and 9.5 for human consumption purposes. Considering this situation, the pH value of the samples was adjusted to be between 7 ± 0.1 with H_2SO_4 or NaOH. The original PAC changed the pH value of the water between 7.63 and 7.74 during the contact times determined after adsorption. It was observed that the M-PAC adsorbent changed the pH of the water in the range of 7.2–7.34 after adsorption. During the predetermined contact times, shaking was carried out in the shaker horizontally at a speed of 100 rpm. Adsorption periods of 2, 4, 8, 12, 24, 36, 48, 72 and 96 hours were examined for kinetic tests at a fixed adsorbent dosage of 300 mg/L. The sample was filtered with 0.45 μm PES filter paper after each contact period to separate the adsorbent particles from the aqueous phase.

Analyses of total organic carbon (TOC) and UV_{254} were performed on the sample obtained from the supernatant portion. UV_{254} analyses included measurements at 254 nm using a UV-1700 Shimadzu UV-visible spectrophotometer. Each sample was measured 3 times and averaged. Before starting the analysis, the spectrophotometer was reset with distilled water.

The difference between the starting and final adsorbate concentrations provided in Equation 1 was used for obtaining the adsorption capacity (adsorbed NOM onto PACs).

$$q = \frac{(C_0 - C)V}{M} \quad (1)$$

Where, C_0 and C are initial and equilibrium concentrations of substance in water samples (mg/L), respectively. Adsorption capacity (mg/g), sample volume (L) and mass of PACs (g) are indicated by q , V and M , respectively.

The TOC removal capabilities of the adsorbents were calculated and suitable kinetic models were found while taking into account the kinetic times. The formula in Equation 2 is used to calculate the adsorption process' rate constant in the pseudo-first order model.

$$\ln(q_e - qt) = (\ln q_e) - K_1 * t \quad (2)$$

The pseudo-second order velocity kinetics were calculated using the formula found in Equation 3 below.

$$\frac{t}{qt} = \frac{1}{K_2 q_e^2} + \frac{1}{q_e} * t \quad (3)$$

K_1 : Pseudo 1st order, adsorption rate constant (1/min)

K_2 : Pseudo 2nd order adsorption rate constant (g/mg.min)

q_e : Amount of substance adsorbed on unit adsorbent (mg/g)

q_t : Amount of pollutant adsorbed in t time (mg/g)

t : Adsorption contact time (min).

RESULTS AND DISCUSSION

Characterization of PAC and M-PAC

Morphological characterization of PAC and M-PAC

The outcomes of SEM analysis on both raw PAC and M-PAC are presented in Figure 2. There are obvious distinctions between PAC and M-PAC when the morphological images are compared. SEM images demonstrate that the original PAC adsorbent features a distinguishing surface feature and pore structure. There were numerous new irregular holes on the M-PAC surface as well as a smooth structure made of nitric acid.

The M-PAC surface area has been slightly reduced. Similarly, there are studies in the literature stating that activated carbon forms a smoother, narrower porous structure after modification with HNO_3 , and this is supported by the decrease in BET surface area [30, 31, 33–35].

The reason for the absence of porosity for M-PAC in SEM analysis may be related to pore clogging and pore destruction by nitric acid. Researchers have reported that this situation can be attributed to two possible effects of nitric acid, i) partial destruction of microporous walls [36, 39] and ii) oxygen functional. They attributed it to the formation of groups and the blockage of the pore entrance [40].

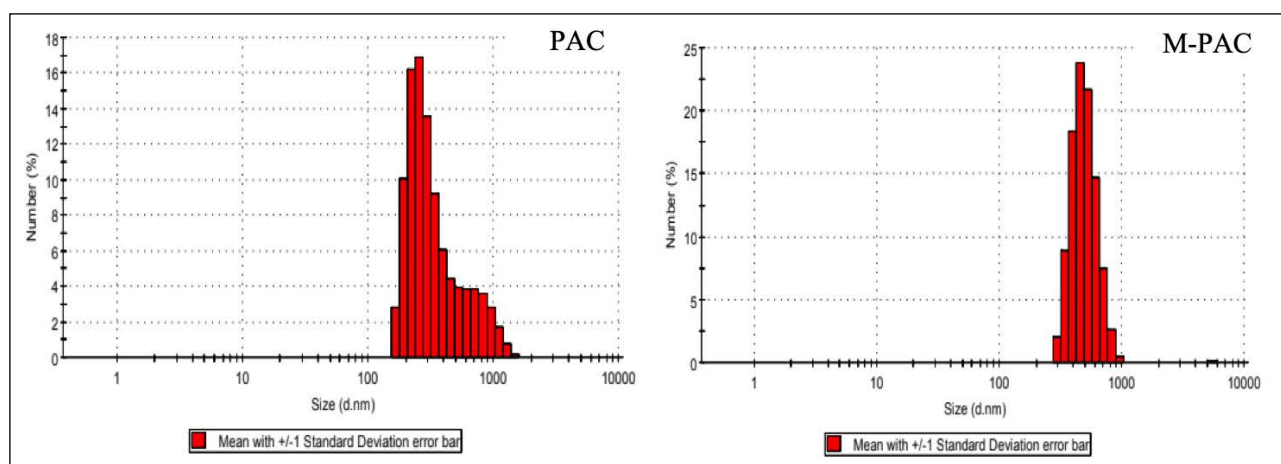


Figure 3. Particle size distribution graph of the original PAC and M-PAC adsorbents.

Table 2. Pore structure and surface chemical characterization of original PAC and M-PAC adsorbents

Adsorbent	BET surface area S_{BET} ($m^2 g^{-1}$)	Total pore volume ($cm^3 g^{-1}$)	Pore diameter (nm)	pH_{pzc}	Total acidic groups		Total basic groups	
					(meq/g)	(meq/m ²)	(meq/g)	(meq/m ²)
PAC	768	0,47	2,45	9.21	3.5	0.005	3.08	0.004
M-PAC	727	0,44	2,44	2.03	4.6	0.006	2.78	0.004

* S_{BET} : Surface area calculated by Brunauer-Emmett-Teller theory; Pore width: It represents the point of adsorption average pore width (BET 4V/A).

It is also seen that the modification with HNO_3 causes the formation of smaller particles on the M-PAC. Activated carbon modified with HNO_3 produces corrosive and particle-eroding properties, according to El-Hendawy et al. [26]. Chingombe et al. [41] observed that the modification of F400 activated carbon with HNO_3 made little difference to the surface morphology other than a significant pore enlargement. In another study, when he examined the SEM image of bamboo charcoal after treatment with HNO_3 , it was observed that the surface became smoother and the cell walls became thicker, and the surface was non-porous [42].

DLS analysis was used to determine the particle size distribution of the unmodified and nitric acid-modified carbon. DLS measurements were carried out using the Malvern NanoZS90 instrument, which has a 633 nm laser, at room temperature. The DLS histogram in Figure 3 indicates the particle size analysis of the PAC and M-PAC adsorbents. The graphs show the particle size diameter in nm on the x-axis and the particle size as a percentage on the y-axis. The histogram plot demonstrates the original PAC's broad particle distribution, which spans the wavelength range of 164.2 nm to 1484 nm.

The weighted average calculation method obtained an average particle size of 387.65 nm for the original PAC adsorbent. This value increased in the M-PAC adsorbent as a result of the nitric acid alteration, and it was determined to be 502.07 nm. Additionally, the M-PAC adsorbent's particle size distribution accumulated in the 387 nm region by 78%. An indicator of a sample's size-based heterogeneity is the polydispersity index (PDI). If the PDI is less than 0.3, it indicates monodispersity; if it is larger than 0.5, it indicates

that the particle is very heterogeneous. The PDI is near to 0, indicating a homogenous particle size [43]. Particle size distribution range ranging from 80 to 1100 nm with PDI 0.237 is given. PDI refers to the size of 85–850 nm with 0.246 [44]. Considering the particle size distributions calculated in our study (387.65 for original PAC; 502.07 for M-PAC), PDI corresponds to a value of 0.246. This situation indicates monodispersity.

FTIR studies were carried out with Perkin Elmer 400 Ft-IR/FT-FIR spectrometer in the wavelength range of 400–4000 cm^{-1} . An important technique for analyzing the distributions of functional groups on surfaces qualitatively is the use of FTIR spectra. FTIR spectra of original PAC and M-PAC are shown in Figure 4. It was observed that the 2900 cm^{-1} and 2094 cm^{-1} bands, which characterize the C-H group in the original PAC, FTIR spectra, remained almost the same in the M-PAC spectrum. These bands result from symmetrical and asymmetrical C – H stretching vibrations [45]. The PAC adsorbent was modified with HNO_3 and the 1987 cm^{-1} band indicating the C N group eliminated as a result [46]. C-O stretching vibrations can be seen in the original PAC's 1242 cm^{-1} band [47, 48]. This demonstrates that acid modification lead to the C-O stretching vibrations disappear in the M-PAC adsorbent.

The M-PAC adsorbent's 1000–1100 cm^{-1} bands are the alcohol C–O stretching vibration structures, and the 1387.4 cm^{-1} band is the COOH group [49]. While other vibrations at 888 cm^{-1} and 749 cm^{-1} are linked to the C-H deformation vibration of the benzene ring, bands emerging at approximately 1400 cm in the literature are related to the O-C-O symmetrical vibration of the carboxylic acid group

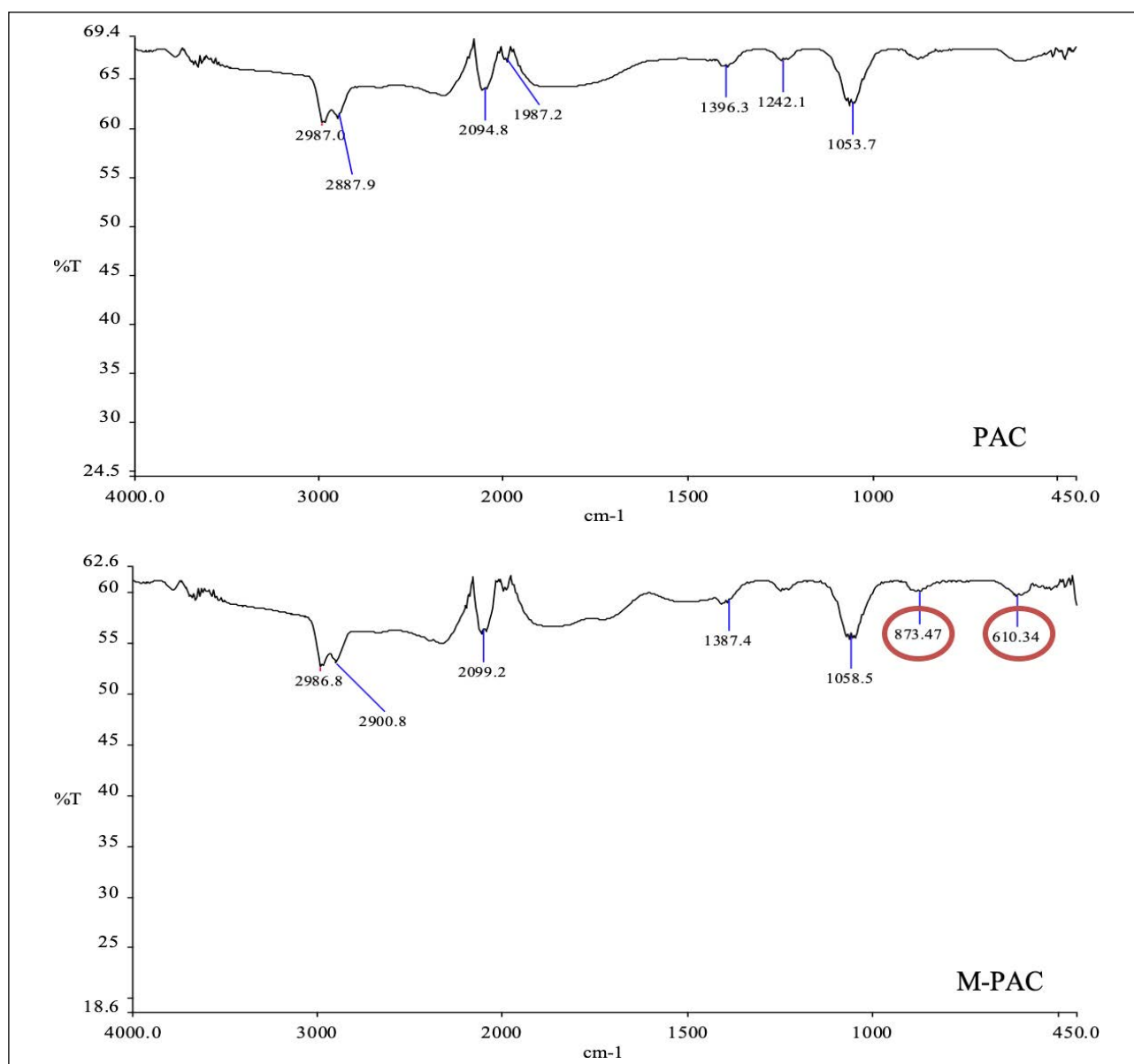


Figure 4. FTIR spectra of original PAC and M-PAC.

[50]. According to Aguiar et al. [51] and Wang et al. [52] bands obtained between 795 and 881 cm^{-1} are indicative of the existence of heteroaromatic chemicals and aromatic rings. As a result of the original PAC nitric acid modification, two new functional groups (873.47 and 610.34 cm^{-1}) that we can associate with the presence of aromatic rings were added to the M-PAC structure. The 873.47 cm^{-1} band can be associated with the presence of aromatic rings and heteroaromatic compounds. In some studies, bonds between 600–900 cm^{-1} have been associated with the out-of-plane bending mode of the C-H or O-H group [53]. The 610.34 cm^{-1} band in the FTIR spectrum of the M-PAC adsorbent is attributed to the C-H or O-H group.

The average BET area, total pore volume, pore diameter, pH_{pzc} , total acidic and basic groups of adsorbents were given in Table 2. The changes brought about by the modification on the surface area and pore properties were comprehended using N_2 adsorption-desorption isotherms.

The surface area of the M-PAC adsorbent was reduced by 5% as a result of the nitric acid modification. Researchers have linked the decrease in surface area caused by acid modification to two possible outcomes: (1) partial destruction of microporous walls [37, 39] and (2) formation of oxygen functional groups due to blockage of the pore entrance [40]. Additionally, the M-PAC adsorbent's total pore volume exhibited a slight decrease from 0.47 cm^3/g to 0.44 cm^3/g . Similar to this, other researchers have found that pore blockage and pore destruction caused by nitric acid modification lead to a decrease in pore volume and surface area [54].

Measurements of pH_{pzc} are made at the zero charge point, where carbon is neutrally charged, to calculate the pH of the solution [55, 56]. At pH below pH_{pzc} , the adsorbent surface will be positively charged, and at a pH above pH_{pzc} , the surface will be negatively charged. According to Dabrowski et al. [57] that event has an impact on the

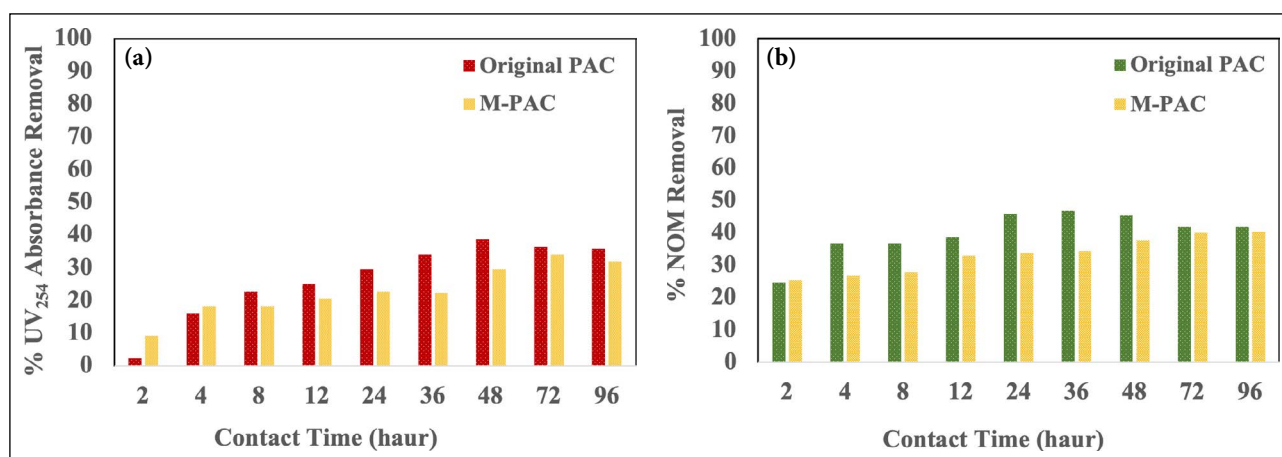


Figure 5. UV₂₅₄ (a) and NOM (b) removal efficiencies (%) for original PAC and M-PAC adsorbents.

adsorbate-adsorbent system's ability to remove pollutants during adsorption. Nitric acid modification caused the pH_{pzc} value of the original PAC adsorbent decrease substantially, from 9.21 to 2.03. This indicates that the acidic properties are more dominant at these carbons and are the result of a greater number of weakly acidic functional groups than others. Total surface acidic and basic group amounts were defined by the Boehm method. An increase was observed in the total acid groups (meq/g) of M-PAC adsorbent after nitric acid modification. The total amount of acidic group for the original PAC increased from 3.5 meq/g to 4.6 meq/g for the M-PAC adsorbent. When the results reported in the literature for acid functional groups were examined, it was concluded that the use of HNO₃ had a dominant effect on carboxylic group formation.

Adsorption Kinetic Analysis

Effect of Contact Time

Adsorption periods of 2, 4, 8, 12, 24, 36, 48, 72 hours and 96 hours were tried at a fixed adsorbent dose of 300 mg/L in order to allow the adsorbents to approach equilibrium. The NOM removal efficiencies were calculated taking into consideration the TOC parameter. Figure 5 shows the UV₂₅₄ (a) and NOM (b) removal efficiencies, which depend on to the adsorbents contact time.

The contact time of 48 hours was found to be adequate after taking into account the removal efficiencies as a result of the kinetic testing. The maximum removal effectiveness was found to be 39% in the 48 hour contact time in the findings of the kinetic investigation, which observed at the removals of UV₂₅₄ absorbance in the original PAC adsorbent. On the other hand, for M-PAC, contact period of 72 hours resulted in the maximum UV₂₅₄ absorbance removal of 34%. The NOM removal efficiency in the coagulation unit inlet water changed from 25 to 47 percent at the determined adsorbent contact times with original PAC. This situation has been supported by studies in the literature stating that AC alone without coagulation is as effective as 0–76% in the removal of NOM [58]. The highest NOM removal, 47%, was observed in the original PAC at 36 hours of contact time. In contrast,

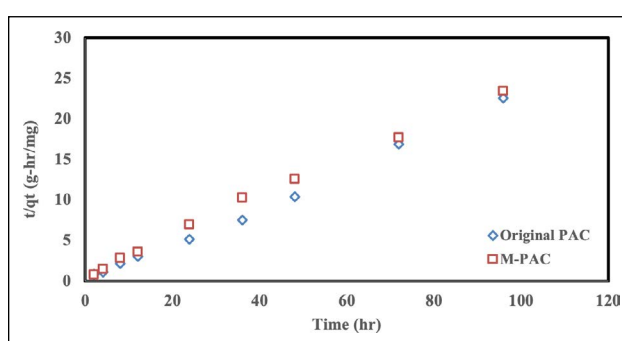


Figure 6. Pseudo-second-order kinetic for NOM adsorption by adsorbents.

M-PAC achieved 40% removal efficiency during contact times of 72 and 96 hours. This revealed that the Purolite AC20 adsorbent modified with nitric acid was not a very efficient adsorbent in UV₂₅₄ absorbance and NOM removal.

Pseudo-kinetic models simulating the total adsorption rate are a widely used method to model the kinetics of adsorption systems, as they accurately reflect real data [59]. The Pseudo-second order (PSO) graph plotting t versus t/qt to determine the organic matter adsorption kinetic rate is shown in Figure 6. The linearity of the t/qt versus t plot confirms the fit of the process to the pseudo-second-order kinetic model. A contact time of 48 hours was chosen to keep the results of the kinetic tests within confidence intervals and to allow comparison with literature searches. In some previous studies on the adsorption of organic substances, it was stated that the time for adsorbents to reach equilibrium ranged from 30 minutes to 72 hours [15, 60, 61].

Adsorption Kinetic Models

Adsorption kinetics were described using pseudo-first order and pseudo-second order models. Table 3 presents the kinetic parameters obtained from pseudo-first order and pseudo-second order models. According to the correlation coefficient of these two models, the pseudo-second order model displayed better fitting than the pseudo-first order model regarding experimental data. Furthermore, compared to the pseudo-first order kinetic model, the calculated

Table 3. Adsorption kinetic model parameters for NOM adsorbed on original PAC and M-PAC

Adsorbents	q_{exp} (mg/g)	Pseudo-first order (PFO)			Pseudo-second order (PSO)		
		q_{cal} (mg/g)	k_1 (1/h)	R^2	q_{cal} (mg/g)	k_2 (g/mg-h)	R^2
Original PAC	4.27	1.56	0.012	0.09	4.35	132.37	0.99
M-PAC	4.07	2.12	0.01	0.76	4.20	0.066	0.99

equilibrium capacity ($q_{e,cal}$) by pseudo-second order kinetic model better predicted the observed equilibrium capacity ($q_{e,exp}$). When the results were examined, it was determined that the R^2 values were high, and considering the correlation between the experimental q_e and the calculated q_e , the adsorption kinetics was in accordance with the Pseudo second order kinetic model. Tafvizi et al. [5] calculated that their kinetic results were the most appropriate kinetic model among all three ACs in the study of pseudo-second-order velocity kinetics. Similarly, Yang and Fox [27] observed that the adsorption of acid modified activated carbon conforms to the pseudo second-order model. Yilmaz et al. [62] found that in the adsorption of the original powdered activated carbon with 2 different properties over the TOC parameter, the contact time of 72 hours was sufficient to reach equilibrium and fit the second-order kinetic model.

Chemisorption or the valence force are the driving forces in the pseudo-second order model. The pseudo-second-order model provides the best fit in this situation because of the interplay between valence force and negatively charged organic matter at the surface functional group. Moreover, pseudo-second-order kinetics have been widely reported to explain organic compound sorption on activated carbon, suggesting that functional group interaction is important in the rate control step [27, 63].

The original PAC and M-PAC, q_{exp} values were 4.27 mg/g and 4.07 mg/g, respectively. The R^2 values of both adsorbents are very close to each other. Pseudo-second order kinetic model q_e (calculated) values were calculated as 4.35 mg/g for the original PAC adsorbent and 4.20 for M-PAC. According to the first-order and second-order models for M-PAC, k_1 and k_2 values were calculated as 0.01 1/h and 0.066 g/mg-h, respectively. The fact that the k_2 value frequently varies based on operational conditions including pH, temperature, and shaking strength explains why the k_2 values of the different adsorbents varied from one another. Zhao et al. [15] reported that the adsorption of NOM by GAC was well described by the pseudo-second-order velocity model and the velocity kinetic parameters k_2 , q_e and R^2 values were calculated as 0.24 g/mg.hr, 2.02 mg/g and 0.99, respectively.

CONCLUSION

The performance of nitric acid modified powdered activated carbon during the removal of NOMs from water is still under investigation. In this study, characterization studies were conducted after the original Purolite AC20 activated carbon was modified using nitric acid. Additionally, the NOM adsorption of nitric acid modified AC (M-PAC) in

the water samples taken from the water entering the coagulation unit was estimated using kinetic models, and the NOM adsorption capacity was assessed.

The surface area of the M-PAC adsorbent was reduced by 5% as a result of the nitric acid modification. The original PAC adsorbent's PH_{pzc} value decreased significantly after nitric acid modification, from 9.21 to 2.03. It also indicates that there are more weakly acidic functional groups than other functional groups at these carbons, which is why the acidic features are more prominent there.

It was shown in the SEM pictures that the M-PAC surface had developed several new, irregular holes as well as a smooth structure. As a result of the original PAC nitric acid modification, two new functional groups were added to the M-PAC structure, which we can associate with the presence of aromatic rings. At 48 hours of contact time, it was found that the original PAC's UV_{254} absorbance removal reached a maximum of 39%. For M-PAC, a maximum UV_{254} absorbance removal of 34% was observed at contact time of 72 hours. The highest NOM removal, 47%, was observed in the original PAC at 36 hours of contact time. In contrast, M-PAC achieved 40% removal efficiency during contact times of 72 and 96 hours. The original PAC and M-PAC, q_{exp} values were 4.27 mg/g and 4.07 mg/g, respectively. As a result of the calculations, it was concluded that the pseudo-second order kinetic model better describes the NOM adsorption of the original PAC and M-PAC. This study will provide preliminary data especially in the evaluation of NOM removal with modified AC adsorbent in real natural water resources.

M-PAC adsorbent was expected to increase NOM adsorption. There are many reasons why removal efficiency does not increase. For example, the properties of water, the appropriate amount of adsorbent and the concentration of nitric acid used for modification are some of these. Modification studies can be carried out with different and lower nitric acid concentrations to increase removal efficiency. Additionally, different mixing times and different acid modifications can be tried. In our study, water source has a low SUVA value. Considering this situation, NOM removal of activated carbon modified with nitric acid from a high SUVA water source can be investigated.

ACKNOWLEDGEMENTS

The authors would like to thank the financial support from the Scientific and Technological Research Council of Türkiye (TUBITAK) 1001 Research Projects Funding Program with project number 118Y402.

DATA AVAILABILITY STATEMENT

The author confirm that the data that supports the findings of this study are available within the article. Raw data that support the finding of this study are available from the corresponding author, upon reasonable request.

CONFLICT OF INTEREST

The author declared no potential conflicts of interest with respect to the research, authorship, and/or publication of this article.

USE OF AI FOR WRITING ASSISTANCE

Not declared.

ETHICS

There are no ethical issues with the publication of this manuscript.

REFERENCES

- [1] T. I. Nkambule, R. W. M. Krause, J. Haarhoff, and B. B. Mamba, “A three step approach for removing organic matter from South African water sources and treatment plants,” *Physics and Chemistry of the Earth*, Vol. 50–52, pp. 132–139, 2012. [\[CrossRef\]](#)
- [2] C. O’Driscoll, J. L. Ledesma, J. Coll, J. G. Murnane, P. Nolan, E. M. Mockler, and L. W. Xiao, “Minimal climate change impacts on natural organic matter forecasted for a potable water supply in Ireland,” *Science of Total Environment*, Vol. 630, pp. 869–877, 2018. [\[CrossRef\]](#)
- [3] J. C. Rodríguez-Murillo, J. Zobrist, and M. Filella, “Temporal trends in organic carbon content in the main Swiss rivers, 1974–2010,” *Science of Total Environment*, Vol. 502, pp. 206–217, 2015. [\[CrossRef\]](#)
- [4] J. Adusei-Gyamfi, B. Ouddane, L. Rietveld, J. P. Cornard, and J. Criquet, “Natural organic matter-cations complexation and its impact on water treatment: A critical review,” *Water Research*, Vol. 160, pp. 130–147, 2019. [\[CrossRef\]](#)
- [5] H. Tafvizi, S. Chowdhury, and T. Husain, “Low cost activated carbon for removal of NOM and DBPs: Optimization and comparison,” *Water (Switzerland)*, Vol. 13(16), pp. 1–23, 2021. [\[CrossRef\]](#)
- [6] A. Matilainen, M. Vepsäläinen, and M. Sillanpää, “Natural organic matter removal by coagulation during drinking water treatment: A review,” *Advances in Colloid and Interface Science*, Vol. 159(2), pp. 189–197, 2010. [\[CrossRef\]](#)
- [7] K. Y. Park, Y. J. Yu, S. J. Yun, and J. H. Kweon, “Natural organic matter removal from algal-rich water and disinfection by-products formation potential reduction by powdered activated carbon adsorption,” *Journal of Environmental Management*, Vol. 235, pp. 310–318, 2019. [\[CrossRef\]](#)
- [8] A. Bhatnagar, and M. Sillanpää, “Removal of natural organic matter (NOM) and its constituents from water by adsorption – A review,” *Chemosphere*, Vol. 166, pp. 497–510, 2017. [\[CrossRef\]](#)
- [9] I. Kristiana, C. Joll, and A. Heitz, “Powdered activated carbon coupled with enhanced coagulation for natural organic matter removal and disinfection by-product control: Application in a Western Australian water treatment plant,” *Chemosphere*, Vol. 83(5), pp. 661–667, 2011. [\[CrossRef\]](#)
- [10] J. I. Álvarez-Uriarte, U. Iriarte-Velasco, N. Chimeño-Alanís, and J. R. González-Velasco, “The effect of mixed oxidants and powdered activated carbon on the removal of natural organic matter,” *Journal of Hazardous Materials*, Vol. 181(1–3), pp. 426–431, 2010. [\[CrossRef\]](#)
- [11] L. Joseph, J. R. V. Flora, Y. G. Park, M. Badawy, H. Saleh, and Y. Yoon, “Removal of natural organic matter from potential drinking water sources by combined coagulation and adsorption using carbon nanomaterials,” *Separation and Purification Technology*, Vol. 95, pp. 64–72, 2012. [\[CrossRef\]](#)
- [12] Y. Zhang, X. Zhao, X. Zhang, and S. Peng, “A review of different drinking water treatments for natural organic matter removal,” *Water Science and Technology: Water Supply*, Vol. 15(3), pp. 442–455, 2015. [\[CrossRef\]](#)
- [13] P. Rao, I. M. C. Lo, K. Yin, and S. C. N. Tang, “Removal of natural organic matter by cationic hydrogel with magnetic properties,” *Journal of Environmental Management*, Vol. 92(7), pp. 1690–1695, 2011. [\[CrossRef\]](#)
- [14] S. Singh, A. Srivastava, and S. P. Singh, “Inexpensive, effective novel activated carbon fibers for sample cleanup: application to multipesticide residue analysis in food commodities using a QuEChERS method,” *Analytical and Bioanalytical Chemistry*, vol. 410(8), pp. 2241–2251, 2018. [\[CrossRef\]](#)
- [15] Z. Zhao, W. Sun, and M. B. Ray, “Adsorption isotherms and kinetics for the removal of algal organic matter by granular activated carbon,” *Science of Total Environment*, Vol. 806, Article 150885, 2022. [\[CrossRef\]](#)
- [16] K. Azam, N. Shezad, I. Shafiq, P. Akhter, F. Akhtar, F. Jamil, and M. Hussain, “A review on activated carbon modifications for the treatment of wastewater containing anionic dyes,” *Chemosphere*, Vol. 306, Article 135566, 2022. [\[CrossRef\]](#)
- [17] C. Y. Yin, M. K. Aroua, and W. M. A. W. Daud, “Review of modifications of activated carbon for enhancing contaminant uptakes from aqueous solutions,” *Separation and Purification Technology*, Vol. 52(3), pp. 403–415, 2007. [\[CrossRef\]](#)
- [18] A. Bhatnagar, W. Hogland, M. Marques, and M. Sillanpää, “An overview of the modification methods of activated carbon for its water treatment applications,” *Chemical Engineering Journal*, Vol. 219, pp. 499–511, 2013. [\[CrossRef\]](#)
- [19] W. Shen, Z. Li, and Y. Liu, “Surface chemical functional groups modification of porous carbon,” *Recent Patents on Chemical Engineering*, Vol. 1(1), pp. 27–40, 2010. [\[CrossRef\]](#)

- [20] Ç. Öter, and Ö. Selçuk Zorer, "Adsorption behaviours of Th(IV) and U(VI) using nitric acid (HNO₃) modified activated carbon: equilibrium, thermodynamic and kinetic studies," *International Journal of Environmental Analytical Chemistry*, Vol. 101(14), pp. 1950–1965, 2021.
- [21] Y. Gokce, and Z. Aktas, "Nitric acid modification of activated carbon produced from waste tea and adsorption of methylene blue and phenol," *Applied Surface Science*, Vol. 313, pp. 352–359, 2014. [CrossRef]
- [22] J. Valentín-Reyes, R. B. García-Reyes, A. García-González, E. Soto-Regalado, and F. Cerino-Córdova, "Adsorption mechanisms of hexavalent chromium from aqueous solutions on modified activated carbons," *Journal of Environmental Management*, Vol. 236, pp. 815–822, 2019. [CrossRef]
- [23] Z. Li, H. Hanafy, L. Zhang, L. Sellaoui, M. S. Netto, M. L. Oliveira, and Q. Li, "Adsorption of congo red and methylene blue dyes on an ashitaba waste and a walnut shell-based activated carbon from aqueous solutions: Experiments, characterization and physical interpretations," *Chemical Engineering Journal*, Vol. 388, Article 124263, 2020. [CrossRef]
- [24] P. Su, J. Zhang, J. Tang, and C. Zhang, "Preparation of nitric acid modified powder activated carbon to remove trace amount of Ni(II) in aqueous solution," *Water Science and Technology*, Vol. 80(1), pp. 86–97, 2019. [CrossRef]
- [25] B. Aykut-Şenel, Ş. Ş. Kaplan-Bekaroğlu, and N. Ateş, "Toz aktif karbonun nitrik asit ve sülfonik asit ile kimyasal modifikasyonu ve karakterizasyonu," *Mühendislik Bilimleri ve Tasarım Dergisi*, Vol. 10(4), pp. 1333–1340, 2022. [Turkish] [CrossRef]
- [26] A. N. A. El-Hendawy, "Influence of HNO₃ oxidation on the structure and adsorptive properties of corncob-based activated carbon," *Carbon NY*, Vol. 41(4), pp. 713–722, 2003. [CrossRef]
- [27] K. Yang, and J. T. Fox, "Adsorption of humic acid by acid-modified granular activated carbon and powder activated carbon," *Journal of Environmental Engineering*, Vol. 144(10), 2018. [CrossRef]
- [28] J. P. Chen, and S. Wu, "Acid/base-treated activated carbons: characterization of functional groups and metal adsorptive properties," *Langmuir*, Vol. 20, no. 6, pp. 2233–2242, 2004. [CrossRef]
- [29] S. X. Liu, X. Chen, X. Y. Chen, Z. F. Liu, and H. L. Wang, "Activated carbon with excellent chromium(VI) adsorption performance prepared by acid-base surface modification," *Journal of Hazardous Materials*, Vol. 141(1), pp. 315–319, 2007. [CrossRef]
- [30] H. T. Ma, V. T. T. Ho, N. B. Pham, L. G. Bach, and T. D. Phan, "The comparison of surface modification methods of the heavy metals adsorption of activated carbon from rice husk," *Applied Mechanics and Materials*, Vol. 876, pp. 91–96, 2018. [CrossRef]
- [31] W. S. Chen, Y. C. Chen, and C. H. Lee, "Modified activated carbon for copper ion removal from aqueous solution," *Processes*, Vol. 10(1), 2022. [CrossRef]
- [32] S. A. Dastgheib, T. Karanfil, and W. Cheng, "Tailoring activated carbons for enhanced removal of natural organic matter from natural waters," *Carbon NY*, Vol. 42(3), pp. 547–557, 2004. [CrossRef]
- [33] A. Guha, W. Lu, T. A. Zawodzinski, and D. A. Schiraldi, "Surface-modified carbons as platinum catalyst support for PEM fuel cells," *Carbon NY*, Vol. 45(7), pp. 1506–1517, 2007. [CrossRef]
- [34] M. E. de Oliveira Ferreira, B. G. Vaz, C. E. Borba, C. G. Alonso, and I. C. Ostroski, "Modified activated carbon as a promising adsorbent for quinoline removal," *Microporous and Mesoporous Materials*, vol. 277, pp. 208–216, 2019. [CrossRef]
- [35] N. Bader, S. Souissi-Najar, and A. Ouederni, "A controlled nitric acid oxidation of an olive stones-based activated carbon: effect of oxidation time," *Lignocellulose Journal*, Vol. 3(1), pp. 22–36, 2014.
- [36] J. Rivera-Utrilla, M. Sánchez-Polo, V. Gómez-Serrano, P. M. Álvarez, M. C. M. Alvim-Ferraz, and J. M. Dias, 'Activated carbon modifications to enhance its water treatment applications. An overview', *Journal of Hazardous Materials*, Vol. 187(1–3), pp. 1–23, 2011. [CrossRef]
- [37] O. Adam, M. Bitschené, G. Torri, F. De Giorgi, P. M. Badot, and G. Crini, "Studies on adsorption of propiconazole on modified carbons," *Separation and Purification Technology*, Vol. 46(1–2), pp. 11–18, 2005. [CrossRef]
- [38] G. Huang, J. X. Shi, and T. A. G. Langrish, "Removal of Cr (VI) from aqueous solution using activated carbon modified with nitric acid," Vol. 152, pp. 434–439, 2009. [CrossRef]
- [39] S. Yao, J. Zhang, D. Shen, R. Xiao, S. Gu, M. Zhao, and J. Liang, "Removal of Pb(II) from water by the activated carbon modified by nitric acid under microwave heating," *Journal of Colloid and Interface Science*, Vol. 463, pp. 118–127, 2016. [CrossRef]
- [40] A. Khelifi, M. C. Almazán-Almazán, M. Pérez-Mendoza, M. Domingo-García, F. J. López-Domingo, L. Temdrara, and A. Addoun, "Influence of nitric acid concentration on the characteristics of active carbons obtained from a mineral coal," *Fuel Processing Technology*, Vol. 91(10), pp. 1338–1344, 2010. [CrossRef]
- [41] P. Chingombe, B. Saha, and R. J. Wakeman, "Surface modification and characterisation of a coal-based activated carbon," *Carbon NY*, Vol. 43(15), pp. 3132–3143, 2005. [CrossRef]
- [42] H. Xu, B. Shen, P. Yuan, F. Lu, L. Tian, and X. Zhang, "The adsorption mechanism of elemental mercury by HNO₃-modified bamboo char," *Fuel Processing Technology*, Vol. 154, pp. 139–146, 2016. [CrossRef]
- [43] Y. P. Lestari, and A. Amaria, "Effect of ammonia-ethanol mole ratio on the silica nanoparticles synthesized for rhodamine b dyes adsorption," *Jurnal Kimia Riset*, Vol. 8(1), pp. 92–104, 2023.
- [44] V. Soshnikova, Y. J. Kim, P. Singh, Y. Huo, J. Markus, S. Ahn, and D. C. Yang, "Cardamom fruits as a

- green resource for facile synthesis of gold and silver nanoparticles and their biological applications,” *Artificial Cells, Nanomedicine, and Biotechnology*, Vol. 46(1), pp. 108–117, 2018. [CrossRef]
- [45] X. Ge, Z. Wu, Z. Wu, Y. Yan, G. Cravotto, and B. C. Ye, “Enhanced PAHs adsorption using iron-modified coal-based activated carbon via microwave radiation,” *Journal of the Taiwan Institute of Chemical Engineers*, Vol. 64, pp. 235–243, 2016. [CrossRef]
- [46] K. Y. Foo, and B. H. Hameed, “Factors affecting the carbon yield and adsorption capability of the mangosteen peel activated carbon prepared by microwave assisted K₂CO₃ activation,” *Chemical Engineering Journal*, Vol. 180, pp. 66–74, 2012. [CrossRef]
- [47] M. Rajabi, A. Rezaie, and M. Ghaedi, “Simultaneous extraction and preconcentration of some metal ions using eucalyptus-wood based activated carbon modified with silver hydroxide nanoparticles and a chelating agent: Optimization by an experimental design,” *RSC Advances*, Vol. 5(108), pp. 89204–89217, 2015. [CrossRef]
- [48] K. Koczyński, D. Pęziak-Kowalska, K. Lota, T. Buchwald, A. Parus, and G. Lota, “Persulfate treatment as a method of modifying carbon electrode material for aqueous electrochemical capacitors,” *Journal of Solid State Electrochemistry*, Vol. 21(4), pp. 1079–1088, 2017. [CrossRef]
- [49] J. Xue, L. Huang, F. Jin, Q. Liu, G. Liu, M. Wang, and S. Zhou, “Two novel and simple strategies for improvement of the traditional activation method for activated carbon preparation: Nano-copper catalysis and Cu(II) doping,” *RSC Advances*, Vol. 5(100), pp. 81857–81865, 2015. [CrossRef]
- [50] M. Hasanzadeh, A. Simchi, and H. Shahriyari Far, “Nanoporous composites of activated carbon-metal organic frameworks for organic dye adsorption: Synthesis, adsorption mechanism and kinetics studies,” *Journal of Industrial and Engineering Chemistry*, Vol. 81, pp. 405–414, 2020. [CrossRef]
- [51] C. R. L. Aguiar, É. Fontana, J. A. B. Valle, A. A. U. Souza, A. F. Morgado, and S. M. A. G. U. Souza, “Adsorption of basic yellow 28 onto chemically-modified activated carbon: Characterization and adsorption mechanisms,” *Canadian Journal of Chemical Engineering*, Vol. 94(5), pp. 947–955, 2016. [CrossRef]
- [52] H. Wang, Z. Tian, L. Jiang, W. Luo, Z. Wei, S. Li, and W. Wei, “Highly efficient adsorption of Cr(VI) from aqueous solution by Fe³⁺ impregnated biochar,” *Journal of Dispersion Science and Technology*, Vol. 38(6), pp. 815–825, 2017. [CrossRef]
- [53] A. A. Ceyhan, Ö. Şahin, C. Saka, and A. Yalçın, “A novel thermal process for activated carbon production from the vetch biomass with air at low temperature by two-stage procedure,” *Journal of Dispersion Science and Technology*, Vol. 104, pp. 170–175, 2013. [CrossRef]
- [54] M. H. Kasnejad, A. Esfandiari, T. Kaghazchi, and N. Asasian, “Effect of pre-oxidation for introduction of nitrogen containing functional groups into the structure of activated carbons and its influence on Cu (II) adsorption,” *Journal of the Taiwan Institute of Chemical Engineers*, Vol. 43(5), pp. 736–740, 2012. [CrossRef]
- [55] S. Žalac, and N. Kallay, “Application of mass titration to the point of zero charge determination,” *Journal of Colloid and Interface Science*, Vol. 149(1), pp. 233–240, 1992. [CrossRef]
- [56] H. P. Boehm, “Surface oxides on carbon and their analysis: A critical assessment,” *Carbon NY*, Vol. 40(2), pp. 145–149, 2002. [CrossRef]
- [57] A. Dabrowski, P. Podkościelny, Z. Hubicki, and M. Barczak, “Adsorption of phenolic compounds by activated carbon - A critical review,” *Chemosphere*, Vol. 58(8), pp. 1049–1070, 2005. [CrossRef]
- [58] V. Uyak, S. Yavuz, I. Toroz, S. Ozaydin, and E. A. Genceli, “Disinfection by-products precursors removal by enhanced coagulation and PAC adsorption,” *Desalination*, Vol. 216(1–3), pp. 334–344, 2007. [CrossRef]
- [59] J. Yu, L. Lv, P. Lan, S. Zhang, B. Pan, and W. Zhang, “Effect of effluent organic matter on the adsorption of perfluorinated compounds onto activated carbon,” *Journal of Hazardous Materials*, Vol. 225–226, pp. 99–106, 2012. [CrossRef]
- [60] Y. Shimizu, M. Ateia, and C. Yoshimura, “Natural organic matter undergoes different molecular sieving by adsorption on activated carbon and carbon nanotubes,” *Chemosphere*, Vol. 203, pp. 345–352, 2018. [CrossRef]
- [61] R. Guilloisou, J. Le Roux, R. Mailler, C. S. Pereira-Derome, G. Varrault, A. Bressy, and J. Gasperi, “Influence of dissolved organic matter on the removal of 12 organic micropollutants from wastewater effluent by powdered activated carbon adsorption,” *Water Research*, Vol. 172, 2020. [CrossRef]
- [62] E. Yilmaz, E. Altıparmak, F. Dadaser-celik, and N. Ates, “Impact of natural organic matter competition on the adsorptive removal of acetochlor and metolachlor from low-specific uv absorbance surface waters,” *ACS Omega*, Vol. 8(35), pp. 31758–31771, 2023. [CrossRef]
- [63] T. S. Anirudhan, P. S. Suchithra, and S. Rijith, “Amine-modified polyacrylamide-bentonite composite for the adsorption of humic acid in aqueous solutions,” *Colloids and Surfaces A: Physicochemical and Engineering Aspects*, Vol. 326(3), pp. 147–156, 2008. [CrossRef]



Research Article

Dispersion model of NO_x emissions from a liquefied natural gas facility

İlker TÜRKYILMAZ¹, S. Levent KUZU²

¹Department of Environmental Engineering, Yıldız Technical University, İstanbul, Türkiye
²Department of Environmental Engineering, İstanbul Technical University, İstanbul, Türkiye

ARTICLE INFO

Article history

Received: 09 January 2024

Revised: 20 February 2024

Accepted: 27 February 2024

Key words:

AERMOD; Dispersion model;
Emissions; Liquefied natural gas

ABSTRACT

Natural gas is widely used in energy production, one of the most prominent sectors for human-kind. Combustion processes inevitably produce air pollutants. The major pollutant during a combustion process is nitrogen oxide emissions. The term of nitrogen oxides primarily include nitrogen monoxide and nitrogen dioxide. These pollutants are generated regardless of the fuel content since air composition itself is the major source for these pollutants. It is possible to calculate emissions through the activity data and emission factors. Calculation of emissions is not enough for an environmental assessment. The impact of pollutants on human health relies on their concentration in the atmosphere. In order to determine their concentrations several modelling practices are developed. In this study, AERMOD used for modelling purpose of NO_x emissions from a liquefied natural gas facility. It was observed that the pollutants were dispersed mostly towards south-southwest of the facility, where Marmaraeğlisi district is located. Although the pollutants transported directly to the settlement, the concentrations remained limited. During operation conditions, the highest daily NO_x concentration was 1.7 µg/m³ and the highest annual concentration was 0.1 µg/m³. At maximum operating conditions, the highest daily NO_x concentration was 16.2 µg/m³ and the highest annual concentration was 2.5 µg/m³. At minimum operating conditions, the highest daily NO_x concentration was 1.1 µg/m³ and the highest annual concentration was 0.2 µg/m³.

Cite this article as: Türkyılmaz İ, Kuzu SL. Dispersion model of NO_x emissions from a liquefied natural gas facility. Environ Res Tec 2024;7(2)212–222.

INTRODUCTION

Air pollution modeling is a numerical tool used to understand the relationship between emissions, meteorology, atmospheric concentrations, soil deposition, and other factors. These models can identify causes and solutions to air quality problems that air pollution measurements cannot provide. Air pollution models can quantitatively evaluate the relationships between emissions and atmospheric concentrations and accumulations, thereby determining the consequences of past and future scenarios as well as the effectiveness of mitigation strategies. These

models are indispensable in scientific, regulatory and research practices. The concentrations of substances in the atmosphere are determined by the processes of transport, diffusion, chemical transformation and accumulation. While transport phenomena have been studied for a long time, turbulence and diffusion in the atmosphere are newer research areas [1]. There are some studies that predict nitrogen oxide formation from the combustion chamber [2] or determining excess air for the combustion process by employing artificial neural network [3]. But these studies do not account for the imission after the release from the stack.

*Corresponding author.

*E-mail address: kuzul@itu.edu.tr



Today, modeling the distribution of a pollutant is carried out with several basic mathematical algorithms: box model, Gaussian model, Eulerian model and Lagrangian model. Gaussian models, the most common mathematical models used for distribution in the atmosphere, assume that the pollutant will disperse according to a normal statistical distribution. Eulerian models solve the conservation of continuity, momentum, and mass equation for a given pollutant. The wind field vector normally used is considered turbulent and affects the pollutant concentration. Direct solution of the equation is laborious and therefore various approaches to the turbulent properties of the flow have been included. Lagrangian models predict pollutant distribution based on a reference grid that usually varies based on the prevailing wind direction or vector or the general direction of dust cloud movement. These models are generally suitable for simulating the distribution of dust with a latent form of the pollutant [4].

The AERMOD model was developed through a collaboration between the American Meteorological Society (AMS) and the United States Environmental Protection Agency (USEPA) Regulatory Model Development Committee (AERMIC) formed in 1991. On April 21, 2000, EPA proposed adopting AERMOD as the preferred regulatory model for simple and complex terrain, and it was formally adopted on November 9, 2005, becoming effective December 9, 2005. The development and acceptance process took 14 years in total [5].

The AERMOD model consists of three main modules. The first module is a steady-state dispersion model that simulates the distribution of air pollutants from stationary industrial sources over short distances of up to 50 kilometers. The second module is a meteorological data preprocessor called AERMET. This module calculates the atmospheric parameters required for the dispersion model by processing surface meteorological data, upper air soundings and data from instrument towers. The third module is AERMAP, which provides the relationship between terrain features and the behavior of air pollution plumes and simulates the effects of airflow over the terrain. In addition, the model includes an algorithm called PRIME, which is used to model the effects of downwash from pollution plumes flowing over nearby buildings. The integrated structure of these modules makes AERMOD an effective tool for air pollution analysis [5].

AERMOD, an advanced plume model, includes updated applications of boundary layer theory, understanding of turbulence and dispersion, and includes consideration of terrain interactions. It was evaluated using 10 databases, including those from flat and elevated terrain areas, urban and rural areas, and a mixture of routine monitoring networks with a limited number of fixed monitoring areas as well as tracer experiments [6].

AERMOD shows superior performance in predicting high limit concentrations compared to other applied models. Accurate and detailed input data is required for the model to work successfully. The quality of data inputs and the

model's ability to accurately reflect physical processes increases its ability to reproduce the distribution of observations. These conditions are important to understand when AERMOD can perform best under different scenarios and environmental conditions, and effective use of the model requires considering these conditions as well as the limits and requirements of the model [7].

AERMOD's meteorological preprocessor (AERMET) evaluates the structure and growth of the planetary boundary layer (PBL) based on surface effects, dependent on heat and momentum fluxes. The depth of this layer and the distribution of pollutants within it are influenced at the local scale by surface characteristics such as surface roughness, albedo, and available surface moisture. AERMOD uses surface and mixed layer scaling to characterize the structure of the PBL. AERMET uses surface characteristics, cloud cover, morning upper air temperature scanning, and near-surface measurement of wind speed, wind direction, and temperature as input. With these data, the model calculates the friction velocity, Monin-Obukhov length, convective velocity scale, temperature scale, mixing height and surface heat flux [8].

This information is necessary for the model to accurately predict how and where pollutants will spread into the atmosphere. While surface data enables the model to understand meteorological conditions at ground level, additional data provided by AERMET helps the model understand how conditions in the atmosphere change with altitude. This comprehensive data set allows the model to be more accurate and effective in air quality predictions.

Scientific review of ADMS and AERMOD technical documentation shows that many of their components are based on similar state-of-the-art algorithms; both assume a bimodal distribution of turbulent vertical velocities for convective conditions. On the other hand, ISC3 represents the typical Gaussian model that has been widely used for 30 years. It works relatively fast compared to AERMOD ADMS, which has improvements such as processing of terrains. The downstream algorithm in AERMOD does not differ from that in ISC3; whereas the downstream algorithm in ADMS is based on recent wind tunnel experiments and model developments. ADMS is unique in that it can model the transport and distribution of instantaneous oscillations. There are a few differences in input meteorology requirements, as AERMOD will allow vertical wind and temperature profiles to be entered, whereas ADMS only requires input of near-ground observations at some level. Since some components of AERMOD and ADMS are relatively new, it seems necessary to perform a series of sensitivity tests with a wide range of sources, meteorological and terrain conditions to ensure that the solutions are robust [9].

ISC3 requires determining whether the area surrounding a facility is rural or urban, thus creating a set of horizontal and vertical distribution curves (Pasquill-Gifford for rural or McElroy-Pooler for urban). There are no intermediate or other distribution ratios used. AERMOD and ADMS can include surface conditions such as soil moisture (using the Bowen ratio or Priestley parameter), surface albedo (for net

radiation estimates), and surface roughness. Surface roughness affects the vertical profiles of wind and temperature and dispersion rates in the surface layer and is an important variable in assessing dispersion around refineries and other industrial areas [9].

ISC3 uses routine meteorological data to calculate the height of the well-mixed layer. As the smoke rises less than the mixing height, the cloud becomes 'trapped' and continues to mix within the layer by reflection. Once the smoke rises above the mixing height, it can no longer spread to the ground. ADMS and AERMOD contain algorithms that measure the partial penetration of the amplified smoke cloud. Ground-level dispersion depends on the reversal force and the buoyancy force of the smoke. This parameterization is important for very mobile clouds or moderately mobile clouds interacting with relatively low-level inversions [9].

A study conducted in 2007 compares the performance of AERMOD and ISC air distribution models and their PRIME versions in two realistic areas. The study shows that ISC predicts higher air concentrations than AERMOD in areas closer to the study area, but the predictions become more similar as distance increases. It has been found that the largest differences are generally seen in 1-hour average periods. It has been assessed that AERMOD and AERMOD-PRIME tend to predict lower concentrations than ISC [10].

In a 2006 study, field odor sampling data were used to evaluate CALPUFF and ISCST3 Gaussian distribution models to estimate downwind concentrations and back-calculate field-borne odor emission rates. According to this study, CALPUFF could predict mean downwind odor concentrations well, whereas ISCST3 tended to underpredict odor concentration compared to field measurements. Additionally, both CALPUFF and ISCST3 models failed to predict peak odor concentrations using constant mean emission from field measurements [11].

Also, in a study conducted in 2016, AERMOD and CALPUFF air distribution models were used to examine the four-season distribution of SO₂ emitted from a gas refinery. The models' predictions were compared with real data collected at monitoring stations, and as a result of this comparison, it was determined that CALPUFF generally performed better than AERMOD. In particular, CALPUFF predicted higher concentrations than AERMOD over certain time periods and in short-term simulations. Additionally, it has been found that AERMOD may contain some significant errors due to its sensitivity to surface features and land use, whereas CALPUFF performs better in complex terrain conditions [12].

In a study conducted in 2009, PM₁₀ concentrations measured in a feedlot in Texas were evaluated using ISCST3 and AERMOD air distribution models. Analyzes under night conditions showed that AERMOD predicted values three times higher than measured concentrations. A sampling study conducted to determine PM concentrations in cotton pickers and the analysis of these data using the AERMOD

Table 1. Coordinates of the study area

Corner number	Geographical coordinates (UTM 35T)	
	Latitude	Longitude
1	577468	4543970
2	577571	4534003
3	587477	4544090
4	587583	4534118

model are also discussed. AERMOD was found to predict 1.8 times higher Emission Factors (EF) than the ISCST3 model [13]. LNG powered ship emissions were calculated for NO_x [14, 15] but their modelling was not executed. A study calculated ground-level NO_x emissions from an LNG plant in Oman by CALPUFF [16].

In this study, we used AERMOD, the proposed model by USEPA to calculate the ground-level NO_x concentrations. This study gave us the opportunity to determine the contribution of a liquefied natural gas facility over a mid-populated district.

MATERIALS AND METHODS

Study Area

The study area encompasses various potential emission sources, including two port facilities specializing in the transport of liquid fuel, one port facility dedicated to dry cargo transportation, and two liquid fuel storage facilities. Additionally, the region hosts two natural gas cycle power plants contributing to the emissions landscape. Urban emission sources, such as vehicle traffic and fuel utilization for heating and cooking purposes, form another significant component. Furthermore, agricultural activities and the operations of small-scale industrial enterprises in the area contribute to the overall emissions scenario.

The modeling area was determined as 10 km x 10 km, with the center of the area being the liquefied natural gas facility. The facility in question is located within the borders of Tekirdağ's Marmaraereğlisi district and the modeling area also includes the district center. The coordinates of the study area are given in Table 1 and the study area is shown in Figure 1.

While selecting the study area, care was taken to ensure that the settlements located near the facility remained within the study area. Meteorological station number 19343, where meteorological data is taken, is also shown in Figure 1. The station in question remains within the boundaries of the study area.

Liquefied Natural Gas Facility

The facility is one of Turkey's important energy infrastructure facilities and is located 85 km from Istanbul, 40 km from Tekirdağ, 20 km from Çorlu Airport and 4 km from Marmara Ereğlisi district centre. The terminal started its journey with the basic design studies that started in 1985,



Figure 1. Map of the study area.

construction works started in 1989 and was completed and put into service in 1994. Capacity increase in 2001, filling operations for land tankers and pier expansion works started in 2007 and were completed in 2016. Finally, the terminal's gas sending capacity was increased in 2018.

The main functions of the terminal include unloading and storage from LNG vessel, gasification of stored LNG and delivery of natural gas to the main transmission line and land tanker filling. Design capacity is 37 million Nm³/day. The terminal has three LNG storage tanks with a total capacity of 255,000 m³.

LNG gasification and shipping processes include taking the stored LNG from tanks and sending it via pipeline to the main transmission line 23 km away after natural gas measurement. The land tanker filling ramp is used to send natural gas to regions where natural gas cannot be delivered via pipeline and has a daily filling capacity of 75 tankers.

A significant portion of the facility's emissions come from natural gas submerged combustion vaporizers (SCV) and flare chimneys. SCVs are used to gasify the liquefied natural gas stored in the facility by heating it. This equipment uses natural gas as fuel. Flare chimneys ensure that natural gas is burned and discharged into the atmosphere during sudden pressure increases in the facility.

Determination of Mass Emissions

Five-point emission sources have been determined for the facility: SCV A, SCV B, SCV C, SCV D, and flare chimneys. Consumption of each point source was determined based on the values obtained by reading the flowmeters. Consumption data is in Table 2.

Apart from the consumption under normal operating conditions, the consumption values of these equipment have been determined from their catalogs for the scenarios in which the equipment will operate at full capacity and at minimum capacity. (For SCVs, maximum consumption = 3244 Sm³/hour, minimum consumption = 220 Sm³/hour)

To determine the NO_x emissions resulting from these stacks, the emission measurement that the facility must have in accordance with environmental legislation was used to find the mass emission rates. The mass flow rate value was calculated by dividing the mass concentration measurement data from stack to the volumetric flowrate measured at the stack. When mass emission is divided by the consumption of LNG, the emission factor is calculated. NO_x emission factor was found to be 92.765 mg/Nm³. Mass emission data is included in Table 3.

Data Used by AERMOD Application in the Study

Five-point emission sources have been determined for the facility: SCV A, SCV B, SCV C, SCV D and flare chimneys. Data on emission sources are given in Table 4.

Using the AERMOD modeling system, pollutant concentrations were calculated at ground level every 500 meters from the starting point to 10,000 m.

In the study, the hourly surface data required by the model (wind speed, wind direction, temperature and cloud cover, etc.) were obtained from the Tekirdağ Marmaraereğlisi station affiliated with the General Directorate of State Meteorological Affairs for 2022. Upper air data was taken from radiosonde data at Istanbul Kartal station, which is the closest point to the study area. The wind frequency rose, including wind speeds and wind directions for 2022, is shown in Figure 2.

Table 2. Consumption values

Months	Volumetric flowrates (Sm ³)				
	SCV A	SCV B	SCV C	SCV D	Flare
J	0	0	0	0	98.586
F	0	2.844	29.623	126.787	102.378
M	0	72.992	15.167	71.096	121.337
A	0	0	150.426	148.356	97.638
M	0	0	2.398	12.797	78.679
J	92	0	449	0	54.981
J	14.598	127.972	75.362	35.548	59.720
A	137.524	323895	307457	187882	52137
S	0	39.870	83	0	67304
O	629	10.359	53.629	9.389	55929
N	478	11.192	218.128	0	109961
D	0	0	0	0	99534

AERMET is a data processor and preprocessor that prepares meteorological data for AERMOD. This process involves first collecting data from appropriate meteorological data sources and subjecting these data to quality control. Quality control increases the reliability of the dataset and the accuracy of the model. Then, the collected data is converted into a usable format by AERMET and the meteorological fields (temperature, wind speed and direction, humidity, etc.) needed by the air quality model are created. In the final stage, the processed meteorological data are presented in a format that can be used by air quality models.

The data AERMET requires include items such as temperature, wind speed and direction, humidity, cloudiness, sunlight, amount and type of precipitation, atmospheric pressure. Additionally, specific data such as local geography and land use are also important to improve the accuracy of the models.

The reliability of the model results can be assessed through quantile-quantile (Q-Q) plots. These can be generated by plotting measured data against modelled data. There are some studies which served for this purpose and showed good agreement between measured and predicted concentrations [5, 17].

RESULTS AND DISCUSSION

A modeling study was carried out using three different scenarios on the distribution of NO_x emissions originating from and potentially arising from Marmaraeğlisi LNG Terminal. Calculations were made using the AERMOD program for 441 receptor points. Two different time averages used to generate figures for each scenario. In the first, the maximum daily concentrations at each of the points. In the second, the average values of the concentrations calculated throughout the year. These time averages were used to generate figures for three different scenarios. These sce-

Table 3. Mass emission rates

Months	Mass flowrates				
	SCV A (g/s)	SCV B (g/s)	SCV C (g/s)	SCV D (g/s)	Flare (g/s.m ²)
J	–	–	–	–	0.00683
F	–	0.00011	0.00114	0.00486	0.00785
M	–	0.00253	0.00053	0.00246	0.00840
A	–	–	0.00538	0.00531	0.00699
M	–	–	0.00008	0.00044	0.00545
J	0.00001	–	0.00002	0.00000	0.00394
J	0.00051	0.00443	0.00261	0.00123	0.00414
A	0.00476	0.01122	0.01065	0.00651	0.00361
S	–	0.00143	0.00001	–	0.00482
O	0.00002	0.00036	0.00186	0.00033	0.00387
N	0.00002	0.00040	0.00781	–	0.00787
D	–	–	–	–	0.00689

Table 4. Data of emission sources

Source name	Temperature (°K)	Stack gas velocity (m/s)	Stack diameter (m)	Stack height (m)
SCV A	291.55	6.41	0.8	10
SCV B	292.25	6.55	1.2	10
SCV C	291.82	7.41	1.2	10
SCV D	290.72	6.77	1.2	10
Flare	–	–	1.2	60

narios for the facility are as follows: In the first scenario, it is assumed that the facility will operate under normal operating conditions, in the second scenario, it is assumed that the equipment and points determined as emission sources will consume maximum natural gas, and in the third and last scenario, it is assumed that the emission sources will consume natural gas at a minimum level.

NO_x Concentrations in Operating Conditions

The first calculations estimated the maximum of 24-hour average concentrations. The highest concentration in the study area was observed to be 1.70 µg/m³ on 09.08.2022. The lowest concentration was determined to be >0.01 µg/m³ on 27.04.2022. The highest 24-hour average concentrations are found in Figure 3. When the map is examined, it is seen that the highest concentrations are in the facility area. According to the distribution map, it is clearly seen that the pollutants are transported in the direction of the prevailing wind as seen in Figure 2.

Additionally, annual average concentrations were calculated as a result of the modeling study conducted at 441 points. It was observed that the highest concentration average in the study area was 0.11 µg/m³. The lowest concentration average was found to be >0.01 µg/m³. Annual

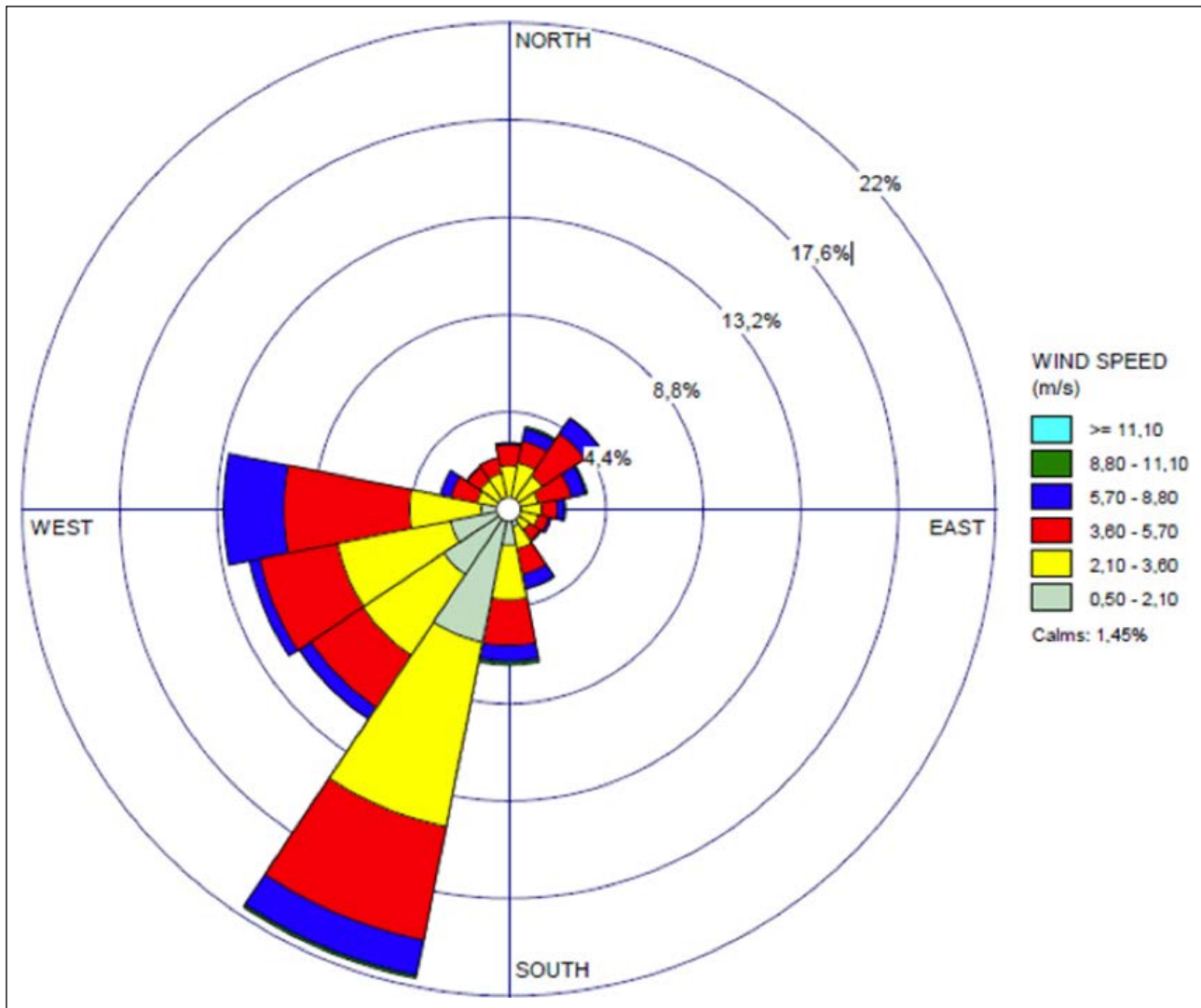


Figure 2. Windrose plot of 2022 for Marmaraereğlisi.

average concentrations are found in Figure 4. When the map is examined, it is seen that the highest concentrations are in the facility area.

NO_x Concentrations at Maximum Operation Capacity

For the situation where the facility operates at maximum capacity throughout the year, the maximum 24-hour concentration averages were found. The highest concentration in the study area was observed to be 16.24 µg/m³ on 09.08.2022. The lowest concentration was determined to be 0.06 µg/m³ on 25.02.2022. The highest 24-hour average concentrations are found in Figure 5. When the map is examined, it is seen that the highest concentrations are in the facility area.

Annual average concentrations were calculated and it was observed that the highest concentration average in the study area was 2.51 µg/m³. The lowest concentration average was found to be >0.01 µg/m³. Annual average concentrations are found in Figure 6. When the map is examined, it is seen that the highest concentrations are in the facility area.

NO_x Concentrations at Minimum Capacity

For the scenario with minimum operation capacity throughout the year, the maximum 24-hour concentration averages were calculated. The highest concentration in the study area was observed to be 1.11 µg/m³ on 09.08.2022. The lowest concentration was determined to be >0.01 µg/m³ on 25.02.2022. The highest 24-hour average concentrations are found in Figure 7. When the map is examined, it is seen that the highest concentrations are in the facility area.

Additionally, annual average concentrations were calculated as a result of the modeling study conducted at 441 points. It was observed that the highest concentration average in the study area was 0.17 µg/m³. The lowest concentration average was found to be >0.01 µg/m³. Annual average concentrations are found in Figure 8. It can be inferred that the highest concentrations are in the facility area.

The escalating severity of air pollution poses a substantiated threat to ecosystems, as evidenced by numerous studies. Heightened levels of pollution intensify apprehensions regarding future implications. Factors such

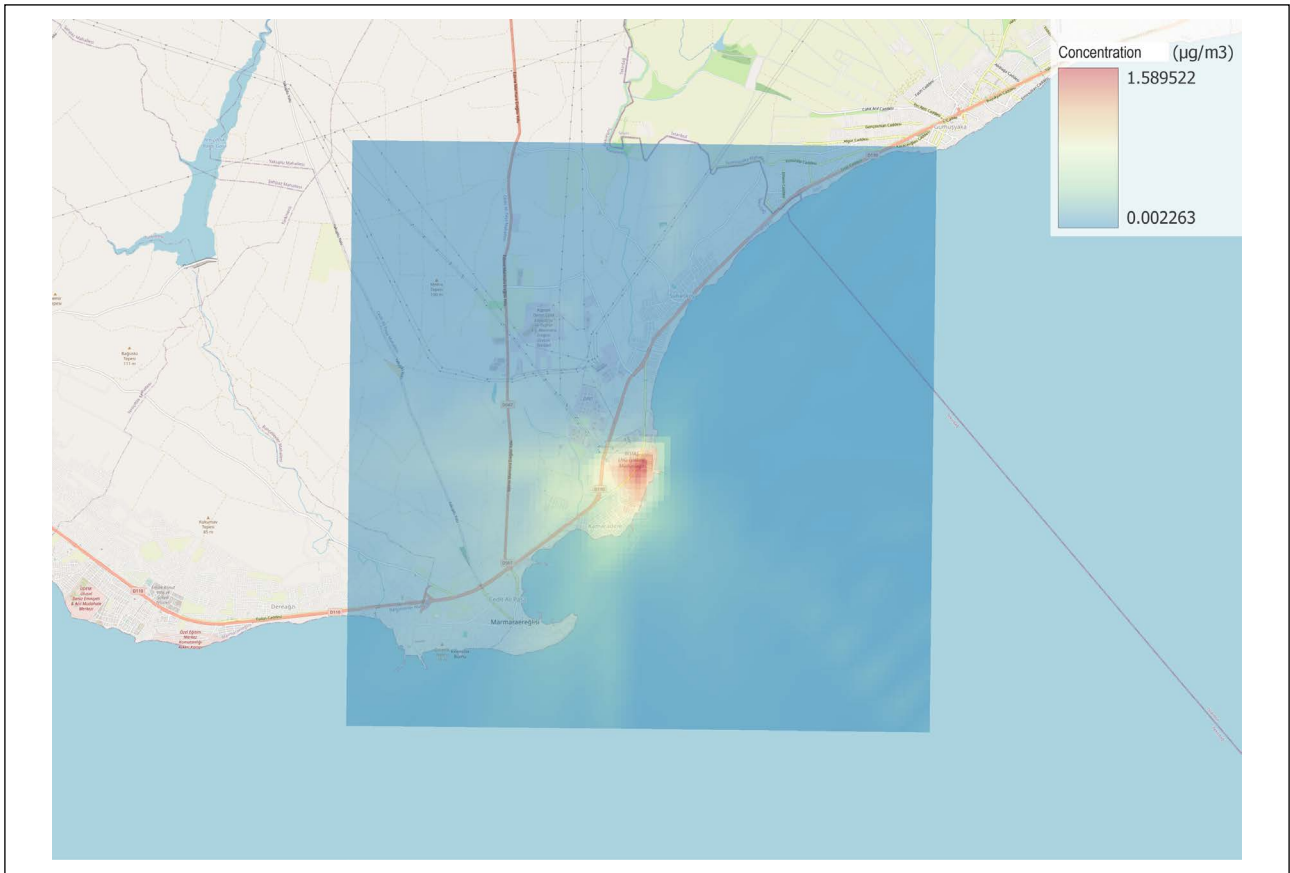


Figure 3. Maximum daily concentrations at operation conditions.

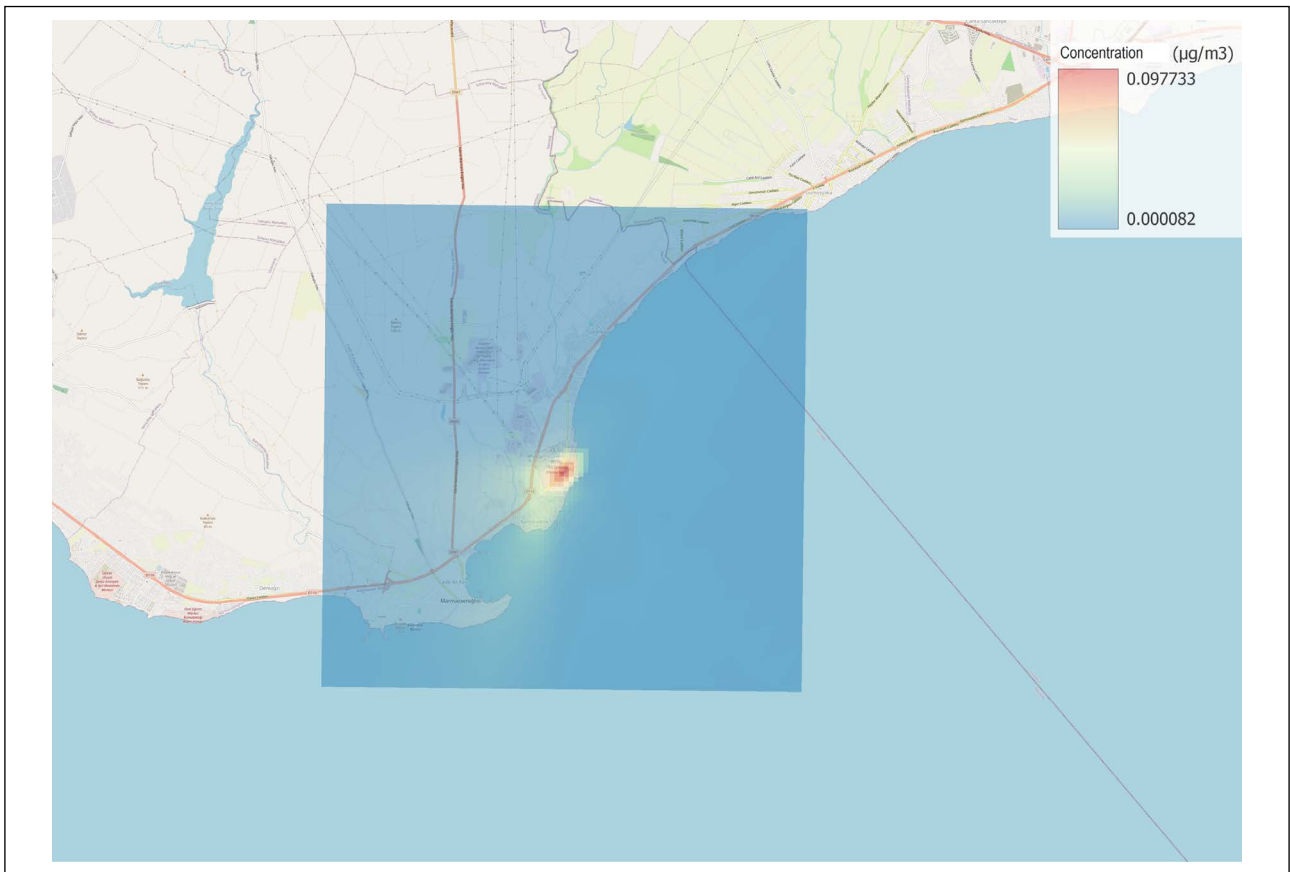


Figure 4. Annual average concentrations at usual operation capacity.

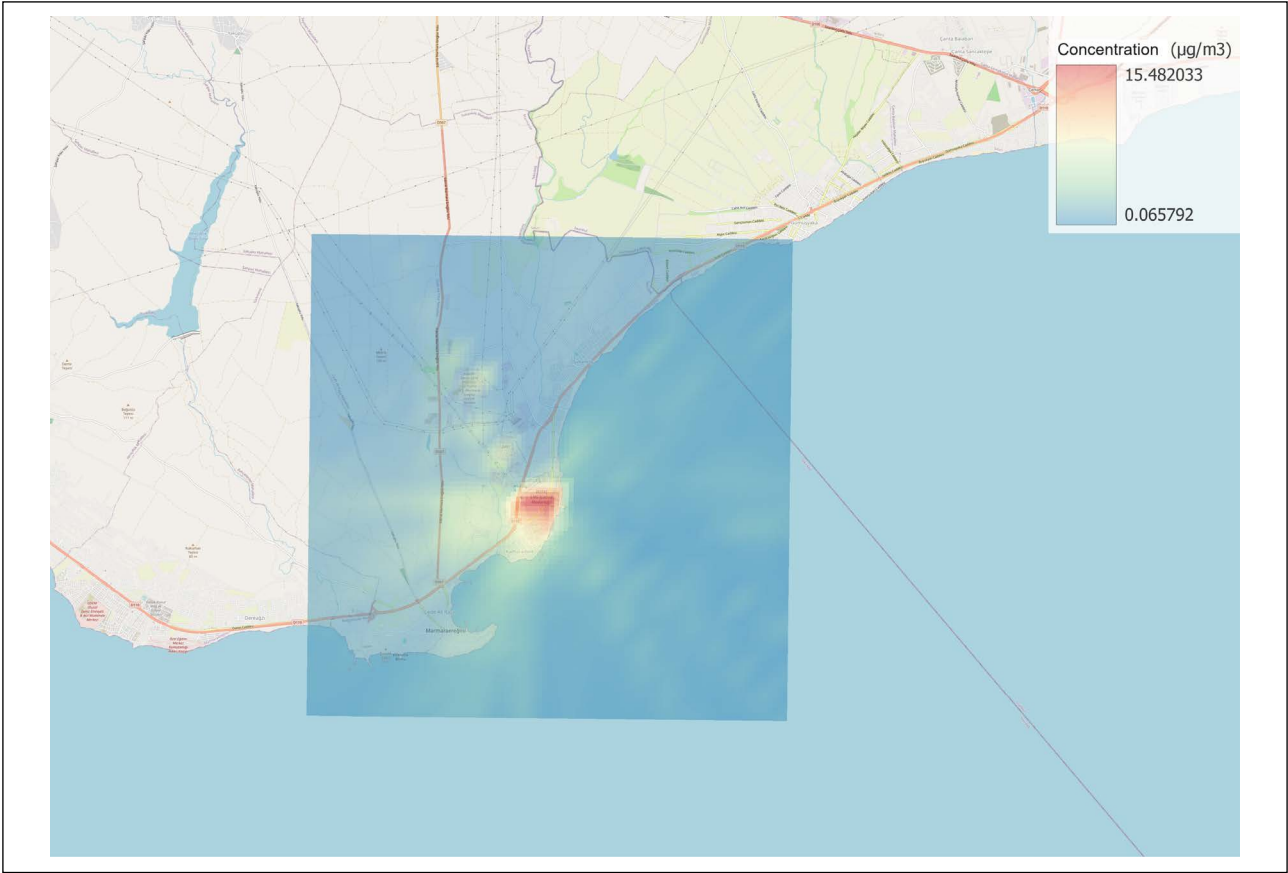


Figure 5. Daily maximum NO_x concentrations during maximum operation conditions.

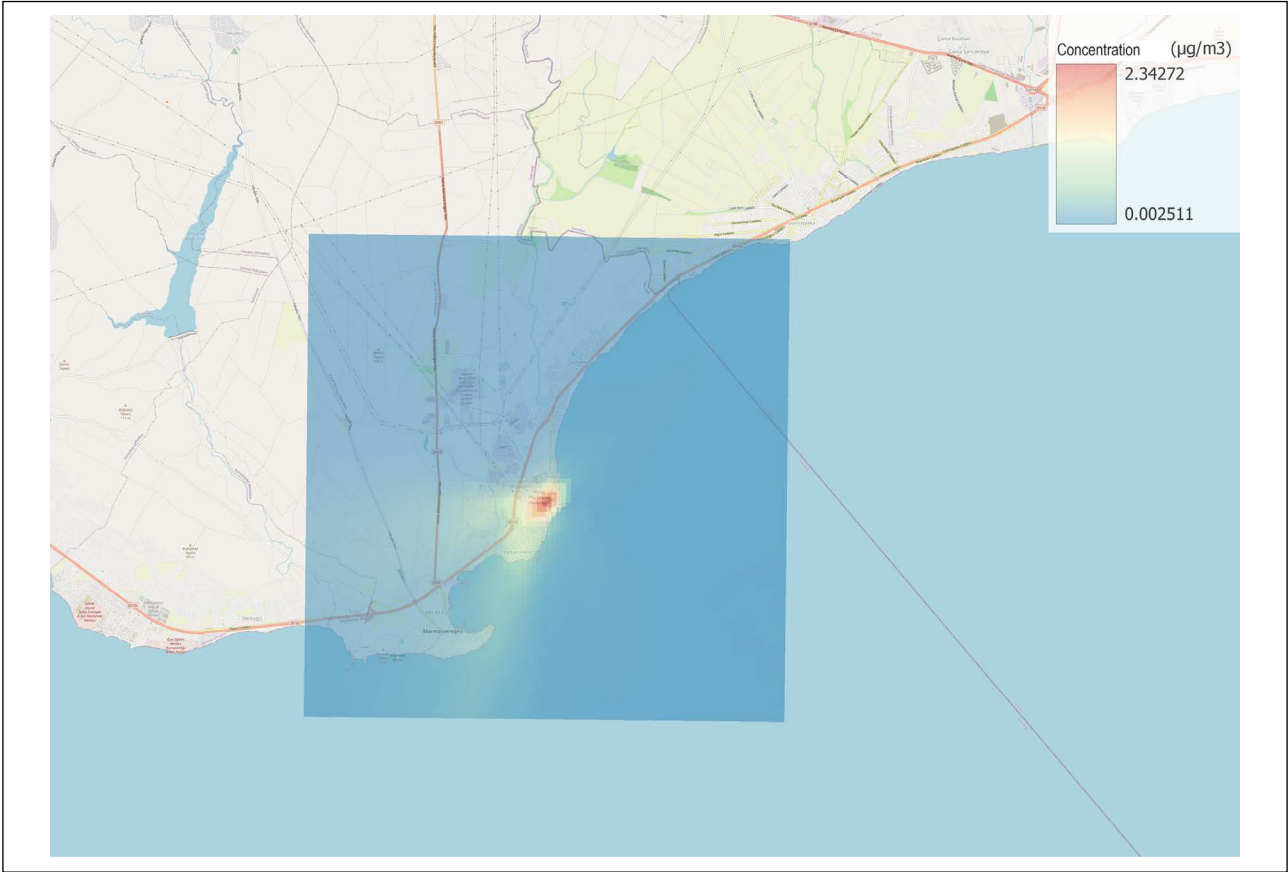


Figure 6. Annual NO_x concentrations during maximum operation conditions.

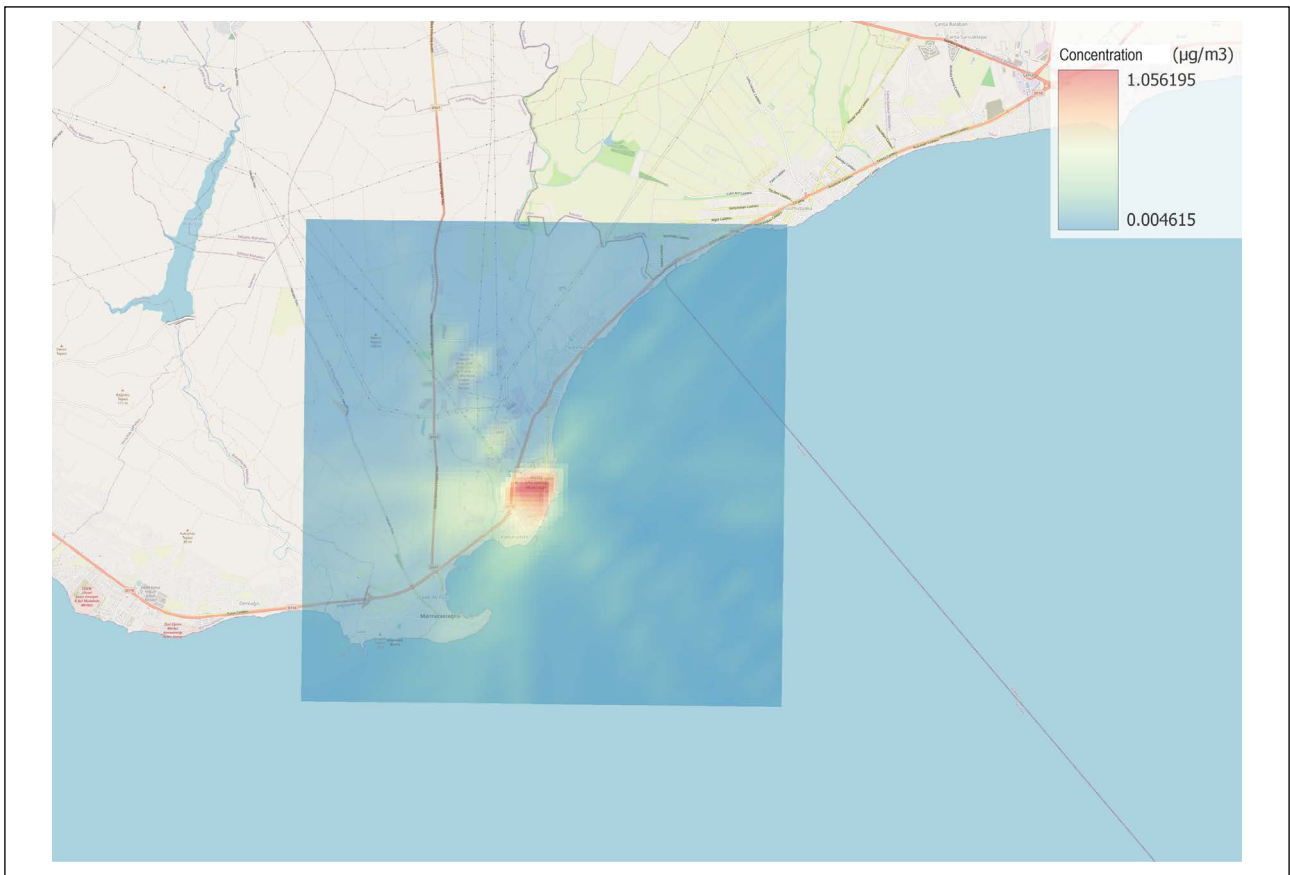


Figure 7. Daily maximum NO_x concentrations during minimum operation conditions.

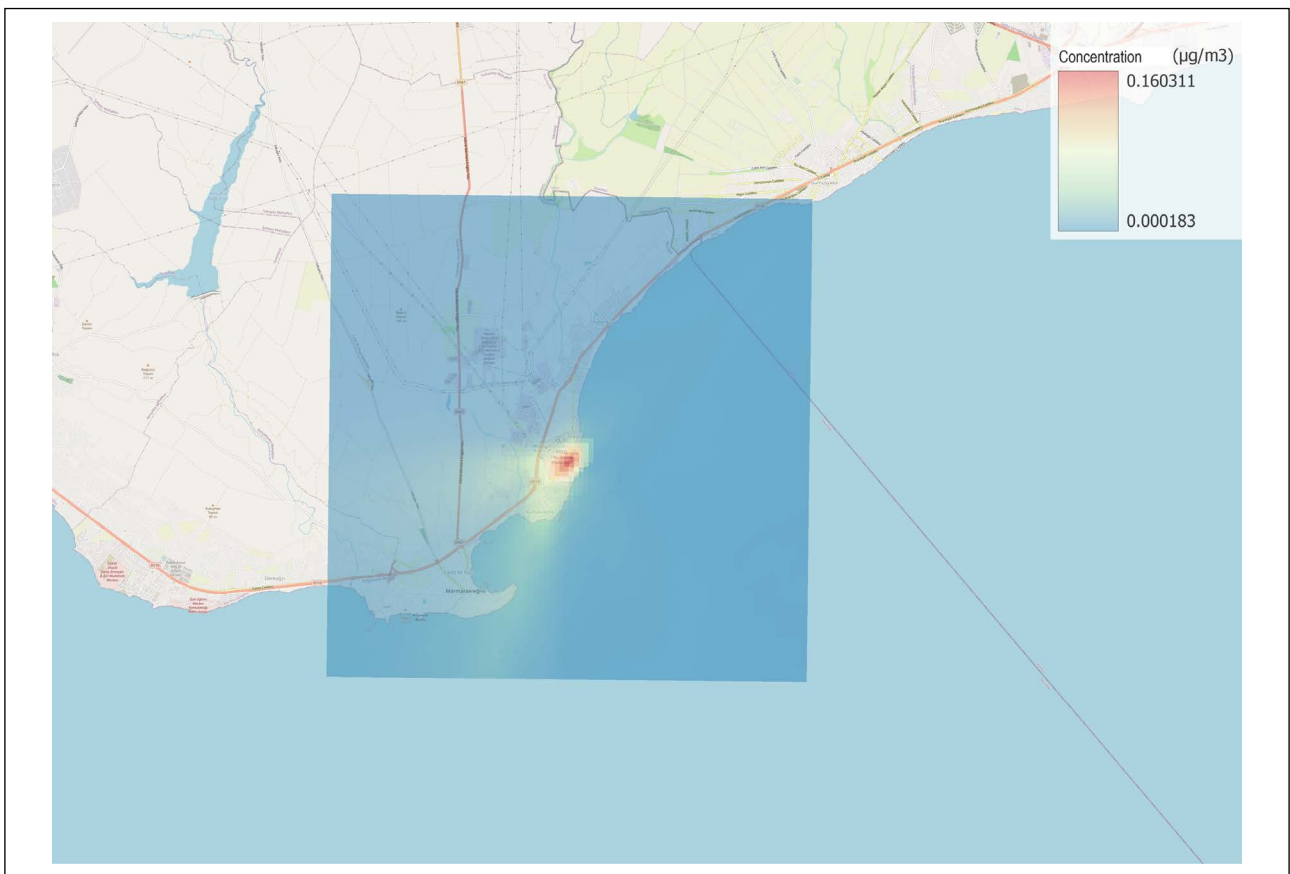


Figure 8. Annual NO_x concentrations during minimum operation conditions.

as burgeoning global population, industrial expansion, unregulated urban development, and escalating energy demands contribute to the exacerbation of air pollution. Consequently, it has become imperative to conduct comprehensive assessments for both newly established and existing facilities to ascertain effective mitigation strategies for combating air pollution.

In this study, emissions from an LNG facility were modeled using AERMOD. The reason for choosing this model is that the required data is at a minimum level and the run time of the model is extremely short. The topography of the area to be modeled is also an extremely important element in model selection. When the AERMOD model is used, reliable results may not be obtained for areas with complex terrain structure. However, AERMOD is a suitable choice since the land structure of the area chosen for the study is quite flat.

When the data obtained through the model is evaluated in terms of the air quality legislation of Türkiye, it is seen that the ground-level concentrations resulting from the facility remain below the limit values. Even if the facility operates at maximum capacity, the highest 24-hour average NO_x concentration would be detected as $16.24 \mu\text{g}/\text{m}^3$. The compared legislation is the Regulation on the Control of Industrial Air Pollution, published in the Official Gazette dated 03.07.2009 and numbered 27277 [18]. The data compared with the value in table 5.1 inside the legislation. It is in accordance with the European Directive [19]. Air quality standard is met in terms of NO_x . When the annual average concentrations for the maximum capacity scenario is considered, the highest expected concentration would be $2.51 \mu\text{g}/\text{m}^3$. This also remains below the long-term limit value determined in the same regulation. The NO_2 limit values are 350, 125, 60, and $25 \mu\text{g}/\text{m}^3$ for hourly, daily, long-term, and winter-time concentrations, respectively.

A study was conducted in Oman around LNG plant to measure air pollutant concentrations [20]. The annual mean was 21.29 ppb for NO_2 . Air quality standards were not exceeded for NO_2 . But this is a cumulative concentration value and does not only consider the plant. It has contribution from all surrounding sources. A modelling study was conducted for the same facility [21]. The highest hourly concentrations were calculated as $2027.4 \mu\text{g}/\text{m}^3$ and $625.54 \mu\text{g}/\text{m}^3$ for winter and summer seasons, respectively. A simple Gaussian model was applied in Nigeria to calculate ground-level concentrations downwind of an LNG plant [22]. According to different scenarios, NO_x concentrations varied between 2.12 and $27.83 \mu\text{g}/\text{m}^3$. There is an agreement with this study to our results.

Previous studies showed that significantly more concentrations above the shoreline can be achieved in the places where are close to ports. Ekmekçiöğlü et al. [23] determined up to $100 \mu\text{g}/\text{m}^3$ annual average NO_x concentration in Kocaeli, on the other hand, they reported annual average NO_x concentration in Ambarlı (Istanbul) around $10 \mu\text{g}/\text{m}^3$. Kuzu et al. [24] found that annual average NO_x concentrations were as high as $520 \mu\text{g}/\text{m}^3$ in Bandırma, which is a district located around a port. Close to the value found in Bandırma, Kuzu

[25] estimated an annual maximum at Atatürk International Airport, with a value of $560 \mu\text{g}/\text{m}^3$. Compared to those reported previous values, the contribution from LNG facility seems quite limited to NO_x concentrations.

CONCLUSIONS

Upon evaluation of the findings, it is evident that the adverse impacts of the liquefied natural gas facility on the environment and nearby settlements are notably minimal. A crucial takeaway from this investigation underscores the necessity of conducting comprehensive integrated assessments for settlements. While current legislative frameworks and practices typically focus on evaluating individual facilities' impacts on air pollution, this approach alone is insufficient. The efficacy of assessing other emission sources such as industrial facilities, traffic, and heating sources concurrently within the regions earmarked for facility establishment holds greater promise in shaping air quality. The primary limitation of the study is that the modeling only includes encompasses the impacts of the liquefied natural gas facility, potentially overlooking broader environmental considerations when it is compared to the legislation limits. However, the value can be exceeded in the atmosphere. The authors recommend expanding the study by including other local emissions to make a comprehensive modelling in the district. Additionally, marine boundary layer development can be considered in another study.

DATA AVAILABILITY STATEMENT

The author confirm that the data that supports the findings of this study are available within the article. Raw data that support the finding of this study are available from the corresponding author, upon reasonable request.

CONFLICT OF INTEREST

The author declared no potential conflicts of interest with respect to the research, authorship, and/or publication of this article.

USE OF AI FOR WRITING ASSISTANCE

Not declared.

ETHICS

There are no ethical issues with the publication of this manuscript.

REFERENCES

- [1] A. Daly, and P. Zannetti, "Air pollution modeling—An overview," in *Ambient air pollution* P. Zannetti, D. Al-Ajmi, and S. Al-Rashied, The Arab School for Science and Technology (ASST) and The Enviro-Comp Institute, 2007, pp. 15–28.
- [2] S. Golgiyaz, M. Daskin, C. Onat, M.F. Talu, "An artificial intelligence regression model for prediction of nox emission from flame image," *Journal of Soft*

- Computing and Artificial Intelligence, Vol. 3, pp. 93–101, 2022. [CrossRef]
- [3] S. Golgiyaz, M.F. Talu, M. Daskin, and C. Onat, “Estimation of excess air coefficient on coal combustion processes via gauss model and artificial neural network,” Alexandria Engineering Journal, Vol. 61, pp. 1079–1089, 2022. [CrossRef]
- [4] K. E. Kakosimos, M. J. Assael, J. S. Lioumbas, and A. S. Spiridis, “Atmospheric dispersion modelling of the fugitive particulate matter from overburden dumps with numerical and integral models”, Atmospheric Pollution Research, Vol. 2, pp. 24–33, 2011. [CrossRef]
- [5] US EPA (2018). User’s Guide for the AMS/EPA Regulatory Model (AERMOD), US Environmental Protection Agency, EPA-454/B-18-001, RTP, NC.
- [6] R. J. Paine, R. F. Lee, R. W. Brode, R. Wilson, A. J. Cimorelli, S. G. Perry, J. C. Weil, A. Venkatram, and P. Peters, (1999). “AERMOD: MODEL FORMULATION AND EVALUATION RESULTS”, Proceedings of the 92nd Annual Meeting of the Air & Waste Management Association, St. Louis, MO, June 20–24, 1999.
- [7] S. G. Perry, A. J. Cimorelli, R. J. Paine, R. W. Brode, J. C. Weil, A. Venkatram, R. B. Wilson, R. F. Lee, and W. D. Peters, “AERMOD: A dispersion model for industrial source applications. part ii: model performance against 17 field study databases,” Journal of Applied Meteorology, Vol. 44(5), pp. 694–708, 2005. [CrossRef]
- [8] A. J. Cimorelli, S. G. Perry, A. Venkatram, J. C. Weil, R. Paine, R. B. Wilson, R. F. Lee, W. D. Peters, R. and W. Brode, (2005). “AERMOD: A dispersion model for industrial source applications. part i: general model formulation and boundary layer characterization,” Journal of Applied Meteorology, Vol. 44(5), pp. 682–693, 2005. [CrossRef]
- [9] S. R. Hanna, B. A. Egan, J. Purdum, and J. Wagler, “Evaluation of the ADMS, AERMOD, and ISC3 dispersion models with the OPTEX, Duke Forest, Kincaid, Indianapolis and Lovett field datasets,” International Journal of Environment and Pollution, Vol. 16(1-6), pp. 301–314, 2021. [CrossRef]
- [10] K. C. Silverman, J. G. Tell, E. V. Sargent, and Z. Qiu, “Comparison of the industrial source complex and aermოდ dispersion models: case study for human health risk assessment,” Journal of the Air & Waste Management Association, Vol. 57(12), pp. 1439–1446, 2007. [CrossRef]
- [11] L. Wang, D. Parker, C. Parnell, R. Lacey, and B. Shaw, “Comparison of CALPUFF and ISCST3 models for predicting downwind odor and source emission rates,” Atmospheric Environment, Vol. 40(25), pp. 4663–4669, 2006. [CrossRef]
- [12] F. Atabi, F. Jafarigol, F. Moattar, and J. Nouri, “Comparison of AERMOD and CALPUFF models for simulating SO₂ concentrations in a gas refinery,” Environmental Monitoring and Assessment, Vol. 188(9), Article 516, 2016. [CrossRef]
- [13] V. S. V. Botlaguduru, “Comparison of Aermოდ and ISCST3 Models For Particulate Emissions From Ground Level Sources,” Master dissertation, Texas A&M University, College Station, TX, 2009.
- [14] Y. Afon, and D. Ervin, “An assessment of air emissions from liquefied natural gas ships using different power systems and different fuels”, Journal of The Air & Waste Management Association, Vol. 58, pp. 404–411, 2008. [CrossRef]
- [15] M. Anderson, K. Salo, and E. Fridell, “Particle- and Gaseous Emissions from an LNG Powered Ship”, Environmental Science and Technology, Vol. 49(20), pp. 12568–12575, 2015. [CrossRef]
- [16] S. A. Abdul-Wahab, S. O. Fadlallah, M. Al-Riyami, and I. Osman, “A study of the effects of CO, NO₂, and PM₁₀ emissions from the Oman Liquefied Natural Gas (LNG) plant on ambient air quality,” Air Quality, Atmosphere, and Health, Vol. 13, pp. 1235–1245, 2020. [CrossRef]
- [17] A. ul Haq, Q. Nadeem, A. Farooq, N. Irfan, M. Ahmad, and M. R. Ali, “Assessment of AERMOD modeling system for application in complex terrain in Pakistan,” Atmospheric Pollution Research, Vol. 10, pp. 1492–1497, 2019. [CrossRef]
- [18] Sanayi Kaynaklı Hava Kirliliğinin Kontrolü Yönetmeliği, Resmi Gazete, 29211. Available at: Dec 20, 2014. (Turkish legislation)
- [19] European Directive. “Directive 2008/50/EC of the European Parliament and of the Council of 21 May 2008 on ambient air quality and cleaner air for Europe.”, Directive 2008/50/EC, air quality, 2008.
- [20] S. A. Abdul-Wahab, “Monitoring of air pollution in the atmosphere around oman liquid natural gas (OLNG) plant,” Journal of Environmental Science and Health, Vol. 40(3), pp. 559–570, 2005. [CrossRef]
- [21] S. A. Abdul-Wahab, S. O. Fadlallah, M. Al-Riyami, M. Al-Souti, and I. Osman, “A study of the effects of CO, NO₂, and PM₁₀ emissions from the Oman Liquefied Natural Gas (LNG) plant on ambient air quality,” Air Quality, Atmosphere and Health, Vol. 13, pp. 1235–1245, 2020. [CrossRef]
- [22] P. N. Ede, D. O. Edokpa, and O. Ayodeji, “Aspects of air quality status of bonny island, Nigeria attributed to an LNG plant,” Energy and Environment, Vol. 22, pp. 891–909, 2011. [CrossRef]
- [23] A. Ekmekçioğlu, S. L. Kuzu, K. Ünlügençoğlu, and U. B. Çelebi, “Assessment of shipping emission factors through monitoring and modelling studies,” Science of the Total Environment, Article 140742, 2020. [CrossRef]
- [24] S. L. Kuzu, L. Bilgili, and A. Kılıç, “Estimation and dispersion analysis of shipping emissions in Bandırma Port, Turkey,” Environment, Development and Sustainability, Vol. 23, pp. 10288–10308, 2021. [CrossRef]
- [25] S. L. Kuzu, “Estimation and dispersion modeling of landing and take-off (LTO) cycle emissions from Atatürk International Airport,” Air Quality Atmosphere and Health, Vol. 11, pp. 153–161, 2018. [CrossRef]



Research Article

Factorial experimental design for removal of Indigo Carmine and Brilliant Yellow dyes from solutions by coagulation

Mustafa KORKMAZ*

Department of Environmental Engineering, Balıkesir University Faculty of Engineering, Balıkesir, Türkiye

ARTICLE INFO

Article history

Received: 21 December 2023

Revised: 22 February 2024

Accepted: 27 February 2024

Key words:

Acid dye; Azo dye; Coagulation;
Dye removal; Factorial design;
Iron chloride

ABSTRACT

Textile and food industries produce huge amounts of wastewaters containing dye residues. When these wastewaters are discharged to receiving surface waters like as lakes and rivers, aesthetically unpleasant situations form. Therefore, these wastewaters should be treated. Wastewater treatment is sometimes an expensive operation and cheap methods should be developed. The removal of Indigo Carmine (I.C., Acid dye) and Brilliant Yellow (B.Y., Azo dye) from synthetically prepared solutions was studied by coagulation using iron chloride salt in a batch reactor at room temperature. As an experimental approach, two leveled factorial design with three factors was applied as a function of pH (4–12), iron chloride amount (0.1–0.4 g/500 mL) and dye concentration (100–200 mg/L). Low pHs supported to removal of these two dyes. The results showed that 100% I.C. dye removal and 90.5% B.Y. dye removal were achieved. The all parameters were statistically insignificant for both the dyes. Indigo Carmine and Brilliant Yellow dyes were removed from solutions successfully. The applied treatment method was evaluated as promising due to low sludge production, low cost, low coagulation duration and high performance. A time span of 5 minutes was found as enough for removals of both of the dyes. After treatment of I.C. and B.Y. dyes by coagulation, the coagulated dyes were determined as un reusable due to iron complex by these dyes. Flocculation was found to be ineffective. A continuous flow reactor was successfully adopted for these dyes.

Cite this article as: Korkmaz M. Factorial experimental design for removal of Indigo Carmine and Brilliant Yellow dyes from solutions by coagulation. Environ Res Tec 2024;7(2)223–232.

INTRODUCTION

Textile and food industries use many different types of dyes to color their products [1]. Approximately 1.6 million tons of textile dyes are produced yearly throughout the World and 10–15% of this volume is scrapped as wastewater [2]. The wastewaters of textile industries contain dense color, heavy metals, high COD and BOI, suspended solid materials and salt at high concentration [3]. Some textile dyes are toxic for humans and animals [4]. The receiving mediums like as lakes and rivers are badly affected by these dye wastewaters as dyes aesthetically ruin water view, inhibit the ox-

xygen and the sunlight penetration into receiving water, and thus dyes prevent the photosynthesis activity in the water body [5]. Therefore, food coloring and textile industries wastewaters should be treated by applying one of the following methods like as adsorption, coagulation, electrocoagulation, biosorption, membrane separation and advanced oxidation. An adsorption method can be applied effectively, if the adsorbent material is regenerable and has a high adsorption capacity. Adsorption is a remarkable method due to its simple and low cost application and high efficiency [2]. In electrocoagulation treatment of dyes, iron or aluminum plates are used. An electrocoagulation method works

*Corresponding author.

*E-mail address: korkmazm@balikesir.edu.tr



by electrical current transfer from a cathode plate to an anode plate which is dissolved to produce coagulating cations like as iron and aluminum for removals of dye molecules [6, 7]. Dye molecules are coagulated by dissolved cations and also converted to H_2O and CO_2 in an electrocoagulation reactor by electrical deterioration of organic dye [7]. Electrocoagulation produces high iron or aluminum sludge at high current densities and long operation durations. Similar to adsorption, biosorption of dyes is suitable in the usage of the regenerable biosorbent with high capacity. Also, surface functional groups of biosorbent play an important role for dye adsorption and adsorbent regeneration [8]. Further, the surface area of the biosorbent as well as the other key point for dye adsorption [9]. Membrane separation is an appropriate process, if the pore diameter of the used membrane is smaller than molecule size of dye [10]. An electrooxidation process works by electrical current transportation from a cathode plate to an anode plate and has a high dye shredding performance to H_2O and CO_2 [7]. The difference between electrooxidation and electrocoagulation is the absence of coagulating cation and is that the plates in electrooxidation are indissoluble. The plates in electrooxidation can be graphite, boron-doped diamond, and rubeidum-coated titanium or others. A coagulation process forms from rapidly dispersion of coagulant and the flocculation [11]. In dye removal by coagulation using iron or aluminum chloride salts, the cations aggregate dye molecules and enable to filtration, sedimentation or centrifugation of these flocks. A coagulation process for dye removal is the more advantageous and cheap technology because aluminum or iron salts are cheap and vast in marked. Also, there would not be any important sludge amount. In addition to this, coagulation-flocculation of dyes by these harmless cations is generally a rapid process. Therefore, the reactor volume for dye removal by coagulation and flocculation process would be small. But, dye recovery after the coagulation process may be impossible due to iron or aluminum complexion with treated dye. Brilliant Yellow dye is an anionic azo dye that can be used in the electrochemical synthesis of polypyrrol films and to dye wool, nylon, and silk fibers [12]. Indigo Carmine dye is a colorant mainly used in the pharmacy, textile, leather, and food industries [13].

Optimization is an useful approach for treatment of wastewaters by applying one of the methods like as taguchi, response surface, artificial neural network and factorial design [14]. In this study, the factorial design method was applied. Factorial optimization design is sometimes used to be initial stage for central composite design. If the experimental matrix limits are not certain for factorial design, it is necessary to carry out several preliminary experiments to determine the experimental matrix. When this situation is required in factorial optimization method, the most suitable way of determination of experimental matrix is the classical single parameter experiments. However, in other optimization experiments (Central composite design and Taguchi), the optimum condition can be determined in a wider cage and in these statistical methods, experimental numbers are too than the factorial design [14]. Thus, the factorial design is

advantageous. This applied coagulation process using iron chloride is a cheap method for dyes (Indigo Carmine and Brilliant Yellow) removal from the textile and food industries wastewaters. In a study, Disperse Blue 106, Disperse Yellow 54, Reactive Blue 49, Reactive Yellow 84 dyes removals were studied using ferric chloride and optimum pHs were determined as 6, 5, 6, 6, respectively [15]. Optimum $FeCl_3 \cdot 6H_2O$ dosages for these dyes were reported between 1 and 2 mM [15]. In another study, Acid Black 1, Acid Violet 5, Reactive Black 5 dyes removals were reported to be increase at 35–50 mg/L chitosan concentrations in coagulation treatment [16]. Shi et al. [17] studied the removal of Direct Black 19, Direct Red 28, Direct Blue 86 dyes by different aluminum species and removals of dyes increased by increasing amounts of aluminum species which were $AlCl_3$, $PACl$ and Al_{13} .

In this study, Brilliant Yellow (B.Y., Azo dye) and Indigo Carmine (I.C., Acid dye) removals by iron chloride coagulation in a batch reactor applying 2^3 factorial design were investigated at room temperature. The applied experimental parameters were pHs (4 and 12), concentrations (100 and 200 mg/L) and iron chloride dosages (0.1 and 0.4 g/500 mL). The advantages and selection reasons of the applied coagulation method from other methods can be summarized as follows. The coagulation method is more effective than adsorption, electrocoagulation, and biosorption because the produced sludge is low. The coagulation method is superior to electrocoagulation due to zero electrical requirements. Membrane separation has an electrical cost for pressure pump operation and membrane fouling is the drawback. Electrooxidation is a very effective technology for dye removal from wastewaters but the residual persistent dye by-products are still a very important problem for treated water discharge. Therefore, iron coagulation of Brilliant Yellow and Indigo Carmine dyes is very advantageous due to the low cost of operation, the easily handling of process and the low operation duration. In addition to batch reactor, a continuous reactor was applied to these two dyes. The I.C. is used in the food and textile industries, and B.Y. is used in the textile industry, therefore, their removals were selected.

MATERIALS AND METHODS

pH Effect Experiments

Experiments for pH effect were carried out in a temperature controlled incubator shaker. For this purpose, 50 mL solutions with 100 mg/L concentrations were adjusted to 4, 6, 8, 10 and 12 pHs and 0.01 g $FeCl_3$ was added to each 100 mL polyethylene bottles with 50 mL dye solution. The other parameters were 20 °C, 5 minutes agitation time and 100 rpm agitation speed. These experiments were carried out for both Indigo Carmine and Brilliant Yellow dyes. After coagulation, 10 mL dye solutions were filtered with Whatman filter paper and measured by using UV-vis spectrophotometer at 610 nm for Indigo Carmine dye and 400 nm for Brilliant Yellow dye. The reason of selection 100 mg/L concentration was the concentration range of 100 and 200 mg/L in factorial design.

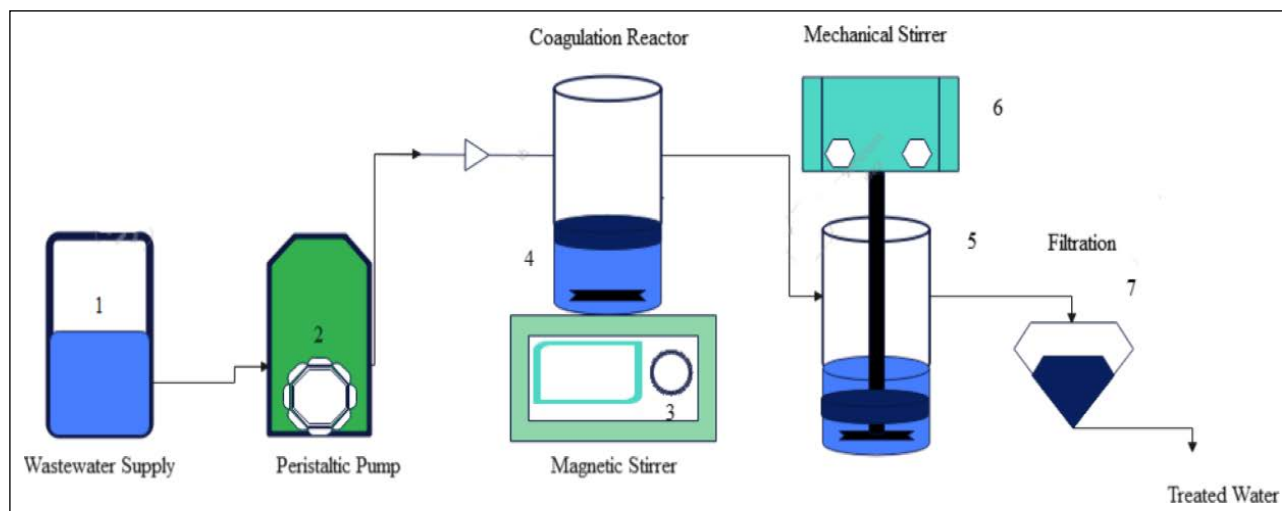


Figure 1. Total Experimental setup.

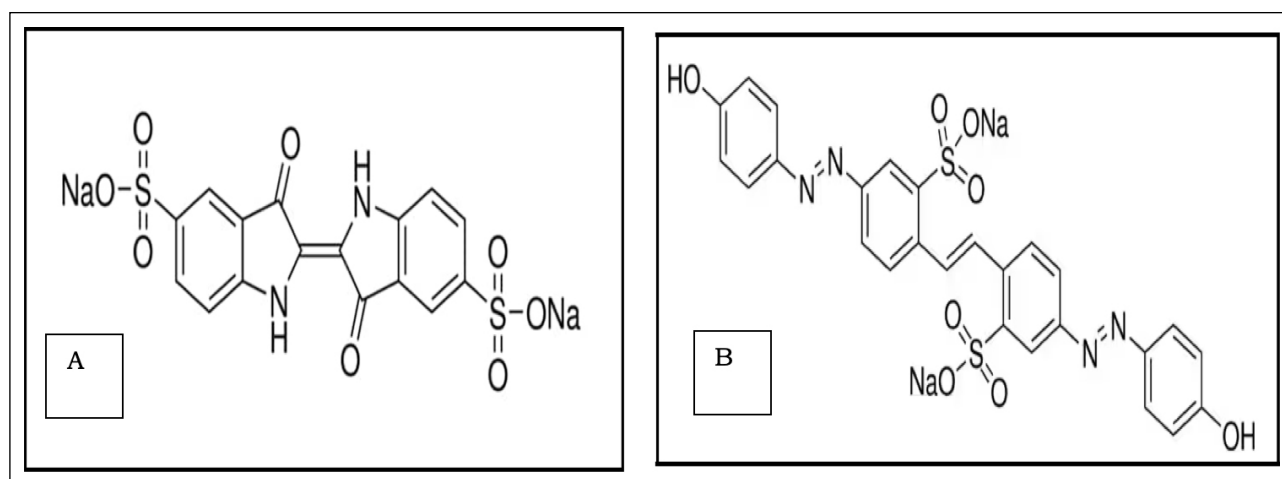


Figure 2. (a) Chemical structure of Indigo Carmine dye. (b) Chemical structure of Brilliant Yellow dye.

Factorial Experimental Design Experiments for Coagulation of Dyes

In this study, Indigo Carmine and Brilliant Yellow dyes removals by coagulation using iron chloride were studied. The experimental setup is given in Figure 1. The batch coagulation reactor had 1.3 L volume and was filled with 500 mL dye solution. In this study, only coagulation was applied and flocculation was omitted. The coagulation reactor was stirred at 1,000 rpm stirring rate by a magnetic stirrer. In batch experiments, 2^3 factorial design was applied for pH, concentration and iron chloride dosage. Parameters were iron chloride dosage (0.1–0.4 g/500 mL), concentration (100–200 mg/L), and pH (4–12). Firstly, dye concentrations of working solutions with 500 mL volume were prepared from 2,000 mg/L stock dye solution (I.C. and B.Y.). pHs of solutions were adjusted and iron chloride salt solution at predetermined volume was added from 10 g FeCl_3 /250 mL stock solution to the working solutions. The reactor content was stirred during 5 minutes and a volume of 10 mL of treated solution was pipetted by automatic pipette and filtered by Whatman filter paper. The filtered solution was diluted and its absorbance value was measured by a spectrophotometer (UV-visible) at 610 nm

for I.C. and at 400 nm for B.Y. The diluted solutions had absorbance values within calibration curve. The experimental error due to dilution was around 3% in removal percentages. The experiments were carried out according to optimization experimental matrix parameters determined by Minitab 16.0 software. The dye chemical structures are given in Figure 2. The iron chloride salt had 98% purity (Merck product). The solution temperatures were 20 °C throughout the experiments. The pure water was used in preparation of dye solutions. Calibration curves of dyes (I.C. and B.Y.) were prepared within 0–10 mg/L concentrations. B.Y. dye had 70% purity and this ratio was taken into consideration in dye concentration calculation. I.C. dye had analytical grade.

Flocculation Experiments

Solutions with 200 mg/L concentrations for B.Y. and I.C. dyes were treated with 0.4 g FeCl_3 in a batch reactor. Coagulation experiments were carried out in a batch reactor and then flocculation experiments were carried out in a Jar test device. The other parameters were kept as constant at 20 °C, 1,000 rpm, 500 mL and natural pHs for coagulation. The flocculation experiments were carried out at 20

Table 1. The intervals of the factors used in optimization

Dye type	Parameter	Abbreviation	Low level (-1)	High level (1)
Indigo Carmine	pH	pH	4	12
	Coagulant Dosage (g/500 mL)	CD	0.1	0.4
	Concentration (mg/L)	C	100	200
Brilliant Yellow	pH	pH	4	12
	Coagulant Dosage (g/500 mL)	CD	0.1	0.4
	Concentration (mg/L)	C	100	200

Table 2. Experimental matrix for dye removal

Trial	pH	(CD, g/500 mL)	(C, mg/L)	I.C. (%)	I.C. model (%)	B.Y. (%)	B.Y. model (%)
1	-1	-1	-1	79.69	86.86	82.14	83.52
2	-1	-1	1	77.73	70.36	90.50	87.12
3	-1	1	-1	100.00	92.62	88.10	84.72
4	-1	1	1	95.31	102.02	79.17	80.56
5	1	-1	-1	47.66	40.48	58.33	56.94
6	1	-1	1	6.64	14.02	55.36	58.74
7	1	1	-1	12.50	19.88	34.52	37.90
8	1	1	1	26.95	19.78	33.33	31.94

CD: Coagulant dosage, C: Concentration.

°C, 60 rpm, natural pHs. After treatment of dye solutions with iron chloride, 500 mL solutions were flocculated and filtered with Whatman filter paper. Because the gathered flocks should be dewatered by filtration.

Dye removal percentages of I.C. and B.Y. were calculated using following equation.

$$\eta = \left(\frac{C_0 - C_t}{C_0} \right) \times 100 \quad (\text{Eq. 1})$$

Here, η is removal percentage (%), C_0 is initial dye concentration (mg/L), C_t is treated water dye concentration (mg/L).

RESULTS AND DISCUSSION

pH Effect

The effect of pH was studied at range of 4–12 for Indigo Carmine and Brilliant Yellow dyes removal by coagulation using iron chloride salt. Indigo Carmine and Brilliant yellow dyes removal as a function of pH were carried out at 100 rpm agitation speed, 20 °C, 50 mL solution volume, 100 mg/L dye concentration, 5 minutes coagulation time, 0.01 g/50 mL iron chloride dosage. The removal was carried out in an incubator shaker. The results are given in Figure 3. The results showed that I.C. and B.Y. dyes removals were constant at 100% and 90 % removal yields from pH 4 to pH 10, respectively, but dyes removals decreased at pH 12. This result can be related with competitive adsorption of anionic dyes and hydroxyl ions for iron cation and iron hydroxyl surface at pH 12. Similar results were reported for anionic dyes adsorption onto coffee waste [18]. In another

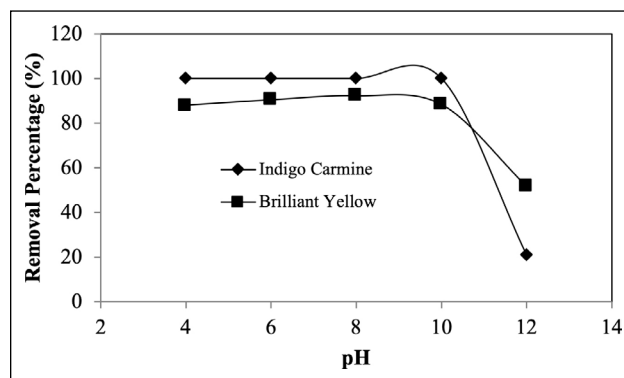
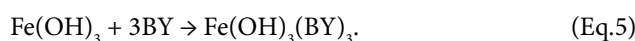
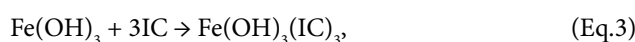


Figure 3. pH effect on removal of Indigo Carmine and Brilliant Yellow dyes from water (100 rpm, 20 °C, 50 mL, 100 mg/L dye, 5 minutes, 0.01 g FeCl₃/50 mL).

study, the anionic dyes removals by spent mushroom waste were decreased at high pHs [19]. The removal mechanism of I.C and B.Y. dyes by iron cation and iron hydroxide can be summarized as follows.



Factorial Optimization Design of Experiments

Science and industry sometimes use optimization methods to upgrade their outputs. Optimization of experiments generally reduces the experiment number. There

Table 3. Analysis of ANOVA

Term	Indigo Carmine			Brilliant Yellow		
	Coefficient	T-value	p	Coefficient	T-value	p
Constant	55.81	7.67	0.083	65.18	27.34	0.023
pH	-32.37	-4.45	0.141	-19.80	-8.30	0.076
Coagulant Dosage (CD)	2.88	0.40	0.760	-6.40	-2.69	0.227
Concentration (C)	-4.15	-0.57	0.670	-0.59	-0.25	0.845
pH-CD	-6.59	-0.91	0.531	-5.06	-2.12	0.280
pH-C	-2.49	-0.34	0.790	-0.45	-0.19	0.882
CD-C	6.59	0.91	0.531	-1.94	-0.81	0.565

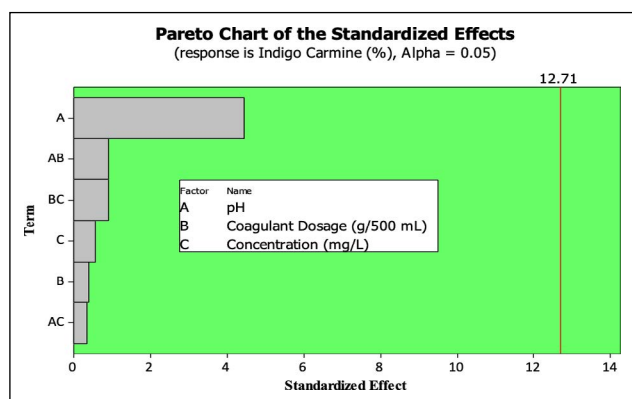


Figure 4. Pareto chart of analysis (Indigo Carmine dye).

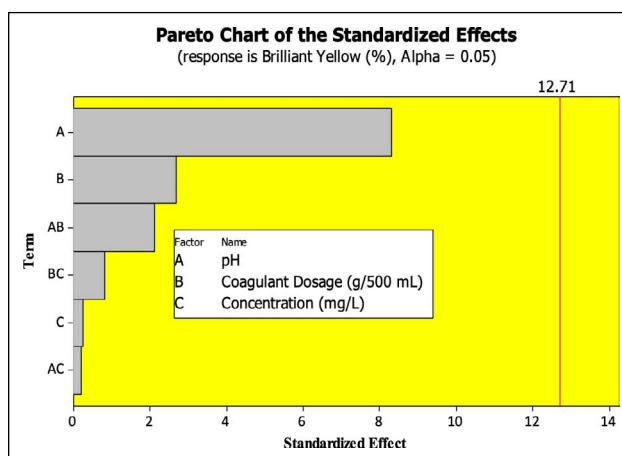


Figure 5. Pareto chart of analysis (Brilliant Yellow dye).

are several optimization methods like as response surface, taguchi, full factorial design, artificial neural network and traditional single parameter optimization. The central composite design tool of response surface method requires more experimental runs containing the matrix conditions of factorial design. If the limits of parameters matrix conditions are unknown, the analysis of central composite design would become more complicated and effort requiring and costly. Traditional single parameter optimization analyzes data separately, and therefore it is not advantageous. Therefore, the factorial design is advantageous than single parameter experiments and central composite design. A factorial experimental design was applied to Indigo Carmine and Brilliant Yellow dyes removals. For analysis of main and interaction effects of parameters, the experimental matrix of the factorial design should be determined before. For the present study, the effect of parameters such as pH, coagulant dosage and concentration were optimized by 2³ factorial design using Minitab 16.0 software. In this study, the response for the analysis and model development was selected as removal percentage. The p values (confidence constants) were used as control parameter to check the reliability of the developed statistical model. When the p value is small from confidence level, the corresponding parameter or interaction were determined as statistically important [20, 21]. The confidence level was selected as 95% for the present study. An example of the general regression model equation for the factorial design can be given as follows.

$$\text{Removal (\%)} = b + b_1X_1 + b_2X_2 + b_3X_3 + b_4X_1X_2 + b_5X_1X_3 + b_7X_2X_3 + b_8X_1X_2X_3 \quad (\text{Eq.6})$$

Here; b, b₁, b₂, b₃, b₄, b₅, b₇, b₈ are model constants and X₁, X₂, X₃ are coded factors representing pH, coagulant dosage, concentration. X₁X₂, X₁X₃, X₂X₃, X₁X₂X₃ are their interactions.

The low and high levels of parameters are given in Table 1. The low and high levels of coagulant dosage (iron chloride) were 0.1 and 0.4 g/500 mL, the low and high levels of pH were 4 and 12 and the low and high levels of concentration were 100 and 200 mg/L. The factorial matrix of experimental design is given in Table 2. The ANOVA analysis (student-t test and confidence levels, p) was performed and was given in Table 3. The confidence limit value (p) for the main and the interaction effects of the parameters was selected as 95%. The maximum dye removal was obtained as 100% in I.C. for pH (4), 0.4 g/500 mL coagulant dosage, 100 mg/L dye concentration. The maximum dye removal was obtained as 90% in B.Y. for pH (4), 0.1 g/500 mL coagulant dosage, 200 mg/L dye concentration. All the parameters were found as statistically insignificant (p values above 0.05). Pareto charts of removals are given in Figures 4 and 5 showing parameters effect above significance. As can be seen in Figures 4 and 5, the all parameters were determined as above confidence values because the parameters lines below the limit value of 12.71. This nu-

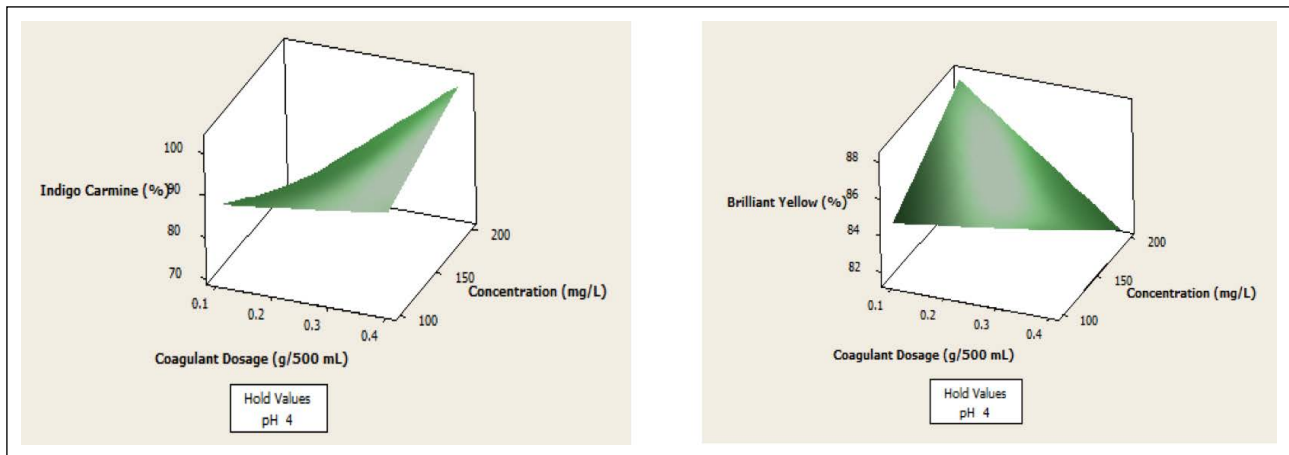


Figure 6. Concentration-coagulant dosage effect on Indigo carmine and Brilliant yellow removal.

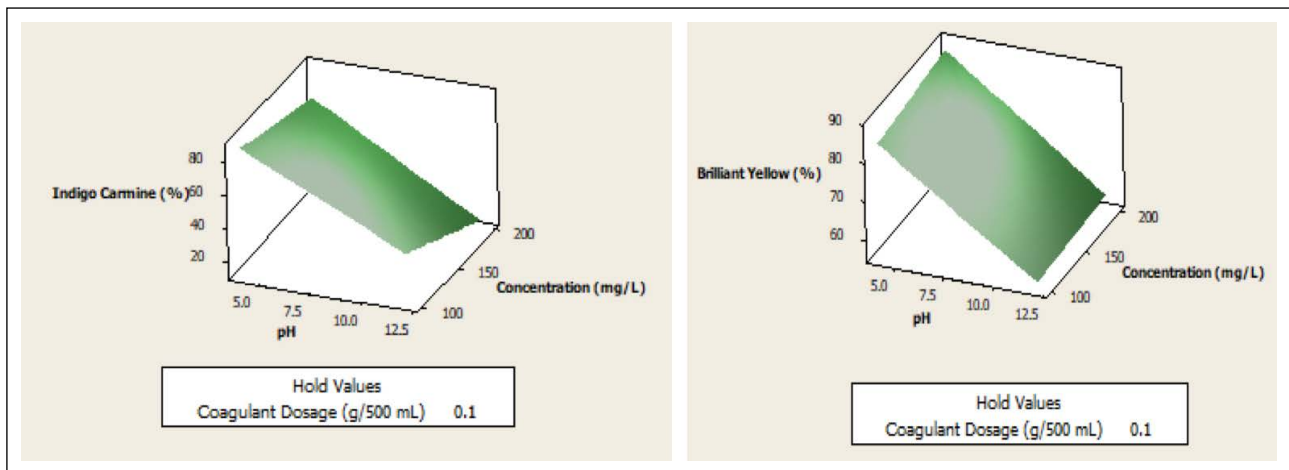


Figure 7. pH-concentration effect on Indigo carmine and Brilliant yellow removal.

merical value is determined by the Minitab 16.0 software. Experimental matrix is given in Table 2. As can be seen in Table 2, I.C. dye removal is changed from 6.64 to 100% and B.Y. dye removal is changed from 33.33 to 90.50%. For Indigo Carmine dye, correlation coefficients were calculated as $R\text{-Sq}=95.66\%$, $R\text{-Sq}(\text{predicted})=0.00\%$, $R\text{-Sq}(\text{Adjusted})=69.62\%$. For Brilliant Yellow dye, correlation coefficients were calculated as $R\text{-Sq}=98.79\%$, $R\text{-Sq}(\text{predicted})=22.51\%$, $R\text{-Sq}(\text{Adjusted})=91.52\%$. According to model estimation values of removal percentages, the dye removal percentages were well recalculated and given in Table 2. The Anova analysis of data was done according to coded factors. The $R\text{-Sq}$ value for Indigo Carmine dye was calculated as 95.66% and the $R\text{-Sq}$ value for Brilliant Yellow dye was calculated as 98.79%. These results show that the developed regression models estimated the data at enough degree and these conclusions were corrected with recalculated data given in Table 2. The statistically insignificant parameter effects are thought that the factorial design assumes the linear lines in two values of one factor and there is a slope. For instance, pH shows very different slopes for all parameter interactions like as pH-concentration, pH-dosage and these different slopes can cause to statistically insignificant (p) values. Also, these results were

related with selection of confidence limit value in Minitab 16.0 software. In this study, the confidence value was selected as 95% and it can be selected to be less. In a study, the confidence value was reported as 90% [14] and in another study, the confidence value was reported as 88% [22]. In Table 3, while the negative coefficients indicate the decreasing effect on data calculation by regression model, the positive coefficients indicate the increasing effect on data calculation by regression model.

The regression models were developed as follows.

$$\text{I.C. removal (\%)} = 55.81 - 32.37 \cdot \text{pH} + 2.88 \cdot \text{CD} - 4.15 \cdot \text{C} - 6.59 \cdot \text{pH} \cdot \text{CD} - 2.49 \cdot \text{pH} \cdot \text{C} + 6.59 \cdot \text{CD} \cdot \text{C} \quad (\text{Eq. 7})$$

$$\text{B.Y. removal (\%)} = 65.18 - 19.80 \cdot \text{pH} - 6.40 \cdot \text{CD} - 0.59 \cdot \text{C} - 5.06 \cdot \text{pH} \cdot \text{CD} - 0.45 \cdot \text{pH} \cdot \text{C} - 1.94 \cdot \text{CD} \cdot \text{C} \quad (\text{Eq. 8})$$

Concentration-Coagulant Dosage Effect on Indigo Carmine and Brilliant Yellow Removal

The results are given in Figure 6. For Indigo Carmine dye removal, high concentration and high coagulant dosage increased the removal and maximum removal was obtained as 100%. For Brilliant Yellow dye removal, maximum removal was obtained at high concentration and low coagulant dosage and maximum removal was obtained as

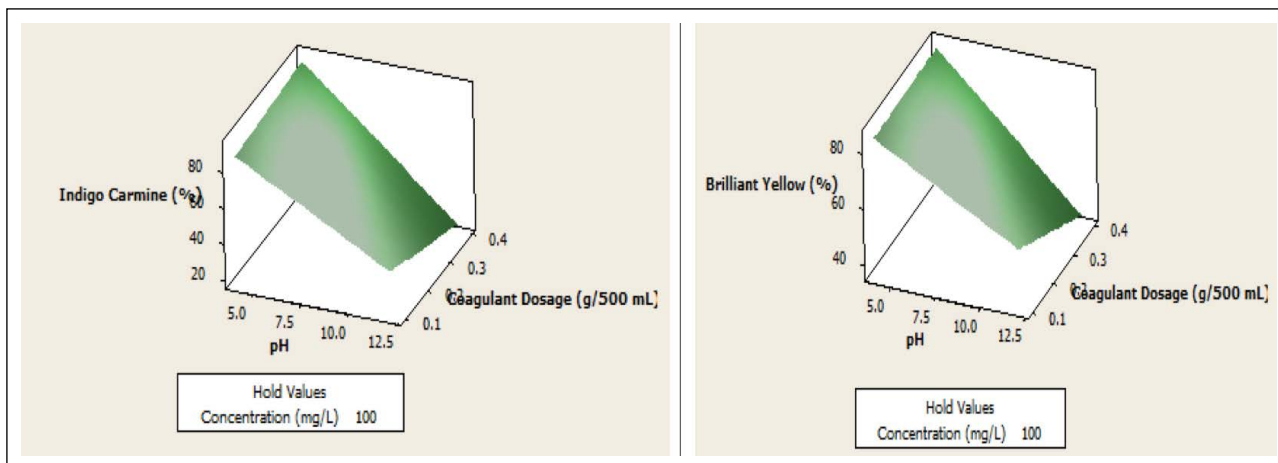


Figure 8. pH-coagulant dosage effect on Indigo Carmine and Brilliant Yellow removal.

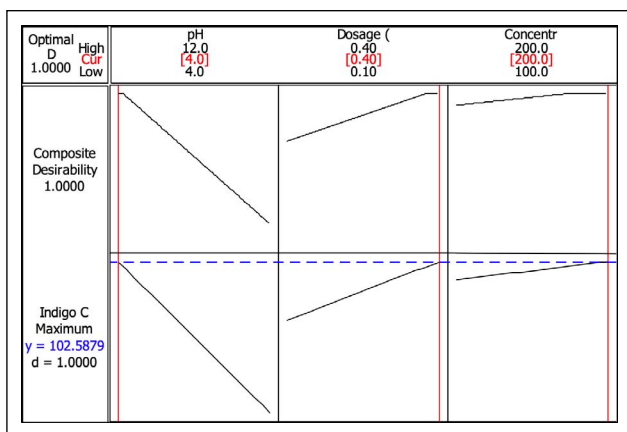


Figure 9. Optimization graphs of Indigo Carmine dye.

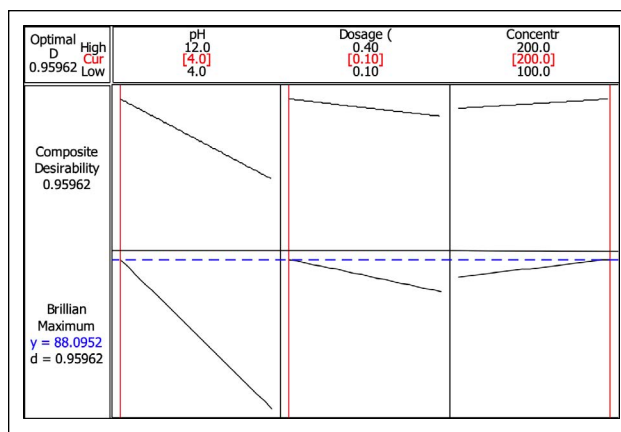


Figure 10. Optimization graphs of Brilliant Yellow dye.

87%. In Indigo Carmine removal, the reason of maximum removal at high concentration and high coagulation dosage was increasing active site number for increasing dosage and driving force of high concentration [9]. The maximum removal reason at low coagulant dosage and high concentration was probably the equilibrium between dye and coagulant for Brilliant Yellow [23]. In different studies, iron chloride dosages were applied as 100 mg/L and 5.6 mg/L for dye removals [24, 25]. Dye concentration was selected as 50 mg/L in a study [25].

pH-Concentration Effect on Indigo Carmine and Brilliant Yellow Removal

The results are given in Figure 7. The Indigo Carmine dye removal increased at low concentration and low pH. The brilliant yellow dye removal increased at high concentration and low pH. At low pHs, the Indigo Carmine dye adsorption was realized at more positive surface of iron hydroxide and iron cations [9]. Also, low concentration of Indigo Carmine dye increased the removal percentage due to high surface of coagulant for decreasing concentration [9]. Low pHs for Brilliant Yellow dye solution increased the positive surface charge of iron hydroxide and iron cations for more removal [9]. High concentration of Brilliant Yellow dye increased the removal due to high driving force [23].

pH-Coagulant Dosage Effect on Indigo Carmine and Brilliant Yellow Removal

The results are given in Figure 8. Indigo Carmine dye removal increased at low pHs and constant coagulant dosages. Brilliant Yellow dye removal increased at low pHs and constant coagulant dosage. While low pHs increase the positive surface charge of coagulants for adsorption of both of the dyes, constant coagulant effect was related with solid-to-solution ratio [9, 22].

Optimization of Indigo Carmine Dye and Brilliant Yellow Dye Removal by Coagulation

Indigo Carmine and Brilliant Yellow dyes removals by iron coagulation were optimized and given in Figures 9 and 10. Maximum removals of I.C. and B.Y. dyes were selected from experimental matrix as 100% and 90.4%, respectively. The removal of I.C. dye at 100% extent was obtained at conditions of pH (4), dosage (0.4 g/500 mL) and concentration (200 mg/L). The removal of B.Y. dye at 88.1% extent was obtained at conditions of pH (4), dosage (0.1 g/500 mL) and concentration (200 mg/L). Optimization graphs of dyes are given in Figures 9 and 10.

Mechanism of Removal of Indigo Carmine and Brilliant Yellow Dyes

Both the dyes have dissociable sodium cation releasing to solution after dissolution by water. Sulfite groups of both of the

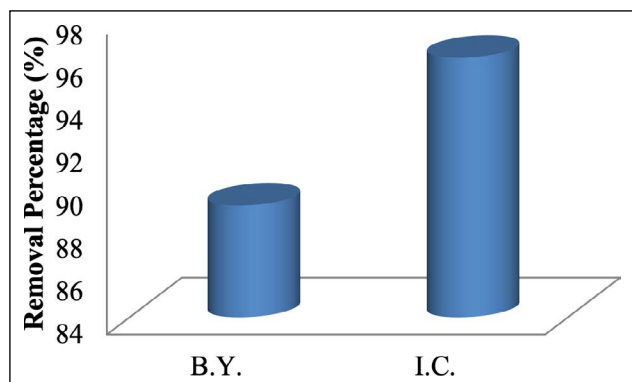


Figure 11. Brilliant Yellow and Indigo Carmine removal after 3.5 hydraulic retention time (The exit dye was collected completely in a baker and the color value was measured as was).

dyes molecules produce negative molecule tips that can form flocks by iron (III) cations. Iron cations combined with the three dye molecules for both of the dyes and long chains for coagulated flocks formed. This formed dye-iron (III) bonds were thought as to be partial ionic and partial covalent bonds between oxygen atoms of sulfite groups and iron (III) ions. These bonding types are depended on bond energies [26].

Continuous Reactor Application for Brilliant Yellow and Indigo Carmine Dye Removal

Brilliant Yellow and Indigo Carmine dyes removals were studied in a continuous reactor with 100 mL volume. In the experiments, natural pH, 1,000 rpm stirring speed, 20 °C, per 5 minutes 0.04 g FeCl₃ dosage, 400 mL dye reservoir volume and 10.084 mL/min volumetric flow rate were applied. The results are given in Figure 11. As can be seen in Figure 11, I.C. dye removal was 96% and B.Y. dye removal was 89%. These results were accordance with the results of factorial design but, B.Y. dye removal was found as high. These results showed that the batch coagulation reactor could be operated as successfully by converting to the continuous reactor. The results belong to total collected 400 mL treated water (3.5 hydraulic retention time) for B.Y. and I.C dyes, separately.

Flocculation Removal of Indigo Carmine and Brilliant Yellow Dyes

After coagulation of Indigo Carmine and Brilliant Yellow dyes, flocculation of these dyes by iron cations and iron hydroxides were realized at 20 °C, 60 rpm stirring speed, 500 mL volume and 0.4 g FeCl₃/500 mL. After flocculation operation, I.C. dye removal remained as the same with coagulation, but B.Y. dye removal increased at about 7%. B.Y. dye adsorption on Whatman filter paper was measured below 5%. Therefore, flocculation for these two dyes was ineffective. I.C. and B.Y. dyes removals were 90.52 and 96.52, respectively. Results are given in Figure 12.

CONCLUSION

Indigo Carmine (I.C.) and Brilliant Yellow (B.Y.) dyes removals were investigated using 2³ factorial design. Optimum conditions for I.C. were determined as 100 mg/L

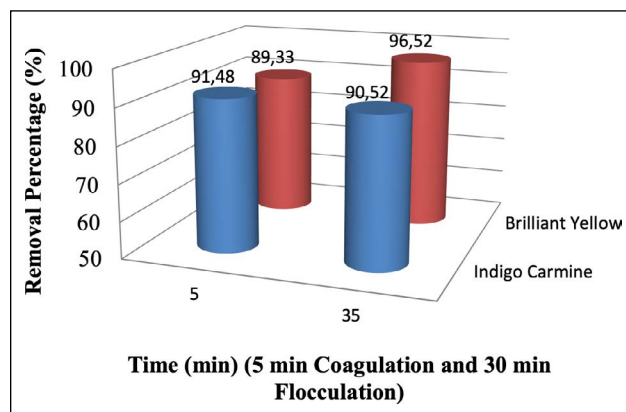


Figure 12. Coagulation and flocculation effect for removal of dyes.

concentration, 0.4 g/500 mL coagulant dosage and pH (4). Optimum conditions for B.Y. were determined as 200 mg/L concentration, 0.1 g/500 mL coagulant dosage and pH (4). Maximum removal for I.C. and B.Y. were obtained as 100% and 90.5%, respectively. The removal of both of dyes by iron coagulation was found as successful. The all parameters were insignificant in respect to statistic for both the dyes.

- For Indigo Carmine dye removal, high concentration and high coagulant dosage increased the removal and maximum removal was obtained as 100%. For Brilliant Yellow dye removal, maximum removal was obtained at high concentration and low coagulant dosage and maximum removal was obtained as 87%.
- The Indigo Carmine dye removal increased at low concentration and low pH. The Brilliant Yellow dye removal increased at high concentration and low pH.
- Indigo Carmine dye removal increased at low pHs and constant coagulant dosage. Brilliant Yellow dye removal increased at low pHs and constant coagulant dosage.
- Optimization graph was designed by selection maximum removal values of 100 and 90.4% for I.C. and B.Y. dyes, respectively and desirability values were obtained as 1 and 0.95962, respectively.
- After treatment of 400 mL Brilliant Yellow and Indigo Carmine dyes in a 100 mL continuous reactor, removal percentages for dyes were calculated as 89 and 96%, respectively.
- Flocculation was determined as ineffective.

DATA AVAILABILITY STATEMENT

The author confirm that the data that supports the findings of this study are available within the article. Raw data that support the finding of this study are available from the corresponding author, upon reasonable request.

CONFLICT OF INTEREST

The author declared no potential conflicts of interest with respect to the research, authorship, and/or publication of this article.

USE OF AI FOR WRITING ASSISTANCE

Not declared.

ETHICS

There are no ethical issues with the publication of this manuscript.

REFERENCES

- [1] X. R. Xu, H.B. Li, W.H. Wang, and J.D. Gu, “Degradation of dyes in aqueous solutions by the Fenton process,” *Chemosphere*, Vol. 57(7), pp. 595–600, 2004. [CrossRef]
- [2] B. Erdem, S. B. Avşar, S. Erdem, and N. Tekin, “Adsorption of light green and brilliant yellow anionic dyes using amino functionalized magnetic silica (Fe₃O₄@SiO₂@NH₂) nanocomposite,” *Journal of Dispersion Science and Technology*, Vol. 40 (9), pp.1227–1235, 2019. [CrossRef]
- [3] N. Viktorová, A. Szarka, and S. Hrouzková, “Recent developments and emerging trends in paint industry wastewater treatment methods,” *Applied Science*, Vol. 12, Article 10678, 2022. [CrossRef]
- [4] B. A. Fil, M. Korkmaz, and C. Özmetin, “Application of nonlinear regression analysis for methyl violet (MV) dye adsorption from solutions onto illite clay,” *Journal of Dispersion Science and Technology*, Vol. 37, pp. 991–1001, 2016. [CrossRef]
- [5] V. Selvaraj, T.S. Karthika, C. Mansiya, and M. Alagar, “An over review on recently developed techniques, mechanisms and intermediate involved in the advanced azo dye degradation for industrial applications,” *Journal of Molecular Structure*, Vol. 1224, Article 129195, 2021.
- [6] T. Arslan, “Kompleks olarak bağlı ağır metal içerikli atıkların elektrokoagülasyon ile arıtımı” Available at: <https://tez.yok.gov.tr/UlusalTezMerkezi/tezSorguSonucYeni.jsp> Accessed on Nov 06, 2023.
- [7] D. R. Ryan, “Electrocoagulation-electrooxidation for mitigating trace organic compounds in model source waters” Available at: https://epublications.marquette.edu/cgi/viewcontent.cgi?article=1532&context=theses_open, Accessed on Nov 06, 2023.
- [8] Y. S. Ho, G. McKay, “Sorption of dye from aqueous solution by peat,” *Chem Eng J*, Vol. 70, pp. 115–124, 1998. [CrossRef]
- [9] M. Korkmaz, C. Özmetin, B.A. Fil, E. Özmetin, and Y. Yaşar, “Methyl violete dye adsorption onto clinoptilolite (natural zeolite): isotherm and kinetic study,” *Fresenius Environmental Bulletin*, Vol. 22(5a), pp. 1524–1533, 2013.
- [10] Y. Hu, and W. Wu “Application of membrane filtration to cold sterilization of drinks and establishment of aseptic workshop food and environmental,” *Virolgy*, Vol. 15, pp. 89–106, 2023. [CrossRef]
- [11] Davis, M. L. *Water and wastewater engineering design principles and practice*; The McGraw-Hill Companies, Inc., Newyork (USA) 2010.
- [12] D. Bingol, N. Tekin, and M. Alkan, “Brilliant Yellow dye adsorption onto sepiolite using a full factorial design,” *Applied Clay Science*, Vol. 50(3), pp. 315–321, 2010. [CrossRef]
- [13] M. B. Ahmad, U. Soomro, M. Muqet, and Z. Ahmed, “Adsorption of Indigo Carmine dye onto the surface-modified adsorbent prepared from municipal waste and simulation using deep neural network,” *Journal of Hazardous Materials*, Vol.408, Article 124433, 2021. [CrossRef]
- [14] M. Korkmaz, C. Özmetin, E. Özmetin, E. Çalgan, and Y. Süzen, “Boron removal by aluminum modified pumice and aluminum hydroxide from boron mine wastewater-Full factorial experimental design,” *Nevşehir Bilim ve Teknoloji Dergisi*, Vol. 10 (1), pp. 1–13, 2021.
- [15] T. H. Kima, C. Park, J. Yang, and S. Kima, “Comparison of disperse and reactive dye removals by chemical coagulation and fenton oxidation,” *Journal of Hazardous Materials*, Vol. 112, pp. 95–103, 2004. [CrossRef]
- [16] A. Szygulaa, E. Guibal, M. Ruiz, and A. M. Sastrec, “The removal of sulphonated azo-dyes by coagulation with chitosan,” *Colloids and Surfaces A: Physicochemical Engineering Aspects*, Vol. 330, pp. 219–226, 2008. [CrossRef]
- [17] B. Shi, G. Li, D. Wang, C. Feng, and H. Tang, “Removal of direct dyes by coagulation: The performance of preformed polymeric aluminum species,” *Journal of Hazardous Materials*, Vol. 143, pp. 567–574, 2007. [CrossRef]
- [18] S. Wong, N. A. Ghafar, N. Ngadi, F. A. Razmi, I. M. Inuwa, R. Mat, and N. A. S. Amin, “Effective removal of anionic textile dyes using adsorbent synthesized from coffee waste,” *Scientific Reports*, Vol. 10, Article 2928, 2020. [CrossRef]
- [19] A. Alhujaily, H. Yu, X. Zhang, and F. Ma, “Adsorptive removal of anionic dyes from aqueous solutions using spent mushroom waste,” *Applied Water Science*, Vol. 10, pp. 183–195, 2020. [CrossRef]
- [20] M. Korkmaz, B. A. Fil, C. Özmetin, and Y. Yaşar, “Full factorial design of experiments for boron removal from Colemanite mine wastewater using Purolite S 108 resin,” *Bulgarian Chemical Communications*, Vol. 46, pp. 594–601, 2014.
- [21] D. Kavak, “Removal of boron from aqueous solutions by batch adsorption on calcined alunite using experimental design,” *Journal of Hazardous Materials*, Vol. 163, pp. 308–314, 2009. [CrossRef]
- [22] M. Korkmaz, C. Özmetin, E. Özmetin, E. Çalgan and Ö. Ziyanak, “Boron removal from colemanite mine wastewater by coagulation using zinc hydroxide–A factorial optimization study” *Celal Bayar University Journal of Science* Vol. 18(1), pp. 77–83, 2022. [CrossRef]
- [23] C. Özmetin, and M. Korkmaz, “ Full factorial design of experiments for boron removal by iron hydroxide from colemanite mine wastewater,” *Journal of BAUN Institute Science and Technology*, Vol. 21(1),

- pp. 244–253, 2019. [\[CrossRef\]](#)
- [24] F. Mcyottoa, Q. Wei, D.K. Macharia, M. Huang, C. Shen, C.W.K. Chow, “Effect of dye structure on color removal efficiency by coagulation,” *Chemical Engineering Journal*, Vol. 405 (1), Article 126674, 2021. [\[CrossRef\]](#)
- [25] Q. Wei, Y. Zhang, K. Zhang, J. I. Mwasiagi, X. Zhao, C. W. K. Chow and R. Tang, “Removal of direct dyes by coagulation: Adaptability and mechanism related to the molecular structure,” *Korean Journal of Chemical Engineering*, Vol. 39(7), pp. 1850–1862, 2022. [\[CrossRef\]](#)
- [26] C. E. Mortimer, “Modern Üniversite Kimyası,” Cilt 1, Çağlayan Kitap Evi, 1990.



Review Article

Impact of dissolved organic nitrogen (DON) to the formation of disinfection byproducts (DBP) during water/wastewater treatment: A review

Ashik AHMED^{*1}, Sumaya TABASSUM², Debo Brata PAUL ARGHA³, Pranta ROY⁴

¹Department of Nanoengineering, North Carolina A&T State University, Greensboro, North Carolina, USA

²Department of Water and Environment, Khulna University, Sher-E-Bangla Rd, Khulna, Bangladesh

³Department of Civil Engineering, Texas State University, Ingram School of Engineering, San Marcos, Texas USA

⁴Virginia Tech, Biological Systems Engineering, Blacksburg, Virginia, USA

ARTICLE INFO

Article history

Received: 30 October 2023

Revised: 09 January 2024

Accepted: 05 February 2024

Key words:

DBPs mitigation; Disinfection byproducts (DBPs); Dissolved organic nitrogen (DON); DBPs precursors; Wastewater treatment

ABSTRACT

Disinfection byproduct (DBP) formation during water and wastewater treatment is a concern for public health and environmental preservation. Dissolved organic nitrogen (DON) serves as a recognized precursor to DBP formation, which can potentially jeopardize human health. This review article offers a comprehensive insight into DON's influence on DBP formation during water and wastewater treatment processes. It delves into DON's sources, properties, and concentrations in water and wastewater, underlining the variability dependent on water source and environmental conditions. The mechanisms of DBP formation from DON, encompassing formation pathways and influencing factors, are meticulously examined. Different treatment methods, like chlorination, ozonation, and UV disinfection, are carefully examined to see how they affect the formation of DON and DBP. Factors that sway DON's impact on DBP formation are also explored. The review also presents various DBP reduction techniques, spanning physical, chemical, and biological treatment methods, their efficacy in curtailing DON's influence, and their potential pros and cons. It addresses challenges, outlines future research directions, identifies knowledge gaps, and highlights the necessity for regulatory measures and policies, providing recommendations for prospective research avenues. It is clear from this in-depth review that more research is needed to understand how DON affects the formation of DBP entirely. It is also essential to protect human health and the environment and follow the rules first when treating wastewater. In conclusion, it analyzes DON's part in forming DBP in water and wastewater treatment. This emphasizes the need for ongoing research and mitigation strategies to protect public health and water quality.

Cite this article as: Ashik Ahmed, Sumaya Tabassum, Debo Brata Paul Argha, Pranta Roy. Impact of dissolved organic nitrogen (DON) to the formation of disinfection byproducts (DBP) during water/wastewater treatment: A review. Environ Res Tec 2024;7(2)233–255.

INTRODUCTION

Water is an indispensable and precious resource for human survival, and safeguarding its availability and quality is of utmost significance. Wastewater treatment is a pivotal measure in ensuring responsible water resource management. It effectively treats domestic, industrial, and municipal waste-

water before it is released into the environment or reused for various applications [1]. Disinfection, as a vital step in the wastewater treatment process, is aimed at neutralizing or eliminating harmful microorganisms that may pose potential health hazards to human populations, animals, such as fish, amphibians, and aquatic invertebrates, can be adversely affected by exposure to disinfection compounds in water [2, 3].

*Corresponding author.

*E-mail address: mahmed1@aggies.ncat.edu



Water/wastewater disinfection is commonly accomplished using chemical or physical techniques, such as chlorination, ozonation, UV radiation, and other advanced oxidation processes [4–7]. These methods effectively eliminate or deactivate microorganisms, which helps reduce the spread of waterborne diseases and safeguard public health [4, 8]. However, one drawback is that disinfection can trigger reactions between disinfectants and organic matter in wastewater, forming DBPs [9].

DBPs encompass various chemical compounds that can arise from chemical reactions between disinfectants and organic matter in wastewater [10]. Examples of DBPs include trihalomethanes (THMs), haloacetic acids (HAAs), haloacetonitriles (HANs), N-nitrosodimethylamine (NDMA), nitrosamines, aldehydes, and other halogenated and organic compounds [11]. DBPs have been recognized as potential carcinogens and mutagens, prompting concerns about their health risks to humans and the environment when present in treated water or wastewater.

Wastewater treatment plants (WWTPs) typically use chlorine or ultraviolet (UV) light for final disinfection before discharging treated wastewater. Research on the formation of DBPs in treated wastewater has involved various methods such as gas chromatography/mass spectrometry (GC/MS) for identifying unknown DBPs [12], target-compound analyses for specific known DBPs [13], and bulk parameters like total organic halogen (TOX) [14]. The types and amounts of DBPs formed from organic matter in wastewater effluent depend on factors such as the level of wastewater treatment and concentrations of ammonia (NH₃) and DON [13, 15]. Well-nitrified WWTP effluents with low ammonia concentration (<0.5 mg/L as N) tend to produce large amounts of THMs, while poorly nitrified effluents (e.g., NH₃-N >5 mg/L) generally inhibit THM production [16]. Chlorination (oxidation) of amino acids can result in the formation of aldehydes and nitriles, with subsequent chlorine substitution forming chloral hydrate (trichloroacetaldehyde) and dichloroacetonitrile [17]. Chlorinated wastewater from an extended aeration treatment plant has been found to produce chloroform, dichloroacetonitrile, and chloral hydrate at specific concentration levels (0.032–0.080, 0.007–0.014, and 0.020–0.038 mg/L respectively) [17]. Higher chlorine doses can destroy the aromatic ring and the formation of chloral hydrate and HAAs [16].

Certain methods exhibit varying degrees of effectiveness in treating DON in drinking water sources. Jar tests involving natural organic matter fractions showed the least removal (~10%) for hydrophobic neutrals, while hydrophobic bases (~30%), hydrophilic bases (~35%), and hydrophilic neutrals (~50%) demonstrated improved but still lower removal rates compared to fulvic (70%) or humic (80%) acids [18]. Alum coagulation in an Australian river achieved moderate DON removal for hydrophobic acid fractions (~50%), hydrophilic acid fractions (64%), and unfractionated material (~64%), but no removal for the neutral fraction [19]. Bio-filtration holds the potential to either remove or generate DON in drinking water sources [20]. Powdered activated

carbon has the capacity to eliminate up to 72% of DON, while the sole study employing the emerging metal organic framework adsorbent for DON removal demonstrated a 98.1% removal efficiency [21, 22].

Recently, DON, which refers to the portion of organic nitrogen that remains in solution after removing particulate organic nitrogen during wastewater treatment, has gained recognition as a significant factor in forming DBPs. A substantial portion of DON, up to 85%, is found in treated wastewater effluent [23]. This DON comprises various compounds such as proteins, amino acids, and humic substances, although a significant portion, approximately 50%, remains unidentified and uncharacterized [23]. DON can originate from diverse sources, such as human and animal waste, agricultural runoff, and industrial discharges [24], and its concentration in wastewater can vary depending on the composition of the wastewater and treatment processes employed [9, 25].

The presence of DON in wastewater can have noteworthy implications for DBP formation during disinfection [26]. The mechanisms by which DON influences DBP formation are intricate and may involve multiple pathways, including the formation of nitrogenous disinfection byproducts (N-DBPs), as well as interactions with other organic and inorganic constituents of effluent organic matters [27, 28]. The influence of DON on the formation of DBPs during wastewater treatment is an increasingly essential and researched area due to its potential impacts on water quality, human health, and environmental protection. A thorough understanding of the underlying mechanisms and factors that affect the role of DON in DBP formation is essential for optimizing disinfection processes and ensuring the safety of treated wastewater [29].

Hence, this review presents a comprehensive summary of the current knowledge on how DON affects the formation of DBPs during water/wastewater treatment. This review will explore the mechanisms through which DON impacts DBP formation, the factors that influence these mechanisms, and the strategies that can be utilized to mitigate DBP formation. Additionally, any gaps in knowledge and research needs in this field will be highlighted, and the regulatory and policy implications of the relationship between DON and DBPs will be discussed.

DISINFECTION BYPRODUCTS: HIDDEN THREAT IN WATER/WASTEWATER TREATMENT

Disinfection byproducts can silently jeopardize the effectiveness of wastewater treatment processes, as they can be generated during the disinfection stage and have the potential to impact water quality negatively. Various factors, such as the level of wastewater treatment, concentrations of ammonia and DON, and the amount of chlorine used, can all influence the formation of DBPs [30–32]. Therefore, it is essential to carefully manage and monitor DBP formation to guarantee the safety and quality of treated wastewater before it is discharged into the environment. By implementing effective strategies to minimize DBP formation, wastewater treatment plants can help protect the environment and pub-

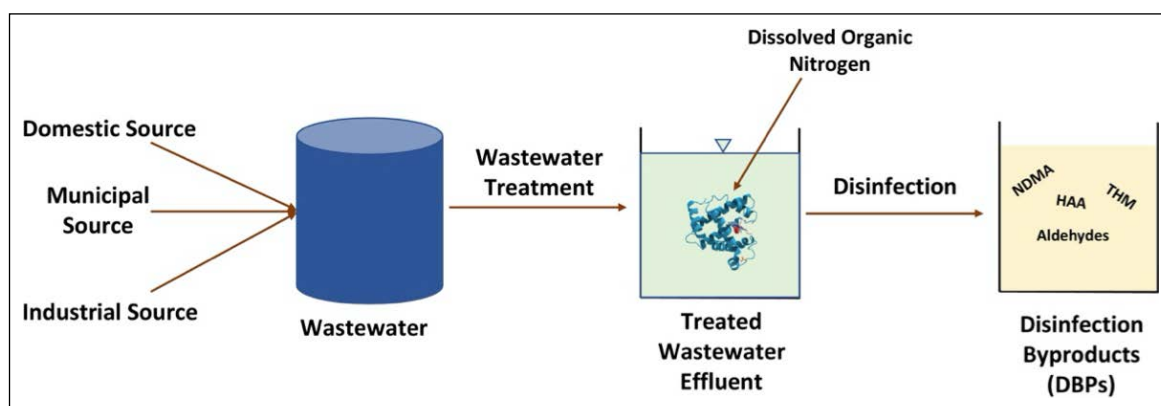


Figure 1. DBP formation in wastewater treatment and disinfection with DON presence.

lic health [28, 29]. The general procedure of DBP formation from wastewater through treatment and disinfection in the presence of DON is illustrated in Figure 1 [30–33].

Types and Properties of DBPs

DBPs can be classified into various types based on their chemical composition, including THMs, HAAs, HANs, NDMA, chlorate, chlorite, bromate, and among others [34–36]. Figure 2 represents the chemical formula of the different readily formed DBPs during disinfection. THMs can be produced during chlorination, chloramination, and ozonation, followed by chlorination [37]. Similarly, HAAs can form during chlorination and chloramination processes. NDMA can be formed through reactions between nitrogen-containing precursors, such as dimethylamine (DMA), and disinfectants, particularly chloramines (formed by the reaction of chlorine with ammonia) [38, 39]. Chlorite (ClO_2^-) and chlorate (ClO_3^-) can be produced during disinfection processes that involve the use of chlorine-based disinfectants, such as chlorine gas (Cl_2), sodium hypochlorite (NaClO), or chlorine dioxide (ClO_2) [40, 41]. Bromate (BrO_3^-) can be produced during disinfection processes that involve the use of bromide (Br^-) ions and an oxidizing agent, such as ozone (O_3) or chlorine-based disinfectants, particularly in waters with high bromide concentrations [42, 43].

DBPs encompass several properties, including solubility, volatility, stability, reactivity, and toxicity, collectively contributing to their potential impact on water quality and human health. The solubility of DBPs can exhibit variability, with some being volatile and prone to evaporation from water due to low solubility, while others may possess a higher solubility and persist in water for longer durations. The stability of DBPs can also vary, ranging from relatively stable compounds to those that degrade or transform into other substances over time [44]. Furthermore, DBPs can display differing reactivity, influencing their interactions with other chemical compounds in water and the environment. Toxicity is another significant property of DBPs, as some may be associated with potential carcinogenic and adverse reproductive effects [10, 40]. It is important to note that the properties of DBPs can be influenced by various factors, such as the type and concentration of disinfectants used, water quality parameters, and environmental conditions [45].

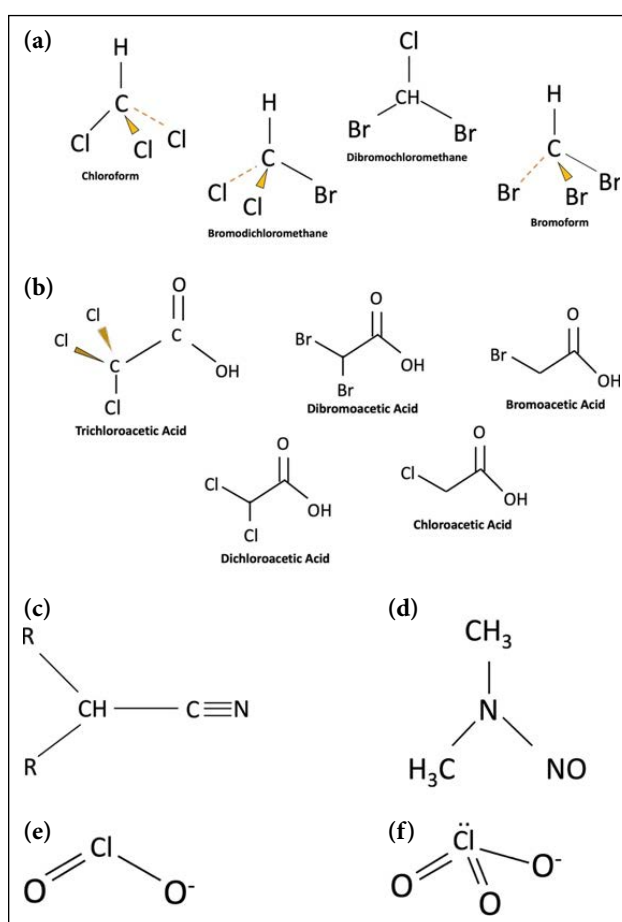


Figure 2. Chemical formula of the different types of DBPs; (a) THMs, (b) HAAs, (c) HANs, (d) NDMA, (e) chlorite (f) chlorate.

Formation Mechanisms of DBPs

Trihalomethane Formation

Trihalomethane formation is a chemical process that occurs during water disinfection when halogen-based disinfectants, such as chlorine, react with organic matter present in water. Chlorination involves oxidation and substitution [46]. Oxidized organic compounds are formed when chlorine reacts with organic matter [47]. In the substitution reaction, chlorine replaces hydrogen atoms in organic matter to form chlorinated organic compounds [48]. Chlorine further reacts with water to form chlorine radicals (Cl^\cdot), which

react with organic matter to form halogenated organic compounds [49]. This step usually limits trihalomethane formation. The most common THMs are chloroform (CHCl_3), bromodichloromethane (CHCl_2Br), dibromochloromethane (CHClBr_2), and bromoform (CHBr_3) [50–52].

Haloacetic Acid Formation

Figure 3 represents the formation mechanisms of HAAs. Through chlorination and chloramination, haloorganic intermediate compounds are formed. The haloorganic intermediates can further react with chlorine or chloramines to form haloacetic acid intermediates through halogenation reactions. The haloacetic acid intermediates can then undergo hydrolysis or oxidation reactions to form HAAs as the final product [53].

Haloacetonitriles Formation

HANs can be formed by the presence of organic nitrogen compounds and through the Cl_2 and NH_2Cl disinfection processes [54]. Chlorine or chloramines can react with the organic nitrogen to form N-chloramines. The produced N-chloroamines can undergo hydrolysis, which involves the addition of water molecules, resulting in the formation of N-chloroimine. The N-chloroimine species can further react with other organic nitrogen compounds in the wastewater effluent, such as amino acids or other organic matter, through nucleophilic substitution or addition or rearrangement reactions, resulting in the formation of HANs [53, 54].

N-nitrosodimethylamine (NDMA) Formation

Dimethylamine (DMA) and amide are two common organic nitrogen compounds found in water, that can undergo nitrosation. Nitrite ions (NO_2^-) react with DMA to form NDMA as an intermediate and nitrosation of amide can form N-Nitrosamide intermediates [55]. N-Nitrosamine intermediates, formed through nitrosation of DMA or amides, can undergo dimethylation, where dimethylating agents, such as formaldehyde (HCHO) or other methylating agents, react with the intermediates to form NDMA [55]. Figure 4 shows the formation mechanisms of NDMA.

Chlorite and Chlorate Formation

Chlorite (ClO_2^-) and chlorate (ClO_3^-) formation can occur during water disinfection processes that involve the use of Cl_2 or NH_2Cl [56]. Chlorine can react with natural organic matter (NOM) or other precursors in water, leading to the formation of chlorite through a series of oxidation reactions [57]. Chlorine can also oxidize chloride ions (Cl^-) in water to form hypochlorite (ClO^-), and further oxidation of hypochlorite can result in the formation of chlorate [57]. The specific mechanisms and pathways of chlorite and chlorate formation can vary depending on pH, temperature, and chlorine dosage.

Bromate Formation

Bromate (BrO_3^-) formation is involved with the use of O_3 for disinfection. O_3 reacts with bromide ions (Br^-) in water to form bromate through a series of oxidation reactions

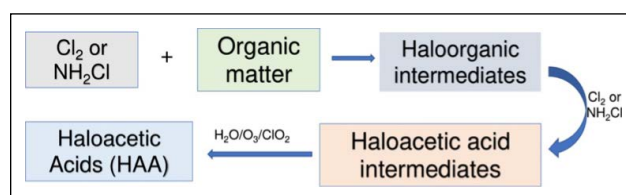


Figure 3. Formation mechanisms of the HAAs.

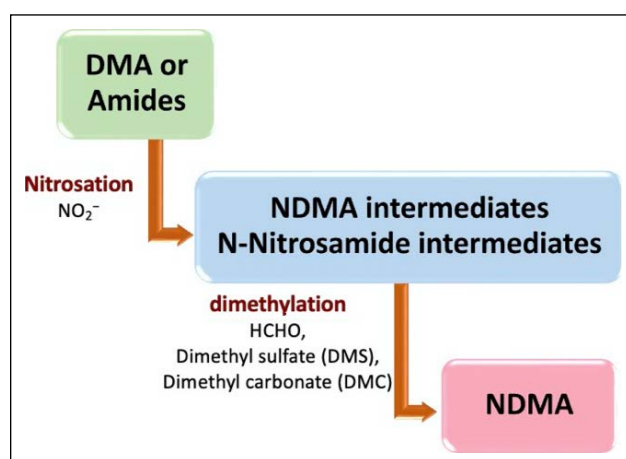


Figure 4. NDMA formation mechanisms.

[43]. The formation of bromate is highly dependent on factors such as pH, temperature, ozone dosage, and bromide ion concentration [58].



Or,



Challenges in Controlling DBPs

Controlling DBPs poses several challenges due to their diverse nature and the complexities associated with their formation and control. Some of the specific challenges for controlling DBPs include formation variability, multiple DBP types, changing regulations, treatment trade-offs, cost implications, monitoring and optimization, public awareness, and communication, etc. DBP has a complex and multifaceted nature. Several factors, such as the type and concentration of disinfectants, water quality parameters, and environmental conditions, make it challenging to predict and mitigate the formation of specific DBPs [60]. Besides, reducing disinfectant dosages or changing disinfection methods, may have trade-offs with other treatment goals, such as pathogen removal or other water quality parameters. Balancing DBP control with other treatment objectives can be challenging.

The factors such as temperature, pH, and chlorine dosage make the DBP control more challenging. The concentrations of regulated DBPs can vary significantly in household tap water due to changes in water temperature [61]. Specifically, when water is heated for bathing or spa use at higher temperatures (e.g., 35–50 °C), there can be a rapid increase in the levels of THMs and HAAs within 0.5 h [62]. This highlights the potential for significant fluctuations in DBP

levels in tap water in response to changes in water temperature, which may have implications for human exposure to these contaminants. Chuang et al. [28] stated that the concentrations of chloroform are 0.028, 0.057, 0.128, 0.171, and 0.304 mg/L for 4, 15, 25, 35, and 50 °C, respectively. He also found a similar pattern for dichloroacetic acid and trichloroacetic acid also got higher DBP concentrations when the temperature changes from 10 to 25 °C [63]. It is hard to control the DBPs with these varying concentrations for different temperatures.

The formation of chlorine DBPs is known to be influenced by pH, as most chlorine reactions are pH dependent. Lower, more acidic pH conditions typically result in less chloroform formation, with a corresponding increase in the concentration of HAAs [64]. This trend of reduced chloroform formation with decreasing pH was also observed in a study by Özbek [65], where hypochlorite was adjusted to pH 4, 7, and 10 and added to resorcinol in different ratios. No chloroform was formed at pH 4, and a 1:3 ratio, but at pH 7 and 10, 50% and 95% of the resorcinol were converted to chloroform, respectively [65]. With varying pH, different controlling measures need to be taken to control DBPs.

Potential Effects on Human Health

Human exposure to DBPs can occur through three main pathways: dermal contact, ingestion, or inhalation [66, 67]. Several epidemiological studies have demonstrated associations between DBP exposure and increased risks of cancer development, liver and kidney defects, central nervous system issues, adverse reproductive outcomes, and endocrine disruption, causing concern for human health in areas where DBPs are present in drinking water [68–70]. Consistently linked to chlorination DBPs as one of the health risks associated with DBP exposure is urinary bladder cancer [70–73]. Another study discovered a potential association between high concentrations of DBPs and increased risks of colon and rectal cancer, especially with individual DBPs such as THMs and HAAs, with the most consistent association observed for rectal cancer. To better comprehend these associations, additional research is required [73].

Emerging DBPs formed in distribution systems during chlorination and chloramination, such as THMs, HAAs, and HANs, have been reported to cause symptoms related to liver, kidney, and nervous system diseases. Unregulated DBPs have been associated with spontaneous abortions, congenital disabilities, stillbirths, and other negative reproductive effects [74]. Recent research has focused on maternal exposure to emerging DBPs during pregnancy, particularly THMs and dichloroacetic acid, and some DNA anomalies have been observed in cord blood, leading to foetal growth restriction or other adverse reproductive outcomes [75–78]. Emerging DBPs may also be classified as carcinogenic substances or have other detrimental effects on human health, such as alterations in pregnancy duration, menstrual cycle, pregnancy loss, foetal development, and congenital malformations, as well as cancer risks, as reported in various studies [79–81].

According to López-Roldán et al. [82], the risk of developing cancer or diseases from ingesting THMs is higher compared to the risk from inhalation during showering or dermal exposure [83]. This highlights the significant danger posed to human health by drinking water contaminated with DBPs, particularly THMs and HAAs. The risks may be higher when the raw water source is surface water, but they may be lower when it is a mix of surface water and groundwater, or solely groundwater.

I-aldehydes, cyanides, halonitromethanes, halo ketones, haloacetamides, iodinated-DBPs, and N-nitrosamines are just some of the DBPs that have been the subject of recent studies. Andersson et al., Chaukura et al., and Chen et al. [84–86] all report that these DBPs are more cytotoxic, genotoxic, and mutagenic than their brominated and chlorinated counterparts, suggesting they pose serious health risks. The N-nitrosamine NDMA (N-nitrosodimethylamine) has been the focus of much attention because even trace amounts (ng/L) have been linked to a 10-fold higher risk of cancer over a lifetime. Among the N-nitrosamines, NDMA (N-nitrosodimethylamine) has garnered significant attention due to its presence in drinking water at low levels of ng/L, which has been associated with a lifetime excess cancer risk of 10^{-6} .

DON: A KEY PLAYER IN DBP FORMATION

DON has been identified as a key player in the formation of DBPs such as THMs, HAAs, HANs, and NDMA in water treatment systems [87]. DON is a complex mixture of organic compounds that can originate from various sources, such as natural organic matter, wastewater, and agricultural runoff. During water treatment processes, disinfectants, such as chlorine, can react with DON, leading to the formation of DBPs, including THMs, HAAs, and other classes of DBPs. Amino acids, nitrogen-containing heterocyclic compounds found in nucleic acids (e.g., cytosine), cells of algae, and extracellular organic matter have been proposed as potential precursors for halogenated acetonitriles (HANs) when they react with chlorine or chloramines. This suggestion is supported by studies conducted by [63, 88, 89].

When free chlorine is present in organic fractions with a high concentration of DON, dichloroacetonitrile (DCAN) is more likely to form at higher concentrations, as reported by Lee et al. and Dotson et al. [87, 90] and Yang et al. [91] show that during chloramination in natural waters, the relationship between DCAN and DON is not well established. According to a hypothesis by Yang et al. [91] DCAN can be formed during chloramination via the hydrolysis of N-chloroimine, which is generated via the direct incorporation of chloramines into diketone moieties of DOM. DCAN is positively correlated with SUVA in chlorinated natural waters [91], suggesting that aromatic content within DOM may be related to the formation of diketone moieties for HAN formation.

Oftentimes, N-DBPs like halonitromethanes (HNMs), N-nitrosamines (NAs), and halonitromethanes (HANs) have been found in chloraminated or chlorinated wastewa-

ter effluent at concentrations ranging from nanograms per liter to micrograms per liter [15, 92, 93]. Compared to other disinfection byproducts that are regulated, like THMs and HAAs, these N-DBPs have been found to be more toxic and to pose more health risks [11, 94, 95].

DON Sources in WWTP

DON in WWTPs comes from both the wastewater that is being treated and the microorganisms that are already present at the site. Low DON concentrations, between 3 and 7 mg/L, are typical in raw municipal wastewater [96, 97]. Carbamate and pyrimidine compounds are major contributors to DON in wastewater from industries producing pesticides, textiles, dairy, fertilizer, leather, and pharmaceuticals, with concentrations ranging from 12 to 71 mg/L [98]. A study found that approximately 88–91% of the TDN in the wastewater generated by the yoghurt production industry comprises DON [99]. A notable origin of DON in wastewater is the use of agricultural fertilizer [20]. An additional research finding revealed that the leather industry contributes 111.5 mg/L of total nitrogen (TN) in wastewater, with a notable portion being attributed to DON [100]. Prior to discharge into municipal wastewater collection systems, DON levels can be reduced to around 10–15 mg/L through industrial wastewater treatment processes [98]. The breakdown of organic materials in the waste material field can also increase the concentration of DON in landfill leachate and coincide with the WWTP influent [94–99], which in turn can react with DBPs precursors in drinking water treatment processes, potentially increasing the formation of DBPs [101–103]. Therefore, DON from municipal waste can play a significant role in forming DBPs in potable water [104, 105].

Microbially derived DON (mDON) is another source of DON at WWTPs. It is found in soluble microbial products (SMP) released during cell metabolism and biomass decay [15, 106]. Lab-scale aerobic bioreactors treating synthetic organic wastewater with ammonium chloride as the sole nitrogen source have been shown to produce up to 3.45 mg/L of DON in the effluent [107]. mDON is largely made up of bioavailable substances for algae, such as proteins, enzymes, nucleic acids, amino acids, and fulvic acid-like substances [108]. There is no chemical difference between DON from the influent and mDON in domestic WWTPs. Recent research, however, has suggested that model predictions indicate mDON may account for nearly 50% of the effluent DON in the activated sludge process [109]. Figure 5 represents the various sources that can generate DON in wastewater system.

Characteristics and Properties of DON

DON's unique properties can contribute to DBP formation, making it an important component of wastewater and natural water systems. DON's varied properties make it a key player in DBP formation. DON can form nitrogenous DBPs, for instance. The composition and concentration of DON in water, disinfectants used, and environmental conditions can affect DON's unique ability to form DBP.

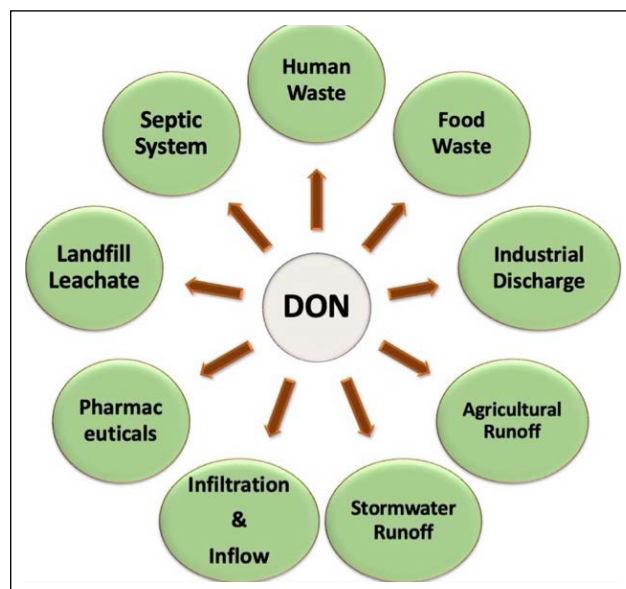


Figure 5. Some anthropogenic sources of DON in wastewater.

Studies from Bolyard and Reinhart and Liu et al. [110, 111] show that the bioavailability of DON is linked to its chemical properties. Effluent with a higher tryptophan to humic substances fluorescence ratio was found to have more bioavailable DON, which could promote algal growth, according to research by [111]. In addition, the bioavailability of effluent DON was shown to increase with molecular weight for DON molecules smaller than 1 kDa [107]. The varying bioavailability of DON in natural waters is likely due to differences in DON's chemical composition. Free amino acids [112–115], urea [116, 117], and nucleic acids [115, 116] are readily taken up by heterotrophic bacteria and/or marine and freshwater algae. The research of Carlsson and Granéli [118] shows that in N-limited systems, algae are less able to make use of humic substances and other forms of DON for growth. Photochemical reactions in natural waters may convert DON into more labile compounds like primary amines [119] or ammonia [120], although these reactions can also have a negative impact on the bioavailability of DON [120]. DON exhibits biodegradability over time, as evidenced by a study that observed variations in the biodegradation of DON among effluent samples from four examined plants before filtration. Specifically, a decline in DON was noted in prefiltration samples from two of the four plants, with these two plants experiencing a reduction of organic nitrogen ranging between one-quarter to one-third over a 20-day period [121].

As wastewater progresses through various treatment stages in a conventional biological nutrient removal (BNR) process, the concentration of DON typically decreases, with the majority of DON removal occurring in the anaerobic zone of the anaerobic/anoxic/oxic process [97]. In cases where the DON concentration in the influent is already low (between 1.1 and 3.9 mg/L), only a small amount of DON is removed during wastewater treatment, leaving concentrations of 0.5 to 1.3 mg/L in the effluent [122]. Studies by Sattayatewa et al. and Huo et al. [96, 97] show that the ac-

tual efficiency of DON removal can vary greatly between different wastewater treatment plants, from 30% to 90%. Furthermore, the composition of domestic wastewater typically consists of proteins, amino acids, and humic-like substances. However, in the effluent, the composition changes to include amino acids, EDTA, and specific proteins that are newly produced compounds, as reported in studies by [97, 123]. In addition, the low molecular weight dissolved organic nitrogen (LMW DON) concentration, which initially ranges from 4.2–4.4 mg/L, undergoes changes during treatment in the effluent, resulting in a range of 1.5–3.5 mg/L (LMW DON), accounting for 50–65% of the effluent DON [119, 120]. According to Huo et al. [97], more than 80% of the effluent DON are hydrophilic and these hydrophilic fractions are mostly bioavailable (almost 85% of the hydrophilic DON) [124, 125]. Secondary effluent DON is well-characterized, with abundant presence of proteins, amino acids, and EDTA [126], whereas DON in raw wastewater is poorly characterized. 60% of the DON in the effluent is made up of proteins, while only 13% is amino acids [126]. Huo et al. [97] also reported that between 50% and 66% of the total DON in WWTP effluent is made up of LMW compounds. Urea, amino acids, DNA, peptides, and synthetic nitrogenous compounds like pesticides and pharmaceuticals are all examples of LMW compounds. In contrast, Pagilla et al. [127] reported that fulvic acids, proteins, and humic acids make up the bulk of the HMW DON in the effluent.

DON Species: Precursors of N-DBPs

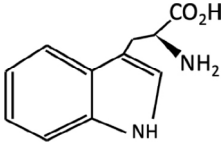
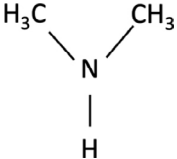
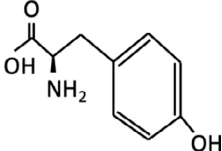
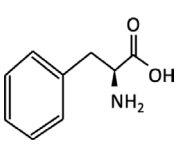
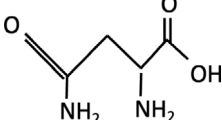
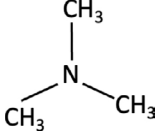
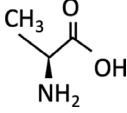
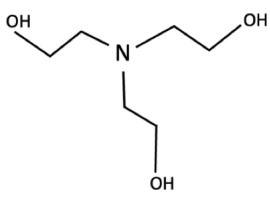
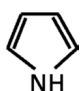
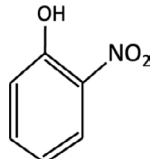
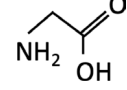
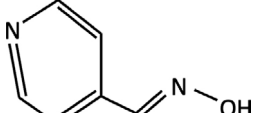
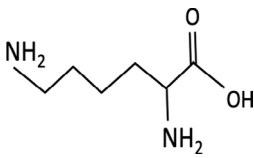
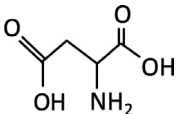
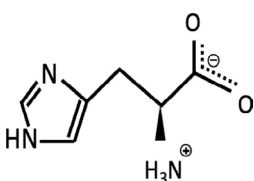
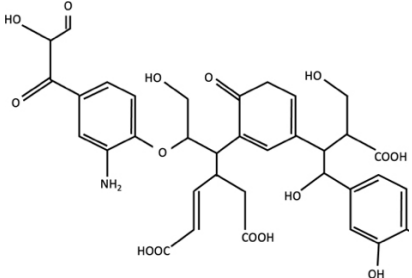
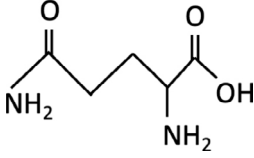
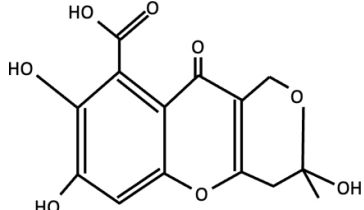
N-DBPs were identified during the chlorination of natural water, which include haloacetonitriles, halonitromethanes, haloacetamides, and NDMA [128]. If excess disinfectants are added, the amount of N-DBP species formed can be used to estimate the formation potential of N-DBPs. This method neutralizes any residual chlorine or chloramine after disinfection reactions have concluded. After that, typical N-DBP species like dichloroacetonitrile and trichloronitromethane are extracted using liquid/liquid extraction (LLE) and analyzed using gas chromatography (GC) with electron capture detection. According to Hu et al. and Plumlee et al. [29, 129], the most frequently detected N-DBP is NDMA, which is concentrated using solid phase extraction (SPE) or LLE and measured using liquid chromatography-tandem mass spectrometry (LC-MS/MS) or GC coupled to an ion trap MS/MS. NDMA accounts for greater than 90% of the total proportion and can be found in wastewater effluent at concentrations greater than 0.0001 mg/L. Najm and Trussell [130] point out that the use of recycled water raises concerns due to the high levels of NDMA present in this water source. The formation of 2,2-dichloroacetamide is primarily attributed to amino acids such as aspartic acid, histidine, tyrosine, glutamine, asparagine, and phenylalanine [131]. Similarly, chloroacetonitrile is derived from nitriles, amino acids including tryptophan, tyrosine, asparagine, and alanine, as well as pyrrole, as reported by Yang et al. [132]. Trichloronitromethane shares similar amino acid precursors with chlo-

roacetonitrile, including glycine [132]. On the other hand, NDMA is primarily formed from dimethylamine (DMA) and tertiary amines that contain DMA functional groups [133]. The formation of cyanogen chloride (CNCl), another type of N-DBP, is often attributed to the presence of glycine and fulvic/humic substances, as identified by [134]. Hydrophilic acids (HiA), hydrophilic bases (HiB), and hydrophobic acids (HoA) all have varying degrees of potential for dichloroacetamide (DCA) formation, but HiAs have the most [135]. DCA is most likely formed from protein-like substances made up of amino acids in the HiA fraction [135]. The amino acids aspartic acid, histidine, tyrosine, tryptophan, glutamine, asparagine, and phenylalanine are all candidates for DCA formation when exposed to chlorine [135]. The precursors capable of forming chloropicrin, with yield capacities ranging from 0.4% to 53%, include 2-nitrophenol, 3-nitrophenol, 4-pyridinealdoxime, trimethylamine, nitromethane, glycine, lysine, and triethanolamine [43, 136, 137]. Chlorination of certain free amino acids [138], heterocyclic nitrogen in nucleic acids [139], proteinaceous materials, and combined and bound amino acids in humic structures generates dihaloacetonitriles and other haloacetonitriles [140]. Table 1 shows the chemical structure of different precursor organic compounds. Compared to other naturally occurring organic compounds, the identified N-DBP precursors typically have a low molecular weight and electrostatic charge [53]. Because of this trait, common water treatment processes, such as coagulation, are ineffective against them. However, it is anticipated that many of these N-DBP precursors will be biodegradable, making them amenable to removal via nanofiltration [53].

IMPACTS OF DON ON DBP FORMATION

An extensive amount of literature has investigated the possible link between the transformation of DON in wastewater treatment plants and the formation of N-DBPs; this includes studies by Aitkenhead-Peterson et al. and Chang et al. [141, 142], among others. The proportion of amphiphilic bases to neutrals in DON has been found to be the most important factor in determining N-DBP formation potentials [143]. Tertiary amines with benzyl functional groups were also found to be associated with an increased likelihood of NDMA formation [144]. The majority of these analyses, however, have only looked at how DON and its N-DBP change before and after the disinfection process. According to research by Selbes et al. [145] and Ding et al. [54], N-DBPs can be roughly divided into two categories: non-halogenated N-DBPs (such as N-nitrosamines) and halogenated N-DBPs. According to previous studies, secondary amines are a major contributor to N-nitrosamine compounds formed during the chlorination process, especially NDMA, as demonstrated by [146]. Bond et al. [88] point out that the formation of halogenated N-DBPs is more complicated than that of non-halogenated ones. Another two study note that haloacetamides, halonitriles, and organic halamines have received a great deal of attention in the study of halogenated DON in wastewater [54, 147].

Table 1. Chemical structures of different DBPs precursors

Tryptophan		Dimethylamine	
Tyrosine		Phenylalanine	
Asparagine		Trimethylamine	
Alanine		Triethanolamine	
Pyrrole		2-nitrophenol	
Glycine		4-pyridinealdehyde	
Lysine		Aspartic acid	
Histidine		Humic acid	
Glutamine		Fulvic acid	

DON in Wastewater Treatment Produce DBP

The formation of N-DBPs from DOM is influenced by a number of DOM properties, including its nitrogen content, hydrophobicity, specific UV absorbance (SUVA), and molecular weight (MW) distribution. A study has shown

that a lower ratio of DOC to DON in DOM indicates higher nitrogen contents in DOM, and thus a greater likelihood of the formation of N-DBPs like HANs, halonitromethanes (HNMs), and N-nitrosamines during chloramination [148]. Same study also shows that the LMW fractions of DOM with

a size of less than 1 kDa tend to have a higher contribution to the formation of N-DBPs during chloramination compared to the high MW fractions (>3 kDa) [148]. Another study reports that hydrophilic DOM fractions have a higher propensity for the formation of HANs and N-nitrosamines than hydrophobic and transphilic DOM fractions [149]. However, they found that the hydrophobic fractions of DOM contribute more to the formation of HNMs during chloramination than the other fractions [149]. In addition to the natural organic matter in surface water, Chow et al. [150] notes that effluent organic matter from biological wastewater treatment plants can affect the formation of N-DBPs due to differences in physicochemical properties, such as molecular size distribution, and higher concentrations of DON (0.7–1.9 mg/L in effluent organic matter vs. a median value of 0.3 mg/L in NOM). Effluent organic matter contains a high concentration of microbially derived DON, which is rich in amines, peptides, and amino acids [151] and therefore has the potential to be converted into N-DBPs via chloramination [152]. It is expected that the yields of N-DBPs from reclaimed water will be greater than those from surface water in situations where wastewater is reused. This is because recycled water is chemically and physically distinct from surface water. In addition, organic matter from effluents is a major contributor to N-DBP precursors in drinking water supplies vulnerable to wastewater discharges [153].

Nitrosamines, halonitroalkanes, and nitriles are just some of the chemical compounds found in the N-DBPs [154]. The N-DBPs also have a wide range of $-NO_2$ and $-CN$ derivatives. The genotoxicity of these chemicals toward mammalian cells is much higher than that of halogen-containing DBPs [155]. An increase in N-DBPs in drinking water supplies has been linked to increased contributions from wastewater discharge. This is why DON is getting so much interest in the wastewater treatment sector. DON is a precursor for the formation of carcinogenic N-DBPs during disinfection, making its presence in wastewater effluent significant in the context of indirect or direct potable wastewater reuse. Recent studies have highlighted the importance of determining the sources of N-DBPs in wastewater effluents, and have found that DON is a major precursor [143, 156]. The formation of N-DBPs can also be aided by organic nitrogen particulate matter in effluents, such as bacterial cells. To a greater extent than dissolved nitrogenous organic matter in secondary effluent, Chuang et al. [28] discovered that Gram-negative *Escherichia coli* and Gram-positive *Enterococcus faecalis* bacterial cells were capable of forming N-DBPs like dichloroacetonitrile, dichloroacetamide, and trichloroacetamide during chlorination.

Effect of DON on DBP Formation

Significant precursors to the formation of nitrogenous N-DBPs are thought to be DON compounds. Dichloroacetonitrile is one N-DBP that can be formed from DON; it is extremely toxic and has an LC50 value that is orders of magnitude higher than carbonaceous DBPs [157]. This indicates that highly toxic by-products may be present in water due to the formation of N-DBPs from DON during

disinfection processes, highlighting the need for effective monitoring and mitigation strategies to ensure water safety. A study reports that several DBPs, including dichloroacetonitrile (DCAN), dissolved organic chlorine (AOCl), and three nitrosamines (N-nitrosodibutylamine (NDBA), N-nitrosodiethylamine, and N-nitrosodipropylamine), were formed during the chlorination of mDON that accumulated during denitrification with various carbon sources and C/N ratios [158]. Sodium acetate as a carbon source and relatively high C/N ratios generally increased the formation potentials of NDBA, DCAN, and AOCl. This indicates that the formation of particular DBPs during the chlorination of mDON can be affected by the carbon source and C/N ratio used during denitrification. Upon chloramination, THMs, dichloroacetic acids, and dihaloacetonitrile originate from similar precursors, and HANs, HAAs, and THMs originate from similar structures within DOM [28]. Also, the precursor of HANs was only about 10% (on a molar basis) of that of THMs and HAAs [28]. DON/DOC in hydrophilic and transphilic fractions correlates with the potential for NDMA formation. The HAA showed a clear trend of increasing concentration only with storage time of long-term DBP changes across storage times (up to 20 days) and temperatures (5 to 20 °C) [159]. Chen et al. [160] took into account the effect of temperature and found that as the temperature was raised (from 25 to 60 °C), there was a decrease in the formation of the four DBP categories that were being studied (THMs, HAAs, HANs, and NDMA). Hua et al. [161] developed a model for the role of lignin phenols in NOM product DBP formation based on concentrations and DBP yields. Trichloroacetic acid is the most formed DBP, followed by dichloroacetic acid and chloroform in terms of the contribution of lignin phenols to the formation of DBP during chlorination. Trichloroacetic acid > dichloroacetic acid & DCAN > chloroform is the formation order of these DBPs due to the lignin phenols in the chloramination [161]. Table 2 shows some potential DBPs formation during the disinfection process by using chlorine, chloramines, chlorine dioxide, and the combined UV and chlorine due to the different complex structured emerging organic micropollutants (EOMPs). Industrial wastewater discharge, municipal sewage discharge, and agricultural runoff are all major contributors to EOMPs in aquatic environments. Toxins from pharmaceuticals and personal care products (PPCPs), endocrine-disrupting chemicals (EDCs), and brominated flame retardants (BFRs) are just a few examples [162].

Factors Influencing the Impact of DON on DBP Formation

The impact of DON on DBP formation can be influenced by several factors.

Concentration and Composition of DON

The concentration and composition of DON in water are key factors that can influence its impact on DBP formation. DON is a complex mixture of organic nitrogen-containing compounds. The concentration of DON in water can vary widely depending on the source of water, season, and oth-

Table 2. Different EOMPs with their chemical structures and the respective DBPs formation with the disinfection process

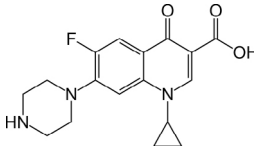
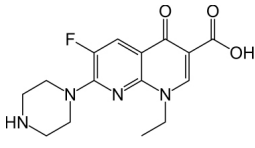
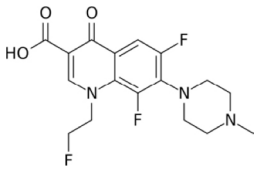
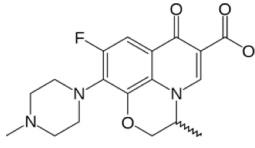
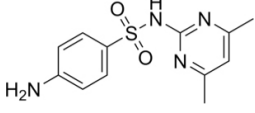
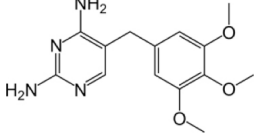
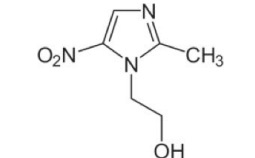
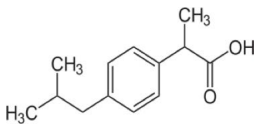
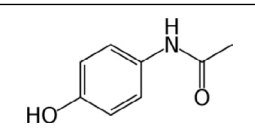
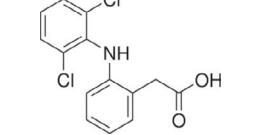
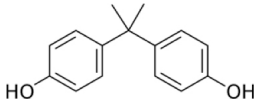
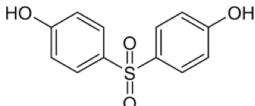
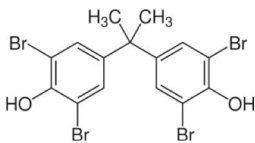
Different EOMPs (PPCPs, EDCs, BFRs)	EOMP structure	Disinfectant use	Potential DBPs formation	Ref
1. Ciprofloxacin		Chlorine	Antibiotic transformation products (TP305, TP262, TP262, TP290, TP292, TP 296, ETC.)	[163]
2. Enoxacin		Chlorine dioxide	THMs, HAAs, HANs, HKs (Haloketones), HAL (Haloacetaldehydes)	[164]
3. Fleroxacin		Chlorine or Chlorine dioxide	Haloacetonitriles, Trihalomethanes, Haloaceticacids	[165]
4. Ofloxacin		Chlorine	Antibiotic transformation products (TP305, TP262, TP262, TP290, TP292, TP 296, ETC.)	[73]
5. Sulfamethazine		Chlorine	Transformation products (TP305, TP262, TP292, TP 296, ETC.)	[166]
6. Trimethoprim		UV and Chlorine	Trichloromethane, Chloral hydrate, Dichloroacetonitrile, Trichloronitromethane	[167]
7. Metronidazole		Chloramine	Dichloroacetonitrile, Trichloroacetamide, Dichloroacetamide, Trichloromethane	[168]
8. Ibuprofen		UV and Chlorine	Trichloromethane, Chloral hydrate; 1,1-dichloro-2-propanone; 1,1,1-trichloropropanone; Dichloroacetic acid, Trichloroacetic acid	[169]
9. Acetaminophen/ Paracetamol		Chloramines	Trichloromethane, Dichloroacetonitrile, Dichloroacetamide, Trichloroacetamide	[54]
10. Diclofenac		Chlorine dioxide	Enhanced-hazardousness transformation products	[170]

Table 2 (cont). Different EOMPs with their chemical structures and the respective DBPs formation with the disinfection process

Different EOMPs (PPCPs, EDCs, BFRs)	EOMP structure	Disinfectant use	Potential DBPs formation	Ref
11. Bisphenol A		Chloramine	Halogenated bisphenol A, Trihalomethane, Haloaceticacids, Haloacetonitriles	[171]
12. Bisphenol S		Chlorine	Monochloro-, dichloro-, trichloro-, tetrachloro-bisphenol; biphenyl ether dimer and trimers	[172]
13. Tetrabromobisphenol A		Chlorine	Transformation products (TP305, TP262, TP292, TP 296, ETC.)	[173]

er environmental factors [174]. Higher concentrations of DON, as well as specific types of organic nitrogen-containing compounds, may increase the potential for DBP formation during disinfection processes. When using sludge alkaline fermentation liquid (SAFL) as the carbon source, the DON concentration in the effluent (1.52 mg/L DON) was higher when compared to when using sodium acetate (0.56 mg/L DON) [175]. However, compared to sodium acetate, SAFL resulted in effluent formation potentials that were 43% and 55% lower for dichloroacetonitrile (7.63 g/mg DON) and nitrosamines (1.57 g/mg DON), respectively. Alanine, glycine, and tyrosine were found to be important precursors to N-DBPs [175]. Protein- and lignin-like compounds made up the bulk of the DON molecules in the effluent [175].

Type and Dosage of Disinfectants

The type and dosage of disinfectants used during water treatment can significantly influence the formation of DBPs from DON. Different disinfectants, such as chlorine, chloramines, chlorine dioxide, and ozone, may react differently with DON and result in varying levels of DBP formation. For instance, chlorine is known to react with DON to form various DBPs, such as trihalomethanes and haloacetic acids, while chloramines can also react with DON to form nitrosamines, another type of DBP [37]. As an example, the amount of chlorine added to reclaimed water during the chlorination process can affect the production of chlorinated DBPs [176]. Slightly oxidized unsaturated aliphatic compounds and polycyclic aromatic compounds have been discovered to be produced during chlorination [177]. In addition, the proportion of polycyclic aromatic chlorinated DBPs with one chlorine atom and highly oxidized unsaturated aliphatic chlorinated DBPs with two chlorine atoms was found to increase with increasing chlorine dosage [177].

Co-occurring Water Constituents

Other naturally occurring water constituents, such as bromide, iodide, and NOM, are also capable of having an impact on the relationship between DON and DBP formation. For example, during the process of disinfection, bro-

midide can react with chlorine to produce brominated DBPs [178]. These brominated DBPs, which include bromoform and bromodichloromethane, are known to have a higher level of toxicity in comparison to their chlorinated counterparts [178]. Bromoform and bromodichloromethane are both classified as Group 2B, possibly carcinogenic to humans [179]. Studies have shown that long-term exposure to elevated levels of bromoform and bromodichloromethane in drinking water may be associated with an increased risk of certain adverse health effects, including bladder cancer, reproductive and developmental effects, and liver and kidney damage [180]. The toxicity of bromoform and bromodichloromethane is primarily attributed to their potential to induce genotoxicity, oxidative stress, and disruption of cellular functions. These DBPs can bind to DNA and proteins, causing DNA damage and impairing cellular processes [181]. During the disinfection process, NOM, which is a complex mixture of organic compounds derived from decaying plant and animal materials, can interact with DON, and affect the formation of DBP. NOM is a byproduct of decomposition of plant and animal matter [182].

Water Treatment Processes

The specific water treatment processes employed, such as pre-oxidation, coagulation, and filtration, can also affect the impact of DON on DBP formation [183]. These processes can modify the concentration and composition of DON, as well as other water constituents, which can subsequently influence DBP formation during disinfection. For example, pre-oxidation processes, such as ozonation or chlorination, can alter the reactivity and characteristics of DON, affecting its potential to form DBPs during subsequent disinfection processes [184].

Reaction Time and Conditions

The reaction time and conditions during disinfection, including contact time, temperature, and pH, can impact the extent of DBP formation from DON. The reaction time refers to the duration for which the disinfectant and

water are in contact during the disinfection process. Longer contact times can lead to increased DBP formation as more time allows for greater interaction between the disinfectant and organic or inorganic precursors in water [185]. For example, higher levels of THMs and HAAs have been observed with longer chlorine contact times during water treatment processes [186]. Higher temperatures can accelerate the rate of DBP formation as reactions are generally more rapid at elevated temperatures [187]. For instance, warm water used in hot tubs, spas, or showers can lead to higher levels of DBPs due to increased reaction rates. The pH of the water can also affect DBP formation, as some DBPs are more likely to form under acidic or basic conditions [187].

Water Quality Regulations

Water quality regulations play a significant role in managing DBP formation, including the impact of DON. Compliance with regulatory standards may necessitate adjustments in water treatment processes, disinfection practices, and monitoring strategies to mitigate DBP formation from DON. Regulatory guidelines, such as maximum contaminant levels (MCLs) established by regulatory agencies, dictate the permissible levels of DBPs in drinking water, and are typically based on extensive research and risk assessments to safeguard public health [188]. Ensuring compliance with these regulations may require utilities to implement additional treatment steps or optimize existing treatment processes to control DBP formation, including addressing the contribution of DON [189]. To prevent harmful effects on the environment, it is essential that industrial wastewater discharge standards do not include nitrogen species, especially when dealing with situations where DON levels are high. Strict compliance with regulations helps protect aquatic ecosystems, lessens the likelihood of eutrophication, and promotes ecological harmony in the receiving environment. Hence, understanding and adhering to water quality regulations are critical factors in effectively managing DBP formation, including the role of DON, in drinking water supplies [190].

DBP MITIGATION TECHNIQUES FOR WASTEWATER TREATMENT

DBP mitigation is important due to the potential health risks associated with DBPs, such as carcinogenicity, genotoxicity, and reproductive and developmental effects. Compliance with regulatory standards for DBP levels in drinking water is necessary to ensure the safety of the water supply and protect public health. Different countries have different regulatory standards for DBPs [191]. For example, the maximum allowable limits for THMs, HAAs, bromate, and inorganic DBPs are 0.08, 0.06, 0.01, and 1 mg/L respectively whereas there has no set limit for NDMA [27]. Therefore, effective DBP mitigation strategies are essential in wastewater treatment to reduce the formation of DBPs and ensure compliance with regulatory requirements.

Techniques for DBP Control

Physical treatment methods are employed to decrease the formation of DBPs in wastewater by physically removing or altering wastewater constituents. Sedimentation [192], filtration [193], and membrane processes [194] are some examples of physical treatment techniques. Sedimentation facilitates the settling of suspended particles in wastewater, reducing the availability of precursor materials for DBP formation [192]. Filtration, on the other hand, involves passing wastewater through filters to remove particulate matter, organic matter, and other contaminants that can contribute to DBP formation [193]. Membrane processes utilize semipermeable membranes to selectively eliminate particles, dissolved substances, and microorganisms from wastewater [194].

Chemical treatment methods involve the utilization of chemicals to modify or eliminate DBP precursors in wastewater. Coagulation [195], oxidation [196], and advanced oxidation processes [197] are examples of chemical treatment techniques. Coagulation entails the addition of chemicals that form flocs, aiding in the removal of suspended particles and dissolved organic matter from wastewater [195]. Oxidation processes employ chemicals like chlorine or ozone to oxidize DBP precursors, reducing their reactivity toward DBP formation [198]. Advanced oxidation processes, such as UV irradiation in combination with hydrogen peroxide, generate highly reactive hydroxyl radicals that can effectively degrade DBP precursors [191, 199].

Biological treatment methods, on the other hand, employ microorganisms to transform or remove DBP precursors in wastewater. Activated sludge processes [200], biofiltration [201], and biological nutrient removal [202], are examples of biological treatment techniques. Activated sludge processes utilize microorganisms in the presence of oxygen to biodegrade organic matter and remove it from wastewater. Biofiltration involves the use of microorganisms attached to a solid support medium to biologically degrade organic matter [201]. Biological nutrient removal processes use microorganisms to remove nutrients, such as nitrogen and phosphorus, from wastewater, which can also indirectly reduce DBP formation by limiting the availability of DBP precursors [203].

Effectiveness of Physical, Chemical, and Biological Treatments in Reducing the Impact of DON on DBP Formation

The effectiveness of these treatments in mitigating the impact of DON on DBP formation is contingent upon several factors, including the specific treatment technique employed, the characteristics of the wastewater being treated, and the concentration and reactivity of DON. Physical treatment methods, such as sedimentation and filtration, can be successful in removing particulate and organic matter, including DON, from wastewater, thereby reducing the availability of DON for DBP formation [192, 201]. Chemical treatment methods, such as coagulation and oxidation, can also be effective in modifying or eliminating

DON from wastewater, thus mitigating its contribution to DBP formation [195, 198]. Biological treatment methods, such as activated sludge processes and biological nutrient removal, employ microbial processes to transform or remove DON, which can also diminish its impact on DBP formation [200, 202].

Potential Benefits and Drawbacks of Using These Treatments

The utilization of physical, chemical, and biological treatment methods in wastewater treatment for controlling DBP formation has both advantages and disadvantages. These treatments have the potential to reduce DBP formation, improve water quality, and comply with regulatory standards. Physical methods, chemical methods, and biological methods can selectively modify or remove DBP precursors through transformation via chemical reaction and microbials, all of which can lead to improved water quality and reduced health risks associated with DBPs [23].

However, there are also drawbacks to consider. Physical and chemical methods may require additional equipment, chemicals, and operational costs, which can increase the overall cost of wastewater treatment [204]. Chemical methods may also generate residuals or by-products that need proper handling and disposal [205]. Moreover, some physical and chemical methods may not effectively remove all types of DBP precursors, and additional treatment steps may be needed. Biological methods may require careful control of environmental conditions, such as temperature, pH, and nutrient levels, to optimize microbial activity and DBP precursor removal [206]. Additionally, biological methods may have longer treatment times and may not be suitable for all types of wastewater or treatment plant configurations [207]. While physical, chemical, and biological treatment methods offer potential benefits in mitigating DBP formation in wastewater treatment, it is important to also consider their drawbacks.

CHALLENGES AND FUTURE DIRECTIONS

The field of DBPs control in wastewater treatment has several knowledge gaps and research requirements. Further investigation is needed in key areas such as identifying and characterizing DBP precursors, understanding the mechanisms of DBP formation, optimizing treatment efficacy, and assessing the toxicity and health risks of DBPs. Comprehensive research is necessary to identify and characterize different types of DBP precursors in wastewater, including their sources, reactivity, and fate during treatment processes.

The complex mechanisms of DBP formation, including pathways and reaction kinetics, require further understanding. While various treatment methods have been proposed for DBP control, their efficacy and optimization in different wastewater treatment scenarios need more investigation. Limited information is available on the toxicity and health risks associated with different types of DBPs, including genotoxicity, carcinogenicity, and potential adverse

effects on human health and the environment. Further research is necessary to better understand the toxicological properties of DBPs and their impacts on public health and the environment. Long-term monitoring and assessment of DBP precursors, formation, and treatment efficacy in full-scale wastewater treatment plants are needed to understand the effectiveness of different treatment methods under real-world conditions, aiding in the identification of suitable treatment strategies for different wastewater treatment scenarios.

CONCLUSION

In conclusion, the formation of DBPs in wastewater treatment is a complex issue that requires careful consideration of the impacts of DON, health effects of DBPs, and mitigation strategies. DON has been found to influence DBP formation in wastewater treatment, which has potential implications for water quality and public health. The health effects of DBPs, including genotoxicity and carcinogenicity, underscore the need for further research and understanding of their toxicological properties. Various mitigation strategies, such as physical, chemical, and biological treatment methods, offer potential benefits in reducing DBP formation, improving water quality, and complying with regulatory standards. However, it's important to note that these methods also have drawbacks, including additional costs and the potential generation of chemical residuals or by-products.

To address the knowledge gaps and research requirements in this field, future investigations should prioritize identifying and characterizing DBP precursors, understanding mechanisms of DBP formation, optimizing treatment efficacy, and assessing toxicity and health risks of DBPs. Long-term monitoring and assessment of DBP precursors, formation, and treatment efficacy in real-world wastewater treatment plants would provide valuable insights for effective mitigation strategies. Regulatory and policy measures should also be considered to ensure appropriate guidelines and standards are in place to mitigate DBP formation and protect public health.

In summary, it is crucial to carefully balance the benefits and drawbacks of DBP control methods and continue research efforts to advance our understanding of DBP formation, health effects, and mitigation strategies in wastewater treatment. This will enable the development of sustainable and effective approaches to minimize DBP formation, ensure safe water quality, and protect public health and the environment. By addressing the challenges and knowledge gaps in this field, we can work towards achieving efficient wastewater treatment practices that prioritize human health, environmental sustainability, and regulatory compliance.

DATA AVAILABILITY STATEMENT

The author confirm that the data that supports the findings of this study are available within the article. Raw data that support the finding of this study are available from the corresponding author, upon reasonable request.

CONFLICT OF INTEREST

The author declared no potential conflicts of interest with respect to the research, authorship, and/or publication of this article.

USE OF AI FOR WRITING ASSISTANCE

Not declared.

ETHICS

There are no ethical issues with the publication of this manuscript.

REFERENCES

- [1] D.Niat [1] A. Voulgaropoulos, “Mitigation of PFAS in U.S. public water systems future steps for ensuring safer drinking water,” *Environmental Progress & Sustainable Energy*, Vol. 41(2), Article e13800, 2022. [\[CrossRef\]](#)
- [2] S. Albolafio, A. Marín, A. Allende, F. H. García, P. J. Simón-Andreu, M. A. Soler, and M. I. Gil, “Strategies for mitigating chlorinated disinfection byproducts in wastewater treatment plants,” *Chemosphere*, Vol. 288(2), Article 132583, 2021. [\[CrossRef\]](#)
- [3] C. Casado, J. Moreno-SanSegundo, I. D. la Odra, B. E. García, J. A. S. Pérez, and J. Marugán, “Mechanistic modelling of wastewater disinfection by the photo-Fenton process at circumneutral pH,” *Chemical Engineering Journal*, Vol. 403(1), Article 126335, 2021. [\[CrossRef\]](#)
- [4] J. Wang and H. Chen, “Catalytic ozonation for water and wastewater treatment: Recent advances and perspective,” *Science of The Total Environment*, Vol. 704, Article 135249, 2020. [\[CrossRef\]](#)
- [5] S.-S. Liu, H. Qu, D. Yang, H. Hu, W. Liu, Z. Qiu, A. Hou, J. Guo, J.-W. Li, Z. Shen, and M. Jin, “Chlorine disinfection increases both intracellular and extracellular antibiotic resistance genes in a full-scale wastewater treatment plant,” *Water Research*, Vol. 136, pp. 131–136, 2018. [\[CrossRef\]](#)
- [6] A. C. Mecha, M. S. Onyango, A. Ochieng, C. J. S. Fourie, and M. N. B. Momba, “Synergistic effect of UV-vis and solar photocatalytic ozonation on the degradation of phenol in municipal wastewater: A comparative study,” *Journal of Catalysis*, Vol. 341, pp. 116–125, 2016. [\[CrossRef\]](#)
- [7] F. J. Beltrán, J. Encinar, and J. F. G. González, “Industrial wastewater advanced oxidation. Part 2. Ozone combined with hydrogen peroxide or UV radiation,” *Water Research*, Vol. 31(10), pp. 2415–2428, 1997. [\[CrossRef\]](#)
- [8] T. Bond, M. R. Templeton, and N. Graham, “Precursors of nitrogenous disinfection by-products in drinking water—A critical review and analysis,” *Journal of Hazardous Materials*, Vol. 235–236, pp. 1–16, 2012. [\[CrossRef\]](#)
- [9] Y. Huang, Y. Zhang, Q. Zhou, A. Li, P. Shi, J. Qiu, and Y. Pan, “Detection, identification and control of polar iodinated disinfection byproducts in chlor(am)inated secondary wastewater effluents,” *Environmental Science*, Vol. 5, 397–405, 2019. [\[CrossRef\]](#)
- [10] T. Manasfi, B. Coulomb, and J.-L. Boudenne, “Occurrence, origin, and toxicity of disinfection byproducts in chlorinated swimming pools: An overview,” *International Journal of Hygiene and Environmental Health*, Vol. 220(3), pp. 591–603, 2017. [\[CrossRef\]](#)
- [11] S. D. Richardson, M. J. Plewa, E. D. Wagner, R. Schoeny, and D. M. DeMarini, “Occurrence, genotoxicity, and carcinogenicity of regulated and emerging disinfection by-products in drinking water: a review and roadmap for research,” *Mutation Research-Reviews in Mutation Research*, Vol. 636(1–3), pp. 178–242, 2007. [\[CrossRef\]](#)
- [12] W. H. Glaze and J. E. Henderson IV, “Formation of organochlorine compounds from the chlorination of a municipal secondary effluent,” *Water Pollution Control Federation*, pp. 2511–2515, 1975.
- [13] S. Krasner, P. Westerhoff, B. Chen, G. L. Amy, S. Nam, S. R. Chowdhury, S. Sinha, and B. E. Rittmann, “Contribution of wastewater to DBP formation,” *International Water Association (IWA)*, 2008.
- [14] M. R. Jekel, and P. V. Roberts, “Total organic halogen as a parameter for the characterization of reclaimed waters: measurement, occurrence, formation, and removal,” *Environmental Science & Technology*, Vol. 14, pp. 970–975, 1980. [\[CrossRef\]](#)
- [15] S. W. Krasner, P. Westerhoff, B. Chen, B. E. Rittmann, S.-N. Nam, and G. Amy, “Impact of wastewater treatment processes on organic carbon, organic nitrogen, and DBP precursors in effluent organic matter,” *Environmental Science & Technology*, Vol. 43, pp. 2911–2918, 2009. [\[CrossRef\]](#)
- [16] R. L. Jolley, *Water chlorination: chemistry, environmental impact and health effects*, Lewis Publishers, 1990.
- [17] M. L. Trehy, R. A. Yost, and C. J. Miles, “Chlorination byproducts of amino acids in natural waters,” *Environmental Science & Technology*, Vol. 20, pp. 1117–1122, 1986. [\[CrossRef\]](#)
- [18] P. Bose, “Selected physico-chemical properties of natural organic matter and their changes due to ozone treatment: Implications for coagulation using alum,” [Master Thesis]. University of Massachusetts Amherst, 1995.
- [19] T. Carroll, S. King, S. R. Gray, B. A. Bolto, and N. A. Booker, “The fouling of microfiltration membranes by NOM after coagulation treatment,” *Water Research*, Vol. 34, pp. 2861–2868, 2000. [\[CrossRef\]](#)
- [20] P. Westerhoff and H. Mash, “Dissolved organic nitrogen in drinking water supplies: a review,” *Journal of Water Supply: Research and Technology-Aqua*, Vol. 51, pp. 415–448, 2002. [\[CrossRef\]](#)
- [21] M. Pishnamazi, S. Koushkbaghi, S. S. Hosseini, M. Darabi, A. Yousefi, and M. Irani, “Metal organic framework nanoparticles loaded-PVDF/chitosan nanofibrous ultrafiltration membranes for the removal of BSA protein and Cr(VI) ions,” *Journal of Molecular Liquids*, Vol. 317, Article 113934, 2020. [\[CrossRef\]](#)

- [22] G. F. Parkin, and P. L. McCarty, “A comparison of the characteristics of soluble organic nitrogen in untreated and activated sludge treated wastewaters,” *Water Research*, Vol. 15, pp. 139–149, 1981. [\[CrossRef\]](#)
- [23] F. Zheng, J. Wang, R. Xiao, W. Chai, D. Xing, and H. Lu, “Dissolved organic nitrogen in wastewater treatment processes: Transformation, biosynthesis and ecological impacts,” *Environmental Pollution*, Vol. 273, Article 116436, 2021. [\[CrossRef\]](#)
- [24] J. D. Rouse, C. A. Bishop, and J. Struger, “Nitrogen pollution: an assessment of its threat to amphibian survival,” *Environmental Health Perspectives*, Vol. 107(10), pp. 799–803, 1999. [\[CrossRef\]](#)
- [25] N.-B. Chang, D. Wen, A. M. McKenna, and M. P. Wanielista, “The Impact of Carbon Source as Electron Donor on Composition and Concentration of Dissolved Organic Nitrogen in Biosorption-Activated Media for Stormwater and Groundwater Co-Treatment,” *Environmental Science & Technology*, Vol. 52(16), pp. 9380–9390, 2018. [\[CrossRef\]](#)
- [26] S. M. Iskander, T. Zeng, E. Smiley, S. C. Bolyard, J. T. Novak, and Z. He, “Formation of disinfection by-products during Fenton’s oxidation of chloride-rich landfill leachate,” *Journal of Hazardous Materials*, Vol. 382(15), 2020, Article 121213, 2020. [\[CrossRef\]](#)
- [27] X.-X. Wang, L. Baoming, M.-F. Lu, L. Yuping, Y.-Y. Jiang, M. Zhao, Z.-X. Huang, Y. Pan, M. Hengfeng, and W.-Q. Ruan, “Characterization of algal organic matter as precursors for carbonaceous and nitrogenous disinfection byproducts formation: Comparison with natural organic matter,” *Journal of Environmental Management*, Vol. 282, Article 111951, 2021. [\[CrossRef\]](#)
- [28] Y.-H. Chuang, A. Y.-C. Lin, X. H. Wang, and H. H. Tung, “The contribution of dissolved organic nitrogen and chloramines to nitrogenous disinfection byproduct formation from natural organic matter,” *Water Research*, Vol. 47(3), pp. 1308–1316, 2013. [\[CrossRef\]](#)
- [29] H. Hu, C. Jiang, H. Ma, L. Ding, J. Geng, K. Xu, H. Huang, and H. Ren, “Removal characteristics of DON in pharmaceutical wastewater and its influence on the N-nitrosodimethylamine formation potential and acute toxicity of DOM,” *Water Research*, Vol. 109, pp. 114–121, 2017. [\[CrossRef\]](#)
- [30] L.-S. Wang, D. Wei, J. Wei, and H.-Y. Hu, “Screening and estimating of toxicity formation with photobacterium bioassay during chlorine disinfection of wastewater,” *Journal of Hazardous Materials*, Vol. 141(1), pp. 289–294, 2007. [\[CrossRef\]](#)
- [31] H. Zhang, J. Qu, H. Liu, and X. Zhao, “Isolation of dissolved organic matter in effluents from sewage treatment plant and evaluation of the influences on its DBPs formation,” *Separation and Purification Technology*, Vol. 64(1), pp. 31–37, 2008. [\[CrossRef\]](#)
- [32] J. L. Roux, H. Gallard, and J.-P. Croué, “Chloramination of nitrogenous contaminants (pharmaceuticals and pesticides): NDMA and halogenated DBPs formation,” *Water Research*, Vol. 45, pp. 3164–3174, 2011. [\[CrossRef\]](#)
- [33] P. Roy, M. A. Ahmed, S. Islam, A. K. Azad, S. Islam, and R. Islam, “Water Supply, Sanitation System and Water-borne Diseases of Slum Dwellers of Bastuhara Colony,” Khulna, Department of Civil Engineering, KUET, Khulna, Bangladesh, 2020. [\[CrossRef\]](#)
- [34] J. L. Roux, M. J. Plewa, E. D. Wagner, M. Nihemaiti, A. Dad, and J.-P. Croué, “Chloramination of wastewater effluent: Toxicity and formation of disinfection byproducts,” *Journal of Environmental Sciences*, Vol. 58, pp. 135–145, 2017. [\[CrossRef\]](#)
- [35] G. Ding, X. Zhang, M. Yang, and Y. Pan, “Formation of new brominated disinfection byproducts during chlorination of saline sewage effluents,” *Water Research*, Vol. 47, pp. 2710–2718, 2013. [\[CrossRef\]](#)
- [36] Y. Zhong, W. Gan, Y. Du, H. Huang, Q. Wu, Y. Xiang, C. Shang, and X. Yang, “Disinfection by-products and their toxicity in wastewater effluents treated by the mixing oxidant of ClO_2/Cl_2 ,” *Water Research*, Vol. 162, pp. 471–481, 2019. [\[CrossRef\]](#)
- [37] G. Hua, and D. A. Reckhow, “Comparison of disinfection byproduct formation from chlorine and alternative disinfectants,” *Water Research*, Vol. 41, pp. 1667–1678, 2007. [\[CrossRef\]](#)
- [38] W. A. Mitch, and D. L. Sedlak, “Formation of N-nitrosodimethylamine (NDMA) from dimethylamine during chlorination,” *Environmental Science & Technology*, Vol. 36, pp. 588–595, 2002. [\[CrossRef\]](#)
- [39] W.-H. Chen, and T. M. Young, “Influence of nitrogen source on NDMA formation during chlorination of diuron,” *Water Research*, Vol. 43, pp. 3047–3056, 2009. [\[CrossRef\]](#)
- [40] B. Ye, Y. Cang, J. Li, and X. Zhang, “Advantages of a $\text{ClO}_2/\text{NaClO}$ combination process for controlling the disinfection by-products (DBPs) for high algae-laden water,” *Environmental Geochemistry and Health*, Vol. 41, pp. 1545–1557, 2019. [\[CrossRef\]](#)
- [41] S. Sorlini, F. Gialdini, M. Biasibetti, and C. Colli-vignarelli, “Influence of drinking water treatments on chlorine dioxide consumption and chlorite/chlorate formation,” *Water Research*, Vol. 54, pp. 44–52, 2014. [\[CrossRef\]](#)
- [42] J.-Y. Fang and C. Shang, “Bromate Formation from Bromide Oxidation by the UV/Persulfate Process,” *Environmental Science & Technology*, Vol. 46, pp. 8976–8983, 2012. [\[CrossRef\]](#)
- [43] T. Lin, S. Wu, and W. Chen, “Formation potentials of bromate and brominated disinfection by-products in bromide-containing water by ozonation,” *Environmental Science and Pollution Research International*, Vol. 21, pp. 13987–14003, 2014. [\[CrossRef\]](#)
- [44] L. Li, Y. Jeon, H. Ryu, J. W. Santo Domingo, and Y. Seo, “Assessing the chemical compositions and disinfection byproduct formation of biofilms: Application of fluorescence excitation-emission

- spectroscopy coupled with parallel factor analysis,” *Chemosphere*, Vol. 246, Article 125745, 2020. [CrossRef]
- [45] P. Roy, M. A. Ahmed, and A. Kumer, “An overview of hygiene practices and health risks related to street foods and drinking water from roadside restaurants of Khulna city of Bangladesh,” *Eurasian Journal of Environmental Research*, Vol. 3, pp. 47–55, 2019.
- [46] B. Li, X. Ma, Q. Li, W. Chen, J. Deng, G. Li, G. Chen, and W. Liao, “Factor affecting the role of radicals contribution at different wavelengths, degradation pathways and toxicity during UV-LED/chlorine process,” *Chemical Engineering Journal*, vol. 392, Article 124552, 2020. [CrossRef]
- [47] S. Onodera, “Formation mechanism and chemical safety of nonintentional chemical substances present in chlorinated drinking water and wastewater,” *Yakugaku Zasshi*, Vol. 130, pp. 1157–1174, 2010. [CrossRef]
- [48] N. Clarke, K. Fuksová, M. Gryndler, Z. Lachmanová, H.-H. Liste, J. Rohlenová, R. Schroll, P. Schröder, and M. Matucha, “The formation and fate of chlorinated organic substances in temperate and boreal forest soils,” *Environmental Science and Pollution Research*, Vol. 16, pp. 127–143, 2009. [CrossRef]
- [49] T. Li, Y. Jiang, X. An, H. Liu, C. Hu, and J. Qu, “Transformation of humic acid and halogenated by-product formation in UV-chlorine processes,” *Water Research*, Vol. 102, pp. 421–427, 2016. [CrossRef]
- [50] R. Loyola-Sepulveda, G. Lopez-Leal, J. Munoz, C. Bravo-Linares, and S. M. Mudge, “Trihalomethanes in the drinking water of Concepción and Talcahuano, Chile,” *Water and Environment Journal*, Vol. 23, pp. 286–292, 2009. [CrossRef]
- [51] M. Panyakapo, S. Soontornchai, and P. Paopuree, “Cancer risk assessment from exposure to trihalomethanes in tap water and swimming pool water,” *Journal of Environmental Sciences*, Vol. 20, pp. 372–378, 2008. [CrossRef]
- [52] A. M. Abdullah, “Assessment of potential risks from trihalomethanes in water supply at Alexandria Governorate,” *Journal of Pollution Effects & Control*, Vol. 2, pp. 1–4, 2014.
- [53] T. Bond, E. H. Goslan, S. A. Parsons, and B. Jefferson, “A critical review of trihalomethane and haloacetic acid formation from natural organic matter surrogates,” *Environmental Technology Reviews*, Vol. 1, pp. 93–113, 2012. [CrossRef]
- [54] S. Ding, W. Chu, T. Bond, Q. Wang, N. Gao, B. Xu, and E. Du, “Formation and estimated toxicity of trihalomethanes, haloacetoneitriles, and haloacetamides from the chlor(am)ination of acetaminophen,” *Journal of Hazardous Materials*, Vol. 341, pp. 112–119, 2018. [CrossRef]
- [55] J. C. Beard, and T. M. Swager, “An organic chemist’s guide to n-nitrosamines: their structure, reactivity, and role as contaminants,” *The Journal of Organic Chemistry*, Vol. 86, pp. 2037–2057, 2021. [CrossRef]
- [56] M. S. Abdel-Rahman, D. Couri, and R. J. Bull, “Metabolism and pharmacokinetics of alternate drinking water disinfectants,” *Environmental Health Perspectives*, Vol. 46, pp. 19–23, 1982. [CrossRef]
- [57] V. Uyak, and I. Toroz, “Enhanced coagulation of disinfection by-products precursors in Istanbul water supply,” *Environmental Technology*, Vol. 26, pp. 261–266, 2005. [CrossRef]
- [58] I. H. Aljundi, “Bromate formation during ozonation of drinking water: A response surface methodology study,” *Desalination*, Vol. 277, pp. 24–28, 2011. [CrossRef]
- [59] A. N. Gounden, and S. B. Jonnalagadda, “Advances in treatment of brominated hydrocarbons by heterogeneous catalytic ozonation and bromate minimization,” *Molecules*, Vol. 24, Article 3450, 2019. [CrossRef]
- [60] R. A. Li, J. A. McDonald, A. Sathasivan, and S. J. Khan, “A multivariate Bayesian network analysis of water quality factors influencing trihalomethanes formation in drinking water distribution systems,” *Water Research*, Vol. 190, Article 116712, 2021. [CrossRef]
- [61] B. Liu, and D. A. Reckhow, “Disparity in disinfection byproducts concentration between hot and cold tap water,” *Water Research*, Vol. 70, pp. 196–204, 2015. [CrossRef]
- [62] P. Roccaro, H.-S. Chang, F. G. Vagliasindi, and G. V. Korshin, “Differential absorbance study of effects of temperature on chlorine consumption and formation of disinfection by-products in chlorinated water,” *Water Research*, Vol. 42, pp. 1879–1888, 2008. [CrossRef]
- [63] J. Fang, J. Ma, X. Yang, and C. Shang, “Formation of carbonaceous and nitrogenous disinfection by-products from the chlorination of *Microcystis aeruginosa*,” *Water Research*, Vol. 44, pp. 1934–1940, 2010. [CrossRef]
- [64] Y.-C. Hung, B. W. Waters, V. K. Yemmireddy, and C.-H. Huang, “pH effect on the formation of THM and HAA disinfection byproducts and potential control strategies for food processing,” *Journal of Integrative Agriculture*, Vol. 16, pp. 2914–2923, 2017. [CrossRef]
- [65] T. Özbelge, “A study for chloroform formation in chlorination of resorcinol,” *Turkish Journal of Engineering and Environmental Sciences*, Vol. 25, pp. 289–298, 2001.
- [66] S. Chowdhury, M. J. Rodriguez, and R. Sadiq, “Disinfection byproducts in Canadian provinces: associated cancer risks and medical expenses,” *Journal of Hazardous Materials*, Vol. 187, pp. 574–584, 2011. [CrossRef]
- [67] A. Gonsioroski, V. E. Mourikes, and J. A. Flaws, “Endocrine disruptors in water and their effects on the reproductive system,” *International Journal of Molecular Sciences*, Vol. 21, Article 1929, 2020. [CrossRef]
- [68] Y. Chen, T. Xu, X. Yang, W. Chu, S. Hu, and D. Yin, “The toxic potentials and focus of disinfection by-products based on the human embryonic kidney (HEK293) cell model,” *Science of the Total Environment*, Vol. 664, pp. 948–957, 2019. [CrossRef]

- [69] C. Legay, M. J. Rodriguez, J. B. Sérodes, and P. Levallois, "Estimation of chlorination by-products presence in drinking water in epidemiological studies on adverse reproductive outcomes: a review," *Science of the Total Environment*, Vol. 408, pp. 456–472, 2010. [CrossRef]
- [70] R. S. Chaves, C. S. Guerreiro, V. V. Cardoso, M. J. Benoliel, and M. M. Santos, "Hazard and mode of action of disinfection by-products (DBPs) in water for human consumption: Evidences and research priorities," *Comparative Biochemistry and Physiology Part C: Toxicology & Pharmacology*, Vol. 223, pp. 53–61, 2019. [CrossRef]
- [71] M. Diana, M. Felipe-Sotelo, and T. Bond, "Disinfection byproducts potentially responsible for the association between chlorinated drinking water and bladder cancer: a review," *Water Research*, Vol. 162, pp. 492–504, 2019. [CrossRef]
- [72] S. Regli, J. Chen, M. Messner, M. S. Elovitz, F. J. Letkiewicz, R. A. Pegram, T. J. Pepping, S. D. Richardson, and J. M. Wright, "Estimating potential increased bladder cancer risk due to increased bromide concentrations in sources of disinfected drinking waters," *Environmental Science & Technology*, Vol. 49, pp. 13094–13102, 2015. [CrossRef]
- [73] R. R. Jones, C. T. DellaValle, P. J. Weyer, K. Robien, K. P. Cantor, S. Krasner, L. E. B. Freeman, and M. H. Ward, "Ingested nitrate, disinfection by-products, and risk of colon and rectal cancers in the Iowa Women's Health Study cohort," *Environment International*, Vol. 126, pp. 242–251, 2019. [CrossRef]
- [74] C. Quintiliani, C. Di Cristo, and A. Leopardi, "Vulnerability assessment to trihalomethane exposure in water distribution systems," *Water*, Vol. 10, Article 912, 2018. [CrossRef]
- [75] L. A. Salas, M. Bustamante, J. R. Gonzalez, E. Garcia-Lavedan, V. Moreno, M. Kogevinas, and C. M. Villanueva, "DNA methylation levels and long-term trihalomethane exposure in drinking water: an epigenome-wide association study," *Epigenetics*, Vol(7), pp. 650–661, 2015. [CrossRef]
- [76] P. Yang, B. Zhou, W.-C. Cao, Y.-X. Wang, Z. Huang, J. Li, W.-Q. Lu, and Q. Zeng, "Prenatal exposure to drinking water disinfection by-products and DNA methylation in cord blood," *Science of the Total Environment*, Vol. 586, pp. 313–318, 2017. [CrossRef]
- [77] W.-C. Cao, Q. Zeng, Y. Luo, H.-X. Chen, D.-Y. Miao, L. Li, Y.-H. Cheng, M. Li, F. Wang, and L. You, "Blood biomarkers of late pregnancy exposure to trihalomethanes in drinking water and fetal growth measures and gestational age in a Chinese cohort," *Environmental Health Perspectives*, Vol. 124(4), pp. 536–541, 2016. [CrossRef]
- [78] B. E. Holmes, L. Smeester, R. C. Fry, and H. S. Weinberg, "Identification of endocrine active disinfection by-products (DBPs) that bind to the androgen receptor," *Chemosphere*, Vol. 187, pp. 114–122, 2017. [CrossRef]
- [79] C. Di Cristo, A. Leopardi, C. Quintiliani, and G. de Marinis, "Drinking water vulnerability assessment after disinfection through chlorine," *Procedia Engineering*, Vol. 119, pp. 389–397, 2015. [CrossRef]
- [80] T. W. Ng, B. Li, A. Chow, and P. K. Wong, "Effects of bromide on inactivation efficacy and disinfection byproduct formation in photocatalytic inactivation," *Journal of Photochemistry and Photobiology A: Chemistry*, Vol. 324, pp. 145–151, 2016. [CrossRef]
- [81] C. M. Villanueva, S. Cordier, L. Font-Ribera, L. A. Salas, and P. Levallois, "Overview of Disinfection By-products and Associated Health Effects," *Current Environmental Health Reports*, Vol. 2(1), pp. 107–115, 2015. [CrossRef]
- [82] R. López-Roldán, A. Rubalcaba, J. Martin-Alonso, S. González, V. Martí, and J. L. Cortina, "Assessment of the water chemical quality improvement based on human health risk indexes: Application to a drinking water treatment plant incorporating membrane technologies," *Science of the Total Environment*, Vol. 540, pp. 334–343, 2016. [CrossRef]
- [83] R. Dyck, G. Cool, M. Rodriguez, and R. Sadiq, "Treatment, residual chlorine and season as factors affecting variability of trihalomethanes in small drinking water systems," *Frontiers of Environmental Science & Engineering*, Vol. 9(1), pp. 171–179, 2015. [CrossRef]
- [84] A. Andersson, M. J. Ashiq, M. Shoeb, S. Karlsson, D. Bastviken, and H. Kylin, "Evaluating gas chromatography with a halogen-specific detector for the determination of disinfection by-products in drinking water," *Environmental Science and Pollution Research*, Vol. 26(8), pp. 7305–7314, 2019. [CrossRef]
- [85] N. Chaukura, S. S. Marais, W. Moyo, N. Mbali, L. C. Thakalekoala, T. Ingwani, B. B. Mamba, P. Jarvis, and T. T. I. Nkambule, "Contemporary issues on the occurrence and removal of disinfection byproducts in drinking water - A review," *Journal of Environmental Chemical Engineering*, Vol. 8(4), Article 103659, 2020. [CrossRef]
- [86] S. Chen, J. Deng, L. Li, and N. Gao, "Evaluation of disinfection by-product formation during chlor(am)ination from algal organic matter after UV irradiation," *Environmental Science and Pollution Research*, Vol. 25(6), pp. 5994–6002, 2018. [CrossRef]
- [87] W. Lee, P. Westerhoff, and J.-P. Croué, "Dissolved organic nitrogen as a precursor for chloroform, dichloroacetonitrile, N-nitrosodimethylamine, and trichloronitromethane," *Environmental Science & Technology*, Vol. 41(15), pp. 5485–5490, 2007. [CrossRef]
- [88] T. Bond, O. Henriët, E. H. Goslan, S. A. Parsons, and B. Jefferson, "Disinfection byproduct formation and fractionation behavior of natural organic matter surrogates," *Environmental Science & Technology*, Vol. 43(15), pp. 5982–5989, 2009. [CrossRef]
- [89] X. Yang, W. Guo, and Q. Shen, "Formation of disinfection byproducts from chlor(am)ination of algal

- organic matter," *Journal of Hazardous Materials*, Vol. 197, pp. 378–388, 2011. [CrossRef]
- [90] A. Dotson, P. Westerhoff, and S. W. Krasner, "Nitrogen enriched dissolved organic matter (DOM) isolates and their affinity to form emerging disinfection by-products," *Water Science and Technology*, Vol. 60(5), pp. 135–143, 2009. [CrossRef]
- [91] X. Yang, C. Shang, W. Lee, P. Westerhoff, and C. Fan, "Correlations between organic matter properties and DBP formation during chloramination," *Water Research*, Vol. 42(8-9), pp. 2329–2339, 2008. [CrossRef]
- [92] K. E. Furst, B. M. Pecson, B. D. Webber, and W. A. Mitch, "Tradeoffs between pathogen inactivation and disinfection byproduct formation during sequential chlorine and chloramine disinfection for wastewater reuse," *Water Research*, Vol. 143, pp. 579–588, 2018. [CrossRef]
- [93] Z. Li, X. Liu, Z. Huang, S. Hu, J. Wang, Z. Qian, J. Feng, Q. Xian, and T. Gong, "Occurrence and ecological risk assessment of disinfection byproducts from chlorination of wastewater effluents in East China," *Water Research*, Vol. 157, pp. 247–257, 2019. [CrossRef]
- [94] M. J. Plewa, Y. Kargalioglu, D. Vankerk, R. A. Minear, and E. D. Wagner, "Mammalian cell cytotoxicity and genotoxicity analysis of drinking water disinfection by-products," *Environmental and Molecular Mutagenesis*, Vol. 40(2), pp. 134–142, 2002. [CrossRef]
- [95] E. D. Wagner, and M. J. Plewa, "CHO cell cytotoxicity and genotoxicity analyses of disinfection by-products: an updated review," *Journal of Environmental Sciences*, Vol. 58, pp. 64–76, 2017.
- [96] C. Sattayatewa, K. Pagilla, R. Sharp, and P. Pitt, "Fate of organic nitrogen in four biological nutrient removal wastewater treatment plants," *Water Environment Research*, Vol. 82(11), pp. 2306–2315, 2010. [CrossRef]
- [97] S. Huo, B. Xi, H. Yu, Y. Qin, F. Zan, and J. Zhang, "Characteristics and transformations of dissolved organic nitrogen in municipal biological nitrogen removal wastewater treatment plants," *Environmental Research Letters*, Vol. 8(4), Article 044005, 2013. [CrossRef]
- [98] Y. Lester, H. Mamane, I. Zucker, and D. Avisar, "Treating wastewater from a pharmaceutical formulation facility by biological process and ozone," *Water Research*, Vol. 47(13), pp. 4349–4356, 2013. [CrossRef]
- [99] S. Kucukcongar, Z. Gok, M. K. Oden, and S. Dursun, "Biodegradability of dissolved organic nitrogen in yoghurt and cheese production wastewaters," *International Journal of Environmental Science and Technology*, Vol. 20, pp. 4031–4040, 2023. [CrossRef]
- [100] X. X. Gao, Y. W. Wang, Y. C. An, R. Y. Ren, Y. H. Lin, N. Wang..., and N. Q. Ren, "Molecular insights into the dissolved organic matter of leather wastewater in leather industrial park wastewater treatment plant," *Science of the Total Environment*, Vol. 882, Article 163174, 2023. [CrossRef]
- [101] T. Khan, D. B. P. Argha, and M. S. Anita, "An analysis of existing medical waste management and possible health hazards in Jhenaidah municipality. Proceedings of International Conference on Engineering Research, Innovation and Education. Bandung, Indonesia: University of Pendidikan Indonesia," 2021.
- [102] M. A. Ahmed, and M. Redowan, "Fate and transport of the biologically treated landfill leachate induced Dissolved Organic Nitrogen (DON)," 2023. <https://par.nsf.gov/biblio/10431230-fate-transport-biologically-treated-landfill-leachate-induced-dissolved-organic-nitrogen-don>. Accessed on May 2, 2024.
- [103] M. R. Rashid, and M. Ashik, "Evaluation of physico-chemical treatment technologies for landfill leachate induced Dissolved Organic Nitrogen (DON)," 2023. <https://par.nsf.gov/biblio/10431232-evaluation-physicochemical-treatment-technologies-landfill-leachate-induced-dissolved-organic-nitrogen-don>. Accessed on May 2, 2024.
- [104] A. Ahmed, and S. M. Moniruzzaman, "A study on plastic waste recycling process in Khulna City," *Proceedings of 4th International Conference on Civil Engineering for Sustainable Development (ICCESD)*. Khulna, Bangladesh, 2018.
- [105] A. Ahmed, and S. Chakrabarti, "Analysis on solid waste management practices and development of integrated solid waste management model for developing country with special reference to Jhenaidah municipal area, Bangladesh," *Proceedings of 4th International Conference on Civil Engineering for Sustainable Development (ICCESD)*. Khulna, Bangladesh, 2018.
- [106] Y. N. A. Soh, C. Kunacheva, R. D. Webster, and D. C. Stuckey, "Identification of the production and biotransformational changes of soluble microbial products (SMP) in wastewater treatment processes: A short review," *Chemosphere*, Vol. 251, Article 126391, 2020. [CrossRef]
- [107] S. He, L. Ding, K. Li, H. Hu, L. Ye, and H. Ren, "Comparative study of activated sludge with different individual nitrogen sources at a low temperature: Effluent dissolved organic nitrogen compositions, metagenomic and microbial community," *Bioresource Technology*, Vol. 247, pp. 915–923, 2018. [CrossRef]
- [108] W. M. Xie, B. J. Ni, G. P. Sheng, T. Seviour, and H. Q. Yu, "Quantification and kinetic characterization of soluble microbial products from municipal wastewater treatment plants," *Water Research*, Vol. 88, pp. 703–710, 2016. [CrossRef]
- [109] H. Hu, K. Liao, W. Xie, J. Wang, B. Wu, and H. Ren, "Modeling the formation of microorganism-derived dissolved organic nitrogen (mDON) in the activated sludge system," *Water Research*, Vol. 174, Article 115604, 2020. [CrossRef]

- [110] S. C. Bolyard, and D. R. Reinhart, “Evaluation of leachate dissolved organic nitrogen discharge effect on wastewater effluent quality,” *Waste Management*, Vol. 65, pp. 47–53, 2017. [CrossRef]
- [111] H. Liu, J. Jeong, H. Gray, S. Smith, and D. L. Sedlak, “Algal uptake of hydrophobic and hydrophilic dissolved organic nitrogen in effluent from biological nutrient removal municipal wastewater treatment systems,” *Environmental Science & Technology*, Vol. 46(2), pp. 713–721, 2012. [CrossRef]
- [112] S. Pantoja, C. Lee, “Cell-surface oxidation of amino acids in seawater,” *Limnology and Oceanography*, Vol. 39(7), pp. 1718–1726, 1994. [CrossRef]
- [113] M. Middelboe, N. H. Borch, and D. L. Kirchman, “Bacterial utilization of dissolved free amino acids, dissolved combined amino acids and ammonium in the Delaware Bay estuary: effects of carbon and nitrogen limitation,” *Marine Ecology Progress Series*, Vol. 128(1–3), pp. 109–120, 1995. [CrossRef]
- [114] J. D. Thomas, “The role of dissolved organic matter, particularly free amino acids and humic substances, in freshwater ecosystems,” *Freshwater Biology*, Vol. 38(1), pp. 1–36, 1997. [CrossRef]
- [115] T. Berman, and D. A. Bronk, “Dissolved organic nitrogen: A dynamic participant in aquatic ecosystems,” *Aquatic Microbial Ecology*, Vol. 31(3), pp. 279–305, 2003. [CrossRef]
- [116] N. O. Jørgensen, L. Tranvik, H. Edling, W. Granéli, and M. Lindell, “Effects of sunlight on occurrence and bacterial turnover of specific carbon and nitrogen compounds in lake water,” *FEMS Microbiology Ecology*, Vol. 25(3), pp. 217–227, 1998. [CrossRef]
- [117] J. B. Rondell, K. W. Finster, and B. A. Lomstein, “Urea and DON uptake by a *Lyngbya gracialis* dominated microbial mat: A controlled laboratory experiment,” *Aquatic Microbial Ecology*, Vol. 21, pp. 169–175, 2000. [CrossRef]
- [118] P. Carlsson, and E. Granéli, Availability of humic bound nitrogen for coastal phytoplankton,” *Estuarine, Coastal and Shelf Science*, Vol. 36, pp. 433–447, 1993. [CrossRef]
- [119] K. L. Bushaw-Newton, and M. A. Moran, “Photochemical formation of biologically available nitrogen from dissolved humic substances in coastal marine systems,” *Aquatic Microbial Ecology*, Vol. 18, pp. 285–292, 1999. [CrossRef]
- [120] A. V. Vähätalo, and R. G. Zepp, “Photochemical mineralization of dissolved organic nitrogen to ammonium in the Baltic Sea,” *Environmental Science & Technology*, Vol. 39(18), pp. 6985–6992, 2005. [CrossRef]
- [121] S. Murthy, K. Jones, S. Baidoo, and K. Pagilla, “Biodegradability of dissolved organic nitrogen: Adaptation of the BOD test,” *Proceedings of the Water Environment Federation 2006* (pp. 1550–1559). Chicago, Illinois, USA, 2006. [CrossRef]
- [122] K. Czerwionka, J. Makinia, K. R. Pagilla, and H. D. Stensel, “Characteristics and fate of organic nitrogen in municipal biological nutrient removal wastewater treatment plants,” *Water Research*, Vol. 46(7), pp. 2057–2066, 2012. [CrossRef]
- [123] P. J. Westgate, and C. Park, “Evaluation of proteins and organic nitrogen in wastewater treatment effluents,” *Environmental Science & Technology*, Vol. 44, pp. 5352–5357, 2010. [CrossRef]
- [124] H. Eom, D. Borgatti, H. W. Paerl, and C. Park, “Formation of low-molecular-weight dissolved organic nitrogen in predenitrification biological nutrient removal systems and its impact on eutrophication in coastal waters,” *Environmental Science & Technology*, Vol. 51(7), pp. 3776–3783, 2017. [CrossRef]
- [125] K. Lu, “Biogeochemical Processes of Dissolved Organic Nitrogen in Aquatic Environments,” 2018. <https://repositories.lib.utexas.edu/items/4a45560b-5c6f-42e8-90bd-700c0bf6b946>. Accessed on May 2, 2024.
- [126] E. Pehlivanoglu-Mantas, and D. L. Sedlak, “Measurement of dissolved organic nitrogen forms in wastewater effluents: concentrations, size distribution and NDMA formation potential,” *Water Research*, Vol. 42(14), pp. 3890–3898, 2008. [CrossRef]
- [127] K. R. Pagilla, M. Urgun-Demirtas, K. Czerwionka, and J. Makinia, “Nitrogen speciation in wastewater treatment plant influents and effluents - The US and Polish case studies,” *Water Science and Technology*, Vol. 57(10), pp. 1511–1517, 2008. [CrossRef]
- [128] H. V. M. Nguyen, S. Tak, J. Hur, and H. S. Shin, “Fluorescence spectroscopy in the detection and management of disinfection by-product precursors in drinking water treatment processes: A review,” *Chemosphere*, Vol. 343, Article 140269, 2023. [CrossRef]
- [129] M. H. Plumlee, M. López-Mesas, A. Heidlberger, K. P. Ishida, and M. Reinhard, “N-nitrosodimethylamine (NDMA) removal by reverse osmosis and UV treatment and analysis via LC-MS/MS,” *Water Research*, Vol. 42(1–2), pp. 347–355, 2008. [CrossRef]
- [130] I. Najm, and R. R. Trussell, “NDMA formation in water and wastewater,” *Journal-American Water Works Association*, Vol. 93(2), pp. 92–99, 2001. [CrossRef]
- [131] K. O. Kusk, A. M. Christensen, and N. Nyholm, “Algal growth inhibition test results of 425 organic chemical substances,” *Chemosphere*, Vol. 204, pp. 405–412, 2018. [CrossRef]
- [132] X. Yang, Q. Shen, W. Guo, J. Peng, and Y. Liang, “Precursors and nitrogen origins of trichloronitromethane and dichloroacetonitrile during chlorination/chloramination,” *Chemosphere*, Vol. 88(1), pp. 25–32, 2012. [CrossRef]
- [133] W. A. Mitch, and D. L. Sedlak, “Characterization and fate of N-nitrosodimethylamine precursors in municipal wastewater treatment plants,” *Environmental Science & Technology*, Vol. 38(5), pp. 1445–1454, 2004. [CrossRef]
- [134] J. H. Lee, C. Na, R. L. Ramirez, and T. M. Olson, “Cyanogen chloride precursor analysis in chlorinated

- river water,” *Environmental Science & Technology*, Vol. 40(5), pp. 1478–1484, 2006. [\[CrossRef\]](#)
- [135] W. H. Chu, N. Y. Gao, Y. Deng, and S. W. Krasner, “Precursors of dichloroacetamide, an emerging nitrogenous DBP formed during chlorination or chloramination,” *Environmental Science & Technology*, Vol. 44(10), pp. 3908–3912, 2010. [\[CrossRef\]](#)
- [136] W. A. Mitch, and I. M. Schreiber, “Degradation of tertiary alkylamines during chlorination/chloramination: Implications for formation of aldehydes, nitriles, halonitroalkanes, and nitrosamines,” *Environmental Science & Technology*, Vol. 42(13), pp. 4811–4817, 2008. [\[CrossRef\]](#)
- [137] N. Merlet, H. Thibaud, and M. Dore, “Chloropicrin formation during oxidative treatments in the preparation of drinking water,” *The Science of the Total Environment*, Vol. 47, pp. 223–228, 1985. [\[CrossRef\]](#)
- [138] T. I. Bieber, “Dihaloacetonitriles in chlorinated natural water,” *Water Chlorination Environmental Impact and Health Effects*, Vol. 4, pp. 85–96, 1983.
- [139] M. S. Young, and P. C. Uden, “Byproducts of the aqueous chlorination of purines and pyrimidines,” *Environmental Science & Technology*, Vol. 28(9), pp. 1755–1758, 1994. [\[CrossRef\]](#)
- [140] H. Ueno, T. Moto, Y. Sayato, and K. Nakamuro, “Disinfection by-products in the chlorination of organic nitrogen compounds: By-products from kynurenine,” *Chemosphere*, Vol. 33(8), pp. 1425–1433, 1996. [\[CrossRef\]](#)
- [141] J. A. Aitkenhead-Peterson, M. K. Steele, N. Nahar, and K. Santhy, “Dissolved organic carbon and nitrogen in urban and rural watersheds of south-central Texas: land use and land management influences,” *Biogeochemistry*, Vol. 96, pp. 119–129, 2009. [\[CrossRef\]](#)
- [142] H. Chang, C. Chen, and G. Wang, “Identification of potential nitrogenous organic precursors for C-, N-DBPs and characterization of their DBPs formation,” *Water Research*, Vol. 45(12), pp. 3753–3764, 2011. [\[CrossRef\]](#)
- [143] H. Chang, C. Chen, and G. Wang, “Characteristics of C-, N-DBPs formation from nitrogen-enriched dissolved organic matter in raw water and treated wastewater effluent,” *Water Research*, Vol. 47(8), pp. 2729–2741, 2013. [\[CrossRef\]](#)
- [144] A. Piazzoli, F. Breider, C.G. Aquillon, M. Antonelli, and U. von Gunten, “Specific and total N-nitrosamines formation potentials of nitrogenous micropollutants during chloramination,” *Water Research*, Vol. 135, pp. 311–321, 2018. [\[CrossRef\]](#)
- [145] M. Selbes, W. Beita-Sandí, D. Kim, and T. Karanfil, “The role of chloramine species in NDMA formation,” *Water Research*, Vol. 140, pp.100–109, 2018. [\[CrossRef\]](#)
- [146] W. Wang, S. Ren, H. Zhang, J. Yu, W. An, J. Hu, and M. Yang, “Occurrence of nine nitrosamines and secondary amines in source water and drinking water: Potential of secondary amines as nitrosamine precursors,” *Water Research*, Vol. 45(16), pp. 4930–4938, 2011. [\[CrossRef\]](#)
- [147] Z. T. How, K. L. Linge, F. Buseti, and C. A. Joll, “Formation of odorous and hazardous by-products from the chlorination of amino acids,” *Water Research*, Vol. 146, pp. 10–18, 2018. [\[CrossRef\]](#)
- [148] H. Han, H. Miao, Y. Zhang, M. Lu, Z. Huang, and W. Ruan, “Carbonaceous and nitrogenous disinfection byproduct precursor variation during the reversed anaerobic–anoxic–oxic process of a sewage treatment plant,” *Journal of Environmental Sciences*, Vol. 65, pp. 335–346, 2018. [\[CrossRef\]](#)
- [149] C. Fang, X. Yang, S. Ding, X. Luan, R. Xiao, Z. Du..., and W. Chu, “Characterization of Dissolved Organic Matter and Its Derived Disinfection Byproduct Formation along the Yangtze River,” *Environmental Science & Technology*, Vol. 55(18), pp. 12326–12336, 2021. [\[CrossRef\]](#)
- [150] C. W. K. Chow, R. Fabris, J. van Leeuwen, D. Wang, and M. Drikas, “Assessing natural organic matter treatability using high performance size exclusion chromatography,” *Environmental Science & Technology*, Vol. 42(17), pp. 6683–6689, 2008. [\[CrossRef\]](#)
- [151] J. A. Leenheer, A. Dotson, and P. Westerhoff, “Dissolved organic nitrogen fractionation,” *Annals of Environmental Science*, Vol. 1, pp. 45–56, 2007.
- [152] J. K. Choe, L. C. Hua, Y. Komaki, A. M. A. Simpson, D. L. McCurry, and W. A. Mitch, “Evaluation of histidine reactivity and byproduct formation during peptide chlorination,” *Environmental Science & Technology*, Vol. 55(3), pp. 1790–1799, 2021. [\[CrossRef\]](#)
- [153] T. Bond, J. Huang, M. R. Templeton, and N. Graham, “Occurrence and control of nitrogenous disinfection by-products in drinking water – A review,” *Water Research*, Vol. 45(15), pp. 4341–4354, 2011. [\[CrossRef\]](#)
- [154] S. W. Krasner, H. S. Weinberg, S. D. Richardson, S. J. Pastor, R. Chinn, M. J. Scimanti..., and A. D. Thruston, “Occurrence of a new generation of disinfection byproducts,” *Environmental Science & Technology*, Vol. 40(23), pp. 7175–7185, 2006. [\[CrossRef\]](#)
- [155] S. Brosillon, M. Lemasle, E. Renault, D. Tozza, V. Heim, and A. Laplanche, “Analysis and occurrence of odorous disinfection by-products from chlorination of amino acids in three different drinking water treatment plants and corresponding distribution networks,” *Chemosphere*, Vol. 77(8), pp. 1035–1042, 2009. [\[CrossRef\]](#)
- [156] W. Qi, L. Fang Yee, and H. Jiangyong, “Relationship between organic precursors and N-nitrosodimethylamine (NDMA) formation in tropical water sources,” *Journal of Water and Health*, Vol. 12(4), pp. 736–746, 2014. [\[CrossRef\]](#)
- [157] P. Jutaporn, M. D. Armstrong, and O. Coronell, “Assessment of C-DBP and N-DBP formation potential and its reduction by MIEX® DOC and MIEX® GOLD resins using fluorescence spectroscopy and parallel factor analysis,” *Water Research*, Vol. 72, Article 115460, 2020. [\[CrossRef\]](#)

- [158] J. Wang, F. Zheng, Z. Yu, J. Chen, and H. Lu, “Dissolved organic nitrogen derived from wastewater denitrification: Composition and nitrogenous disinfection byproduct formation,” *Journal of Hazardous Materials*, Vol. 440, Article 129775, 2022. [CrossRef]
- [159] P. G. Jang, H. G. Cha, “Long-term changes of disinfection byproducts in treatment of simulated ballast water,” *Ocean Science Journal*, Vol. 55(2), pp. 265–277, 2020. [CrossRef]
- [160] H. Chen, M. S. Ersan, N. Tolić, R. K. Chu, T. Karanfil, and A. T. Chow, “Chemical characterization of dissolved organic matter as disinfection byproduct precursors by UV/fluorescence and ESI FT-ICR MS after smoldering combustion of leaf needles and woody trunks of pine (*Pinus jeffreyi*),” *Water Research*, Vol. 209, Article 117962, 2022. [CrossRef]
- [161] G. Hua, J. Kim, and D. A. Reckhow, “Disinfection byproduct formation from lignin precursors,” *Water Research*, Vol. 63, pp. 285–295, 2014. [CrossRef]
- [162] M. Altarawneh, A. Saeed, M. Al-Harashseh, and B.Z. Dlugogorski, “Thermal decomposition of brominated flame retardants (BFRs): Products and mechanisms,” *Progress in Energy and Combustion Science*, Vol. 70, pp. 212–259, 2019. [CrossRef]
- [163] G. He, T. Zhang, Q. Zhang, F. Dong, and Y. Wang, “Characterization of enoxacin (ENO) during ClO₂ disinfection in water distribution system: Kinetics, byproducts, toxicity evaluation and halogenated disinfection byproducts (DBPs) formation potential,” *Chemosphere*, Vol. 283, Article 131251, 2021. [CrossRef]
- [164] G. He, T. Zhang, F. Zheng, C. Li, Q. Zhang, F. Dong, and Y. Huang, “Reaction of fleroxacin with chlorine and chlorine dioxide in drinking water distribution systems: Kinetics, transformation mechanisms and toxicity evaluations,” *Chemical Engineering Journal*, Vol. 374, pp. 1191–1203, 2019. [CrossRef]
- [165] G. He, T. Zhang, Y. Li, J. Li, F. Chen, J. Hu, and F. Dong, “Comparison of fleroxacin oxidation by chlorine and chlorine dioxide: Kinetics, mechanism and halogenated DBPs formation,” *Chemosphere*, Vol. 286(Part 1), Article 131585, 2022. [CrossRef]
- [166] Y. Yang, J. Shi, Y. Yang, J. Yin, J. Zhang, and B. Shao, “Transformation of sulfamethazine during the chlorination disinfection process: Transformation, kinetics, and toxicology assessment,” *Journal of Environmental Sciences*, Vol. 76, pp. 48–56, 2019. [CrossRef]
- [167] Z. Wu, J. Fang, Y. Xiang, C. Shang, X. Li, F. Meng, and X. Yang, “Roles of reactive chlorine species in trimethoprim degradation in the UV/chlorine process: Kinetics and transformation pathways,” *Water Research*, Vol. 104, pp. 272–282, 2016. [CrossRef]
- [168] S. Zhang, T. Lin, W. Chen, H. Xu, and H. Tao, “Degradation kinetics, byproducts formation and estimated toxicity of metronidazole (MNZ) during chlor(am)ination,” *Chemosphere*, Vol. 235, pp. 21–31, 2019. [CrossRef]
- [169] E. Aghdam, Y. Xiang, J. Sun, C. Shang, X. Yang, and J. Fang, “DBP formation from degradation of DEET and ibuprofen by UV/chlorine process and subsequent post-chlorination,” *Journal of Environmental Sciences*, Vol. 58, pp. 146–154, 2017. [CrossRef]
- [170] Y. Wang, H. Liu, G. Liu, and Y. Xie, “Oxidation of diclofenac by aqueous chlorine dioxide: Identification of major disinfection byproducts and toxicity evaluation,” *Science of The Total Environment* Vol. 473–474, pp. 437–445, 2014. [CrossRef]
- [171] J. Li, J. He, Md. T. Aziz, X. Song, Y. Zhang, and Z. Niu, “Iodide promotes bisphenol A (BPA) halogenation during chlorination: Evidence from 30 X-BPAs (X = Cl, Br, and I),” *Journal of Hazardous Materials*, Vol. 414, Article 125461, 2021. [CrossRef]
- [172] S. Zheng, J. Shi, J. Zhang, Y. Yang, J. Hu, and B. Shao, “Identification of the disinfection byproducts of bisphenol S and the disrupting effect on peroxisome proliferator-activated receptor gamma (PPAR γ) induced by chlorination,” *Water Research*, Vol. 132, pp. 167–176, 2018. [CrossRef]
- [173] Y. Gao, S. Y. Pang, J. Jiang, J. Ma, Y. Zhou, J. Li..., and L. P. Yuan, “Transformation of flame retardant tetrabromobisphenol a by aqueous chlorine and the effect of humic acid,” *Environmental Science & Technology*, Vol. 50(17), pp. 9608–9618, 2016. [CrossRef]
- [174] P. Durand, L. Breuer, P. J. Johnes, G. Billen, A. Butturini, G. Pinay..., and R. Wright, “Nitrogen processes in aquatic ecosystems,” 2011. <https://centaur.reading.ac.uk/20855/8/Chapter%25207%2520ENA%2520Durand%2520Breuer%2520Johnes%25202011.pdf>. Accessed on May 3, 2024.
- [175] F. Zheng, S. Xu, W. Chai, D. Liu, and H. Lu, “Fermentation liquid as a carbon source for wastewater nitrogen removal reduced nitrogenous disinfection byproduct formation potentials of the effluent,” *Science of The Total Environment*, Vol. 832, Article 155115, 2022. [CrossRef]
- [176] Y. Du, X. T. Lv, Q. Y. Wu, D. Y. Zhang, Y. T. Zhou, L. Peng, and H. Y. Hu, “Formation and control of disinfection byproducts and toxicity during reclaimed water chlorination: A review,” *Journal of Environmental Sciences*, Vol. 58, pp. 51–63, 2017. [CrossRef]
- [177] J. K. Liang, Y. Lu, Z. M. Song, B. Ye, Q. Y. Wu, and H. Y. Hu, “Effects of chlorine dose on the composition and characteristics of chlorinated disinfection byproducts in reclaimed water,” *Science of the Total Environment*, Vol. 824, Article 153739, 2022. [CrossRef]
- [178] H. Zhai, X. Zhang, X. Zhu, J. Liu, and M. Ji, “Formation of brominated disinfection byproducts during chloramination of drinking water: New polar species and overall kinetics,” *Environmental Science & Technology*, Vol. 48, pp. 2579–2588, 2014. [CrossRef]
- [179] H. Komulainen, “Experimental cancer studies of chlorinated by-products,” *Toxicology*, Vol. 198(1–3), pp. 239–248, 2004. [CrossRef]
- [180] D. Baytak, A. Sofuoglu, F. Inal, S. C. Sofuoglu, “Seasonal variation in drinking water concentrations of

- disinfection by-products in IZMIR and associated human health risks,” *Science of The Total Environment*, Vol. 407(1), pp. 286–296, 2008. [CrossRef]
- [181] M. Khallef, R. Liman, M. Konuk, İ. H. Cigerci, D. Benouareth, M. Tabet, A. Abda, “Genotoxicity of drinking water disinfection by-products (bromoform and chloroform) by using both Allium anaphase-telophase and comet tests,” *Cytotechnology*, Vol. 67(2), pp. 207–213, 2015. [CrossRef]
- [182] T. I. T. Nkambule, “Natural Organic Matter (NOM) in South African waters : Characterization of NOM, treatability and method development for effective NOM removal from water,” 2012. <https://www.proquest.com/docview/2566004979/abstract/FB-5C4113E93B43BAPQ/1>. Accessed on May 3, 2024.
- [183] F. Dong, Q. Lin, C. Li, G. He, and Y. Deng, “Impacts of pre-oxidation on the formation of disinfection byproducts from algal organic matter in subsequent chlor(am)ination: A review,” *Science of The Total Environment*, Vol. 754, Article 141955, 2021. [CrossRef]
- [184] B. Sun, Y. Wang, Y. Xiang, and C. Shang, “Influence of pre-ozonation of DOM on micropollutant abatement by UV-based advanced oxidation processes,” *Journal of Hazardous Materials*, Vol. 391, Article 122201, 2020. [CrossRef]
- [185] K. Doederer, W. Gernjak, H. S. Weinberg, and M. J. Farré, “Factors affecting the formation of disinfection by-products during chlorination and chloramination of secondary effluent for the production of high quality recycled water,” *Water Research*, Vol. 48, pp. 218–228, 2014. [CrossRef]
- [186] X. Yang, C. Shang, and J. C. Huang, “DBP formation in breakpoint chlorination of wastewater,” *Water Research*, Vol. 39(19), pp. 4755–4767, 2005. [CrossRef]
- [187] G. Hua, and D. A. Reckhow, “DBP formation during chlorination and chloramination: Effect of reaction time, pH, dosage, and temperature,” *Journal AWWA*, Vol. 100(8), pp. 82–95, 2008. [CrossRef]
- [188] C. Tsaridou, A. J. Karabelas, “Drinking water standards and their implementation—A critical assessment,” *Water*, Vol. 13(20), Article 2918, 2021. [CrossRef]
- [189] J. C. Vickers, M. A. Thompson, and U. G. Kelkar, “The use of membrane filtration in conjunction with coagulation processes for improved NOM removal,” *Desalination*, 102(1–3), pp. 57–61, 1995. [CrossRef]
- [190] D. Ghernaout, B. Ghernaout, and A. Kellil, “Natural organic matter removal and enhanced coagulation as a link between coagulation and electrocoagulation,” *Desalination and Water Treatment*, Vol. 2(1–3) pp. 203–222, 2009. [CrossRef]
- [191] X. Wang, Y. Mao, S. Tang, H. Yang, Y. F. Xie, “Disinfection byproducts in drinking water and regulatory compliance: A critical review,” *Frontiers of Environmental Science & Engineering*, Vol. 9(1), pp. 3–15, 2015. [CrossRef]
- [192] Y. Qian, Y. Chen, Y. Hu, D. Hanigan, P. Westhoff, and D. An, “Formation and control of C- and N-DBPs during disinfection of filter backwash and sedimentation sludge water in drinking water treatment,” *Water Research*, Vol. 194, Article 116964, 2021. [CrossRef]
- [193] J. M. Laine, J. G. Jacangelo, E. W. Cummings, K. E. Carns, and J. Mallevalle, “Influence of bromide on low-pressure membrane filtration for controlling DBPs in surface waters,” *Journal AWWA*, Vol. 85(6), pp. 87–99, 1993. [CrossRef]
- [194] J. G. Jacangelo, R. Rhodes Trussell, and M. Watson, “Role of membrane technology in drinking water treatment in the United States,” *Desalination*, Vol. 113(2–3), pp. 119–127, 1997. [CrossRef]
- [195] V. Uyak, and I. Toroz, “Disinfection by-product precursors reduction by various coagulation techniques in Istanbul water supplies,” *Journal of Hazardous Materials*, Vol. 141(1), pp. 320–328, 2007. [CrossRef]
- [196] T. Bond, E. H. Goslan, B. Jefferson, F. Roddick, L. Fan, and S. A. Parsons, “Chemical and biological oxidation of NOM surrogates and effect on HAA formation,” *Water Research*, Vol. 43(10), pp. 2615–2622, 2009. [CrossRef]
- [197] G. S. Wang, S. T. Hsieh, and C. S. Hong, “Destruction of humic acid in water by UV light—catalyzed oxidation with hydrogen peroxide,” *Water Research*, 34(15), pp. 3882–3887, 2000. [CrossRef]
- [198] Y. Jiang, J. E. Goodwill, J. E. Tobiasson, and D. A. Reckhow, “Comparison of ferrate and ozone pre-oxidation on disinfection byproduct formation from chlorination and chloramination,” *Water Research*, Vol. 156, pp. 110–124, 2019. [CrossRef]
- [199] Y. H. Chuang, A. Szczuka, F. Shabani, J. Munoz, R. Aflaki, S. D. Hammond, and W.A. Mitch, “Pilot-scale comparison of microfiltration/reverse osmosis and ozone/biological activated carbon with UV/hydrogen peroxide or UV/free chlorine AOP treatment for controlling disinfection byproducts during wastewater reuse,” *Water Research*, Vol. 152, pp. 215–225, 2019. [CrossRef]
- [200] Y. Lu, F. Tang, Y. Wang, J. Zhao, X. Zeng, Q. Luo, and L. Wang, “Biodegradation of dimethyl phthalate, diethyl phthalate and di-n-butyl phthalate by *Rhodococcus* sp. L4 isolated from activated sludge,” *Journal of Hazardous Materials*, Vol. 168(2–3), pp. 938–943, 2009. [CrossRef]
- [201] E. S. Peterson, R. S. Summers, and S. M. Cook, “Control of pre-formed halogenated disinfection byproducts with reuse biofiltration,” *Environmental Science & Technology*, Vol. 57(6), pp. 2516–2526, 2023. [CrossRef]
- [202] J. Hu, Q. Yang, and J. L. Wang, “Biodegradation of di-n-butyl phthalate in sequencing batch reactor bioaugmented with *Micrococcus* sp. and the bacterial community analysis,” *International Journal of Environmental Science and Technology*, Vol. 12, pp. 2819–2828, 2015. [CrossRef]
- [203] M. A. Zazouli, and L. R. Kalankesh, “Removal of precursors and disinfection by-products (DBPs) by membrane filtration from water; a review,” *Journal*

- of Environmental Health Science and Engineering, Vol. 15, pp. 25, 2017. [[CrossRef](#)]
- [204] I. Petrinic, J. Korenak, D. Povodnik, and C. Hélix-Nielsen, “A feasibility study of ultrafiltration/reverse osmosis (UF/RO)-based wastewater treatment and reuse in the metal finishing industry,” *Journal of Cleaner Production*, Vol. 101, pp. 292–300, 2015. [[CrossRef](#)]
- [205] E. Molina Alcaide, and A. Nefzaoui, “Recycling of olive oil by-products: Possibilities of utilization in animal nutrition,” *International Biodeterioration & Biodegradation*, Vol. 38(3–4), pp. 227–235, 1996. [[CrossRef](#)]
- [206] N. T. Holland, M. T. Smith, B. Eskenazi, and M. Bastaki, “Biological sample collection and processing for molecular epidemiological studies,” *Mutation Research/Reviews in Mutation Research*, Vol. 543(3), pp. 217–234, 2003. [[CrossRef](#)]
- [207] C. M. López-Vázquez, C. M. Hooijmans, D. Brdjanovic, H. J. Gijzen, and M. C. M. van Loosdrecht, “Factors affecting the microbial populations at full-scale enhanced biological phosphorus removal (EBPR) wastewater treatment plants in The Netherlands,” *Water Research*, Vol. 42(10–11), pp. 2349–2360, 2008. [[CrossRef](#)]



Review Article

Fostering sustainability: The environmental advantages of natural fiber composite materials – a mini review

Sivasubramanian PALANISAMY¹, Thulasi Mani MURUGESAN², Murugesan PALANIAPPAN³,
Carlo SANTULLI⁴, Nadir AYRILMIŞ⁵

¹*PTR College of Engineering and Technology, Madurai, Tamilnadu, India*

²*Department of Mechanical and Aerospace Engineering, Carleton University, Ottawa, Canada*

³*Department of Mechanical Engineering, College of Engineering, Imam Mohammad Ibn Saud Islamic University, Riyadh, Saudi Arabia*

⁴*School of Science and Technology, Università di Camerino, Camerino, Italy*

⁵*Department of Wood Mechanics and Technology, Faculty of Forestry, İstanbul University-Cerrahpaşa, İstanbul, Türkiye*

ARTICLE INFO

Article history

Received: 29 November 2023

Revised: 10 February 2024

Accepted: 27 February 2024

Key words:

Applications; Chemical and mechanical properties; Exploring characteristics; Environmental protection; Natural fiber composites; Sustainability

ABSTRACT

In recent decades, natural fiber reinforced composites (NFRCs) have become an attractive substitute for conventional materials such as glass fiber and have attracted considerable interest from researchers and academics, particularly in the context of environmental protection. Environmental factors and their impact on the fundamental properties of renewable materials are becoming an increasingly popular area of study, particularly natural fibers and their composites. While this area of research is still expanding, natural fiber-reinforced polymer composites (NFRCs) have found widespread use in a variety of engineering contexts. Natural fibers (NFs) such as pineapple leaf (PALF), bamboo, abaca, coconut fibers, jute, banana, flax, hemp, sisal, kenaf, and others have many desirable properties, but their development and use present researchers with a number of obstacles. These fibers have attracted attention due to their various advantageous properties, such as lightness, economy, biodegradability, remarkable specific strength, and competitive mechanical properties, which make them promising candidates for use as biomaterials. As a result, they can serve as alternative materials to traditional composite fibers such as glass, aramid, and carbon in various applications. In addition, natural fibers have attracted the interest of an increasing number of researchers because they are readily available in nature and as by-products of agricultural and food systems, contributing to the improvement of the environmental ecosystem. This interest coincides with the search for environmentally friendly materials to replace synthetic fibers used in the construction, automotive, and packaging industries. The use of natural fibers is not only logical but also practical, as their fibrous form can be easily extracted and strengthened by chemical, physical, or enzymatic treatments. This article provides a brief overview of NFRCs, looking at their chemical, physical, and mechanical properties. It also highlights some of the significant advances associated with NFRCs from an economic, environmental, and sustainability perspective. Additionally, it provides a concise discussion of their diverse applications, all with a focus on their positive impact on the environment.

Cite this article as: Palanisamy S, Murugesan TM, Palaniappan M, Santulli C, Ayrılmış N. Fostering sustainability: The environmental advantages of natural fiber composite materials – a mini review. Environ Res Tec 2024;7(2)256–269.

*Corresponding author.

*E-mail address: nadiray@istanbul.edu.tr



INTRODUCTION

In recent decades, natural fiber, also known as plant fibers have gained an increasing attention for polymer composites as a possible alternative to traditional polymer composites reinforced with synthetic fibers. Reasons for this include their affordable price and good mechanical properties [1]. There is an increasing focus on the potential to produce bio-composites with minimal environmental impact and a trend towards carbon neutrality. This applies to both thermosets and thermoplastics and has received considerable attention [2, 3]. Since the initial research efforts, the expansion of the natural fiber market into the composites sector has been steadily increasing worldwide. It is reasonable to assume that one or more natural fibers suitable for this purpose can be identified in each global region [4]. Based on assessments carried out between 2011 and 2016, the global output of companies specializing in natural fiber composites is expected to grow by 10% [5]. In particular, the refinement of hybridization processes with aramid, glass, carbon and natural fibers has been the focus of progress in their application in composites. Additionally, there has been an exploration of distinct and more targeted treatments, diverging from the expertise traditionally gained in textile products [5, 6].

The polymer matrix, a critical component of natural fiber reinforced composites (NFRCs), prevents mechanical abrasion and environmental hazards from reaching the fiber surface [7]. The incorporation of resilient and low-density plant fibers in polymer matrix, ensuring robust integration, can result in composites with increased specific strength. This applies to both thermoplastics and thermosets, with recent applications extending to bio-based matrices. Table 1 provides an inventory of globally popular and commercially viable natural fibers, along with total global fiber production. An upward trend in the use of sustainable materials in the manufacture of automotive components [8, 9]. The majority of these NFRCs are composed of sixty to seventy percent NFs, with the remaining portion consisting of adhesive and matrix. A variation of microbes and ecological factors, such as humidity and temperature, influence the

degradation of NF in an open environment [10, 11]. There is a significant cause for concern in construction applications regarding the environmental conditions of NFRCs. The degradation of natural fiber components at higher temperatures alters the mechanical properties of the composite [12–14]. These components include cellulose, hemicellulose, and lignin.

This study focused on the characteristics of commercial natural fibers, manufacturing techniques for NFRCs, and their diverse economic, environmental, and sustainability perspectives. Moreover, the future prospects of the NFRCs were discussed.

FIBERS MADE FROM NATURAL SOURCES

Natural fibers (NFs) can be derived from minerals plants, or animals [22]. Within the category of animal fibers, notable examples include protein fibers such as silk, human hair and even wool [23, 24]. Figure 1 illustrates different examples of fiber classification. According to their origin, plant fibers can be classified as stem, stalk, bast, wood, fruit, leaf, grass or seed. Cell walls in plant fibers use randomly oriented hemicellulose and lignin to bind the mostly amorphous cellulose [25]. Amorphous lignin forms a protective layer between the fibers, increasing the strength of the cellulose and hemicellulose network [26]. Hemicellulose formulae a matrix encapsulating the Crystallized cellulose microfibrils and acts as a binder in the cell wall. As shown in Figure 2, the mechanical properties of the fiber are determined by the secondary walls (S2) of the crystalline cellulose microfibrils. When used independently, whether in nanometric or micrometric arrangement, the fiber exhibits excellent tensile strength [26, 27]. Surface modification of polypropylene resulted in improved mechanical properties, indicating that the arrangement had a positive effect [28].

Bast fibers such as sisal, hemp, flax, jute, coir, including kenaf are widely used in polymer based composites due to their unique properties such as high tensile properties, low density, low-cost [3,29,30]. In particular, flax, hemp and

Table 1. Global production of natural fibers around the world and their quantities [15–21]

Source of fiber	Leading Countries in Production	Production in the world (10 ³ tons)
Abaca	Philippines, Costa Rica, Ecuador	70
Bamboo	India, China, Indonesia	30000
Coir	India, Sri Lanka	100
Flax	Canada, France, Belgium	830
Hemp	China, France, Philippines	214
Jute	India, China, Bangladesh	2300
Kenaf	India, Bangladesh, US	970
Ramie	China, Brazil, Philippines, India	100
Sisal	Tanzania, Brazil	375
Sugarcane bagasse	Brazil, India, China	75000
Cotton	China, India, US	25000

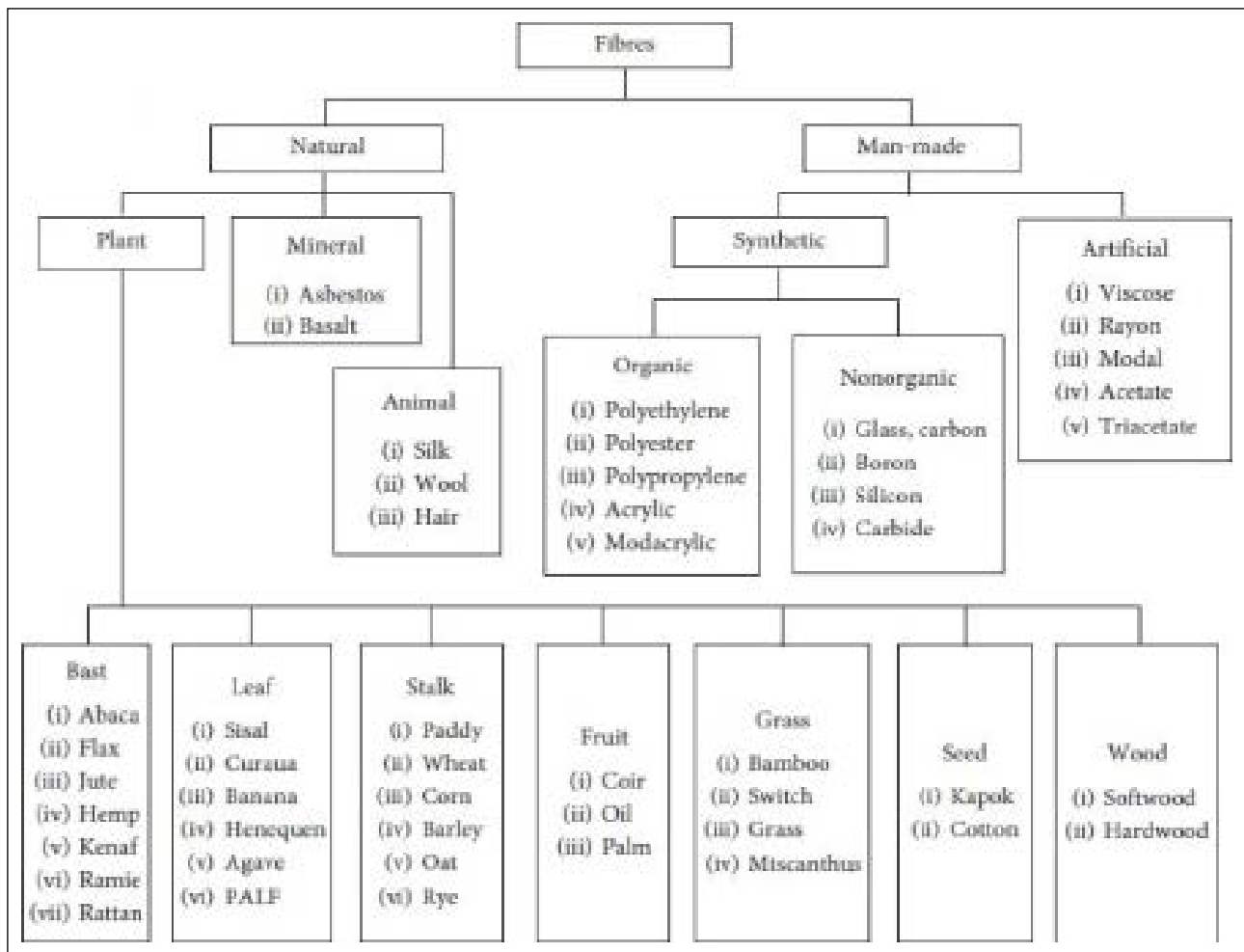


Figure 1. Classification of natural and man-made fibers.

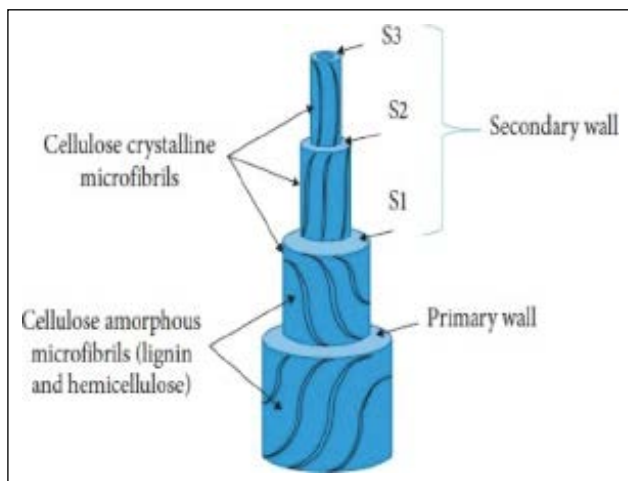


Figure 2. Natural fiber structure [29].

jute were used in polymer composites at an early experimental stage. Over time, however, the scope of research has expanded to include a wide range of species [31]. Jute, grown in South Asian countries and several Latin American countries, is a fiber known for its significant mechanical properties, making it suitable for applications such as ropes and sacks [32]. Flax is the most important and sought-after

bast fiber in Europe, although certain varieties are naturally grown in China [33]. The quality of natural fibers depends on geographic conditions such as weather, harvesting time, soil properties. The geographic conditions affects the chemical composition and cellulose crystallinity, which determines the physical, mechanical, and thermal properties of the polymer composites [34].

The aspect ratio of the fiber is affected by other properties of the fibers include the microfibrillar angle, which is the angle at which the technical (extractable) fiber is formed by winding together the fibers, the dimensions of the lumen and porosity, and the cell length and diameter. Together, these factors affect [33, 35, 36]. All these properties have the potential to influence the mechanical characteristics of the fiber. The mechanical characteristics of various natural based fibers are compared to E-glass synthetic fibers in Table 2. At the composite stage, factors such as fiber extraction, polymer matrix type, interfacial bond performance, distribution of fiber in polymer matrix, manufacturing processes, fiber orientation and porosity emerge as key elements influencing the strength of the resulting composite [8]. In addition, the modulus of natural fibers tends to decrease with increasing diameter, as shown in a previous study [35]. This phenomenon was mainly attributed to the fibrillation

Table 2. Mechanical properties of certain fibers derived from [8]

Fibers	Density (g/cm ³)	Tensile strength (MPa)	Specific tensile strength (MPa/g.cm ³)	Stiffness (GPa)	Specific stiffness (GPa/g.cm ³)
E-glass	2.5	2000–3000	800–1400	70	29
Wool	1.3	50–315	38–242	2.3–5	1.8–3.8
Chicken feather	0.9	100–203	112–226	3–10	3.3–11
Ramie	1.5	400–938	270–620	44–128	29–85
Flax	1.5	345–1830	230–1220	27–80	18–53
Jute	1.3–1.5	393–800	300–610	10–55	7.1–39
Hemp	1.5	550–1110	370–740	58–70	39–47
Cotton	1.5–1.6	287–800	190–530	5.5–13	3.7–8.4
Sisal	1.3–1.5	507–855	362–610	9.4–28	6.7–20
Silk	1.3	100–1500	100–1500	5–25	4–20

of natural fibers and increase in the percentage of porosity within the fibers [36]. Natural fibers, due to their chemical composition, have a notable drawback for their applications - hygroscopicity. The absorption of moisture adversely affects their properties [37, 38].

Pure microcrystalline cellulose occupies its maximum theoretical density, which is somewhat less than 1.6 g/cm³, is linked to that of natural lignocellulosic fiber [39, 37]. Natural fibers are undoubtedly less dense than the theoretical maximum due to their high porosity content and cellulose composition [15]. In composites made of natural fibers, the density is significantly lower since the matrix is usually lighter than the fibers. Table 3 displays the densities of commercially used natural based fibers in polymeric composite materials.

The proportions of cellulose, hemicellulose and lignin in natural fibers are the main factors influencing their chemical composition. Cellulose is a naturally occurring molecule that is abundant and degradable. In addition, NFRCs can be biodegraded with other polymers after they have served their useful purpose [44-46]. NFRCs reduce the risk of atmospheric impact and generate positive carbon credits. In this case, NFRCs consist mainly of NFs (60-70%), with the adhesive and matrix making up the remainder [6]. A variety of microbes, as well as environmental factors such as temperature and humidity, influence NF degradation in an open environment. The degradation process involves the breakdown of various fiber components, including hemicelluloses, lignin and cellulose. This allowed for the observation of the overall failure of the mechanical properties of NFRCs [45]. Furthermore, a characteristic that defines the structural potential of the fibers is their degree of crystallinity. Normal fibers often contain very little pectin and waxes, and the amount of residual ash is usually only a few percent. Selected studies reporting structural components of some natural fibers are presented in Tables 4, 5 and 6, respectively.

Coconut is a rigid and decomposable lignocellulosic type of fiber derived from the the outer shell of the coconut fruit, which makes up approximately 25% of the husk. Coconut fiber is also called coir fiber [49]. Coconut (*Cocos nucifera*) is

Table 3. The density of various natural fibers

Fiber	Density (g/cm ³)	Reference
Abaca	1.5	[38]
Alfa	0.89	[38]
Bamboo	0.6–1.1	[40]
Banana	1–1.5	[41]
Coir	1.25	[1]
Cotton	1.5–1.6	[41]
Flax	1.4	[1]
Hemp	1.48	[1]
Henequen	1.2	[38]
Jute	1.3–1.49	[40]
Kenaf	1.45	[42]
PALF	1.53	[43]
Palm	1.03	[24]
Ramie	1.5	[1]
Sisal	1.33	[1]
Wool	1.3	[41]
Vakka	0.81	[30]

widely grown in tropical countries such as Thailand, Philippines, India, Indonesia, and Lanka. The high amount of the lignin of coir fibers makes them weather resistant, relatively waterproof durable, and also Chemically changeable. The fibers also have a higher elongation at break. The unique properties of coconut fiber, characteristics such as a low specific gravity and an excellent flexural as well as tensile strength, among others, make it a potential alternative to synthetic fibers such as glass fibers in polymer composites [50]. Tensile properties of plant fibers, tensile modulus along with tensile and impact strength are critical characteristics for considering the performance in polymer composites. The physical, mechanical, thermal and morphological properties of coir fiber have been reported in the literature [50].

Table 4. Amount of cellulose in some commercial natural fibers

Source of natural fiber	Cellulose(% by weight)	Reference
Abaca	56–66	[38]
Alfa	45	[38]
Bamboo	30–65	[40]
Banana	62–64	[46]
Cotton	82–7–90	[38]
Flax	71	[47]
Hemp	57–75	[47]
Henequen	60–77.6	[38]
Jute	59–71.5	[40]
Kenaf	45–57	[42]
Ramie	68–91	[47]
Sisal	78	[48]

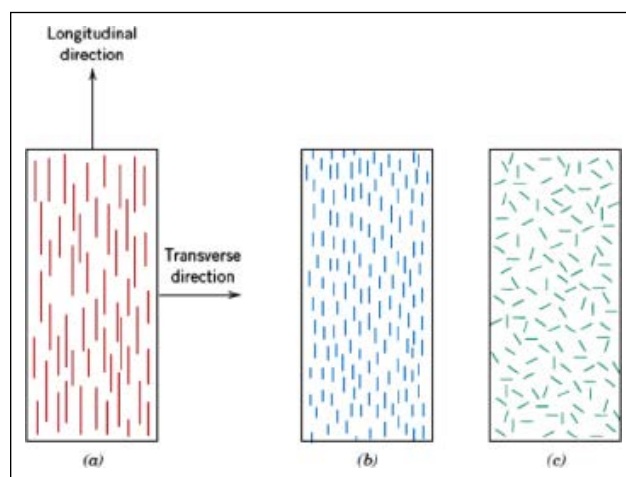
Table 5. Amount of hemicellulose in several plant fibers

Source of natural fiber	Hemicellulose (% by weight)	Reference
Abaca	20–25	[38]
Alfa	38.5	[38]
Bamboo	30	[40]
Banana	19	[46]
Cotton	5.7	[38]
Flax	18.6–21.6	[47]
Hemp	14–22.4	[47]
Henequen	4–28	[38]
Jute	13.6–20.4	[40]
Kenaf	8–13	[42]
Ramie	5–16.7	[47]
Sisal	25.7	[48]

In composites, several fiber factors may influence the mechanical as well as physical properties. These include fiber length, orientation, dispersion within the polymeric matrix, loading level, and form [51]. The shape and arrangement of the fibers, e.g. continuous fibers, fabric fibers, discontinuous fibers (discrete fibers that are both aligned and orientated in a random manner), flakes and particles, influences the composite's strength [52,53]. The schematic representations of orientation of continuous and discontinuous fibers are presented in Figure 3 [54]. Short fibers are more evenly distributed throughout the matrix, but tend to have a lower stiffness than longer fibers. When the short fibers are used randomly and uniformly in the polymer matrix, the resulting composite has homogeneous strength in all directions. In general, the production process of polymer composites with short fibers are simpler than long fibers. In particular, short-fiber reinforced polymer based composites are more suitable for applications requiring impact resistance [52, 53, 55].

Table 6. Amount of lignin of some commercial natural fibers

Source of natural fiber	Lignin (% by weight)	Reference
Abaca	7–13	[38]
Alfa	14.9	[38]
Bamboo	5–31	[40]
Banana	5	[46]
Cotton	<2	[38]
Flax	2.2	[47]
Hemp	3.7–13	[47]
Henequen	8–13.1	[38]
Jute	11.8–13	[40]
Kenaf	21.5	[42]
Ramie	0.6–0.7	[47]
Sisal	12.1	[48]

**Figure 3.** Arrangement of fibers in polymer matrix, (a) continuous and aligned, (b) discontinuous and aligned, (c) discontinuous and randomly oriented fiber reinforced polymer composites [54].

MANUFACTURING METHODS FOR NATURAL FIBER-REINFORCED POLYMER COMPOSITES (NFRCS)

Fiber-reinforced plastics can be produced using a variety of techniques, all based on the idea of polymerization, depending on the geometry of the target component. A collection of research on natural fiber composites produced using a range of production techniques and processes is shown in Table 7.

Hand Layup

The molding process described is a manual process in which fiber-reinforcements are placed by hand and polymer resin is poured over them. An additional layer of fiber-reinforcement is then applied to the surface of the polymer matrix. To ensure a seamless and air-free surface, a lightly pressurized roller is then moved over the layers. This step not only prevents air from being trapped between the layers but also ensures a smooth and uniform surface [75, 78]. After

Table 7. Different composite manufacturing procedures and methods

Method	Composite produced	References
Hand layup	Sisal, jute, and glass fibers with Polyester resin	[56]
	bi-directional jute fiber with epoxy resin	[57]
	Banana fiber with epoxy	[58]
	Glass and sisal/jute fibers with Epoxy	[56]
	Calotropis Gigantea fruit fiber with Polyester	[59]
Spray layup	Rice straw waste in a box made of Kraft paper with a natural rubber seal.	[60, 61]
	Composites using different flax topologies and nanosilica particles	[45, 62, 63]
	Epoxy with coconut sheath fiber	[64]
	Epoxy containing jute and sisal fibers	[65]
Filament winding	Kraft paper and cellulose combine to form cellulose aceto-butyrate (CAB) or natural rubber (NR).	[66]
	Composites reinforced with ramie fiber yarn	[67]
	composites consisting of biopol and jute yarn	[68]
	High density pre-preg polyethylene made of sisal fiber	[69]
	Filament-wound epoxy composites reinforced with natural fibers	[70]
Compression moulding	Composites of cellulose and natural rubber reinforcing short natural fibers made of polyethylene	[71]
	Jute fibers in matrices of polyester and epoxy	[72]
	reinforcement for composites using sisal and banana	[56]
	Natural fibers used to reinforce PLA composites	[73]
	Polypropylene/sugarcane bagasse fibers composite	[74]
Injection winding	Sisal woven fibers with an epoxy matrix modified by natural rubber	[71, 72]
	Vetiver/polypropylene	[75]
	Bamboo-glass fibers/polypropylene hybrids	[76]
	Reinforced polypropylene composites using sugarcane bagasse fibers	[74]
	Reinforced polypropylene with palm fibers	[53, 77]

the initial steps, the manufacturing technique described is repetitive for each polymer matrix and fiber to build up the required layers. This stacking allows for the necessary curing time. The process is particularly suitable for small size composite batches. To facilitate manual handling, the viscosity of the resin must be low, which is often achieved by increasing the diluent/styrene content. However, this adjustment may result in a slight reduction in mechanical properties. A single-sided hand lay-up produces a seamless and better excellence finish to the product. This method offers greater flexibility in material design. However, the trade-off is a longer curing cycle, typically 24 to 48 hours. This time frame is critical to ensure proper curing and to achieve the desired structural integrity and performance of the composite [53,54].

Spray Layup

Spray lay-up is a hand molding technique that is an extension of hand lay-up, similar to hand lay-up. This strategy has attracted much interest, particularly in the field of natural fiber composites [79]. In this technique, a spray gun is used to apply pressurized adhesive and reinforcement into the geometry of chopped fibers. It is possible to spray the reinforcement and matrix material

simultaneously or sequentially at various intervals. To release any air entrapped in the layups, a roller is then lightly tensioned as it passes over the sprayed surface. The material is sprayed to the appropriate thickness. Then, it is cured at room temperature for a certain period of time before it is taken out of the mold [80]. This approach preferentially uses low-viscosity matrices; however, low-volume production is the most appropriate manufacturing process, although this choice may affect the mechanical properties of the matrices. The aim is to produce a low-cost composite with an excellent one-sided surface finish [42].

Filament Winding

Depending on the situation, filament winding is often used for both open and closed constructions. Using a mandrel that is swung around a spindle, filaments are wound under stress to create the composite material. By following the axis of the rotating mandrel, a moving eye simultaneously deposits fibers where required. In this way it is possible to produce convex shapes. Low viscosity resins are often preferred [81] and in the case of natural fiber composites, custom grades of epoxy resins have been used [70].

Table 8. Mechanical characteristics of composites reinforced with natural fibers

Fiber	Tensile strength (MPa)	Young's modulus (GPa)	Flexural strength (MPa)	Reference
Abaca	100–980	6.2–20	–	[38]
Bamboo	140–800	11–32	32	[29, 42]
Banana	600	17.85	76.53	[29, 54]
Cotton	400	12	43.3	[1, 93]
Jute	320–800	8–78	45	[42, 68]
Kenaf	930	53	74	[94]
Palm	377	2.75	24.4	[77, 95]
Ramie	500	44	–	[1]
Sisal	600–700	38	288.6	[1]
Henequen	430–570	10.1–16.3	95	[41, 96, 97]

Compression Molding

It is a widely used technique in the field of thermoplastic matrices, especially when dealing with loose chopped fibers, short or long fiber mats and structures that may be very uneven or aligned. This technique can also be used with thermoset matrices. Fibers are usually laid in various configurations with sheets of thermoplastic resin before heat and pressure are applied to form a stronger structure. Typically, the material is heated, placed in an open cavity, reheated and then pressed into the mold. [79, 80, 82].

Injection Molding

The substance contained within a barrel that has been heated an injection molding machine is melted by the combined action of fluctuating temperatures and the frictional motion of the barrel. Following its introduction by an injection nozzle into the mold cavity, the molten plastic solidifies to assume the geometry of the interior structure as it cools. After the components have hardened, the plate is opened, and ejector pins are used to remove the item. A transportable container holds the mold tool in place. Higher volume applications are a good fit for this technique, which produces a clean surface finish. Still, this process's tensile strength is often lower than that of other thermoset systems [83].

MECHANICAL PROPERTIES OF NFRCs

The mechanical characterization of a material includes its response to an applied load, including elastic deformation. These properties not only define the range of use of the material but also influence its durability in everyday applications. To characterize and differentiate between materials and alloys, mechanical properties are essential. The mechanical characteristics of composites reinforced with natural fibers are given in Table 8.

Lignin effectively protects plant fibers from damaging environmental conditions such as humidity and temperature [84, 85], including cellulose, hemicellulose, pectin and wax. Hydrophilicity and exposure to a wide range of weather conditions are two additional factors that shorten the life

of NFRCs. However, in humid environments, plant fibers absorb more water and have more voids in their interior, which changes their structure and affects their mechanical and impact properties [83, 85-87]. The NFRCs have become more popular in recent years due to their environmental advantages over synthetic fibers. These advantages include recyclability, biodegradability, energy efficiency and light-weight [88–92].

SUSTAINABILITY OF NFRCs

The "green" term is frequently linked with NFRCs, which are seen as one of the new materials of current use [94, 98–101]. This is because NFRCs break down into their component parts when composites decompose, making them biodegradable [102]. Sustainability, biodegradability, and recyclability can impact the climate in the present and the future [102-105]. The global movement towards eco-friendly materials is generating significant interest as it advocates for stricter regulations and legislation to combat harmful materials. Specifically, NFRCs are being promoted as a green material by the researchers in this context [106, 107]. A significant amount of NFRCs is produced by NFs. Traditional fiber-reinforced composites, like glass, use 54.7 MJ/kg of energy to produce, while NFRCs use just 9.55 MJ/kg [108]. Compared to fiber composites, non-fiber reinforced plastics have a lower environmental impact. Products with eco-friendly features, such as biodegradability and renewability, are seeing increased demand in the market because of their reduced impact on the environment [109-113]. NFs also generate revenue through the production process, which is an additional significant benefit. Also, the land utilized in the production of NF can be repeatedly cultivated. As an example, in addition to fibers, seeds, substances, and oils are produced during the processing of hemp and flax, which have various significant applications, such as the production of nutritional supplements for people [114]. Additionally, the mass that is made can be broken down naturally at the end of its functioning period. For example, a sector of the economy that generates 64.3 billion nuts annually already produces coir strands as a waste product [115-118].

Table 9. Recent applications of some NFRCs [122]

Fiber	Application
Coir	Cases for mirrors, brooms as well as brushes, doors with flush shutters, cushions for seats, upholstery filler, yarns and ropes for nets, and roofing sheets
Cotton	Industries for furniture, textiles, and yarn
Flax	Bicycle frames, decking, fencing, window frames, tennis rackets, and snowboarding
Hemp	Textile, paper, electrical, cordage, and furniture industries
Jute	Construction panels, chipboards, construction materials, door frames and shutters and geotextiles
Kenaf	Mobile device cases, insulation, bags, packing supplies, and bedding for animals
Ramie	Manufacturing of paper, fishing nets, home furnishings, packaging, sewing threads, and clothes
Sisal	The construction industry produces doors, panels, roofing sheets, and other products.

POTENTIAL APPLICATIONS OF NFRCs

The use of NFRCs as a viable alternative to glass fiber, albeit to a lesser extent than carbon fiber composites, has become increasingly widespread in a wide range of engineering applications. Some of their notable advantages are their low specific weight, affordability, biodegradability at the end of life and renewability. NFRCs are becoming increasingly popular in the transportation (vehicle) industries, especially in the case of indoor uses like boot linings, protection against the sun, door panels, seat backs and external underfloor panels [7, 113]. Already in 2004, the BMW Group used approximately 10,000 tons of natural fibers in its manufacturing processes. In addition, the aerospace industry has embraced the use of natural fiber composites for aircraft interior trim [16]. There is increasing evidence that natural fiber composites (NFRCs) can be efficiently converted into load-bearing structural elements suitable for infrastructure and other structural applications [27, 114]. In addition, current research initiatives aim to promote the use of sisal and coconut fiber composites as a substitute for asbestos in roofing components. [44, 79-82]. The environmental impact of NFRCs is lower than that of synthetic fiber-reinforced composites. Due to their biodegradability, lightweight, affordability and lack of environmental impact, natural plant fibers are promising for use in industrial applications [119, 120]. On the other hand, researchers are promoting the use of NFRCs in particular in this context [110]. Hemp, flax and kenaf are natural plant fibers that have many uses, including in the aerospace, automotive, marine, construction and packaging industries [121]. The sports industry, including water sports, is heavily involved in the application of natural fiber composites (NFRCs) due to the improved performance that can be achieved through their use. Table 9 lists some of the advanced manufacturing applications of NFRCs in this sector.

FUTURE PROSPECTS

Natural fibers are a low-cost, lightweight and environmentally friendly substitute for glass fibers in polymer composites and their use is rapidly becoming the norm. NFRCs are used in a wide range of sectors including transporta-

tion, energy, construction and domestic appliances. When exposed to high levels of moisture, it is inevitable that the fiber/matrix interface will deteriorate, leading to distortion of dimensional properties and poor stress transfer in all plant fiber composites. In addition, moisture distribution within the composite, temperature, humidity, matrix, and fiber content are some of the many factors that influence moisture uptake. Environmental characterization of NFRCs has become an important and time-consuming component of evaluating the physical characteristics of composites in dissimilar ecological circumstances. This review paper has covered a lot of ground in its discussion of the environmental impact of NFRCs, drawing on a large body of literature. Particular attention has been paid to studies that have investigated the effects of moisture uptake by plant fibers on polymer matrices and how these effects manifest themselves in composite laminates that have undergone impact testing at low, elevated and cryogenic temperatures. Several impact characteristics have been highlighted and addressed. While the NFRCs have made great strides in focusing research studies, there are still some gaps that need to be filled.

CONCLUSION

Natural fibers, also known as plant cellulose fibers, are a novel material that can replace composite materials in various industries. Comparative studies of natural fibers with other reinforced composites have highlighted the environmental benefits of natural fibers, making them more suitable for practical use in industry. As a result, the integration of NFRCs with personal armour technologies has been actively explored by materials scientists and engineers. Each type of natural fiber has different chemical characteristics: bamboo and hemp have higher hemicellulose content, cotton has higher cellulose and kenaf content, and bamboo has higher lignin content. The difference in fiber content by weight contributes to the difference in density between natural and synthetic fibers, promoting environmental sustainability. This has led to the widespread adoption of natural fibers as an alternative to synthetic fibers, not only because of their environmentally friendly properties but also for their applications in the engineering and construction industries, promoting eco-

conomic growth in rural areas. The motivation for replacing glass fibers with biofibers is the environmental impact, health problems, cost and energy requirements. Natural based fibers are derived from various parts of plants. The study findings suggest that enhancing the properties of composites using natural fibers could offer promising avenues for improving environmental sustainability. The environmental impact of the NFRCs is quite low, making them suitable for various sustainable engineering applications. Numerical tools can be used to help characterize mechanical properties of composites, which enable the design of innovative composites and saving time.

DATA AVAILABILITY STATEMENT

The author confirm that the data that supports the findings of this study are available within the article. Raw data that support the finding of this study are available from the corresponding author, upon reasonable request.

CONFLICT OF INTEREST

The author declared no potential conflicts of interest with respect to the research, authorship, and/or publication of this article.

USE OF AI FOR WRITING ASSISTANCE

Not declared.

ETHICS

There are no ethical issues with the publication of this manuscript.

REFERENCES

- [1] P. Wambua, J. Ivens, and I. Verpoest, “Natural fibers: can they replace glass in fiber reinforced plastics?,” *Composites Science and Technology*, Vol. 63(9), pp. 1259–1264, 2003. [\[CrossRef\]](#)
- [2] A. K. Mohanty, L. T. Drzal, and M. Misra, “Engineered natural fiber reinforced polypropylene composites: influence of surface modifications and novel powder impregnation processing,” *Journal of Adhesion Science and Technology*, Vol. 16(8), pp. 999–1015, 2002. [\[CrossRef\]](#)
- [3] R. A. Kurien, D. P. Selvaraj, M. Sekar, M. C. P. Koshy, C. Paul, S. Palanisamy, C. Santulli, and P. Kumar, “A comprehensive review on the mechanical, physical, and thermal properties of abaca fiber for their introduction into structural polymer composites,” *Cellulose*, pp. 1–22, 2023.
- [4] S. Palanisamy, K. Vijayananth, T. M. Murugesan, M. Palaniappan, and C. Santulli, “The prospects of natural fiber composites: A brief review,” *International Journal of Lightweight Materials and Manufacture*, 2024. [Epub ahead of print]. doi: 10.1016/j.ijlmm.2024.01.003. [\[CrossRef\]](#)
- [5] N. Uddin, *Developments in fiber-reinforced polymer (FRP) composites for civil engineering*. Elsevier, 2013.
- [6] M. Y. Khalid, A. Al Rashid, Z. U. Arif, W. Ahmed, H. Arshad, and A. A. Zaidi, “Natural fiber reinforced composites: Sustainable materials for emerging applications,” *Results in Engineering*, Vol. 11, Article 100263, 2021. [\[CrossRef\]](#)
- [7] C. Santulli, S. Palanisamy, and S. Dharmalingam, “Natural fibers-based bio-epoxy composites: mechanical and thermal properties,” in *Epoxy-Based Biocomposites*, CRC Press, pp. 163–176, 2023. [\[CrossRef\]](#)
- [8] K. L. Pickering, M. G. A. Efenfy, and T. M. Le, “A review of recent developments in natural fiber composites and their mechanical performance,” *Composites Part A: Applied Science and Manufacturing*, Vol. 83, pp. 98–112, 2016. [\[CrossRef\]](#)
- [9] B. Dahlke, H. Larbig, H. D. Scherzer, and R. Poltrock, “Natural fiber reinforced foams based on renewable resources for automotive interior applications,” *Journal of cellular plastics*, Vol. 34(4), pp. 361–379, 1998. [\[CrossRef\]](#)
- [10] S. Palanisamy, M. Kalimuthu, C. Santulli, R. Nagarajan, and G. Karuppiah, “Effect of Extraction Methods on the Properties of Bast Fibers,” in *Bast Fibers and Their Composites: Processing, Properties and Applications*, Springer, pp. 17–37, 2022. [\[CrossRef\]](#)
- [11] A. C. N. Singleton, C. A. Baillie, P. W. R. Beaumont, and T. Peijs, “On the mechanical properties, deformation and fracture of a natural fiber/recycled polymer composite,” *Composites Part B: Engineering*, Vol. 34(6), pp. 519–526, 2003. [\[CrossRef\]](#)
- [12] N. Shah, J. Fehrenbach, and C. A. Ulven, “Hybridization of hemp fiber and recycled-carbon fiber in polypropylene composites,” *Sustainability*, Vol. 11(11), Article 3163, 2019. [\[CrossRef\]](#)
- [13] M. Asim, M. Jawaid, M. Nasir, and N. Saba, “Effect of fiber loadings and treatment on dynamic mechanical, thermal and flammability properties of pineapple leaf fiber and kenaf phenolic composites,” *Journal of Renewable Materials*, Vol. 6(4), Article 383, 2018. [\[CrossRef\]](#)
- [14] C. Santulli, S. Palanisamy, and M. Kalimuthu, “Pineapple fibers, their composites and applications,” in *Plant Fibers, their Composites, and Applications*, Elsevier, pp. 323–346, 2022. [\[CrossRef\]](#)
- [15] S. Palanisamy, M. Kalimuthu, M. Palaniappan, A. Alavudeen, N. Rajini, C. Santulli, F. Mohammad, and H. Al-Lohedan, “Characterization of acacia caesia bark fibers (ACBFs),” *Journal of Natural Fibers*, Vol. 19(15), pp. 10241–10252, 2022. [\[CrossRef\]](#)
- [16] O. Faruk, A. K. Bledzki, H.-P. Fink, and M. Sain, “Biocomposites reinforced with natural fibers: 2000–2010,” *Progress in Polymer Science*, Vol. 37(11), pp. 1552–1596, 2012. [\[CrossRef\]](#)
- [17] M. J. John, and S. Thomas, “Biofibers and biocomposites,” *Carbohydrate polymers*, Vol. 71(3), pp. 343–364, 2008. [\[CrossRef\]](#)
- [18] S. K. Ramamoorthy, M. Skrifvars, and A. Persson, “A review of natural fibers used in biocomposites: Plant, animal and regenerated cellulose fibers,” *Polymer Reviews*, Vol. 55(1), pp. 107–162, 2015. [\[CrossRef\]](#)

- [19] M. Butnariu, and A. I. Flavius, "General information about cellulose," *Biotechnol Bioprocess*, Vol. 3(3), pp. 2314–2766, 2022.
- [20] E. Zini, and M. Scandola, "Green composites: an overview," *Polymer Composites*, Vol. 32(12), pp. 1905–1915, 2011. [CrossRef]
- [21] M. Jacob, S. Thomas, and K. T. Varughese, "Mechanical properties of sisal / oil palm hybrid fiber reinforced natural rubber composites," *Composites Science and Technology*, Vol. 64, pp. 955–965, 2004. [CrossRef]
- [22] A. Kicińska-Jakubowska, E. Bogacz, and M. Zimniewska, "Review of natural fibers. Part I—Vegetable fibers," *Journal of Natural Fibers*, Vol. 9(3), pp. 150–167, 2012. [CrossRef]
- [23] A. Céline, S. Fréour, F. Jacquemin, and P. Casari, "The hygroscopic behavior of plant fibers: a review," *Frontiers in Chemistry*, Vol. 1, Article 43, 2014. [CrossRef]
- [24] P. Suman, A. L. Naidu, and P. R. Rao, "Processing and mechanical behaviour of hair fiber reinforced polymer metal matrix composites," in *International Conference on Recent Innovations in Engineering and Technology (ICRIET-2k16)*, Organized by Gandhi Institute of Engineering and Technology, Gunpur on 5th & 6th November-2016, 2016.
- [25] H. Chen, "Chemical composition and structure of natural lignocellulose," in *Biotechnology of lignocellulose*, Springer, pp. 25–71, 2014. [CrossRef]
- [26] A. K. Mohanty, M. Misra, and L. T. Drzal, "Natural fibers, biopolymers, and biocomposites," CRC Press, 2005. [CrossRef]
- [27] M. M. Ibrahim, A. Dufresne, W. K. El-Zawawy, and F. A. Agblevor, "Banana fibers and microfibrils as lignocellulosic reinforcements in polymer composites," *Carbohydrate Polymers*, Vol. 81(4), pp. 811–819, 2010. [CrossRef]
- [28] M. Joonobi, J. Harun, P. M. Tahir, L. H. Zaini, S. SaifulAzry, and M. D. Makinejad, "Characteristic of nanofibers extracted from kenaf core," *BioResources*, Vol. 5(4), pp. 2556–2566, 2010. [CrossRef]
- [29] P. H. F. Pereira, M. D. F. Rosa, M. O. H. Cioffi, K. C. C. D. C. Benini, A. C. Milanese, H. J. C. Voorwald, and D. R. Mulinari, "Vegetal fibers in polymeric composites: a review," *Polímeros*, Vol. 25, pp. 9–22, 2015. [CrossRef]
- [30] M. M. Rao, and K. Mohan Rao, "Extraction and tensile properties of natural fibers: Vakka, date and bamboo," *Composite Structures*, Vol. 77, pp. 288–295. [CrossRef]
- [31] G. Karuppiyah, K. C. Kuttalam, and M. Palaniappan, "Multiobjective optimization of fabrication parameters of jute fiber / polyester composites with egg shell powder and nanoclay filler," *Molecules*, Vol. 25(23), Article 5579, 2020. [CrossRef]
- [32] L. Mwaikambo, "Review of the history, properties and application of plant fibers," *African Journal of Science and Technology*, Vol. 7(2), Article 121, 2006.
- [33] Y.-F. Wang, Z. Jankauskiene, C. S. Qiu, E. Gruzdeviene, S. H. Long, E. Alexopoulou, Y. Guo, J. Szopa, D. M. Hao, A. L. Fernando, and H. Wang, H, "Fiber flax breeding in China and Europe," *Journal of Natural Fibers*, Vol. 15(3), pp. 309–324, 2018. [CrossRef]
- [34] K. R. Sumesh, A. Ajithram, S. Palanisamy, and V. Kavimani, "Mechanical properties of ramie/flax hybrid natural fiber composites under different conditions," *Biomass Conversion and Biorefinery*, pp. 1–12, 2023. [CrossRef]
- [35] M. J. A. Van den Oever, H. L. Bos, and M. Van Kemenade, "Influence of the physical structure of flax fibers on the mechanical properties of flax fiber reinforced polypropylene composites," *Applied Composite Materials*, Vol. 7(5), pp. 387–402, 2000.
- [36] S. Sharma, S. S. Nair, Z. Zhang, A. J. Ragauskas, and Y. Deng, "Characterization of micro fibrillation process of cellulose and mercerized cellulose pulp," *RSC Advances*, Vol. 5(77), pp. 63111–63122, 2015. [CrossRef]
- [37] C. C. Sun, "True density of microcrystalline cellulose," *Journal of Pharmaceutical Sciences*, Vol. 94(10), pp. 2132–2134, 2005. [CrossRef]
- [38] D. B. Dittenber, and H. V. S. GangaRao, "Critical review of recent publications on use of natural composites in infrastructure," *Composites Part A: Applied Science and Manufacturing*, Vol. 43(8), pp. 1419–1429, 2012. [CrossRef]
- [39] T. M. Murugesan, S. Palanisamy, C. Santulli, and M. Palaniappan, "Mechanical characterization of alkali treated *Sansevieria cylindrica* fibers–Natural rubber composites," *Materials Today: Proceedings*, Vol. 62, pp. 5402–5406, 2022. [CrossRef]
- [40] E. Jayamani, S. Hamdan, M. R. Rahman, and M. K. Bin Bakri, "Comparative study of dielectric properties of hybrid natural fiber composites," *Procedia Engineering*, Vol. 97, pp. 536–544, 2014. [CrossRef]
- [41] A. L. Naidu, B. Sudarshan, and K. H. Krishna, "Study on mechanical behavior of groundnut shell fiber reinforced polymer metal matrix composites," *International Journal of Engineering Research & Technology*, Vol. 2(2), pp. 1–6, 2013.
- [42] E. Omrani, P. L. Menezes, and P. K. Rohatgi, "State of the art on tribological behavior of polymer matrix composites reinforced with natural fibers in the green materials world," *Engineering Science and Technology, an International Journal*, vol. 19(2), pp. 717–736, 2016. [CrossRef]
- [43] L. U. Devi, S. S. Bhagawan, and S. Thomas, "Mechanical properties of pineapple leaf fiber-reinforced polyester composites," *Journal of Applied Polymer Science*, Vol. 64(9), pp. 1739–1748, 1997. [CrossRef]
- [44] M. Jonoobi, M. Jonoobi, R. Oladi, Y. Davoudpour, K. Oksman, A. Dufresne, Y. Hamzeh, and R. Davoodi, "Different preparation methods and properties of nanostructured cellulose from various natural resources and residues: a review," *Cellulose*, Vol. 22, pp. 935–969, 2015. [CrossRef]

- [45] R. P. de Melo, M. F. V. Marques, P. Navard, and N. P. Duque, "Degradation studies and mechanical properties of treated curauá fibers and microcrystalline cellulose in composites with polyamide 6," *Journal of Composite Materials*, Vol. 51(25), pp. 3481–3489, 2017. [CrossRef]
- [46] R. Badrinath, and T. Senthilvelan, "Comparative investigation on mechanical properties of banana and sisal reinforced polymer based composites," *Procedia Materials Science*, Vol. 5, pp. 2263–2272, 2014. [CrossRef]
- [47] X. Li, and G. L. Tabil, and S. Panigrahi, "Chemical treatments of natural fiber for use in natural fiber-reinforced composites: A review," *Journal of Polymers and the Environment*, Vol. 15(1), pp. 25–33, 2007. [CrossRef]
- [48] N. A. Nordin, F. M. Yusof, S. Kasolang, Z. Salleh, and M. A. Ahmad, "Wear rate of natural fiber: long kenaf composite," *Procedia Engineering*, Vol. 68, pp. 145–151, 2013. [CrossRef]
- [49] G. Karuppiyah, K. C. Kuttalam, N. Ayrilmis, R. Nagarajan, M. I. Devi, S. Palanisamy, and C. Santulli, "Tribological analysis of jute/coir polyester composites filled with eggshell powder (ESP) or nanoclay (NC) using grey rational method," *Fibers*, Vol. 10(7), Article 60, 2022. [CrossRef]
- [50] A. G. Adeniyi, D. V. Onifade, J. O. Ighalo, and A. S. Adeoye, "A review of coir fiber reinforced polymer composites," *Composites Part B: Engineering*, Vol. 176, Article 107305, 2019. [CrossRef]
- [51] S. Palanisamy, M. Kalimuthu, S. Dharmalingam, A. Alavudeen, R. Nagarajan, S. O. Ismail, S. Siengchin, F. Mohammad, and H. A. Al-Lohedan, "Effects of fiber loadings and lengths on mechanical properties of Sansevieria Cylindrica fiber reinforced natural rubber biocomposites," *Materials Research Express*, Vol. 10(8), Article 85503, 2023. [CrossRef]
- [52] S.-J. Park, and M.-K. Seo, "Modeling of fiber-matrix interface in composite materials," *Interface Science and Technology*, Vol. 18, pp. 739–776, 2011. [CrossRef]
- [53] A. Gani, M. Ibrahim, F. Ulmi, and A. Farhan, "The influence of different fiber sizes on the flexural strength of natural fiber-reinforced polymer composites," *Results in Materials*, Vol. 21, Article 100534, 2024. [CrossRef]
- [54] D. C. William, "Materials science and engineering: An introduction," John Wiley, 2014.
- [55] S. Palanisamy, T. M. Murugesan, M. Palaniappan, C. Santulli, and N. Ayrilmis, "Use of hemp waste for the development of myceliumgrown matrix biocomposites: A concise bibliographic review," *BioResources*, Vol. 18(4), pp. 8771–8780, 2023. [CrossRef]
- [56] M. Ramesh, K. Palanikumar, and K. H. Reddy, "Comparative evaluation on properties of hybrid glass fiber-sisal/jute reinforced epoxy composites," *Procedia Engineering*, Vol. 51, pp. 745–750, 2013. [CrossRef]
- [57] V. Mishra and S. Biswas, "Physical and mechanical properties of bi-directional jute fiber epoxy composites," *Procedia Engineering*, Vol. 51, pp. 561–566, 2013. [CrossRef]
- [58] M. Ramesh, T. S. A. Atreya, U. S. Aswin, H. Eashwar, and C. Deepa, "Processing and mechanical property evaluation of banana fiber reinforced polymer composites," *Procedia Engineering*, Vol. 97, pp. 563–572, 2014. [CrossRef]
- [59] G. D. Babu, K. S. Babu, and P. N. Kishore, "Tensile and wear behavior of calotropis gigantea fruit fiber reinforced polyester composites," *Procedia Engineering*, Vol. 97, pp. 531–535, 2014. [CrossRef]
- [60] N. Klinklow, S. Padungkul, S. Kanthong, S. Patcharaphun, and R. Techapiesanchaorenkij, "Development of a kraft paper box lined with thermal-insulating materials by utilizing natural wastes," *Key Engineering Materials*, Vol. 545, pp. 82–88, 2013. [CrossRef]
- [61] S. Ashworth, J. Rongong, P. Wilson, and J. Meredith, "Mechanical and damping properties of resin transfer moulded jute-carbon hybrid composites," *Composites Part B: Engineering*, Vol. 105, pp. 60–66, 2016. [CrossRef]
- [62] M. Praveen Kumar, R. V. Mangalaraja, S. Karazhanov, T. F. de Oliveira, M. Sasikumar, G. Murugadoss, S. Mubarak, S. Palanisamy, and N. Kumaresan, "An overview of noble-metal-free nanostructured electrocatalysts for overall water splitting," *Materials Technology for the Energy and Environmental Nexus*, Vol. 1, pp. 1–3, 2023. [CrossRef]
- [63] S. Siengchin, and R. Dangtungee, "Polyethylene and polypropylene hybrid composites based on nano silicon dioxide and different flax structures," *Journal of Thermoplastic Composite Materials*, Vol. 27(10), pp. 1428–1447, 2014. [CrossRef]
- [64] S. M. S. Kumar, D. and Duraibabu, and K. Subramanian, "Studies on mechanical, thermal and dynamic mechanical properties of untreated (raw) and treated coconut sheath fiber reinforced epoxy composites," *Materials & Design*, Vol. 59, pp. 63–69, 2014. [CrossRef]
- [65] F. Costa, and J. R. M. d'Almeida, "Effect of water absorption on the mechanical properties of sisal and jute fiber composites," *Polymer-Plastics Technology and Engineering*, Vol. 38(5), pp. 1081–1094, 1999. [CrossRef]
- [66] B. Ly, W. Thielemans, A. Dufresne, D. Chaussy, and M. N. Belgacem, "Surface functionalization of cellulose fibers and their incorporation in renewable polymeric matrices," *Composites Science and Technology*, Vol. 68(15–16), pp. 3193–3201, 2008. [CrossRef]
- [67] H. Ma, Y. Li, Y. Shen, L. Xie, and D. Wang, "Effect of linear density and yarn structure on the mechanical properties of ramie fiber yarn reinforced composites," *Composites Part A: Applied Science and Manufacturing*, Vol. 87, pp. 98–108, 2016. [CrossRef]

- [68] A. K. Mohanty, M. A. Khan, S. Sahoo, and G. Hinrichsen, "Effect of chemical modification on the performance of biodegradable jute yarn-Biopol® composites," *Journal of Materials Science*, Vol. 35(10), pp. 2589–2595, 2000.
- [69] M. Dun, J. Hao, W. Wang, G. Wang, and H. Cheng, "Sisal fiber reinforced high density polyethylene pre-preg for potential application in filament winding," *Composites Part B: Engineering*, Vol. 159, pp. 369–377, 2019. [CrossRef]
- [70] P. Lehtiniemi, K. Dufva, T. Berg, M. Skrifvars, and P. Järvelä, "Natural fiber-based reinforcements in epoxy composites processed by filament winding," *Journal of reinforced plastics and composites*, Vol. 30(23), pp. 1947–1955, 2011. [CrossRef]
- [71] M. Abdelmouleh, S. Boufi, M. N. Belgacem, and A. Dufresne, "Short natural-fiber reinforced polyethylene and natural rubber composites: effect of silane coupling agents and fibers loading," *Composites Science and Technology*, Vol. 67(7–8), pp. 1627–1639, 2007. [CrossRef]
- [72] A. Gopinath, M. S. Kumar, and A. Elayaperumal, "Experimental investigations on mechanical properties of jute fiber reinforced composites with polyester and epoxy resin matrices," *Procedia Engineering*, Vol. 97, pp. 2052–2063, 2014. [CrossRef]
- [73] K. Oksman, M. Skrifvars, and J.-F. Selin, "Natural fibers as reinforcement in polylactic acid (PLA) composites," *Composites Science and Technology*, Vol. 63(9), pp. 1317–1324, 2003. [CrossRef]
- [74] S. M. da Luz, A. R. Goncalves, and A. P. Del'Arco Jr, "Mechanical behavior and microstructural analysis of sugarcane bagasse fibers reinforced polypropylene composites," *Composites Part A: Applied Science and Manufacturing*, Vol. 38(6), pp. 1455–1461, 2007. [CrossRef]
- [75] Y. Ruksakulpiwat, N. Suppakarn, W. Sutapun, and W. Thomthong, "Vetiver–polypropylene composites: physical and mechanical properties," *Composites Part A: Applied Science and Manufacturing*, Vol. 38(2), pp. 590–601, 2007. [CrossRef]
- [76] M. M. Thwe and, K. Liao, "Effects of environmental aging on the mechanical properties of bamboo–glass fiber reinforced polymer matrix hybrid composites," *Composites Part A: Applied Science and Manufacturing*, Vol. 33(1), pp. 43–52, 2002. [CrossRef]
- [77] S. Srisuwan, N. Prasoetsopha, and N. Suppakarn, "The effects of alkalized and silanized woven sisal fibers on mechanical properties of natural rubber modified epoxy resin," *Energy Procedia*, Vol. 56, pp. 19–25, 2014. [CrossRef]
- [78] H. Rashnal, I. Aminul, V. V Aart, and V. Ignaas, "Tensile behaviour of environment friendly jute epoxy laminated composite," *Procedia Engineering*, Vol. 56, pp. 782–788, 2013. [CrossRef]
- [79] K. Srinivas, A. L. Naidu, and M. V. A. R. Bahubalendruni, "A review on chemical and mechanical properties of natural fiber reinforced polymer composites," *International Journal of Performability Engineering*, Vol. 13(2), Article 189, 2017. [CrossRef]
- [80] H. Ku, H. Wang, N. Pattarachaiyakoop, and M. Trada, "Composites : Part B A review on the tensile properties of natural fiber reinforced polymer composites," *Composites Part B: Engineering*, Vol. 42, pp. 856–873, 2011. [CrossRef]
- [81] V. Fiore, T. Scalici, G. Di Bella, and A. Valenza, "A review on basalt fiber and its composites," *Composites Part B: Engineering*, Vol. 74, pp. 74–94, 2015. [CrossRef]
- [82] J. Summerscales, A. Virk, and W. Hall, "A review of bast fibers and their composites: Part 3–Modelling," *Composites Part A: Applied Science and Manufacturing*, Vol. 44, pp. 132–139, 2013. [CrossRef]
- [83] Y. Zou, N. Reddy, and Y. Yang, "Reusing polyester/cotton blend fabrics for composites," *Composites Part B: Engineering*, Vol. 42(4), pp. 763–770, 2011. [CrossRef]
- [84] M. Z. Rong, M. Q. Zhang, Y. Liu, G. C. Yang, and H. M. Zeng, "The effect of fiber treatment on the mechanical properties of unidirectional sisal-reinforced epoxy composites," *Composites Science and Technology*, Vol. 61(10), pp. 1437–1447, 2001. [CrossRef]
- [85] S. Palanisamy, M. Kalimuthu, C. Santulli, M. Palaniappan, R. Nagarajan, and C. Fragassa, "Tailoring epoxy composites with acacia caesia bark fibers: Evaluating the effects of fiber amount and length on material characteristics," *Fibers*, Vol. 11(7), Article 63, 2023. [CrossRef]
- [86] F. de Andrade Silva, N. Chawla, and R. D. de Toledo Filho, "Tensile behavior of high performance natural (sisal) fibers," *Composites Science and Technology*, Vol. 68(15–16), pp. 3438–3443, 2008. [CrossRef]
- [87] V. K. Thakur, M. K. Thakur, and R. K. Gupta, "Review : Raw natural fiber – based polymer composites," *International Journal of Polymer Analysis and Characterization*, Vol. 19(3), pp. 256–271, 2014. [CrossRef]
- [88] M. M. Kabir, H. Wang, T. Aravinthan, F. Cardona, and K.-T. Lau, "Effects of natural fiber surface on composite properties: A review," in *Proceedings of the 1st international postgraduate conference on engineering, designing and developing the built environment for sustainable wellbeing (eddBE2011)*, pp. 94–99, 2011.
- [89] A. Moudood, A. Rahman, H. M. Khanlou, W. Hall, A. Öchsner, and G. Francucci, "Environmental effects on the durability and the mechanical performance of flax fiber/bio-epoxy composites," *Composites Part B: Engineering*, Vol. 171, pp. 284–293, 2019. [CrossRef]
- [90] A. B. Nair, P. Sivasubramanian, P. Balakrishnan, K. A. N. Ajith Kumar, and M. S. Sreekala, "Environmental effects, biodegradation, and life cycle analysis of fully biodegradable 'green' composites," *Polymer Composites*, pp. 515–568, 2013. [CrossRef]

- [91] V. P. Arthanarieswaran, A. Kumaravel, and M. Kathirselvam, "Evaluation of mechanical properties of banana and sisal fiber reinforced epoxy composites: Influence of glass fiber hybridization," *Materials & Design*, Vol. 64, pp. 194–202, 2014. [CrossRef]
- [92] I. N. Hidayah, D. N. Syuhada, H. P. S. A. Khalil, Z. A. M. Ishak, and M. Mariatti, "Enhanced performance of lightweight kenaf-based hierarchical composite laminates with embedded carbon nanotubes," *Materials & Design*, Vol. 171, Article 107710, 2019. [CrossRef]
- [93] V. Paul, K. Kanny, and G. G. Redhi, "Mechanical, thermal and morphological properties of a bio-based composite derived from banana plant source," *Composites Part A: Applied Science and Manufacturing*, Vol. 68, pp. 90–100, 2015. [CrossRef]
- [94] B.-H. Lee, H.-J. Kim, and W.-R. Yu, "Fabrication of long and discontinuous natural fiber reinforced polypropylene biocomposites and their mechanical properties," *Fibers and Polymers*, Vol. 10(1), pp. 83–90, 2009. [CrossRef]
- [95] E. R. S. Goutham, S. S. Hussain, C. Muthukumar, S. Krishnasamy, T. S. Muthu Kumar, C. Santulli, S. Palanisamy, J. Parameswaranpillai, and N. Jesuarockiam, "Drilling parameters and post-drilling residual tensile properties of natural-fiber-reinforced composites: A review," *Journal of Composites Science*, Vol. 7(4), Article 136, 2023. [CrossRef]
- [96] M. P. M. Dicker, P. F. Duckworth, A. B. Baker, G. Francois, M. K. Hazzard, and P. M. Weaver, "Green composites: A review of material attributes and complementary applications," *Composites Part A: Applied Science and Manufacturing*, Vol. 56, pp. 280–289, 2014. [CrossRef]
- [97] I. M. De Rosa, J. M. Kenny, D. Puglia, C. Santulli, and F. Sarasini, "Tensile behavior of New Zealand flax (*Phormium tenax*) fibers," *Journal of Reinforced Plastics and Composites*, Vol. 29(23), pp. 3450–3454, 2010. [CrossRef]
- [98] P. S. Kumar, C. U. Kiran, and K. P. Rao, "Effect of fiber surface treatments on mechanical properties of sisal fiber polymer composites—a review," *International Journal of Advanced Research in Science, Engineering and Technology*, Vol. 4, pp. 4411–4416, 2017.
- [99] A. L. Naidu, and P. S. V. R. Rao, "A review on chemical behaviour of natural fiber composites," *International Journal of Chemical Sciences*, Vol. 14(4), pp. 2223–2238, 2016.
- [100] R. Siakeng, M. Jawaid, H. Ariffin, S. M. Sapuan, M. Asim, and N. Saba, "Natural fiber reinforced polylactic acid composites: A review," *Polymer Composites*, Vol. 40(2), pp. 446–463, 2019. [CrossRef]
- [101] O. Onuaguluchi, and N. Banthia, "Plant-based natural fiber reinforced cement composites: A review," *Cement and Concrete Composites*, Vol. 68, pp. 96–108, 2016. [CrossRef]
- [102] A. J. Adeyi, M. O. Durowoju, O. Adeyi, E. O. Oke, O. A. Olalere, and A. D. Ogunsola, "Momordica augustisepala L. stem fiber reinforced thermoplastic starch: Mechanical property characterization and fuzzy logic artificial intelligent modelling," *Results in Engineering*, Vol. 10, Article 100222, 2021. [CrossRef]
- [103] M. Fagone, F. Loccarini, and G. Ranocchiai, "Strength evaluation of jute fabric for the reinforcement of rammed earth structures," *Composites Part B: Engineering*, Vol. 113, pp. 1–13, 2017. [CrossRef]
- [104] N. M. Muhammad Hijas, P. Pramod, P. Prasanth, H. Sivam, and P. Sivasubramanian, "Development of jute fiber reinforced natural rubber composite material & determination of its mechanical properties," *IJIRST*, Vol. 3, pp. 207–212, 2017.
- [105] G. Thilagavathi, E. Pradeep, T. Kannaian, and L. Sasikala, "Development of natural fiber nonwovens for application as car interiors for noise control," *Journal of Industrial Textiles*, Vol. 39(3), pp. 267–278, 2010. [CrossRef]
- [106] N. E. Zafeiropoulos, C. A. Baillie, and J. M. Hodgkinson, "Engineering and characterisation of the interface in flax fiber/polypropylene composite materials. Part II. The effect of surface treatments on the interface," *Composites Part A: Applied Science and Manufacturing*, Vol. 33(9), pp. 1185–1190, 2002. [CrossRef]
- [107] E. A. Elbadry, M. S. Aly-Hassan, and H. Hamada, "Mechanical properties of natural jute fabric/jute mat fiber reinforced polymer matrix hybrid composites," *Advances in Mechanical Engineering*, Vol. 4, Article 354547, 2012. [CrossRef]
- [108] S. V. Joshi, L. T. Drzal, A. K. Mohanty, and S. Arora, "Are natural fiber composites environmentally superior to glass fiber reinforced composites?," *Composites Part A: Applied Science and Manufacturing*, Vol. 35(3), pp. 371–376, 2004. [CrossRef]
- [109] A. K. M. Nayab-Ul-Hossain, S. K. Sela, and S. Bin Sadeque, "Recycling of dyed fiber waste to minimize resistance and to prepare electro thermal conductive bar," *Results in Engineering*, Vol. 3, Article 100022, 2019. [CrossRef]
- [110] S. Mahmud, K. M. F. Hasan, M. A. Jahid, K. Mohiuddin, R. Zhang, and J. Zhu, "Comprehensive review on plant fiber-reinforced polymeric biocomposites," *Journal of Materials Science*, Vol. 56, pp. 7231–7264, 2021. [CrossRef]
- [111] O. S. Palanisamy, M. Kalimuthu, A. Azeez, M. Palaniappan, S. Dharmalingam, R. Nagarajan, and C. Santulli, "Wear properties and post-moisture absorption mechanical behavior of kenaf/banana-fiber-reinforced epoxy composites," *Fibers*, Vol. 10(4), Article 32, 2022. [CrossRef]
- [112] J. P. Correa, J. M. Montalvo-Navarrete, and M. A. Hidalgo-Salazar, "Carbon footprint considerations for biocomposite materials for sustainable products: A review," *Journal of Cleaner Production*, Vol. 208, pp. 785–794, 2019. [CrossRef]

- [113] V. K. Thakur, *Green composites from natural resources*. CRC Press, 2013. [\[CrossRef\]](#)
- [114] R. N. Arancon, “Market and trade of coconut products: Expert’s consultation on coconut sector development in Asia and the Pacific,” Asian and Pacific coconut community, Bangkok, 2013.
- [115] E. C. Botelho, R. A. Silva, L. C. Pardini, and M. C. Rezende, “A review on the development and properties of continuous fiber/epoxy/aluminum hybrid composites for aircraft structures,” *Materials Research*, Vol. 9, pp. 247–256, 2006. [\[CrossRef\]](#)
- [116] A. Ticoalu, T. Aravinthan, and F. Cardona, “A review of current development in natural fiber composites for structural and infrastructure applications,” in *Proceedings of the southern region engineering conference (SREC 2010)*, pp. 113–117, 2010.
- [117] A. Belaadi, A. Bezazi, M. Maache, and F. Scarpa, “Fatigue in sisal fiber reinforced polyester composites: hysteresis and energy dissipation,” *Procedia Engineering*, Vol. 74, pp. 325–328, 2014. [\[CrossRef\]](#)
- [118] S. A. S. Goulart, T. A. Oliveira, A. Teixeira, P. C. Miléo, and D. R. Mulinari, “Mechanical behaviour of polypropylene reinforced palm fibers composites,” *Procedia Engineering*, Vol. 10, pp. 2034–2039, 2011. [\[CrossRef\]](#)
- [119] W. Wang, M. Sain, and P. A. Cooper, “Study of moisture absorption in natural fiber plastic composites,” *Composites Science and Technology*, Vol. 66(3–4), pp. 379–386, 2006. [\[CrossRef\]](#)
- [120] R. Kumar, M. I. Ul Haq, A. Raina, and A. Anand, “Industrial applications of natural fiber-reinforced polymer composites—challenges and opportunities,” *International Journal of Sustainable Engineering*, Vol. 12(3), pp. 212–220, 2019. [\[CrossRef\]](#)
- [121] Y. G. Thyavihalli Girijappa, S. Mavinkere Rangappa, J. Parameswaranpillai, and S. Siengchin, “Natural fibers as sustainable and renewable resource for development of eco-friendly composites: a comprehensive review,” *Frontiers in Materials*, Vol. 6, Article 226, 2019. [\[CrossRef\]](#)
- [122] L. Mohammed, M. N. M. Ansari, G. Pua, M. Jawaid, and M. S. Islam, “A review on natural fiber reinforced polymer composite and its applications,” *International Journal of Polymer Science*, Vol. 2015, Article 243947, 2015. [\[CrossRef\]](#)



Review Article

Application of Scheffe's Simplex Lattice Model in concrete mixture design and performance enhancement

Jonah AGUNWAMBA , Fidelis OKAFOR , Michael Toryila TİZA

Department of Civil Engineering, University of Nigeria, Enugu, Nigeria

ARTICLE INFO

Article history

Received: 17 December 2023

Revised: 01 March 2024

Accepted: 07 March 2024

Key words:

Concrete mix optimization;
Scheffe's Simplex Lattice Model;
Statistical methods; Material
properties; Sustainability

ABSTRACT

This comprehensive literature review delves into the application of Scheffe's Simplex Lattice Model for optimizing cement concrete mixtures, with a particular emphasis on its impact on material properties and sustainability. The review meticulously outlines the principles, historical context, and advantages of Scheffe's model, providing a nuanced understanding of its significance. Comparative analyses with traditional and alternative optimization techniques in concrete mix design illuminate the distinct advantages of statistical methods, especially Scheffe's model. The review critically examines the challenges and limitations associated with applying Scheffe's model, addressing issues related to the complexity of concrete mixtures and computational demands. Potential avenues for improvement are explored, suggesting refinements to handle non-linearity, incorporate advanced optimization algorithms, and streamline computational requirements. Additionally, the review highlights emerging trends in statistical modeling for concrete mixture optimization, such as the integration of machine learning and data-driven approaches, signaling the evolving landscape of concrete technology. In conclusion, the literature underscores Scheffe's Simplex Lattice Model as a valuable and versatile tool with far-reaching implications for the advancement of concrete mixture design methodologies. The call to action encourages ongoing research and development to refine the model, explore emerging trends, and address practical challenges, positioning Scheffe's model as a cornerstone in the pursuit of sustainable, resilient, and high-performance concrete materials.

Cite this article as: Agunwamba J, Okafor F, Tiza MT. Application of Scheffe's Simplex Lattice Model in concrete mixture design and performance enhancement. Environ Res Tec 2024;7(2)270–279.

INTRODUCTION

The optimization of concrete mixtures is crucial for ensuring the strength, durability, and overall performance of structures, especially in the face of growing demands for enhanced material properties and sustainability. The complex nature of concrete mixtures, influenced by numerous variables, poses a challenge in achieving an ideal balance. This literature review focuses on statistical methods in concrete mixture optimization, particularly Scheffe's Simplex Lattice Model, recognized for efficiently exploring and optimizing

multi-variable systems. By unraveling the model's principles and examining its applications, the review aims to contribute insights into its potential to revolutionize concrete mixture design. It comprehensively surveys existing studies, evaluating methodologies and outcomes, with the overarching goal of advancing concrete technology and providing valuable guidance to researchers and practitioners in the field. The scope encompasses a diverse range of studies, methodologies, and outcomes related to Scheffe's model, offering a holistic perspective on its successes, challenges, and future potential in shaping the future of concrete mixture design.

*Corresponding author.

*E-mail address: tizamichael@gmail.com



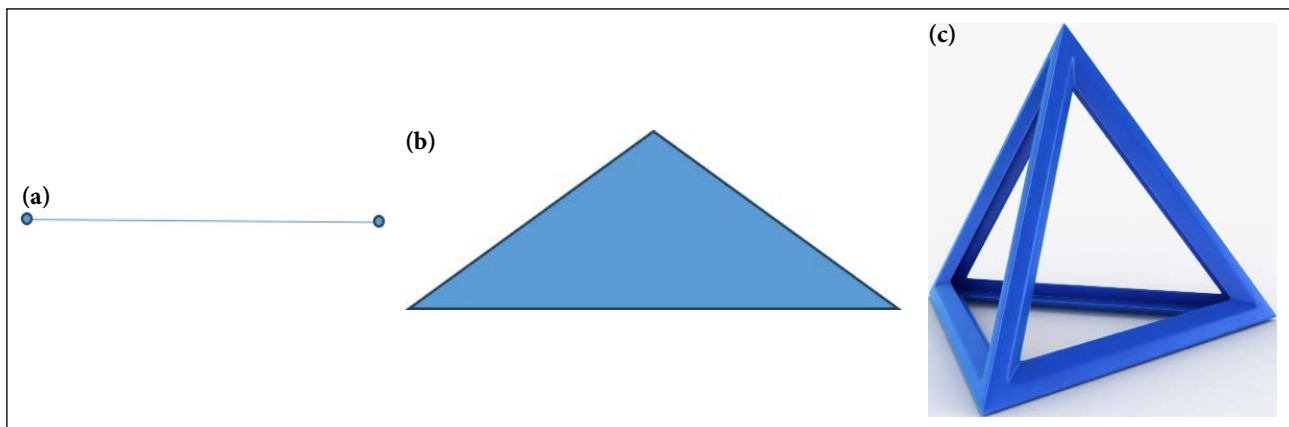


Figure 1. (a) Scheffe's simplex lattice design, when q is 2. (b) Scheffe's simplex lattice when q is 3. (c) Scheffe's simplex lattice design, when q is 4 (Tetrahedron Shape).

SCHEFFE'S SIMPLEX LATTICE MODEL OVERVIEW AND PRINCIPLES

Explanation of Scheffe's Simplex Lattice Model

Scheffe's Simplex Lattice Model is a statistical tool designed for optimizing complex systems with multiple variables. Developed by statistician Henry Scheffe (1958), this model is particularly suited for mixture design, enabling researchers and engineers to navigate intricate parameter spaces efficiently. At its core, the model employs a simplex, a geometric shape formed by connecting points in multi-dimensional space, to iteratively explore and converge towards optimal combinations of variables [1]. By systematically probing the experimental space, Scheffe's Simplex Lattice Model facilitates the identification of optimal concrete mixtures. The process begins by defining parameters $\{q, n\}$ for the Simplex Lattice Model, generating a design with uniformly spaced points for each component.

In a mixture experiment with q components, think of a lattice as a well-ordered pattern of points. For Scheffe's simplex lattice design, when q is 2, it is like 2 points forming a straight line as depicted in Figure 1a. When q is 3, it resembles an equilateral triangle as depicted in Figure 1b, and for q equal to 4, it takes the shape of a regular tetrahedron as depicted in Figure 1c.

Scheffe's idea suggests that each component in the mixture design sits on a corner (vertex) of this lattice, with a factor space of $(q-1)$. If we denote the degree of the polynomial as 'n,' a $\{q, n\}$ simplex lattice for q components has evenly spaced points created by all possible combinations of $(n+1)$ levels for each component.

Concrete properties, according to Scheffe, depend on the right proportioning of its components, not the total mass. So, Scheffe's optimization theory, using polynomial regression, helps model and optimize concrete properties.

Actual ratios are determined through experience, and pseudo ratios are calculated [2]. Experiments are conducted to obtain response values, and model equations are fitted using the Least Squares Method. The model is validated, and

mix proportions are optimized, with experiments verifying predictions. Results are analyzed, and the process concludes [3–5]. Refer to Figure 2 for the visual representation of this comprehensive flowchart.

Historical Context and Development of the Model

The historical evolution of Scheffe's Simplex Lattice Model traces back to the mid-20th century when Henry Scheffe introduced it as a powerful statistical tool [6]. Stemming from advancements in experimental design and statistical analysis, the model emerged as a response to the increasing complexity of industrial processes, including the intricate nature of concrete mixture optimization. Its development represents a pivotal moment in statistical modeling, demonstrating a tailored approach for efficiently exploring and optimizing intricate parameter spaces [7].

Basic Principles and Mathematical Foundations

The model's fundamental principles rest on the simplex method, a mathematical optimization technique used to navigate complex spaces [8]. The simplex is a geometric shape with vertices representing different combinations of variables [9]. Scheffe's model employs a systematic process of moving toward optimal combinations by iteratively adjusting the vertices. Mathematically, this involves solving linear programming problems, minimizing or maximizing an objective function subject to certain constraints [10]. The model's elegance lies in its ability to efficiently converge towards optimal solutions, even in high-dimensional spaces [10, 11].

Advantages and Unique Features of Scheffe's Simplex Lattice Model in the Context of Concrete Mixture Optimization

Scheffe's Simplex Lattice Model offers distinct advantages in the realm of concrete mixture optimization. Its systematic approach allows for the exploration of a wide range of variables simultaneously, enabling researchers to identify optimal combinations efficiently [12]. The model's adaptability to high-dimensional spaces is particularly beneficial in the intricate context of concrete mixtures, where

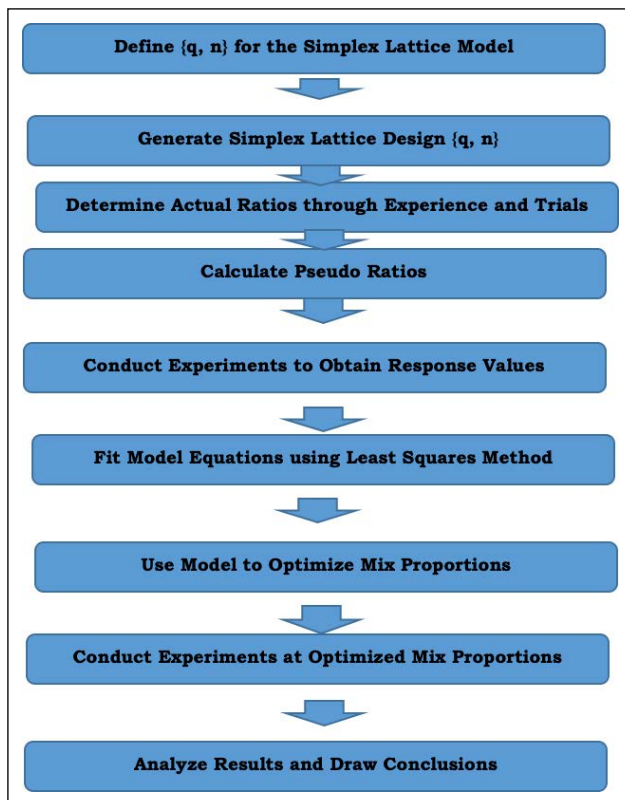


Figure 2. Visual representation of optimization process using Scheffe's Simplex Lattice Model in concrete mix design.

multiple components interact to determine the material's properties [13]. Additionally, Scheffe's model provides a structured methodology for researchers to understand and refine the relationships between variables, offering valuable insights into the optimization process. Its application in concrete mixture design demonstrates a unique ability to balance variables effectively, resulting in improved material performance and durability [14]. Table 1 summarizes the key advantages of Scheffe's Simplex Lattice Model in concrete mixture optimization.

HISTORICAL DEVELOPMENT OF MIXTURE DESIGN TECHNIQUES IN CONCRETE

Evolution of Concrete Mixture Design Methodologies

The evolution of concrete mixture design methodologies reflects a progression from empirical methods to more systematic and scientific approaches [15]. Initially, concrete mixtures were formulated based on experience and rules of thumb. Over time, advancements in material science, engineering, and statistical methods have driven the development of more sophisticated and precise mixture design techniques [16]. The evolution represents a shift towards a more comprehensive understanding of the complex interactions among various components in concrete [16]. As depicted in Figure 3, this flowchart visually represents the evolution of concrete mixture design methodologies. The progression begins with empirical methods rooted in experience and rule of thumb formulations, transitioning

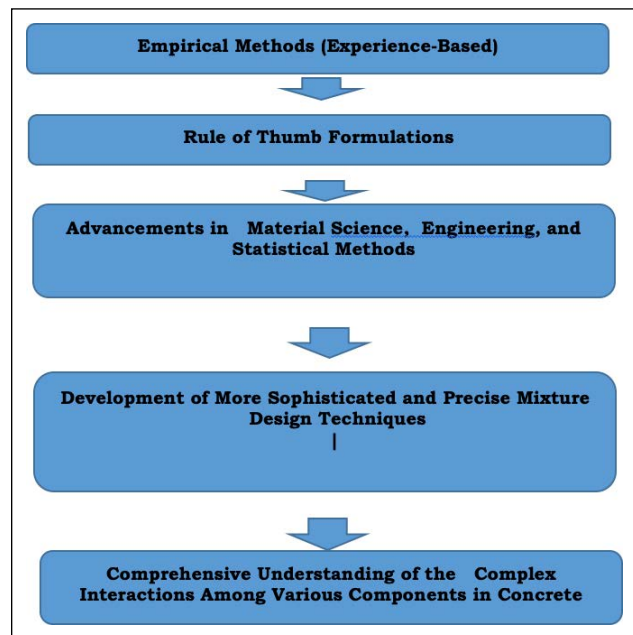


Figure 3. Flowchart visually representing the evolution of concrete mixture design methodologies.

towards more sophisticated and precise techniques driven by advancements in material science, engineering, and statistical methods.

Key Milestones and Advancements Leading to the Adoption of Statistical Methods

Key milestones in concrete mixture design include the recognition of statistical methods as powerful tools for optimizing material properties [17]. As the demand for high-performance concrete increased, researchers sought more rigorous and efficient approaches. The adoption of statistical methods gained momentum with the realization that they could systematically explore the vast design space of concrete mixtures [18]. Milestones include the integration of factorial experiments and response surface methodologies, paving the way for the utilization of advanced statistical models like Scheffe's Simplex Lattice Model [19].

Comparison with Other Optimization Techniques Used in Concrete Mix Design

Comparing statistical methods, such as Scheffe's Simplex Lattice Model, with other optimization techniques in concrete mix design reveals distinct advantages. Traditional methods often rely on trial-and-error approaches, whereas statistical models provide a systematic and data-driven framework for optimization [20]. Statistical methods can efficiently handle multiple variables simultaneously, offering a holistic approach to mixture design. In contrast, deterministic methods may struggle to navigate complex parameter spaces. Moreover, statistical models, by considering interactions between variables, contribute to a more nuanced understanding of the concrete mixture, leading to improved performance and durability compared to some traditional optimization techniques [21].

Table 1. Advantages of Scheffe's Simplex Lattice Model in concrete mixture optimization

Aspect	Description	Reference
Systematic approach	Simultaneous exploration of multiple variables for efficient identification of optimal combinations[12].	[12]
Adaptability to high-dimensional spaces	Crucial in the complex context of concrete mixtures, excelling in navigating intricate, multi-variable systems[13].	[13]
Structured methodology	Provides a systematic framework for understanding and refining relationships between variables in optimization processes[14].	[14]
Effective balancing of variables	Uniquely balances variables, contributing to improved material performance and durability in concrete mixture design[14].	[14]

Table 2. Comparative analysis of statistical methods in concrete mix design

Aspect	Comparison	Reference
Approach	Statistical methods (e.g., Scheffe's Simplex Lattice Model) provide a systematic, data-driven alternative to traditional trial-and-error approaches.	[20]
Handling multiple variables	Statistical methods efficiently manage multiple variables, offering a holistic approach, while deterministic methods may struggle in complex spaces.	[20]
Consideration of interactions	Models like Scheffe's consider interactions, contributing to nuanced understanding and improved performance.	[21]
Evolutionary milestones	Evolution highlights a shift from empirical to statistically driven approaches for precision and efficiency.	[22]
Advantages in design spaces exploration	Statistical models systematically explore complex design spaces, uncovering nuanced relationships, enhancing concrete mix design.	[23]

In summary, the evolution of concrete mixture design methodologies has witnessed a transition from empirical practices to sophisticated, statistically driven approaches. Key milestones underscore the importance of adopting statistical methods for precision and efficiency [22]. When compared with other optimization techniques, statistical models stand out for their systematic exploration of complex design spaces and their ability to uncover nuanced relationships between variables, making them valuable tools in advancing the field of concrete mix design [23]. Table 2 provides a concise comparison of statistical methods, particularly Scheffe's Simplex Lattice Model, with other optimization techniques in concrete mix design, along with relevant references.

METHODOLOGICAL APPLICATIONS IN CEMENT CONCRETE STUDIES

Review of Studies Applying Scheffe's Simplex Lattice Model in Optimizing Concrete Mixtures

Numerous studies have leveraged Scheffe's Simplex Lattice Model to optimize concrete mixtures, showcasing its versatility and effectiveness in enhancing material properties [24]. These investigations span a range of applications, from achieving specific strength requirements to improving durability and sustainability. The review highlights the methodologies employed in these studies, emphasizing the diversity of concrete mixtures addressed and the outcomes achieved through the application of Scheffe's model.

Description of Variables Considered in These Studies

In the studies employing Scheffe's Simplex Lattice Model, a variety of critical variables are systematically considered to optimize concrete mixtures. These variables often include the water-cement ratio, a crucial factor influencing both the workability and strength of concrete [24]. Aggregate types, encompassing size, gradation, and source, are meticulously examined for their impact on mechanical and durability properties [25]. Additionally, the incorporation of admixtures, such as superplasticizers or pozzolans, adds another layer of complexity to the optimization process. The literature review details how these studies strategically manipulate and assess these variables within the context of Scheffe's model to achieve desired concrete performance [26].

Discussion on How the Model Accounts for Interactions Between Different Components in the Concrete Mix

Scheffe's Simplex Lattice Model excels in its ability to account for the intricate interactions between different components in a concrete mix [27]. The model operates by systematically varying the levels of each variable, observing the resulting changes in the mixture's properties. Through this iterative process, Scheffe's model captures not only the individual effects of variables but also their interactions [28]. For instance, it assesses how the water-cement ratio influences the performance of specific aggregate types or how the addition of an admixture interacts with varying proportions of cementitious materials [29]. By comprehensively exploring these interdependencies, the model provides valuable insights into the nuanced relationships among

Table 3. Interactions among concrete Mix Components Using Scheffe's Model

Interaction type	Description	Reference
Water-cement ratio vs. aggregate types	Scheffe's model systematically analyzes how variations in the water-cement ratio influence the performance of specific aggregate types.	[29]
Admixture impact on cementitious materials	The model explores interactions, revealing how the addition of an admixture interacts with varying proportions of cementitious materials.	[29]

Table 4. Performance evaluation of concrete mixtures optimized with Scheffe's Simplex Lattice Model

Performance indicator	Description	Reference
Compressive strength	Assessment of the concrete's ability to withstand loads, a key metric reflecting its structural integrity.	[34]
Durability	Evaluation includes resistance to abrasion, freeze-thaw cycles, and chemical exposure, indicating long-term sustainability.	[34]
Workability	Analysis of the concrete's ease of placement and compaction, contributing to practical application.	[35]
Setting time	Examination of the time taken for the concrete to set, influencing construction timelines.	[35]
Shrinkage	Assessment of the concrete's tendency to shrink during curing, a critical consideration for structural integrity.	[35]

different components, guiding the optimization process towards achieving the desired concrete mixture characteristics [30]. In essence, the studies reviewed demonstrate the efficacy of Scheffe's Simplex Lattice Model in optimizing concrete mixtures by considering and manipulating key variables. The nuanced exploration of interactions between different components, facilitated by the model, contributes to a more profound understanding of the intricate relationships within concrete mixes, ultimately leading to improved and tailored material performance [31]. Table 3 succinctly outlines the ways Scheffe's Simplex Lattice Model addresses and understands the intricate interactions among different components in concrete mixes.

PERFORMANCE EVALUATION OF OPTIMIZED CONCRETE MIXTURES

Evaluation of Concrete Mixtures Optimized Using Scheffe's Simplex Lattice Model

The evaluation of concrete mixtures optimized through Scheffe's Simplex Lattice Model reveals the model's impact on enhancing material properties [32]. This process involves a systematic assessment of the optimized mixtures in real-world conditions. Researchers and practitioners critically examine the performance of the concrete to determine the effectiveness of the Scheffe's model in achieving desired outcomes [33].

Analysis of Performance Indicators

Concrete mixtures optimized using Scheffe's Simplex Lattice Model undergo a thorough analysis of various performance indicators. These indicators encompass fundamental properties such as compressive strength, a key metric reflecting the concrete's ability to withstand loads

[34]. Durability assessments, including resistance to abrasion, freeze-thaw cycles, and chemical exposure, provide insights into the long-term sustainability of the optimized mixtures. Other relevant properties, such as workability, setting time, and shrinkage, contribute to a comprehensive understanding of the concrete's overall performance [35]. The analysis delves into how Scheffe's model influences these indicators, showcasing the model's effectiveness in tailoring concrete mixtures to meet specific performance criteria. Table 4 concisely summarizes the performance evaluation of concrete mixtures optimized through Scheffe's Simplex Lattice Model, covering key indicators and their references.

Comparison with Traditional Mix Designs and Alternative Optimization Methods

A critical aspect of evaluating concrete mixtures optimized with Scheffe's Simplex Lattice Model involves comparing the results with traditional mix designs and alternative optimization methods. This comparative analysis aims to discern the advantages and limitations of Scheffe's model in achieving superior outcomes [36]. Traditional mix designs, often relying on empirical rules or trial-and-error approaches, serve as benchmarks for assessing the efficiency and precision brought about by statistical optimization [36]. Furthermore, alternative optimization methods, such as response surface methodologies or genetic algorithms, provide a basis for evaluating the unique contributions of Scheffe's model to the field of concrete mixture design. This comparative analysis informs researchers and practitioners about the relative merits and contexts in which Scheffe's Simplex Lattice Model excels [37]. Table 5 provides a concise overview of the comparative analysis of concrete mixtures optimized

Table 5. Comparison of concrete mixtures optimized with Scheffe's Simplex Lattice Model, traditional mix designs, and alternative optimization methods

Comparison aspect	Description	Reference
Optimization approach	Comparison between Scheffe's Simplex Lattice Model, traditional mix designs (empirical or trial-and-error), and alternative methods like response surface methodologies or genetic algorithms.	[36]
Efficiency and precision	Assessment of the efficiency and precision achieved by Scheffe's model in comparison to traditional methods, serving as benchmarks.	[36]
Unique contributions	Examination of the unique contributions of Scheffe's model compared to alternative optimization methods, highlighting its specific advantages in concrete mixture design.	[37]
Merits and limitations	Discussion of the relative merits and limitations of Scheffe's Simplex Lattice Model in achieving superior outcomes, informing researchers and practitioners about its contexts of excellence.	[37]

Table 6. Challenges, limitations, and areas for improvement in applying Scheffe's Simplex Lattice Model to concrete mixtures

Discussion aspect	Description	Reference
Complexity of concrete mixture	Challenges arising from the complexity of concrete mixtures involving numerous interacting variables. Model efficacy may be compromised in highly nonlinear relationships or regions where assumptions are not well met.	[37, 38]
Computational demands	Computational challenges, especially in large-scale mixtures or dealing with numerous variables simultaneously. Addressing these demands is crucial for practical applicability.	[39, 40]
Optimization challenges	Potential issues with mathematical optimization when dealing with real-world constraints. Practical constraints in construction scenarios, such as material availability and batching limitations, might not be adequately considered in the optimization process.	[40, 43]
Refinement for nonlinearity and interactions	Areas for improvement include refining the model to better handle nonlinearity and complex interactions among variables. Incorporating advanced optimization algorithms or complementary techniques could enhance adaptability.	[41]
Streamlining computational demands	Efforts to streamline computational demands, making the model more accessible for practical applications.	[39]
Incorporating probabilistic methods	Suggested refinement involves incorporating probabilistic or uncertainty analysis methods within the model to better capture real-world variability, contributing to a more robust optimization process.	[42]
Accommodating practical constraints	Refining the model to accommodate practical constraints in construction, such as material availability and batching limitations, enhancing its utility in real-world scenarios.	[42] [43]

with Scheffe's Simplex Lattice Model, traditional mix designs, and alternative optimization methods, covering key aspects and their respective references.

CHALLENGES AND LIMITATIONS

Discussion of Challenges and Limitations in Applying Scheffe's Simplex Lattice Model to Concrete Mixtures

While Scheffe's Simplex Lattice Model offers significant advantages in optimizing concrete mixtures, it is not without challenges and limitations. One notable challenge lies in the complexity of the concrete mixture itself, which often involves numerous interacting variables [37, 38]. The model's efficacy may be compromised when dealing with highly nonlinear relationships or when the optimization process encounters regions of the parameter space where the model's assumptions are not well met [39]. Additionally, the computational demands of the model may pose challenges, especially when dealing with large-scale mixtures or when considering a plethora of variables simultaneously [39, 40]. Furthermore, the reliance on mathematical optimization might overlook certain practical

constraints that can influence the feasibility of recommended mixtures in real-world construction scenarios.

Identification of Potential Areas for Improvement and Refinement of the Model

To address the challenges and enhance the applicability of Scheffe's Simplex Lattice Model in concrete mixture optimization, several areas for improvement and refinement can be considered [40]. Firstly, refining the model to better handle nonlinearity and complex interactions among variables could significantly improve its performance. Incorporating more advanced optimization algorithms or combining Scheffe's model with other complementary techniques may also enhance its adaptability to diverse concrete mixtures [41]. Moreover, efforts to streamline the computational demands of the model could make it more accessible for practical applications. Additionally, incorporating probabilistic or uncertainty analysis methods within the model could better capture real-world variability, contributing to a more robust optimization process [42]. Lastly, refining the model to accommodate

Table 7. Emerging trends in statistical modeling for concrete mixture optimization and future research directions for improving Scheffe's Simplex Lattice Model

Aspect	Description	Reference
Integration of machine learning	Emerging trend: Integration of machine learning techniques, such as neural networks and genetic algorithms, to handle complex, non-linear relationships within concrete mixtures. This trend enhances the capability to optimize mixtures effectively.	[44]
Data-driven approaches	Emerging trend: Increased use of data-driven approaches, leveraging large datasets and advanced analytics to gain insights into material behaviors. This trend enhances the effectiveness of optimizing concrete mixtures.	[45]
Probabilistic modeling and uncertainty quantification	Emerging trend: Integration of probabilistic modeling and uncertainty quantification, allowing researchers to account for variability and assess the robustness of optimized mixtures in real-world conditions.	[45]
Enhancing adaptability to large-scale designs	Future direction: Research on enhancing Scheffe's Simplex Lattice Model's adaptability to large-scale and complex mixture designs. This may involve refining algorithms or incorporating parallel computing strategies to handle computational demands.	[45, 46]
Integration of machine learning concepts	Future direction: Exploration of integrating machine learning concepts within Scheffe's model to handle non-linear relationships and expand its applicability.	[46]
Development of hybrid models	Future direction: Research on developing hybrid models that combine Scheffe's Simplex Lattice Model with other advanced optimization techniques. This integration aims to capitalize on strengths, overcome limitations, and achieve more robust results.	[46]
Performance under different conditions	Future direction: Investigation of Scheffe's model performance under various environmental conditions and material sources. This research contributes to its applicability in diverse construction scenarios.	[45, 46]
Addressing practical constraints	Future direction: Research focused on addressing practical constraints and incorporating real-world considerations, such as economic feasibility and construction site constraints, to enhance the model's practical utility.	[45, 46]

practical constraints in construction, such as material availability and batching limitations, would further enhance its utility in real-world scenarios [42, 43]. Table 6 summarizes the challenges, limitations, and areas for improvement in applying Scheffe's Simplex Lattice Model to concrete mixtures, providing key insights and corresponding references.

EMERGING TRENDS AND FUTURE DIRECTIONS

Exploration of Emerging Trends in Statistical Modeling for Concrete Mixture Optimization

The exploration of emerging trends in statistical modeling for concrete mixture optimization reveals a dynamic landscape influenced by advancements in technology, data analytics, and materials science [44]. One prominent trend involves the integration of machine learning techniques to complement traditional statistical models. Machine learning algorithms, such as neural networks and genetic algorithms, demonstrate promise in handling complex, non-linear relationships within concrete mixtures. Another trend is the increased use of data-driven approaches, leveraging large datasets and advanced analytics to gain insights into material behaviors and optimize mixtures more effectively [45]. Furthermore, the integration of probabilistic modeling and uncertainty quantification is gaining traction, allowing researchers to account for variability and assess the robustness of optimized mixtures in real-world conditions.

Suggestions for Future Research Directions and Improvements in Applying Scheffe's Simplex Lattice Model to Optimize Concrete Properties

As we look towards the future, several avenues for research and improvement in applying Scheffe's Simplex Lattice Model to optimize concrete properties emerge [45, 46]. Firstly, exploring ways to enhance the model's adaptability to large-scale and complex mixture designs is crucial. This might involve refining the model's algorithms or incorporating parallel computing strategies to handle the computational demands associated with intricate concrete formulations. Additionally, integrating machine learning concepts within Scheffe's model could open new possibilities for handling non-linear relationships and further expanding its applicability [46].

Furthermore, future research could focus on developing hybrid models that combine Scheffe's Simplex Lattice Model with other advanced optimization techniques. This integration could capitalize on the strengths of different approaches, potentially overcoming limitations and achieving more robust results. Moreover, investigating the model's performance under different environmental conditions and varying material sources can contribute to its applicability in diverse construction scenarios. Addressing practical constraints and incorporating real-world considerations, such as economic feasibility and construction site constraints, remains a critical area for future research to enhance the model's practical utility. Table 7 summarizes emerging trends in statistical modeling for concrete mixture optimization and suggests future research directions

for improving Scheffe's Simplex Lattice Model, providing key insights and corresponding references.

CONCLUSION

Summary of Key Findings from the Literature Review

The literature review on the application of Scheffe's Simplex Lattice Model in cement concrete mixture optimization reveals a robust and versatile statistical tool. The model has been successfully employed to navigate the complex landscape of concrete mixtures, showcasing its efficacy in achieving optimal combinations of variables. Studies reviewed demonstrate the model's ability to improve performance indicators, such as compressive strength and durability, through a systematic exploration of the design space. The review underscores Scheffe's model as a valuable asset in the evolution of concrete mixture design methodologies.

Implications for the Field of Concrete Mixture Design and Optimization

The implications for the field of concrete mixture design and optimization are significant. The systematic and data-driven approach offered by Scheffe's Simplex Lattice Model presents a paradigm shift from traditional empirical methods. By efficiently exploring multi-variable systems, the model contributes to a more nuanced understanding of the relationships among concrete components. This has profound implications for achieving tailored material properties, enhancing durability, and optimizing sustainability in concrete construction. The reviewed studies suggest that the adoption of Scheffe's model can lead to more efficient and precise concrete mixture designs, setting the stage for advancements in the construction industry.

Call to Action for Further Research and Development in this Area

The literature review illuminates avenues for further research and development in the application of Scheffe's Simplex Lattice Model to concrete mixture optimization. Researchers are encouraged to delve deeper into refining the model to address challenges such as non-linearity and computational efficiency. Exploring hybrid models that integrate Scheffe's model with emerging machine learning techniques offers a promising direction. Additionally, there is a call for research that extends the model's applicability to diverse environmental conditions, material sources, and practical constraints encountered in real-world construction settings. This comprehensive approach will contribute to the continued evolution of concrete mixture design methodologies, advancing the field towards more sustainable, resilient, and high-performance concrete materials.

In conclusion, the literature review showcases Scheffe's Simplex Lattice Model as a valuable tool in concrete mixture optimization, with implications for improving material properties and sustainability. The call to action emphasizes the need for ongoing research and development to refine the model, explore emerging trends, and address practical challenges, fostering innovation in the field of concrete mixture design and optimization.

ACKNOWLEDGEMENTS

The completion of this article is a testament to the collective dedication and invaluable contributions of all authors, whose diverse perspectives and expertise greatly enriched its content and depth.

DATA AVAILABILITY STATEMENT

The author confirm that the data that supports the findings of this study are available within the article. Raw data that support the finding of this study are available from the corresponding author, upon reasonable request.

CONFLICT OF INTEREST

The author declared no potential conflicts of interest with respect to the research, authorship, and/or publication of this article.

USE OF AI FOR WRITING ASSISTANCE

Not declared.

ETHICS

There are no ethical issues with the publication of this manuscript.

REFERENCES

- [1] M. Adamson, A. Razmjoo, and A. Poursae, "Durability of concrete incorporating crushed brick as coarse aggregate," *Construction and Building Materials*, Vol. 94, pp. 426–434, 2015. [\[CrossRef\]](#)
- [2] E. Avci, and E. Yildirim, "Examination of unconfined compressive strength values by response surface models in grouted sands with microfine cements," *ZBORNIK RADOVA GEO-EXPO*, 2018. [\[CrossRef\]](#)
- [3] R. Kazemi, E. M. Golafshani, and A. Behnood, "Compressive strength prediction of sustainable concrete containing waste foundry sand using meta-heuristic optimization-based hybrid artificial neural network," *Structural Concrete*, 2023. [\[CrossRef\]](#)
- [4] M. A. Mosabepurah and O. Eren, "Statistical flexural toughness modeling of ultra high performance concrete using response surface method," *Computers and Concrete*, Vol. 17(4), pp. 477–488, 2016. [\[CrossRef\]](#)
- [5] V. Muthuraman, R. Ramakrishnan, K. Sundaravadivu, and B. Arun, "Predicting surface roughness of WEDMed Wc-Co composite using box-behnken response surface method," *Advanced Materials Research*, Vol. 651, pp. 361–366, 2013. [\[CrossRef\]](#)
- [6] I. Z. Akobo, S. B. Akpila, and B. Okedeyi, "Optimization of compressive strength of concrete containing rubber chips as coarse aggregate based on Scheffe's model," *International Journal of Civil Engineering*, Vol. 7(7), pp. 93–110, 2020. [\[CrossRef\]](#)
- [7] U. Alaneme George and M. Mbadike Elvis, "Optimization of flexural strength of palm nut fibre concrete using Scheffe's theory," *Materials Science for Energy Technologies*, Vol. 2(2), pp. 272–287, 2019. [\[CrossRef\]](#)

- [8] A. A. Aliabdo, A. M. Abd-Emoatry, and H. H. Hassan, "Utilization of crushed clay brick in concrete industry," *Alexandria Engineering Journal*, Vol. 53(1), pp. 151–168, 2014. [\[CrossRef\]](#)
- [9] A. V. Alves, T. F. Vieira, J. Brito, and J. R. Correia, "Mechanical properties of structural concrete with fine recycled ceramic aggregate," *Construction and Building Materials*, Vol. 64, pp. 103–113, 2014. [\[CrossRef\]](#)
- [10] E. E. Ambrose, D. U. Ekpo, I. M. Umoren, and U. S. Ekwere, "Compressive strength and workability of laterized quarry sand concrete," *Nigerian Journal of Technology*, Vol. 36(3), pp. 605–610, 2018. [\[CrossRef\]](#)
- [11] U. C. Anya, "Models for predicting the structural characteristics of sand-quarry dust blocks," Doctorial Dissertation, University of Nigeria, 2015.
- [12] J. I. Arimanwa, D. O. Onwuka, M. C. Arimanwa, and U. S. Onwuka, "Prediction of the compressive strength of aluminum waste–cement concrete using Scheffe's theory," *Journal of Materials in Civil Engineering*, Vol. 24(2), pp. 177–183, 2012. [\[CrossRef\]](#)
- [13] P. O. Awoyera, J. O. Akinmusuru, and J. M. Ndumbuki, "Green concrete production with ceramic wastes and laterite," *Construction and Building Materials*, Vol. 117, pp. 29–36, 2016. [\[CrossRef\]](#)
- [14] B. Benabed, E. H. Kadri, T. Ngo, and A. Bouvet, "Rheology and strength of concrete made with recycled concrete aggregate as replacement of natural aggregates," *Epitoanyag Journal of Silicate Based and Composite Materials*, Vol. 72(2), pp. 48–58, 2020. [\[CrossRef\]](#)
- [15] L. Bloom, and A. Bentur, "New mix designs for fresh and hardened concrete," *ACI Materials Journal*, Vol. 92(2), pp. 143–150, 1995.
- [16] G. E. P. Box, W. G. Hunter, and J. S. Hunter, "Statistics for experimenters: An introduction to design, data analysis, and model building," John Wiley & Sons, New York, 1978.
- [17] M. Daniyal and S. Ahmad, "Application of waste ceramic tile aggregates in concrete," *International Journal of Innovative Research in Science and Engineering Technology*, Vol. 4(12), pp. 12808–12815, 2015.
- [18] M. A. DeRousseau, J. R. Kasprzyk, and W. V. Srubar, "Computational design optimization of concrete mixture: a review," *Cement and Concrete Research*, Vol. 109, pp. 42–53, 2018. [\[CrossRef\]](#)
- [19] N. R. Draper and F. Pukelsheim, "K-models for mixture experiments," *Journal of Quality Technology*, Vol. 29(4), pp. 420–427, 1997.
- [20] H. Elci, "Utilization of crushed floor and wall tile wastes as aggregate in concrete production," *Journal of Cleaner Production*, Vol. 112, pp. 742–752, 2016. [\[CrossRef\]](#)
- [21] H. N. Ezeh, and O. M. Ibearugbulem, "Statistical optimization of concrete mix proportions using Scheffe's simplex theory," *Journal of Engineering and Applied Sciences*, Vol. 4(1), pp. 1–7, 2009.
- [22] A. Halicka, P. Ogrodnik, and B. Zegardlo, "Using ceramic sanitaryware waste as concrete aggregate," *Construction and Building Materials*, Vol. 48, pp. 295–305, 2013. [\[CrossRef\]](#)
- [23] A. Heidari and D. Tavakoli, "A study of the mechanical properties of ground ceramic powder concrete incorporating nano-SiO₂ particles," *Construction and Building Materials*, Vol. 38, pp. 255–264, 2013. [\[CrossRef\]](#)
- [24] D. M. Kannan, S. H. Aboubakr, A. S. El-Dieb, and M. M. Taha, "High performance concrete incorporating ceramic wastes powder as large partial replacement of Portland cement," *Construction and Building Materials*, Vol. 144, pp. 35–41, 2017. [\[CrossRef\]](#)
- [25] V. M. Malhotra, and P. K. Mehta, "Supplementary cementitious materials," *Cement and Concrete Research*, Vol. 32(9), pp. 1525–1537, 2002. [\[CrossRef\]](#)
- [26] E. M. Mbadike, and N. N. Osadebe, "Application of Scheffe's model in optimization of compressive strength of lateritic concrete," *Journal of Civil Engineering and Construction Technology*, Vol. 4(9), pp. 265–274, 2013.
- [27] C. Medina, M. Frias, and M. I. Rojas, "Microstructure and properties of recycled concrete using ceramic sanitary ware industry waste as coarse aggregate," *Construction and Building Materials*, Vol. 31, pp. 112–118, 2012. [\[CrossRef\]](#)
- [28] N. Mohan, A. Gupta, and S. Singh, "Optimization of mix proportions of mineral aggregates for use in polymer concrete using statistical techniques," *Journal of Materials in Civil Engineering*, Vol. 14(6), pp. 521–526, 2002.
- [29] D. C. Montgomery, "Design and analysis of experiments," John Wiley & Sons, 2017.
- [30] A. M. Neville, "Properties of concrete," 5th ed., Pearson Education, 2011.
- [31] S. O. Obam, "A simplex-centroid design for mixture optimization," *Journal of Quality Technology*, Vol. 30(4), pp. 391–403, 1998.
- [32] F. O. Okafor, and O. Oguaghamba, "Procedures for optimization using Scheffe's model," *Journal of Engineering Science and Application*, Vol. 7(1), pp. 36–46, 2010.
- [33] P. N. Onuamah and N. N. Osadebe, "Development of optimized strength model of lateritic hollow block with 4% mound soil inclusion," *Nigerian Journal of Technology*, Vol. 34(1), pp. 1–11, 2015. [\[CrossRef\]](#)
- [34] N. N. Osadebe, C. C. Mbajorgu, and T. U. Nwakonobi, "An optimization model development for laterized concrete mix proportioning in building constructions," *Nigerian Journal of Technology*, Vol. 26(1), pp. 37–45, 2007.
- [35] F. Pacheco-Torgal and S. Jalali, "Reuse of ceramic wastes in concrete," *Construction and Building Materials*, Vol. 24, pp. 832–838, 2010. [\[CrossRef\]](#)
- [36] H. Scheffe, "Experiments with mixtures," *Journal of the Royal Statistical Society. Series B (Methodological)*, Vol. 20(2), pp. 344–360, 1958. [\[CrossRef\]](#)

- [37] H. G. Shruthi, M. E. Gowtham, T. Samreen, and R. P. Syed, "Reuse of ceramic wastes as aggregate in concrete," *International Research Journal of Engineering and Technology*, Vol. 3(7), pp. 115–119, 2016.
- [38] M. Simon, "Statistical experimental design for performing tests on concrete," *Cement and Concrete Research*, Vol. 33(11), pp. 1841–1847, 2003.
- [39] M. J. Simon, "Concrete mixture optimization using statistical methods: Final Report," Federal Highway Administration, Infrastructure Research and Development, Georgetown Pike McLean, VA, USA, 2003.
- [40] M. Simon, and V. M. Malhotra, "Statistical experimental design for optimizing concrete mixtures," *ACI Materials Journal*, Vol. 94(3), pp. 193–202, 1997.
- [41] Z. Tahar, B. Benabed, E. H. Kadri, T. Ngo, and A. Bouvet, "Rheology and strength of concrete made with recycled concrete aggregate as replacement of natural aggregates," *Epitoanyag Journal of Silicate Based and Composite Materials*, Vol. 72(2) pp. 48–58, 2020. [\[CrossRef\]](#)
- [42] W. C. Tang, Y. Lo, and A. Nadeem, "Mechanical and dryness shrinkage properties of structural-graded polystyrene aggregate concrete," *Cement and Concrete Composite*, Vol. 30(5), pp. 403–409, 2008. [\[CrossRef\]](#)
- [43] A. Torkittikul, and A. Chaipanich, "Utilization of ceramic waste as fine aggregate within Portland cement and fly ash concrete," *Cement and Concrete Composite*, Vol. 32, pp. 440–449, 2010. [\[CrossRef\]](#)
- [44] B. Zegardlo, M. Szelag, and P. Ogrodnik, "Ultra-high strength concrete made with recycled aggregate from sanitary ceramic wastes – the method of production and the interfacial transition zone," *Construction and Building Materials*, Vol. 122, pp. 736–742, 2016. [\[CrossRef\]](#)
- [45] O. Zimbili, W. Salim, and M. Ndambuki, "A review on the usage of ceramic wastes in concrete production," *International Journal of Civil, Environmental, Structural, Construction and Architectural Engineering*, Vol. 8(1), pp. 91–95, 2014.
- [46] E. E. Ambrose, F. O. Okafor, and M. E. Onyia, "Compressive strength and Scheffe's optimization of mechanical properties of recycled ceramics tile aggregate concrete," *Journal of Silicate Based and Composite Materials*, Vol. 73(3), Article 18583, 2021. [\[CrossRef\]](#)



Case Report

Potential recycling of mine tailings for PMC's Padcal Mine, Philippines

Idongesit Ime IKOPBO¹, Melissa May BOADO^{*2}

¹Engineering Program, School of Advanced Studies, Saint Louis University, Baguio City, Philippines

²Department of Chemical and Mining Engineering, School of Engineering and Architecture, Saint Louis University, Baguio City, Philippines

ARTICLE INFO

Article history

Received: 28 December 2023

Revised: 02 March 2024

Accepted: 12 March 2024

Key words:

Mine tailing; Multi-criteria analysis; Recycling; Repurposing; Waste diversion

ABSTRACT

Industrialized countries attempted to obtain minerals, resulting in a developed method to extract valuable minerals from the ground. Consequently, waste mine tailings are produced and, when left to pile up, will potentially be hazardous to the environment and the people. However, more mine tailings become a problem when the organization needs clarification on the minerals' value and what they can be used for. This study focuses on a multi-criteria analysis of the potential repurposing of the Philex Mining Corporation (PMC) tailings in Benguet, Philippines. While mining policies were considered, findings show that piles of mine tailings had not been considered for refining to produce more resources for development, construction, and economic growth. The study employs qualitative inquiry to understand better the grassroots processes and reconnaissance of the stored tailings. The analysis tries to promote sustainable practices – presenting a higher sustainability priority, resource conservation, and the responsible management of mining waste, making it a more favorable alternative to traditional tailing storage facilities. Several industrial uses for the tailings have been suggested to reinforce waste diversion.

Cite this article as: Ikopbo II, Boado MM. Potential recycling of mine tailings for PMC's Padcal Mine, Philippines. Environ Res Tec 2024;7(2)280–289.

INTRODUCTION

The global community benefits from mining because it makes the resources accessible for technology, infrastructure, and energy. Mining pollution can cause water pollution, with heavy metals and radionuclides being the most common pollutants [1]. Today's mining methods contribute to solid waste accumulation, accounting for a significant portion of the world's waste streams. Not only that, but the amount of waste generated each year totals millions of tons [2, 3]. Mining is an unavoidable anthropogenic process that occurs worldwide and frequently alters the land's shape. A large amount of land or earth must be moved, and most of the process involves extracting valuable minerals and elements from waste. In today's world, metal mining is increasingly important. As a result, more metals, particularly copper, are extracted from the ground [4, 5].

Historically, mine tailings have been disposed of in large impoundments or ponds near the mining site. The fact that tailings are typically dumped into lakes, rivers, or even the ocean is a significant source of concern in the mining process. They are backfilled or dumped into gauges as mining waste [6]. It is worth noting that mine tailings are stored in dams, which can be reused for other purposes. Environmental disasters are frequently a problem in mining, and they are unavoidable. This results in social disasters. More than anything else, how mine tailings are handled and controlled determines the likelihood of environmental disasters caused by mining [7].

Mining operations in the Philippines have frequently been complex, harming the environment and making it difficult for people to live their everyday lives. The disposal or stor-

*Corresponding author.

*E-mail address: mmboado@slu.edu.ph



age of large amounts of mining waste, known as tailings, impacts the environment and the people who live there and is an integral part of the mining company [8]. Tailings show the global impact of the mining industry. When precious minerals and metals from mined ore are processed and extracted, a liquid slurry of tiny mineral particles known as tailing is created. Pipes are used to transport these tiny mineral fragments to extensive tailings storage facilities (TSFs), where they are kept for many years or even decades [7].

Heavy metal pollution has always been a significant issue because mining harms people's health. Because of the wind, arsenic, and cadmium move around in nature evenly. As a result, temperatures rise, worsening health conditions [9]. Most mining companies' most significant problem is tailings dam failures, which are said to be the cause of three-fourths of mining-related environmental disasters [10]. Tailings storage capacity can be challenging to manage. In the study of [7], for example, wet storage capacity for wet tailings necessitates a more efficient dam to store the tailings for an extended period. When the handling and storage processes fail, it poses a significant threat to the system and the environment due to radioactive reactions based on time management.

In 2012, a mining incident at Padcal mine, Philex Mining Corporation in Benguet, released 20.6 million tons of toxic tailings into rivers [11]. Recent interest in repurposing mine tailings is growing, with the potential to reduce environmental and social impacts, such as water contamination and habitat destruction.

Large private and governmental mining industries do not repurpose their waste mine tailings to generate additional revenue while ensuring the environment's and its inhabitants' safety [12]. Vitti & Arnold (2022) stated that mining can help the country's economy in a variety of ways, and reusing waste mine tailings can significantly contribute to the country's revenue growth [13, 14].

However, there has been growing interest in exploring potential repurposing opportunities for mine tailings. Despite the fact that more mining companies are doing their part to reduce the damage they cause, most mining companies have established systems for disposing of mine waste, such as dams, embankments, and a variety of other things. One of the main reasons for considering the repurposing of mine tailings is to mitigate the environmental and social impacts associated with their disposal. Traditional tailings storage methods can pose risks such as water contamination, habitat destruction, and the release of potentially harmful substances into the surrounding environment. Repurposing mine tailings can mitigate environmental and social impacts, such as water contamination, habitat destruction, and the release of harmful substances into the environment [15].

As a result, this study focuses on the recycling applicability and potential of PMC's mine tailings in Benguet's Padcal. Also, the study considered how mine tailings, such as iron, aluminum, and other metals, could be reused and recycled to eliminate the requirement for storage facilities and lessen

the impact of mine tailings on the environment. This study looked into how these mine tailings could be repurposed and areas where they could be reused, which justifies the conduct of this study. This would reduce the use of other natural building materials and eliminate the need for extensive land areas to store mine tailings, lowering the economic and environmental costs.

This research intends to promote the reduction of waste generation, to contribute to sustainable resource utilization and the promotion of circular economy principles. Implementing effective tailings recycling practices can contribute to more sustainable and responsible mining operations, benefiting both the industry and the surrounding communities. The implications of the findings will provide valuable insights for policymakers, mining companies, future researchers, students, and stakeholders interested in transforming mine tailings into valuable resources while minimizing their environmental footprint.

MATERIALS AND METHODS

Locale of the Study

Padcal, Benguet in the Philippines, is home to the PMC, a copper-gold Mine. It is situated southeast of Baguio City at a height of around 1500 meters. The rainy season lasts from May to October, with an annual rainfall of about 4500 mm. Since the mine's underground block cave operations began in 1958, copper concentrates containing copper, gold, and silver have been produced. Their mining product is typical porphyry copper, with primary copper ore minerals chalcopyrite and bornite and gold and silver as byproducts [16].

The Padcal mine production capacity generates a total milled ore of 7,945,879 metric tons in 2021, higher than the tonnage of 7,837,536 in 2020 and lower than that of 8,112,791 in 2019. Also, the budget tonnage per day is 23,200 as of 2022. Moreover, as of 2023, the average tonnage per day is 18,968.87, the average tonnage per month is 572,859.9, and the land area covered by the tailing pond for TSF 3 is 165 hectares. Based on the current tailing output, it is projected to be full by the end of October 2025, assuming a 647 m reduced level (mRL) as final crest elevation and 642 mRL slimes elevation. The volume capacity calculation to 642 mRL elevation based on the September 2023 Bathymetric survey is 12.9M DMT.

Population Sampling

The research is based on qualitative inquiry processes, with the goal of better understanding how mine repurposing is beneficial with respect to the current practices of PMC. The study used purposive sampling to identify informants for the investigation, which involved interviewing current informants and suggesting others who meet the criteria. The study focused on the corporation's staff, ensuring that everyone in the sample had experienced the subject matter.

The environmental protection and enhancement officer and the tailing storage facility departmental head working at PMC with three or more years of experience were in-

cluded. The environmental protection and enhancement officer was relevant to this study because the participants gave technical expertise in areas such as environmental impact assessment, mine tailing management, and waste management. The tailing storage facility departmental head was relevant to this study because the participant gave valuable insights into the management and operation of tailing storage facilities.

Data Gathering Procedure

This study's primary data source was a semi-structured, one-on-one interactive session. The researcher spoke with the mining staff and elicited information about mine waste repurposing, the mine tailing characteristics, the possible applications of their tailings, and the benefits of utilizing the mine tailings in Padcal by asking open-ended questions. The interviews were recorded with the informants' permission. Reflective notes were taken throughout the interviews, particularly at the end, and as a result, other information from the PMC's internal and published reports was included. This helped the researcher identify their strengths and weaknesses while also providing some transcription prompts [17]. Each interview lasted about 45 minutes. In addition, the written notes contained immediate personal thoughts about the interview as well as observations of both verbal and nonverbal behaviors as they occurred. The researcher transcribed the audio recording after the interviews ended. The researcher ascertained that the participant's language accurately reflected the meanings embedded in the experience. Through the participants' consent and voluntary participation, the researcher initially established a connection with them. Data collection continued until no new discoveries were made and category saturation was reached.

Ethics approval was obtained from the Saint Louis University Research Ethics Committee, and the various mining companies endorsed the introductory letters before conducting the study. The study participants were protected by getting detailed information via written informed consent, which means that potential research participants were fully informed about the research procedures and dangers before agreeing to participate. Participation in this study was voluntary and posed no significant risk to physical or psychological wellbeing. Up until the point of data analysis, all participants had the option to withdraw from the study for any reason.

The information gathered for this research is private and confidential. There was no personal information about the participants in the study report, such as name or address. After examining the data, the researcher removed all identifying information, and the study results were sent without any identifying information. The data was kept on a password-protected laptop with a locked file. The raw data would be accessible only to the researcher and the research panel. The researcher can decline to ask for the interview if it appears inappropriate for the study, and the participants would not be held liable to the researcher or the study.

Characterization Method of Mine Tailings

During the data gathering, a representative sample of PMC mine tailings was taken from tailing storage facility 3. Three Samples were sourced and labeled North, Middle, and South, respectively, and the analysis was carried out at Saint Louis University Mining Laboratory, Baguio City. The samples were subjected to X-ray Fluorescence Spectroscopy (XRF) to determine the elemental analysis and reported as oxides.

RESULTS AND DISCUSSION

Philippine Regulations

The Department of Environment and Natural Resources (DENR) oversees both the Mines and Geosciences Bureau (MGB) and the Environmental Management Bureau (EMB), which monitor mining activities and ensure compliance when issuing permits for treatment, storage, and disposal (TSD) to facilities with high volume wastes. MGB is in charge of mining operations administration and oversight, while EMB is in charge of monitoring and controlling the environment. Before the MGB issues any permits, the relevant local government units must determine whether a mining plan is viable. Currently, these government agencies only require storage of mine tailings.

PMC conducts its operations under the highest ethical standards, adhering to good governance as a responsible corporate citizen. It strives to abide by its Code of Conduct and all relevant laws, guidelines, and mining industry requirements. Additionally, it provides partners in the mining industry with its expertise and starts enlightening and productive discussions about issues that concern the sector and society.

Tailing Management Practices

PMC has implemented some mine tailing management practices to minimize the environmental impact of its operations. Their mine tailings are not utilized, but instead stored in the tailings pond. The company has constructed TSFs that are designed to collect and store mine tailings, which are the waste materials generated during mining operations. These are engineered to prevent leaks and spills and are regularly monitored to ensure their integrity. They are currently on their third TSF.

Their only plan for their tailings is to store them because their tailings are only allowed to be stored in the tailing storage facilities. If the waste cannot be converted into something useful, mine waste tailing storage is usually beneficial. If waste is not converted into something useful, it tends to accumulate in the environment and cause problems for people there.

While storing mine tailings in a pond can be a viable option for tailings management, it is important for mining companies to carefully consider the specific characteristics of the tailings, the local environment, and regulatory requirements and to implement appropriate monitoring and management measures to ensure the safety and sustainability of the TSF.

Table 1. Composition of PMC tailings and particular regions of samples taken at TSF 3. The numbers displayed are oxide-form reports of the entire elemental analysis

Sample	Composition*						
	Al ₂ O ₃ wt %	CaO wt %	Fe ₂ O ₃ wt %	Cu wt %	MgO wt %	SiO ₂ wt %	S wt %
Sample north	8.23	3.94	8.19	0.048	3.3	32.41	1.29
Sample middle	6.63	3.98	8.53	0.044	2.0	28.78	1.36
Sample south	7.37	3.77	8.79	0.044	2.0	28.66	1.29
Mean average	7.41	3.90	8.50	0.05	2.43	29.95	1.31

The participants were asked how long they intended to store their tailings:

Participant 1 also said:

“Forever, maybe, since there is nowhere else to store it besides our pond. Unless maybe there will be a new technology to help with that.”

Participant 2 explained further from the response of Participant 1 by saying that the effect of constructing TSFs on the environment is mostly deforestation and some accompanying social issues because of the affected owners where they would have to settle claims as needed.

The participants further explained how their tailings are managed.

“We don’t treat the tailings; we just store them. We just separate the solids from the water. We use decanting system here.” (Participant 1)

Also, participant 2 said:

“We do not do any treatment on the tails. Immediately after we have recovered the metals, it goes through tunnels and pipes to the treatment storage disposal TSFs. Our tailings are not toxic. We do monthly monitoring. There are no heavy metals present in our effluent.” there are no significant amounts of mercury, arsenic or cyanide in our tailings. (Participant 2).

Although the participants had a general idea that mine mill tailings can be used in construction materials, they needed to have initiative on how their mill tailings from their company can be reused. They also had their perception toward the repurposing of mine tailing. Participant 1 explained that repurposing these tailings will have a minimal negative impact on the environment but can maybe contribute economically to the country by reducing the cost of constructing storage facilities.

Participant 2 had a perception about the environmental impact if their company pursues repurposing by utilizing their tailing.

“If there is really a diversion of tailings, then definitely, there will be no tailings storage facilities and that means there will be no sub-merged areas, no loss of habitat, no deforestation and reforestation, and there will be no additional cost. But there is no initiative on that at the moment.” (Participant 2)

Reusing these tailings, according to Participant 1, would not cause much environmental harm, but it might speed up construction and boost the economy by making facilities more accessible and affordable for everyone to use. However, they do not recycle their tailings.

“But if we could reuse these tailings, I think there is not much impact on the environment if we would be utilizing the tailing. But if we could use this tailing, I think they will be some sort of economical program. But environmentally, it could be just reprocessing the tailing may be used in the construction materials. I think there will be no environmental impact and if there is, it will be minimal.” (Participant 2)

In all, the repurposing of mine tailings can positively contribute to a country’s national economic growth by generating revenue, creating jobs, reducing environmental impact, and supporting the growth of critical industries. On the aspect of recycling applicability, and potential of tailings based on their characteristics, findings show that the absence of copper (Cu), the corporation’s main mineral, in the samples suggests that the initial beneficiation and separation process was so effective that there was little to no copper left in the tailings. The typical minerals mine by PMC is porphyry copper.

Since their tailings are not treated nor reused, knowing the composition of their tailings was of importance to this research as they generate tons of tailings daily. Participant 2 said their tailings are basically composed of bornite and chalcopyrite. The company’s treatment processes have stayed the same because the still follow the same till date since their tailings are not treated and the quality of the tailings do not cause any degradation.

Characteristics of PMC Mine Tailings at TSF3

The composition of mine tailings varies from one company to another because of the inherent ore characteristics where they mine as well as the processes each employs in mineral beneficiation. The suitability for utilization will be entirely depended on the characterization of the mine tailings. Whether it will require further separation of components or refinement on the intended use. In-depth studies will show the characteristics of mine-tailing composites, such as physical properties, mechanical properties, durability properties, and leaching behavior.

In order to determine how best to use and recycle the tailings, chemical analysis was used to analyze three tailings samples, labeled North, Middle, and South, to determine their potential for recycling and usage using The tables below contain a presentation of the chemical analysis's findings. Based on the analysis, the average mean of the chemical compositions for the mine tailing is presented.

As shown in Table 1, the compositions of copper tailings show that silicon dioxide, iron, and aluminum oxides have higher percentage concentration in the tailings than other metallic oxides. The tailings are composed of low-grade metallic and non-metallic oxides that can be financially recovered and recycled into various manufactured products such as cement manufacturing, glass, ceramics, bricks, etc. in the required percentage. With extensive utilization, the elemental composition of copper tailings, which includes Fe_2O_3 , Al_2O_3 , MgO , and SiO_2 , has good concentration and recovery rates and can be used as additives in construction materials. The concentrations of the compounds present in the PMC tailings are consistent such that as it is, they can be used as an additive or substitute for the fine aggregates added to cement to form concrete. The high silica content makes this a plausible use. Further refinement can mean they can be used in the cement manufacturing industry.

Recycling Applicability and Potential of the PMC Mine Tailings

The mine tailings have good percentages of silicon dioxide, iron, aluminum oxide, and magnesium that can be repurposed for construction materials manufacturing because of their physical properties and chemical composition. Silica-rich mine tailings can also be used as a component in various construction materials, such as concrete, asphalt, tiles, and bricks. The tailings can be mixed with other materials, such as cement, lime, and aggregates to produce high-strength materials.

Several studies have investigated mine tailings as a supplementary cementitious material (SCM) in Portland cement manufacturing and have shown that it is possible to produce high-quality cement with tailings as a partial replacement for traditional raw materials. Due to their high silica content, silica-rich mine tailings can also be used as an SCM. They can react with the calcium hydroxide produced during cement hydration to form additional cementitious compounds [18].

The specific requirements and optimal dosage of mine tailings may vary depending on the type of tailings, their chemical compositions, and the specifications of the cement product. Portland cement is one of the most widely used types of cement. The average composition of Portland cement is CaO , 50–60%; SiO_2 , 20–25%; Al_2O_3 , 5–10%; MgO , 1–3%; Fe_2O_3 , 1–2% and SO_3 , 1–2% [19]. Ordinary Portland cement contains different ingredients with varied proportions. Each ingredient imparts a different property to the cement. To produce good quality cement, it is important to know the proportions, functions and limitations of different cement ingredients.

- Silica (SiO_2). Silica or silicon dioxide is the second largest quantity of cement ingredients which is about 17 to 25%. Silica can be obtained from sand, argillaceous rock, etc. Enough silica helps to form di-calcium and tri-calcium silicates, which impart strength to the cement.
- Alumina (Al_2O_3). Alumina in cement is present in the form of aluminum oxide. The range of alumina in cement should be 3 to 8%. It is obtained from bauxite, alumina, and clay. Alumina imparts quick setting properties to the cement. In general, high temperature is required to produce the required quality of cement.
- Iron oxide (Fe_2O_3). Iron oxide quantity in cement ranges from 0.5 to 6%. It can be obtained from fly ash, iron ore, and scrap iron. The main function of iron oxide is to impart color to the cement.
- Magnesia (MgO). Cement contains Magnesia or Magnesium oxide in the range of 0.1 to 3%. Magnesia in cement in small quantities imparts hardness and color to the cement. If it is more than 3%, the cement becomes unsound, and the strength of the cement also reduces.

Along with lime and other inorganic oxides, these ingredients can widely be used as a cement additive. A material that can bind other materials together is cement, a binder that sets and hardens. In a process known as calcination, clay and other limestone materials are heated to 14500 °C in a kiln to create calcium oxide (CaO) from calcium carbonate (CaCO_3), which is then combined with the additions mentioned above. Portland cement is made by grinding the rigid material, known as clinker, along with a small quantity of gypsum.

To use mine tailings as SCM, they are first ground to a fine powder and then blended with the other raw materials used in cement production, such as limestone and clay [20]. The resulting mixture is then fed into a kiln and heated to high temperatures, which causes chemical reactions that transform the raw materials into cement clinkers to occur. The addition of mine tailings to Portland cement can improve the strength, durability, and workability of the resulting concrete [21].

Mine tailings as a SCM can provide economic benefits by reducing waste disposal costs and creating a new revenue stream. However, careful consideration of chemical composition is necessary to ensure no negative impact on cement performance and safety at the mine site. The use of mine tailings should not compromise the stability of the mine site.

Philex mine tailings are rich in silicon, iron, and aluminum oxides. The composition will be most suitable for cement production, which will eventually make its way to the construction industry, such as in civil works for roads. This environmentally friendly approach offers environmental and economic benefits. However, careful evaluation is necessary to ensure the tailings are not polluting, comply with geotechnical specifications, and are safe. Reprocessing techniques like crushing, grinding, flotation, and leaching may be necessary to remove impurities and adjust chemical composition. The decision to use mine tailings depends on individual mine and cement manufacturing processes. By

Table 2. An analysis based on multiple criteria evaluating the pros and cons of each factor in the reuse and recycling of their mine tailing

Factors	Pros	Cons	Balance
Tailing dam failures	F+ S++ T+		F+ S++ T+
Heavy metal seepage	F+ S+ T+		F+ S+ T+
Tailing dusting	S+ A+		S+ A+
Avoided cost of building more storage facilities	F+ T+		F+ T+
Liberating the area that the tailings dam had previously taken up.	F+		F+
Avoidance of leach collection and treatment	F+ S++ T+		F+ S++ T+
Using up mine tailings	F+ S+		F+ S+
Land recovery	F+		F+
Avoidance cost of post-closure care	F+ T+		F+ T+
Metal recovery	F++		F++
Slag	S+	F-	F- S+
Transport quarry-plant cost		F-	F-
Cost of investment		F-	F-
Machinery		F-	F-
Labour expense		F-	F-
Cost of energy		F-	F-
Cost of maintenance		F-	F-

using mine tailings as a supplementary material in cement manufacturing, the industry can reduce its reliance on virgin raw materials, helping to conserve natural resources and lowering the environmental impact of mining activities. The industry can reduce the energy consumption associated with mining and processing virgin materials, contributing to overall energy conservation.

Ultimately, the decision to reprocess mine tailings for use in cement production will depend on a variety of factors, including the specific characteristics of the tailings, the requirements of the cement manufacturing process, and the applicable regulations and standards.

Multi-Criteria Analysis

One of the objectives of this study is to present a multi-criteria analysis of storing the tailings in comparison to their utilization. After thorough consideration of various factors surrounding the idea of economic and environmental benefits of storing versus utilizing mine tailings, it came out that utilization of mine tailings is more beneficial than storing them. This study emphasizes the potential to reduce the consumption of natural resources by recovering valuable materials, minimizing waste, conserving energy, promoting environmental stewardship, and creating economic incentives for sustainable mining practices. Multi-criteria analysis is a decision-making tool that evaluates options based on multiple criteria, taking into account various factors and their relative importance [22]. It provides a structured approach to assessing and comparing different factors based on various criteria, which helps in making informed decisions that consider environmental sustainability [23]. In

Table 3. Multi-criteria analysis outlining the pros and cons of mine tailing storage

Factors	Pros	Cons	Balance
Slag	S+	F-	F- S+
Transport quarry-plant cost		F-	F-
Cost of investment		F-	F-
Machinery		F-	F-
Labour expense		F-	F-
Cost of energy		F-	F-
Cost of maintenance		F-	F-

conducting a multi-criteria analysis of tailings utilization, it is necessary to evaluate each option and compare them with the advantages and disadvantages of other options for managing mine tailings [24]. The analysis should consider its immediate and prospective pros and cons and the risks and uncertainties associated with each option.

In this regard, the aim is to determine whether the advantages of recycling and reusing mine tailings outweigh the disadvantages. A factor item will be given symbols according to its relevance precedence, a method described by Hillebrandt [25] and used by Lu et al. [26] will be employed here. This is thoroughly integrated with the Bio-Economic Model since it states that the multi-criteria analysis can be a powerful approach in the decision whether to pursue repurposing of mine tailings. This combined allows for a comprehensive evaluation of various criteria and objectives, considering both economic and environmental factors [27].

Table 4. Pros and cons of reusing mine tailings compared to storing them in tailing storage facilities are compared in a brief and preferred order of results

Factors	Mine tailing	Storing tailing	Preferred order	
			Mine tailing	Storing tailing
Tailing dam failures	F+ S++ T+	-	1	2
Heavy metal seepage	F+ S+ T+	-	1	2
Tailing dusting	S+ A+	-	1	2
Avoided cost of building more storage facilities	F+ T+	-	1	2
Liberating the area that the tailings dam had previously taken up.	F+	-	1	2
Avoidance of leach collection and treatment	F+ S++ T+	-	1	2
Using up mine tailings	F+ S+	-	1	2
Land recovery	F+	-	1	2
Avoidance cost of post closure care	F+ T+	-	1	2
Metal recovery	F++	-	1	2
Slag	F-S+	F-S+	1	1
Transport quarry-plant cost	F-	F-	1	1
Cost of investment	F-	F-	1	1
Machinery	F-	F-	1	1
Labour expense	F-	F-	1	1
Cost of energy	F-	F-	1	1
Cost of maintenance	F-	F-	1	1
Totals for preferred orders			17	27
Overall priority			1	2

This means that the multi-criteria analysis of repurposing the tailings should be evaluated not only in terms of economic value, but also in terms of the environmental and social impacts of the repurposing process. When examining environmental challenges, it is often challenging to put clear monetary values on the benefits associated with sustainability initiatives [28].

It is agreed to use an acronym for each of the four scoring criteria: F for financial impact, S for safety, A for abstract, and T for time-efficiency to quantify the immeasurable. These acronyms stand for the annual flow of the advantages and disadvantages of repurposing mine tailings. In addition, a plus symbol (+) and a minus sign (-) will be used to indicate pros and cons, respectively. A double sign will denote greater significance. The advantages and disadvantages of this strategy for recycling tailings and conventionally storing tailings are shown in Tables 2, 3, and 4, respectively.

Multi-criteria analysis has been found to be an effective approach for evaluating the various factors related to the reuse and recycling of mine tailings [29]. By employing a multi-criteria analysis technique, Table 2 outlines the pros and cons associated with recycling and reusing mine tailings. Table 3 illustrates how multi-criteria analysis is a valuable technique in assessing various approaches to managing mine tailings storage, depending on a variety of factors [30]. Lottermoser, B.G. conducted a study in 2011 that analyzed the environmental impacts and management strate-

gies associated with mine wastes, particularly mine tailings [31]. The study is a valuable resource for understanding the advantages and disadvantages of reusing mine tailings compared to storing them in tailings storage facilities from an environmental perspective. Table 4 depicts the decision to reuse mine tailings instead of storing them in tailings storage facilities, which was made after considering the pros and cons presented in Tables 2 and 3.

The advantages of mine environmental quality regulations in terms of economic, health, physical, and social benefits transcend the disadvantages. In a real economic sense, mine environmental regulations benefit citizens by fostering their health, safety, welfare, tranquility, and permanence. The findings from this research study suggest the multi-criteria analysis some sense of direction regarding the systematic approach involved in the mine tailings dam, the danger involved in lathering mine tailings, and possible managerial skills to minimize ecosystem and subsequently improve the industrial benefit of the mine tailings. It showed that there are far more financial advantages in terms of environmental sustainability for utilizing mine tailing than storing them. As a result, using this mine tailings for other purposes presents a higher sustainability priority resource. The acquisition of mine tailings and crushed waste rock from mines is easier and more cost-effective than dredging, quarrying, and mining. The use of mine tailings and waste rock from mines reduces the need to extract these materials from the

earth and thus prevents the disturbance of ecosystems in such environment. Therefore, multi-criteria analysis offers several economic and environmental advantages.

In PMC, tailings are disposed using traditional tailings management procedures, which involve storing them in tailings dams. When valued within the context of the sustainable economy, it is thought that tailings might be regarded as a supply of raw materials. Consequently, there are no links between the academic community and industry that support research for such. The corporation strictly adheres to mining regulations, policies, and laws in the Philippines by making sure the tailings are stored properly. Repurposed tailings are perceived to have minimal to no negative impact on the environment.

The findings indicate that there are elements other than copper in the tailing from the mining process. Exploration could lead to the discovery of more of them, which would aid in other areas of science, technology, and invention. The PMC tailings are rich in silica which has the potential to be used as a supplementary cementitious material in cement production. This finding concurs with [32] the analogy that refined elements such as SiO_2 can be added to cement manufacturing for the construction of buildings. Since the tailings have values in the construction industry, recycling of the tailings should be ascertained.

Repurposing mine tailings, according to Cheng, T. C., Kassimi, F., & Zinck, J. M. (2016), tends to preserve natural resources, reduce dams, reduce environmental impact, and then contribute massively to economic growth by 9% [33]. It emphasizes the importance of promoting tailings recycling in order to reduce excessive consumption of natural resources.

The advantage of recycling can be easily justified and offset by significant savings if we take into account all of the expenses associated with a tailings dam throughout its entire life cycle, including the costs related to closure and rehabilitation, the risk of a potential failure both during operation and after closure, the possibility for the disastrous loss of life, the rebuilding process, remediation of the environment, production loss, damage to the company, and closure costs.

The multi-criteria analysis shows that repurposing mine tailing has far more advantage than traditional way of storing the mine tailings. It provides a robust decision-making framework that considers environmental, economic, social, and long-term liability aspects. This approach promotes sustainable practices, resource conservation, and the responsible management of mining waste, making it a more favorable alternative to traditional tailing storage facilities. It can encourage the development of improved tailings management practices, including innovative methods for tailings dewatering, consolidation, and compaction. These practices can reduce the volume of tailings that need to be stored, thus minimizing the environmental footprint of storage facilities. It can also lead to identifying and evaluating new technologies and approaches for tailings management. Additional research studies can help optimize the use of space within storage facilities, potentially extending their

operational lifespans and reducing the need for expansion or construction of new impounding facilities.

Repurposing mine tailings can offer environmental and economic benefits, but it also comes with potential risks that need to be carefully considered. Some of the risks associated with the repurposing of mine tailings include environmental contamination, geotechnical stability, and long-term stability. To mitigate these risks, several measures can be taken, such as thoroughly characterize the chemical and physical properties of the mine tailings and applying monitoring programs to track any changes in their properties over time. Place measures to contain and isolate the mine tailings to prevent the release of contaminants into the surrounding environment, such as using impermeable liners and barriers. Implement appropriate engineering controls when repurposing mine tailings, such as compaction, reinforcement, and proper slope design to guarantee geotechnical stability and ensure that the repurposing of mine tailings complies with relevant environmental regulations and standards to minimize potential risks to human health and the environment. Develop and implement long-term management plans for the repurposed mine tailings, including ongoing monitoring, maintenance, and contingency measures for potential environmental impacts.

CONCLUSION

The study explores the repurposing of mine tailings, focusing on the impact on the environment and resource recovery. The PMC stores a significant amount of mine tailings without reusing them, believing that repurposed tailings will have minimal environmental impact. However, the sample analysis reveals that the tailings contain elements like silicon, aluminum, and iron dioxide, which could be utilized in construction manufacturing industries. These elements and minerals are beneficial to economic growth and could contribute to the sustainability of the mining sector. The development of new processes and technologies for repurposing mine tailings can drive innovation in the mining sector. This can lead to the creation of new intellectual property, the growth of a technology-driven ecosystem, and the fostering of a culture of continuous improvement within the industry. These advancements can contribute to economic growth by enhancing the sector's competitiveness and attracting investment in research and development. This can create opportunities for job creation and local economic development. New processing facilities, research centers, and reclamation projects related to tailings repurposing can generate employment and economic activity in mining regions, contributing to the diversification and resilience of local economies.

The study also highlights the potential of reusing mine tailings in Portland cement manufacturing, conserving natural resources, and reducing the cost of constructing additional storage facilities. By incorporating these mine tailings into the cement manufacturing process, the need to extract and consume raw materials can be reduced, conserving natural resources and promoting sustainable practices.

A multi-criteria analysis approach for recycling mine tailings offers several advantages, enabling a comprehensive evaluation of various criteria and factors, allowing for a more informed decision-making process. By incorporating mine tailings into the Portland cement manufacturing process, the company can conserve natural resources and promote sustainable practices.

Compared to several developed nations, the Philippines' current rate of mine waste utilization is below average. Vast amounts of mine tailings are just deposited in the tailing storage facilities. To address concerns about the economy and the environment;

1. The research also encourages mining companies to focus on the efficient use of their mine waste in the construction sector. By researching how to use these waste materials in the manufacturing construction materials, it is possible to lessen the detrimental effects of mine tailings and better use the potential uses of mine tailings.
2. Consider the social acceptability of the proposed repurposing methods. Engage with local communities, stakeholders, and Indigenous groups to understand their concerns, interests, and potential benefits. The National Commission on Indigenous People (NCIP) Administrative Order 3 outlines the participation of local communities in the decision-making process of new projects through collaborative and inclusive approaches respecting the socio-political structures of the locale. This could involve assessing impacts on health, livelihoods, cultural heritage, and community wellbeing. Also, develop a clear, transparent, and accessible communication strategies to inform the public about the potential benefits and risks associated with repurposing mine tailings.
3. Mining companies in the Philippines should evaluate their mine tailings and conduct more experimental studies on the characteristics of their mine tailings. They are encouraged to explore reprocessing and recycling their mine tailings to reduce the tailings' environmental impact and maintenance cost of tailing storage facilities.
4. Mining companies should conduct a comprehensive risk assessment to identify and mitigate potential risks associated with the repurposing of their mine tailings. This includes considerations for safety, health hazards, and financial risks. By considering these factors and conducting a thorough multi-criteria analysis, you can effectively identify the resources and potential utilization options for mine tailings.
5. The corporation or government should look into this research study to see the recycling possibility of the tailings due to the concentration of SiO_2 , Al_2O_3 , Fe_2O_3 , Etc., which justifies recycling potential in the cement industry, pottery industry, Etc., for the generation of income to the company and the country as well.

ACKNOWLEDGEMENTS

I would like to express my sincere gratitude to all those who have contributed to the successful completion of this research entitled "Potential Recycling of Mine Tailings for PMC's Padcal Mine, Benguet." First and foremost, I would like to extend my heartfelt appreciation to the Almighty God for the wisdom, knowledge, and understanding that He has bestowed upon me throughout this research journey. I would also like to thank my research supervisor and my Panel members for their time, and their expertise. Their thoughtful input and suggestions have greatly enriched the quality and depth of this research work. I am thankful to Saint Louis University for providing me with the necessary resources and facilities for conducting this research. Last but not least, I would like to acknowledge the contributions of all the participants who took the time to respond to the interviews. Without their cooperation, this research would not have been possible.

DATA AVAILABILITY STATEMENT

The author confirm that the data that supports the findings of this study are available within the article. Raw data that support the finding of this study are available from the corresponding author, upon reasonable request.

CONFLICT OF INTEREST

The author declared no potential conflicts of interest with respect to the research, authorship, and/or publication of this article.

USE OF AI FOR WRITING ASSISTANCE

Not declared.

ETHICS

There are no ethical issues with the publication of this manuscript.

REFERENCES

- [1] S. Liu, Q. Li, and J. Song, "Study on the grinding kinetics of copper tailing powder," *Powder Technology*, Vol. 330, pp. 105–113, 2018. [\[CrossRef\]](#)
- [2] C. Wang, D. Harbottle, Q. Liu, Z. and Xu, "Current state of fine mineral tailings treatment: A critical review on theory and practice," *Minerals Engineering*, Vol. 58, pp. 113–131, 2014. [\[CrossRef\]](#)
- [3] M. Edraki, T. Baumgartl, E. Manlapig, D. Bradshaw, D. M. Franks, and C. J. Morgan, "Designing mine tailings for better environmental, social and economic outcomes: A review of alternative approaches," *Journal of Cleaner Production*, Vol. 84, pp. 411–420, 2014. [\[CrossRef\]](#)
- [4] D. Kossoff, W. E. Dubbin, M. Alfredsson, S. J. Edwards, M. G. Macklin, and K. A. Hudson-Edwards, "Mine tailings dams: Characteristics, failure, environmental impacts, and remediation," *Applied Geochemistry*, Vol. 51, pp. 229–245, 2014. [\[CrossRef\]](#)
- [5] J. N. Moore, and S. N. Luoma, "Hazardous wastes from large-scale metal extraction: A case study," *Environment Science Technology*, Vol. 24(9), pp. 1278–1285, 1990. [\[CrossRef\]](#)

- [6] C. Falagán, B. M. Grail, and D. B. Johnson, “New approaches for extracting and recovering metals from mine tailings,” *Minerals Engineering*, Vol. 106, pp. 71–78, 2017. [CrossRef]
- [7] E. Schoenberger, “Environmentally sustainable mining: The case of tailings storage facilities,” *Resources Policy*, Vol. 49, pp. 119–128, 2016. [CrossRef]
- [8] M. A. Q. Adajar, and M. A. H. Zarco, “An empirical model for predicting the hydraulic conductivity of mine tailings,” *International Journal of Geomate*, Vol. 7(14), pp. 1054–1061, 2014. [CrossRef]
- [9] T. Mashifana, and T. Sithole, “Clean production of sustainable backfill material from waste gold tailings and slag,” *Journal of Cleaner Production*, Vol. 308, Article 127357, 2021. [CrossRef]
- [10] International Institute for Environment and Development (IIED), “Breaking new ground: mining, minerals and sustainable development: The report of the MMSD project (1st ed.),” Earthscan, 2002.
- [11] J. R. Owen, D. Kemp, É. Lébre, K. Svobodova, and G. P. Murillo, “Catastrophic tailings dam failures and disaster risk disclosure,” *International Journal of Disaster Risk Reduction*, Vol. 42, Article 101361, 2020. [CrossRef]
- [12] O. Onuaguluchi, and O. Eren, “Copper tailings as a potential additive in concrete: Consistency, strength and toxic metal immobilization properties,” *Indian Journal of Engineering and Materials Sciences*, Vol. 19(2), pp. 79–86, 2012.
- [13] C. Vitti, and B. J. Arnold, “The reprocessing and revalorization of critical minerals in mine tailings,” *Mining, Metallurgy & Exploration*, Vol. 39, pp. 49–54, 2022. [CrossRef]
- [14] D. M. Reconalla, and R. E. Eguia, “Local content development framework in mining context: The case of Pantukan, Compostela Valley, Philippines,” 2015. <https://www.ijser.in/archives/v4i6/IJSER15831.pdf>. Accessed on May 02, 2024.
- [15] S. Holcombe, and J. Keenan, “Mining as a temporary land use scoping project: Transitions and repurposing,” 2020. <https://www.mineclosure.net/media/resources/352/mining-as-a-temporary-land-use-final200318-f.pdf>. Accessed on May 02, 2024.
- [16] Philex Mining Corporation, “Philex extends P12.9 M assistance to villages,” <https://www.philexmining.com.ph/2020/05/19/philex-extends-p12-9-m-assistance-to-villages/>. Accessed on May 2, 2024.
- [17] H. J. Streubert, and D. R. Carpenter, “Qualitative research in nursing: Advancing the Humanistic Imperative (5th ed.),” Williams & Wilkins; 2011.
- [18] G. Koumal, “Method of environmental clean-up and producing building material using Copper mine tailing waste material,” United States Patent Number US5286427A, 1994.
- [19] C. Snell, B. Tempest, and T. Gentry, “Comparison of the thermal characteristics of Portland cement and geopolymers concrete mixes,” *Journal of Architectural Engineering*, Vol. 23(2), 2017. [CrossRef]
- [20] O. Onuaguluchi, and Ö. Eren, “Reusing copper tailings in concrete: corrosion performance and socio-economic implications for the Lefke-Xeros area of Cyprus,” *Journal of Cleaner Production*, Vol. 112(Part 1), pp. 420–429, 2016. [CrossRef]
- [21] Y. Wang, T. A. Zhang, Y. Zhang, G. Lyu, and W. Zhang, “Mineral transformation in treating low-grade bauxite using the calcification-carbonization process and preparing cement clinker with the obtained residue,” *Minerals Engineering*, Vol. 138, pp. 139–147, 2019. [CrossRef]
- [22] N. Mouter, M. Dean, C. Koopmans, and J. M. Vassallo, “Comparing cost-benefit analysis and multi-criteria analysis,” In *Advances in Transport Policy and Planning*, Vol. 6, pp. 225–254, 2020. [CrossRef]
- [23] N. Mouter, “Chapter one - Standard transport appraisal methods,” *Advances in Transport Policy and Planning*, Vol. 7, pp. 1–7, 2021. [CrossRef]
- [24] I. B. Huang, J. Keisler, and I. Linkov, “Multi-criteria decision analysis in environmental sciences: Ten years of applications and trends,” *Science of the Total Environment*, Vol. 409(19), pp. 3578–3594, 2011. [CrossRef]
- [25] P. M. Hillebrandt, “Economic theory and the construction industry (2nd ed.),” Macmillan; 2000. [CrossRef]
- [26] W. Lu, A. Fung, Y. Peng, C. Liang, and S. Rowlinson, “Cost-benefit analysis of Building Information Modeling implementation in building projects through demystifying time-effort distribution curves,” *Building and Environment*, Vol. 82, pp. 317–327, 2014. [CrossRef]
- [27] D. R. Brown, “A review of bio-economic models,” 2000. <https://citeseerx.ist.psu.edu/document?repid=rep1&type=pdf&doi=02b7a49c0fe95f45910d55d6bb0daa7a4a8f45ad>. Accessed on May 2, 2024.
- [28] A. A. Mahmood, and M. Elektorowicz M. A conceptual cost benefit analysis of tailings matrices use in construction applications. *Proceedings of The 3rd International Conference on Civil and Environmental Engineering for Sustainability*. Hurghada, Egypt, 2016. [CrossRef]
- [29] U. Kaźmierczak, J. Blachowski, and J. Górniak-Zimroz, “Multi-criteria analysis of potential applications of waste from rock minerals mining,” *Applied Sciences*, Vol. 9(3), pp. 441, 2019. [CrossRef]
- [30] V. Monardes, and J. M. Sepúlveda, “Multi-criteria analysis for circular economy promotion in the management of tailings dams: A case study,” *Minerals*, Vol. 13(4), Article 486, 2023. [CrossRef]
- [31] B. G. Lottermoser, “Recycling, reuse and rehabilitation of mine wastes,” *Elements*, Vol. 7(6), pp. 405–410, 2011. [CrossRef]
- [32] A. K. Awasthi, X. Zeng, and J. Li, “Integrated bio-leaching of copper metal from waste printed circuit board-A comprehensive review of approaches and challenges,” *Environmental Science and Pollution Research*, Vol. 23(21), pp. 21141–21156, 2016. [CrossRef]
- [33] Cheng, T. C., Kassimi, F. and Zinck, J. (2016). A holistic approach to green mining innovation in tailings reprocessing and repurposing. *Proceedings Tailings and Mine Waste* (pp. 2–5). Colorado, USA.